Development of a natural product library using hyphenated techniques and evaluation of its constituents as potential anti-cancer agents

by

Patrick Matthew Mc Millan

16037392

Supervisor: Prof. Vinesh J. Maharaj

Submitted in fulfilment of the requirements for the degree

MAGISTER SCIENTIAE CHEMISTRY

In the Faculty of Natural and Agricultural Sciences

University of Pretoria

June 2023

Declaration

I, **PATRICK MATTHEW MC MILLAN** declare that the dissertation, which I hereby submit for the degree *Magister Scientiae* Chemistry at the University of Pretoria, is my own work and has not previously been submitted by me for a degree at this or any other tertiary institution.

Signature: ....

Date: 20 - 06 - 2023

Acknowledgements

I wish to express my recognition and genuine appreciation towards Prof. Vinesh J. Maharaj for his guidance and scientific contribution during my project and for the opportunity to work on such a prestigious scientific endeavour. The persistence, devotion and composure you've shown throughout the project has helped me make it the success it is.

In addition, my special gratitude goes to our collaborators, Dr. Barry O'Keefe at the National Cancer Institute for his support and intellectual contribution as a world leading expert in natural products and Prof. SubbaRao V. Madhunapantula at the JSS Medical College in India for his screening work and contribution to this project.

I also appreciate and recognise all my colleagues in the Biodiscovery Centre for their encouragement and assistance, with special mention to Mr. L. Invernizzi, Mr. WJ. Rudolf and Dr. P. Moyo. I would like to thank Dr. Y. Naudé and Dr. M. Wooding for their years of chromatography and mass spectroscopy guidance. I am also grateful to the entire staff of the Chemistry department with special mention to Mrs. N. Steenkamp, Mrs. R. Swart, Dr. J. Pretorius, Mr. N. van Vuuren, Dr. F. Malan and Prof. M. Rademeyer.

My extend thanks to Dr. B. Okole for his assistance in transferring the plant materials from the Council for Scientific and Industrial Research to the Chemistry Department and Mr. J. Sampson for his assistance in collecting plant material from the Manie van der Schijff Botanical Gardens.

This work would not have been possible without the financial support from the National Research Foundation and the Department of Science and Innovation. Your support is much appreciated.

Finally, I am forever grateful to my family and friends for their support throughout my academic career. Words cannot express my deepest gratitude to my parents, Michael and Margaret, who through their hard work and many sacrifices have given me the opportunity to pursue my education.

Summary

Worldwide, cancer is among the most common public health issues with an estimated death toll in 2020 of close to 10 million individuals. Although cancer treatments are continuously improving as the use of personalised medicinal treatments have shown great potential, the incident rate of cancer is predicted to exponentially increase over the next 10 years. Cancer treatment is still a reductionist approach since cancer is a variety disease at the cellular level, which makes treatment even more challenging. The rising incidence of cancer worldwide and the reductionist approach in treatments emphasises the need for new and more efficient cancer treatments. The use of natural products in medicinal practices is one of mankind's oldest traditions. Since 1982, The FDA has approved over 809 natural products for the treatment and management of communicable and noncommunicable diseases like HIV, bacterial infections and cancers. Natural products still offer novel and chemically diverse compounds that display greater drug-likeness behaviour than synthetic compounds. In the past, natural products have been exceptionally successful in drug discovery which proves their potential for novel therapeutic agents against variety diseases like cancer. South Africa's biodiversity is potentially one of the world's richest and untapped sources for novel natural products. In 2018, it was estimated that South Africa contained over 67 000 animal and 20 401 plant species. Additionally, South Africa has one of the richest multicultural heritages in the world that has established an impressive knowledge on the use of indigenous medicinal plants.

The work completed in this study has created a trusted South African natural product library that is ready for modern HTS against various diseases. In this project, the robust procedures developed for the standardisation of plant extracts and fractions were miniaturised from the high-throughput methods of pre-existing natural product library platforms, primarily the NCI NPNPD project. A validation study that used a paclitaxel spiked extract of *Brassica oleracea* (cabbage) was also conducted to ensure the integrity of plant samples after the plant preparative methods. A second extract of *Brassica oleracea* was used as a negative control and did not contain paclitaxel. The UPLC-PDA-HRMS analysis of the spiked fractions indicated that paclitaxel was concentrated in fraction 6 and was quantified at 0.1409 mg/mL in the final standardised fraction. The recovery of the spiked paclitaxel was calculated to be 6.23 %, which indicated that the preparation of the spiked extract for fractionation was ineffective. The spiked extract and respective fractions were screened against the human lung cancer cell line A549 where the presence of other interfering compounds resulted in a low cell proliferation inhibition for fraction 6 of 31.43 %. Irrespective of the low activity, it was determined that the plant preparative methods did not degrade potential bioactive compounds

nor induce false positives as later in the project the presence of a few extremely bioactive fractions were observed.

Additionally, from a subset of selected medicinal plant species in the South African natural product library at University of Pretoria was evaluated for potential anti-cancer compounds. For plant species selection an ethnopharmacological preferential scoring system was developed that preferentially scored the South African medicinal plants most likely to succeed based on their traditional usage. From a final list of the top 100 preferentially scored medicinal plant species, 34 (representing 21 plant families) were standardised and high-throughput screened against the human cancer cell lines A549, MCF7 and Caco2. The ultrasonic bath extraction method developed produced sufficient high-quality extracts for downstream standardisation from ± 7.0 g of plant material. Of the 34 plant extracts produced, only one required a second extraction. The automated plant extract fractionation method developed by the NCI NPNPD project was used to fractionate 34 plant extracts on C8 SPE cartridges using a single needle Gilson GX-241 ASPEC® liquid handler. Each plant extract was fractionated into 7 unique fractions of decreasing polarity which resulted in the total production of 272 unique fractions. The average mass recovery after fractionation was 46.75 % but a slight revision in the preparation of the plant extracts before fractionation will improve the recovery. The standardisation of the plant extracts and respective fractions followed a multi-step process using a Hamilton Microlab® STARlet™ automated liquid handler. The STARlet™ automated liquid handler successfully standardised more than 97 % of the plant extracts and fractions at 5 mg/mL in DMSO. For the few plant extracts and fractions that had insufficient mass to be standardised, their respective concentrations in 100 µL DMSO were recorded appropriately. All the standardised extracts and fractions were stored in airtight screw capped pre-barcoded polypropylene vials at -20 °C under dry atmospheric conditions inside a Hamilton Verso® Q20 robotic freezer. The unique internal barcoding format and database structure developed in this project was able to successfully catalogue and correlate all the information relating to the preparation, standardisation and storage of each standardised extract and fraction.

It was noted that only 3 standardised fractions showed excellent cell proliferation inhibition above 80 % against the cell line A549 at 50 µg/mL. It was noted that the 3 standardised fractions with potent activity were from fraction numbers 3 and/or 4. At the screening concentration 25 µg/mL, only 7 and 3 standardised fractions showed above 90 % cell proliferation inhibition against the cell lines MCF7 and Caco2, respectively. The potent fractions were concentrated in the fractions number 2 and 4. The benefit of fractionating the plant extracts on a C8 SPE cartridge pre-HTS was demonstrated as most active fractions demonstrated better activity than their respective crude extracts. It was demonstrated that in

a time and cost-efficient manner, the HTS of a small subset of standardised fractionated plant extracts from the South African natural product library has rapidly identified numerous "hits" for the investigation of potentially novel anti-cancer compounds.

Using the *in vitro* HTS results of the South African natural product library, a single hit fraction from *Mikania natalensis* was prioritised for post-HTS investigation. At the time of investigation there was no reported phytochemical analysis or biological activity on *M. natalensis* which made it attractive for potentially novel anti-cancer compounds. The dereplication of the hit fraction used modern UPLC-PDA-HRMS analysis and online databases such as ChemSpider, PubChem, Reaxys and the Dictionary of Natural Products which quickly lead to the tentative identification of a single unique chromatographic peak as mikanin 3-O-sulphate, named M3S. The easy upscaling of the plant preparative methods allowed for the rapid isolation of the biologically active compound. Approximately 18.26 g of dried leaf material from *M. natalensis* was used to produce 2.30 g of an upscaled MeOH/DCM crude extract. Only 0.745 g of the extract was used in upscaled extract fractionation which produced 24.66 mg of the hit fraction for isolation purposes. The 24.66 mg of the hit fraction was prepared in 1.0 mL ACN/H_2O and injected onto the semi-preparative HPLC-PDA-MS. By using mass-directed isolation on the HPLC-PDA-MS, 0.98 mg of the tentatively identified compound M3S was isolated. The identity of M3S was further verified by structural confirmation using both 1D (^1H and ^{13}C) and 2D (HSQC and HMBC) NMR experiments in combination with ACDLabs™ Spectrus Processor. The isolated M3S was rescreened and the IC_{50} concentrations against the cancer cell lines MCF7 and Caco2 were 146.2 µM and 65.36 µM, respectively. The presence dihydromikanolide in the leaf extract of *M. natalensis* was also confirmed by SCXRD analysis of a single crystal from the dried fraction 5 of the upscaled extract fractionation of *M. natalensis*. The absolute configuration of dihydromikanolide was reported to be less uncertain than current literature. This was the first report of dihydromikanolide and M3S, that has shown encouraging anti-cancer activity against the cancer cell lines MCF7 and Caco2, present in the leaf extract of *M. natalensis*.

Keywords: *Anti-cancer, HTS, South Africa, Medicinal plants, Mikania natalensis, Natural products, Natural product library.*

Table of Contents

© University of Pretoria

List of Figures

Chapter 4

List of Tables

List of Equations

List of Supplementary Data

Chapter 3

List of Abbreviations

R^2	Coefficient of determination
^{13}C NMR	Carbon NMR
^1H NMR	Proton NMR
4T1	Mouse breast cancer cell line
A549	Lung cancer cell line
ACN	Acetonitrile
BEH	Ethylene bridged hybrid
BPI	Base peak ion
CAR	Chimeric antigen receptor
CCDC	Cambridge Crystallographic Data Centre
CCK-8	Cell counting kit-8 assay
CD_3OD	Deuterated methanol
CO-RE	Compression-induced O-ring expansion
CSIR	Council for Scientific and Industrial Research
Da	Dalton
DCM	Dichloromethane
DEC	Disposable extraction cartridge
DIA	Data-independent acquisition
DMEM-HG	Dulbecco's Modified Eagle Medium- High glucose
DMEM-LG	Dulbecco's Modified Eagle Medium- Low glucose
DMSO	Dimethylsulfoxide
ED_{50}	Median effective dose
EGFR	Epidermal growth factor receptor
ER	Oestrogen receptor
ESI	Electron spray ionisation
EtOAc	Ethyl acetate
FBS	Foetal bovine serum
FDA	Food and Drug Administration
g	Gram
GRIDD	The Griffith Institute for Drug Discovery
HeLa	Cervical cancer cell line
HEp2	Human larynx carcinoma
HepG 2	Liver cancer cell line
HER2	Epidermal growth factor receptor 2
HER2+	HER2 positive breast cancer
HHS	Hamilton heater shaker
HIV	Human immunodeficiency virus
HMBC	Heteronuclear multiple bond correlation
HPLC	High-performance liquid chromatograph
HPLC-PDA-MS	Waters® Preparative high performance liquid chromatography (HPLC) system equipped with a Waters PDA and ACQUITY QDa detector
HSQC	Heteronuclear single quantum coherence spectroscopy
HTS	High-throughput screening
Hz	Hertz
IC_{50}	Half maximal inhibitory concentration

ICH	International Council For Harmonisation
ICI's	Immune checkpoint inhibitors
ID	Internal diameter
iSwap	Internal swivel arm plate handler
kV	Kilovolts
L/Hr	Litres per hour
LBC	Luminal breast cancer
LC	Liquid chromatography
LD$_{50}$	Median lethal dose
LOD	Limit of detection
LOQ	Limit of quantification
M	Molar
m/z	Mass to charge ratio
M3S **(37)**	Mikanin 3-O-sulfate
MCF7	Breast cancer cell line
mDa	Millidalton
MeOH	Methanol
MFX	Multiflex carrier base
mg	Milligram
Min	Minute
MIT	Minimum intensity threshold
mL	Millilitre
mm	Millimetre
mM	Millimolar
MS	Mass spectroscopy
MTBE	Methyl tert-butyl ether
MTT **(13)**	3-(4,5-dimethylthiazol-2yl)-2,5-diphenyl tetrazolium bromide
NCI	National Cancer Institute
NCI NPNPD	National Cancer Institute Program for Natural Product Discovery
NMR	Nuclear magnetic resonance
NSCLC	Non-small cell lung cancer
OD	Optical density
OD	Outer Diameter
PBS	Phosphate buffered saline
PDA	Photodiode array detector
PP	Polypropylene
ppm	Parts per million
PR	Progesterone receptor
PTFE	Polytetrafluoroethylene
QTOF	Quadrupole time-of-flight mass spectrometer
RT	Retention time
SANBI	South African National Biodiversity Institute
SCLC	Small cell lung cancer
SFC	Supercritical fluid chromatograph
SFE	Supercritical fluid extraction
SPE	Solid-phase extraction
SRB **(15)**	Sulphorhodamine B

SCXRD	Single crystal X-ray diffraction
TCA	Trichloroacetic acid
T-cells	T lymphocytes
TK10	Renal cancer cell line
TNBC	Triple-negative breast cancer
UACC62	Melanoma cell line
µg/mL	Microgram per millimeter
µL	Microlitre
µM	Micromolar
UPLC	Ultra-high pressure liquid chromatography
UPLC-PDA-HRMS	Waters® ACQUITY UPLC® system coupled to a Waters® XEVO-G2-XS-QTOF
V	Volts
Vero cells	African monkey kidney cell line
λ_{max}	Lambda max

Additional outputs based on this work

Poster presentation

H3D Symposium: First Place Poster Prize (Student Category) for the poster titled:
"Creation of a South African natural product library ready for high-throughput screening against multiple diseases".
(25-28 October 2022)

Creation of The South African natural product library

University of Pretoria: The first South African natural product library has become the cornerstone of the Biodiscovery Group founded by Prof. V. Maharaj in the Chemistry Department at the University of Pretoria.

Published work that used The South African natural product library methods

- Mianda, S. M. et al. *In vitro* dual activity of *Aloe marlothii* roots and its chemical constituents against *Plasmodium falciparum* asexual and sexual stage parasites. *J. Ethnopharmacol*. **297**, 115551 (2022).
- Invernizzi, L. *et al.* Use of hyphenated analytical techniques to identify the bioactive constituents of *Gunnera perpensa L*., a South African medicinal plant, which potently inhibit SARS-CoV-2 spike glycoprotein–host ACE2 binding. *Anal. Bioanal. Chem.* **414**, 3971–3985 (2022).

Chapter 1: Introduction

1.1 Natural products in human history

Natural products have been used in medicinal practices since the beginning of mankind. The earliest recorded usage of medicinal plants dates back over five thousand years which listed twelve different medicinal plants formulations referencing over 250 plant species[1]. Since then, mankind has continuously been searching for novel natural therapeutic compounds. Due to the advances in disease screening and chemical analysis technologies, a significant amount of approved drugs worldwide are natural products or derivatives[2]. Natural products have shown to be extremely effective against infectious and non-infectious diseases such as the human immunodeficiency virus (HIV), bacterial infections and cancers. Natural products are still seen as a rich source for chemically diverse and novel therapeutic compounds that are often more drug-like than synthetic compounds[3].

The term natural products refers to the chemical compounds i.e., secondary metabolites produced by living organisms. In the lab, these chemical compounds are targeted by extraction and isolation methods for chemical characterisation and potential therapeutic applications. Living organisms such as plants produce both primary and secondary metabolites. Primary metabolites are directly involved in the normal growth and development of the plant[4]. Plant secondary metabolites are not as crucial for plant development but are essential for other important functions like chemical signalling, chemical defence from predators and the attraction of pollinators[4]. It is reported that specific plant secondary metabolites are commonly confined to a few plant species within a phylogenetic group. It is estimated that less than 15 % of the world's plant species have been chemically analysed implying a high possibility of discovering novel secondary metabolites with therapeutic application[4]. The elemental compositions of plant secondary metabolites are often restricted to hydrogen, carbon, oxygen, nitrogen and sulphur with halogens being less common. Irrespective of the simple elemental compositions, plant secondary metabolites offer diverse chemical scaffolds and molecular complexity that makes discovering novel therapeutic compounds from plants infinite[5]. Plant secondary metabolites can be categorised into different chemical classes based on their chemical scaffolding and function groups. The major chemical classes in plants are: alkaloids, phenolic compounds, sulphur containing compounds and terpenoids[6]. There is an estimated 12 000 alkaloids, over 8 000 phenolic compounds and over 100 000 terpenoids that have been chemically characterised from plant secondary metabolites[7–9].

Between January 1981 and September 2019, the Food and Drug Administration (FDA) approved 1 881 drug entities of which 809 (43 %) were unaltered natural products or synthetic

1

derivatives[10]. For over 38 years, natural products have influenced almost half of the final drug entities approved by the FDA. Shown in Figure 1-1 are a few FDA approved drug entities since 1981:
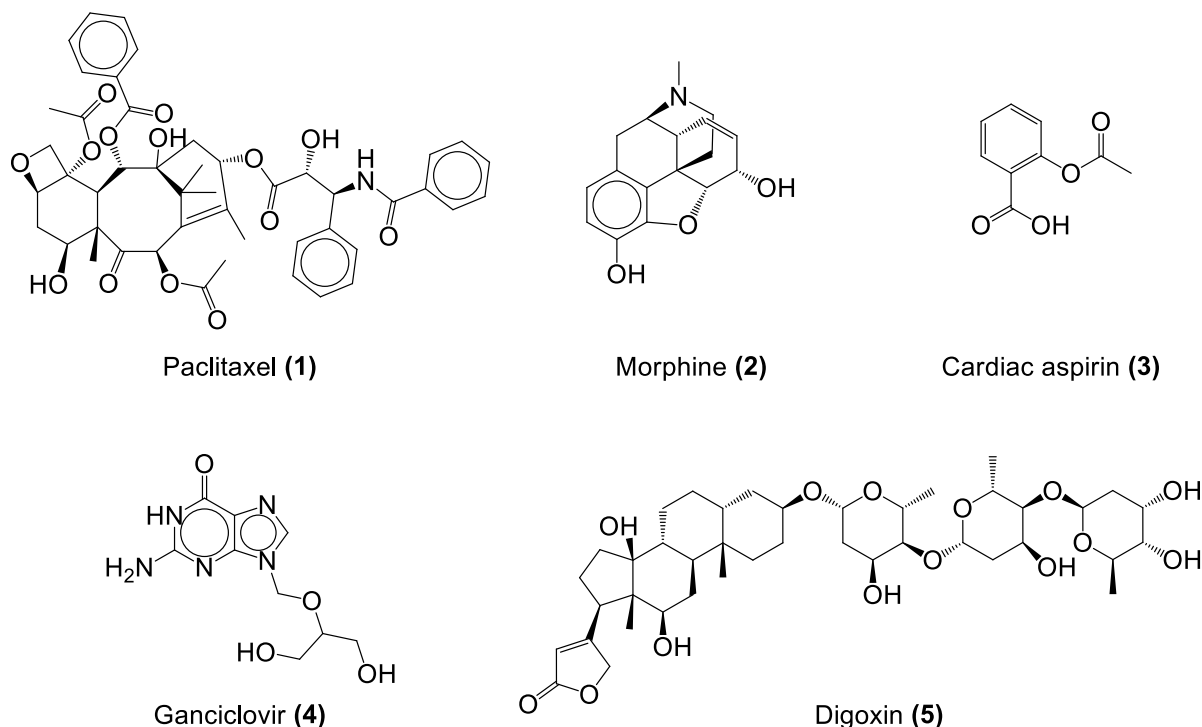
Figure 1-1 Shown above are the chemical structures of the following FDA approved drugs: Paclitaxel **(1)**, morphine **(2)**, cardiac aspirin **(3)**, ganciclovir **(4)** and digoxin **(5)**.

These compounds were all isolated from higher plants but are used in different treatments for different diseases. Paclitaxel **(1)** is widely used in cancer treatments, morphine **(2)** is administered for pain management, cardiac aspirin **(3)** is used as a blood thinner, ganciclovir **(4)** is used as an antiviral and digoxin **(5)** is used to treat cardiac arrhythmias. This illustrates the chemical diversity and complexity of natural products found in plants that are often synthetically unobtainable.

Despite the past successes of natural products, the incompatibility and inconsistency of crude plant extracts in modern drug discovery screening was not appealing to most pharmaceutical corporations. The incompatibility is mainly due to the chemical complexity and presence of interfering compounds in crude plant extracts that has discouraged the use of natural products in drug discovery screening[11]. Pharmaceutical corporations have turned to screening large synthetic drug libraries and combinatorial drug formulations as they've shown to be relatively easier, reproducible and slightly more successful. While such difficulties exist when working

2

with crude natural product extracts, the novelty and chemical diversity is still superior to the simple and restrictive scaffolding of synthetic compounds.

1.2   South Africa's biodiversity and traditional medicinal practises

South Africa has been recognised as one of 17 megadiverse countries in the world. A country is identified as a megadiverse country if it has at minimum 5 000 endemic plant species and a marine ecosystem within its borders[12]. South Africa is one of the smaller megadiverse countries with an approximate 1.2 million km^2 of landmass and 1.1 million km^2 of surrounding ocean. South Africa is also globally ranked within the top ten nations for the largest plant species variety and globally ranked third for marine species endemism. Additionally, three of the world's 36 biodiversity hotspots reside within South Africa[13]. For a realm to be classified as a biodiversity hotspot the following criteria must be met: 1) the region must contain at minimum 1 500 endemic vascular plant species and 2) it must have 30 % of the natural abundance remaining[14]. The three hotspots identified in South Africa is the Succulent Karoo biome, Cape Floristic Region and lastly the Maputaland-Pondoland-Albany region.

Both South Africa's landmass and surrounding oceans contain an approximate two-thirds of the world's biodiversity. In 2018, it was estimated that South Africa contained over 67 000 animal species and an estimated 20 401 plant species. Of all the identified animal and plant species worldwide, approximately 2 % of amphibians, 7 % of birds, 1 % of freshwater fishes, 5 % of mammals, 7 % vascular plants and 4 % of reptile species are found in South Africa[13]. This is possible as the diverse ranges of bioclimatic, oceanographic and geological realms in South Africa have allowed high species diversity and endemism to occur. South Africa's terrestrial realms can be categorised into nine biomes that encompass 458 national vegetation types, of which 80 % are endemic[13]. The different national vegetation types are found within the following nine biomes: Albany thicket, Desert, Forest, Fynbos, Grassland, Indian Ocean Coastal Belt, Succulent Karoo, Nama-Karoo and Savanna. South Africa's biodiversity has a major presence in the country's economy, society and traditional healthcare. In South Africa, there is an estimate 418 000 biodiversity-related jobs with a tourism industry annually worth over R30 billion. Other than economic value, a significant portion of rural communities still depend on harvesting edible plants, fish and insects for nourishment as well as the use of medicinal plants for traditional healthcare. Additionally, the biodiversity has been a major influence in the development of cultural and spiritual practises forming part of South Africa's national identity and heritage[13].

South Africa is well known for its rich multicultural heritage and impressive traditional knowledge on medicinal plants. Animals but mostly plants are regularly used in traditional

medicinal practises and cultural rituals. Of the estimated 20 000 plant species in South Africa, only 2 000 indigenous plant species are used in medicinal practises[13]. It is reported that 656 medicinal plant species are overused and has resulted in 56 threatened plant species due to unsustainable harvesting. In South Africa, animals and medicinal plants are fundamental in the work of over 200 000 traditional health practitioners and in the informal traditional medicine industry valued annually at R18 billion. In 2017, 60 % of the traditional health practitioners in the Limpopo province reported difficulty in accessing desired plant materials due to unsustainable harvesting[13]. This raises the concern about the sustainability of the informal traditional medicine industry and the threat to South Africa's biodiversity. The vast diversity of indigenous plant species and the rich traditional cultures that have utilised the native plants in medicinal practises, South Africa's flora is one of the world's richest untapped sources for potential cancer chemotherapeutic compounds.

1.3 The creation of a South African natural product library

For thousands of years biological sources have been used around the world in traditional medicinal practises. Since 1981, over 800 FDA approved drugs have been isolated or derived from natural products[10]. With biological screening becoming more target specific and high-throughput, the demand for novel chemical diversity has increased while the complexity of the screening samples have decreased[15]. Natural products can keep up with the required novelty and chemical diversity however the complexity of natural product extracts has become incompatible with modern screening. South Africa is a biologically megadiverse country with an immense indigenous knowledge of medicinal plant that can offer guided selection of medicinal plants that could offer novel natural products. Most of South Africa's medicinal plants have not been chemically analysed or screened against prevalent diseases suggesting that the biodiversity is an untapped source of novel therapeutic agents. The most significant attempt was made by Council for Scientific and Industrial Research (CSIR) where most of South Africa's plant biodiversity was collected, prepared, extracted and screened *in vitro* for anti-cancer activity against human cancer cell lines[16]. However, the extracted material was not prepared for high-throughput screening (HTS) campaigns as the technologies for standardisation, rapid compound isolation and structure elucidation were not available. The CSIR created a plant depository containing over 10 000 dry plant materials and over 30 000 plant extracts which represented an estimated 7 000 indigenous South African plant species. The creation of a South African natural product library ready for HTS will enable South Africa to conduct world leading medical research.

1.4   Cancer and modern cancer treatments

1.4.1   Cancer and the causes

Cancer is a noncommunicable disease where genetic mutations result in the accelerated proliferation of abnormal and unregulated cells. Genetic mutations are often caused by genetic disorders or exposure to carcinogenic compounds. In general, genetic mutations or damage to the proto-oncogenes within healthy cells creates abnormalities in the cell-division cycle causing uncharacteristic proliferation[17]. Proto-oncogenes are responsible for regulated cell division and growth under normal conditions but become oncogenes after genetic mutation or damage. Oncogenes characteristically lack tumour suppressor gene regulators which result in uncontrolled and accelerated cell division[18]. Other than genetic disorders and exposure to carcinogenic compounds, environmental factors can directly or indirectly influence the nuclei of healthy cells resulting in genetic mutations[19]. Bacteria, radiation and viruses only cause an estimated 7 % of all reported cancer types[20]. The term cancer refers to over 270 variants of unregulated cell proliferation occurring in different cell types[21]. Unfortunately, at the cellular level cancer is a variety disease making the diagnosis and treatment especially challenging[22,23]. In men, the highest percentages of cancer types occur in the prostate, lung and bronchus. In women, cancer prevalence is the highest in breast, lung and bronchus. Prostate and breast cancer is reported as the major cancer type in men and women, respectively[24]. Breast cancer is the most prevalent cancer type worldwide with an estimated 2.26 million new cases reported in 2020. Similarly in 2020, lung and colorectum cancer were the second and third most prevalent cancer types in with an estimated 2.2 million and 1.9 million new cases reported as seen in Figure 1-2.

Estimated number of new cases in 2020, World, both sexes, all ages

Breast
2 261 419 (11.7%)

Lung
2 206 771 (11.4%)

Colorectum
1 931 590 (10%)

Prostate
1 414 259 (7.3%)

Stomach
1 089 103 (5.6%)

Liver
905 677 (4.7%)

Cervix uteri
604 127 (3.1%)

Other cancers
8 879 843 (46%)

Data source:GLOBOCAN 2020
Graph production: Global Cancer Observatory (http://gco.iarc.fr/)
© International Agency for Research on Cancer 2023

Total : 19 292 789

International Agency for Research on Cancer
World Health Organization

Figure 1-2 The estimated number of new cancer incidents worldwide 2020[25].

1.4.2　Current cancer treatments and the urgency for new treatments

Despite the major advances in cancer treatments, each case is treated on an individual basis. Cancer treatment is still a reductionist approach as the same cancer type may respond differently to the recommended treatments[26]. Of the 809 drug entities approved by the FDA, only 156 (19 %) were approved for use in cancer treatments[10]. This underlines the urgency for the further development of current or new chemotherapeutic drugs. A few common approaches in cancer treatments are excisional surgery, chemotherapy, radiotherapy and immunotherapy.

1.4.2.1　Excisional surgery

Surgical removal is one of the most common treatments for most solid cancers. However, the surgical removal of solid tumours can only be considered if the procedure will not further endanger the patient. Even though the surgical removal of primary or metastatic tumours have shown to save or prolong the patient's life, it may still induce or accelerate the tumour's recurrence[27]. Tumour recurrence is mainly caused by the shedding of tumour cells into the blood and lymphatic system as the tumour and surrounding tissues are damaged during removal[28]. Additionally, simply by handling the tumour may lead to a 10-fold increase in circulating tumour cells[29]. Excisional surgery is often paired with perioperative chemotherapy as it has shown a decrease in metastasis and recurrence caused by tumour removal. Other combinational therapeutic options that decrease the risk of recurrence after surgery include a treatment of antiendotoxin agents or even immunotherapy[30].

1.4.2.2　Chemotherapy approach

Chemotherapy treatment uses cytotoxic compounds to prevent further growth and division of cancer cells by effectively killing them. The use of cytotoxic compounds in cancer treatment was first considered after mustard gas was reported to kill lymphatic tissues and bone marrow[31]. Since cancer cells grow at an accelerated rate when compared to normal cells, the cytotoxic drugs can inhibit the growth or kill cancerous cells more rapidly and effectively than the surrounding healthy cells. Shown below in Figure 1-3 are a few of the FDA approved anti-cancer drugs since 1981:

6
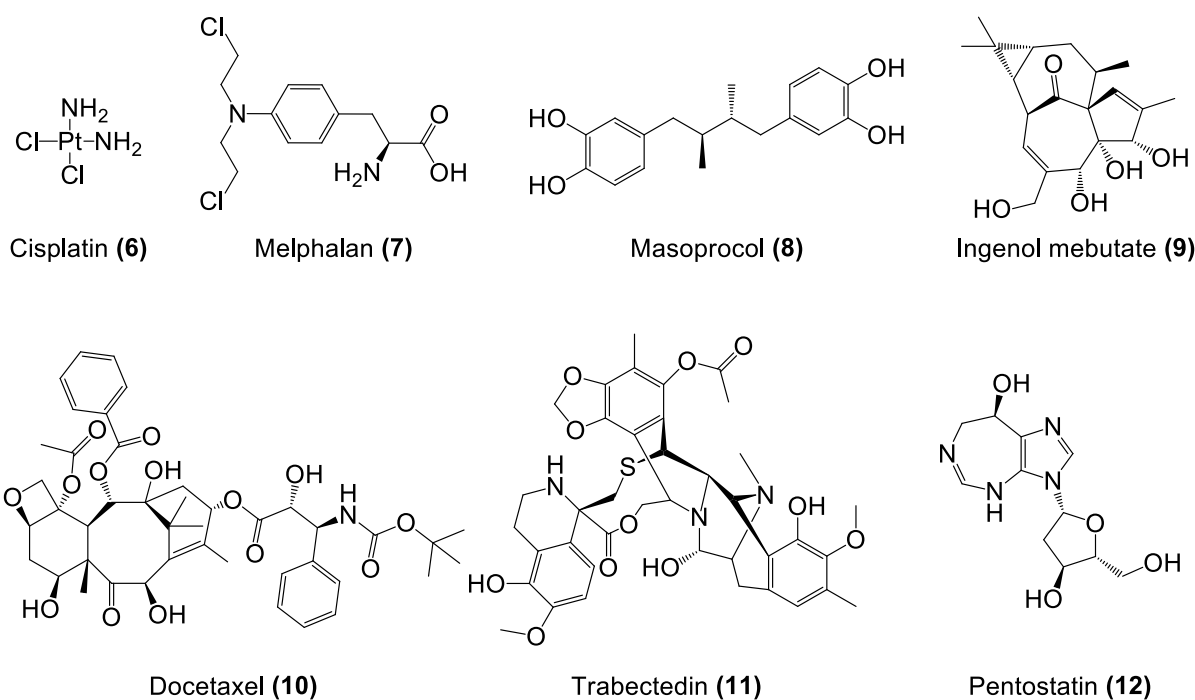
Figure 1-3 Shown above are the chemical structures of the following FDA approved drugs used in chemotherapy: cisplatin **(6)**, melphalan **(7)**, masoprocol **(8)**, ingenol mebutate **(9)**, docetaxel **(10)**, trabectedin **(11)** and pentostatin **(12)**.

Paclitaxel **(1)**, cisplatin **(6)**, melphalan **(7)**, masoprocol **(8)**, ingenol mebutate **(9)**, docetaxel **(10)**, trabectedin **(11)** and pentostatin **(12)** are currently used to treatment different cancer types. Only compounds **(1), (8), (9)** and **(10)** are natural products isolated from higher plants. Compounds **(11)** and **(12)** were natural products isolated from a marine and bacterium source, respectively. This illustrates the chemical diversity and novelty of the natural products that have been approved by the FDA as therapeutic compounds.

However, it is not uncommon for the secondary metabolites that have complex scaffolds such as paclitaxel **(1)**, to be synthesised via semisynthetic or biotechnological routes[15]. Paclitaxel **(1)** is an anti-microtubule agent that is used to treat ovarian, oesophageal, breast and lung cancer[32]. Paclitaxel **(1)** was first isolated in 1979 from the bark of *Taxus brevifolia* but due its low natural abundance, it is commercially prepared from a more abundant precursor isolated from *Taxus baccata*[33].

1.4.2.3   Radiotherapy approach

Ionised radiation is used to cause extensive damage to the genetic material within cancerous cells resulting in cell death[34]. Only cancerous cells are targeted and exposed to high doses of radiation however the genetic material of both the cancerous cells and the surrounding healthy

7

cells are damaged. Usually, healthy cells are able to repair their genetic material and retain their normal function faster and more efficiently than cancerous cells resulting in the differential killing of cancer cells[35]. Radiation therapy is also used as an effective means of relieving patients from symptoms caused by cancer. Shown in Table 1 are the cancer types treatable by radiotherapy alone and in combination therapy with other treatments such as surgery, chemotherapy or immunotherapy[36].

Table 1 The cancer types treatable with radiotherapy alone and in combination with other treatments.

Treatable cancers with radiotherapy alone	Treatable cancers with radiotherapy in combination with other cancer treatments
Cervix carcinomas	Local advanced cervix carcinomas
Head and neck carcinomas	Locally advanced head and neck carcinomas
Lymphomas	Advanced lymphomas
Non-small cell lung carcinomas	Locally advanced lung carcinomas
Prostate carcinomas	Endometrial carcinomas
Skin cancers	Soft tissue sarcomas
	CNS tumours
	Bladder carcinomas
	Breast carcinomas
	Paediatric tumours
	Rectal and anal carcinomas

It is evident that using radiotherapy in combination with other cancer treatments diversifies the application of the treatment to even the most aggressive cancer types.

1.4.2.4 Immunotherapy approach

Cancers are notorious for evading immune detection by suppressing the function of T lymphocytes (T-cells) resulting in a suppressed antitumor immune response. T-cells form part of the immune system that fights off infections and diseases like cancer. Cancer immunotherapy is aimed at reactivating the body's antitumor immune response by overcoming the evading tactics of cancer cells. Immunotherapy approaches allow the immune system to recognise and attack cancer cells. Current immunotherapies currently focus on the applications of immune checkpoint inhibitors (ICI's) i.e., monoclonal antibodies and the chimeric antigen receptor (CAR) T-cells in adoptive cell therapy[37]. To overcome the cancer cell mediated T-cell inhibition, ICI's prevent the immune checkpoint proteins on the T-cells from binding to the cancerous cells thus reactivating normal T-cell function and killing the cancerous cells[38]. The FDA has approved the use of ICI's like ipilimumab, pembrolizumab and

8

nivolumab in the treatment of cancer types like lung cancer (small and non-small cell), melanoma, gastric cancer, head and neck squamous cell carcinoma, Hodgkin's lymphoma, ovarian cancer and renal cancer[37]. Another immunotherapy approach is adoptive cell therapy where the patient's T-cells are biochemically modified (*ex vivo*) to elicit specific antitumor responsiveness. Such an example is the modification of the CAR T-cells that are used to recognise selected antigens associated with a specific tumour. Currently, modified CAR T-cells are used to treat haematological tumours but ongoing investigations indicate potential application in solid tumour treatment[39].

1.5   Problem statement and justification

To date there is no platform that has allowed access to a trusted collection of South Africa's large and unique biodiversity for drug discovery research. South Africa's biodiversity contains a large number of medicinal plant species however a modern drug-discovery platform has not been developed. As modern biological screening protocols have developed towards being more target-specific, more sensitive and higher throughput, crude natural product extracts have become incompatible. The decline in the utility of crude natural product extracts resulted in the creation of semi-purified or fractionated natural product extract libraries[2]. The use of natural product libraries that have standardised both the crude extract and respective fractions in HTS ready formats have shown improved performance during biological screening and in post-screening investigations like bioactive compound isolation and chemical characterisation. Fractionated crude extracts are significantly less complex than crude natural product extracts that can contain well over hundreds of secondary metabolites. The reduction in complexity of an active sample simplifies the dereplication process (identifying known and/or interfering compounds) thus accelerating the isolation and structure elucidation of targeted bioactive compounds[2]. Additionally, standardised natural product libraries are environmentally sustainable as only a minimal amount of biological material is required to create standardised samples in a format that is chemically stable for long-term storage.

As South Africa's biological diversity is diminishing due to unsustainable harvesting and climate change, the prospect of creating an all-inclusive South African natural product library diminishes[13]. Since natural products are a readily available source of chemically diverse and complex novel therapeutic compounds, South Africa's biodiversity has the potential of being a major advantage in medical research. In 2020, it was estimated that South Africa had over 108 000 new cancer cases and close to 60 000 cancer related deaths[40]. Additionally, it was estimated that close to 10 million individuals worldwide lost their lives from cancer in 2020 emphasising the need for new, potentially more efficient cancer treatments.

9

In response, this project intends to develop a trusted access South African natural product library ready for HTS and to evaluate its constituents as potential anti-cancer agents. This will be accomplished by adopting the CSIR plant repository and integrating the current technologies used in natural product drug-lead discovery with the intellectual guidance from world leading experts. The platform will also serve to accelerate the identification of potential drug leads thus improving the efficiency of drug discovery efforts by the inclusion of larger numbers of natural product scaffolds. This approach has already been adopted by many countries across the world e.g., the US National Cancer Institute's (NCI) and the Griffith Institute for Drug Discovery in Australia[5,41].

1.6   Aims and objectives

The aims of this study were:

a) The development of a South African natural product library platform that is ready for HTS against numerous diseases.

b) The evaluation of a subset of the natural product library as potential anti-cancer agents.

c) The investigation of a "hit" to rapidly isolate and characterise a biologically active compound using state of the art hyphenated analytical techniques.

The overall objectives of the study were:

- To develop high-throughput plant material standardisation methods in an HTS ready format for the South African natural product library platform.

- Validate the high-throughput standardisation methods against a cancer cell line in an NCI-60 1-dose-assay.

- Plant selection from the material available in the plant repository using a preferential scoring system.

- High-throughput standardisation of the plant materials collected.

- *In vitro* screening of the standardised extracts and fractions against different cancer cell lines.

- Selection of a "hit" from the *in vitro* screening data for further investigation.

- Hit investigation and identification of the bioactive compound using analytical instruments such as UPLC-PDA-HRMS and online chemical databases like ChemSpider, PubChem, Reaxys and the Dictionary of Natural Products.

- Mass-directed isolation and structural confirmation of the bioactive compound using instruments like HPLC-PDA-MS and NMR.

- *In vitro* dose-response study of the isolated bioactive compound for IC_{50} determination.

Chapter 2 describes the following:

- The creation of high-throughput standardisation methods for extraction, fractionation and standardisation of plant materials.
- The validation of the developed high-throughput standardisation methods using a positive and negative method control against the lung cancer cell line A549 in an NCI-60 1-dose-assay.

Chapter 3 describes the following:

- A literature survey on the medicinal plant species used in South Africa.
- The creation of a preferential scoring system.
- Scoring and selection of the most preferential medicinal plant species for screening against cancer.
- High-throughput standardisation of the selected plant species.
- *In vitro* screening of the standardised samples against different cancer cell lines using different assays.
- The selection of a "hit" for further investigation.

Chapter 4 describes the following:

- The UPLC-PDA-HRMS analysis of the "hit" fraction from *Mikania natalensis* for the identification of the bioactive compound using online databases like ChemSpider, PubChem, Reaxys and the Dictionary of Natural Products.
- The mass-directed isolation of the identified bioactive compound in *M. natalensis* leaf extract using HPLC-PDA-MS techniques.
- The structural confirmation of the isolated bioactive compound using ^{1}H and ^{13}C NMR in combination with ACDLabs™ Spectrus Processor.
- The IC_{50} determination of the isolated bioactive compound using a dose-response *in vitro* assay against the cancer cell lines MCF7 and Caco2.
- The X-ray diffraction analysis of a single crystal from the upscaled fractionation of *M. natalensis* leaf extract.

Chapter 5 provides a general conclusion of the study.

1.7   References

1.   Petrovska, B. B. Historical review of medicinal plants' usage. *Pharmacognosy reviews* **6**, 1–5 (2012).
2.   Wilson, B. A. P., Thornburg, C. C., Henrich, C. J., Grkovic, T. & O'Keefe, B. R. Creating and screening natural product libraries. *Natural product reports* **37**, 893–918 (2020).
3.   Atanasov, A. G., Zotchev, S. B., Dirsch, V. M., International Natural Product Sciences Taskforce & Supuran, C. T. Natural products in drug discovery: advances and opportunities. *Nature reviews. Drug discovery* **20**, 200–216 (2021).

4. Nwokeji Paul Anulika, Enodiana Osamiabe Ignatius, Ezenweani Sunday Raymond, Osaro-Itota Osasere & Akatah Hilda Abiola. The Chemistry Of Natural Product: Plant Secondary Metabolites. *International Journal of Technology Enhancements and Emerging Engineering Research* **4**, 1–9 (2016).

5. Thornburg, C. C. *et al.* NCI Program for Natural Product Discovery: A Publicly-Accessible Library of Natural Product Fractions for High-Throughput Screening. *ACS chemical biology* **13**, 2484–2497 (2018).

6. Guerriero, G. *et al.* Production of Plant Secondary Metabolites: Examples, Tips and Suggestions for Biotechnologists. *Genes* **9**, 309 (2018).

7. Bribi, N. Pharmacological activity of Alkaloids: A Review. *Asian Journal ofBotany* **1**, 1–6 (2018).

8. Tungmunnithum, D., Thongboonyou, A., Pholboon, A. & Yangsabai, A. Flavonoids and Other Phenolic Compounds from Medicinal Plants for Pharmaceutical and Medical Aspects: An Overview. *Medicines* **5**, 93 (2018).

9. Bergman, M. E., Davis, B. & Phillips, M. A. Medically Useful Plant Terpenoids: Biosynthesis, Occurrence, and Mechanism of Action. *Molecules (Basel, Switzerland)* **24**, 1–23 (2019).

10. Newman, D. J. & Cragg, G. M. Natural Products as Sources of New Drugs over the Nearly Four Decades from 01/1981 to 09/2019. *Journal of natural products* **83**, 770–803 (2020).

11. Zhang, L. & Demain, A. L. *Natural Products. Natural Products: Drug Discovery and Therapeutic Medicine* (Humana Press, 2005). doi:10.1007/978-1-59259-976-9.

12. Mittermeier, R. A. & Mittermeier, C. G. *Megadiversity: Earth's Biologically Wealthiest Nations.* (1997).

13. Skowno, A. L. *et al. National Biodiversity Assessment 2018: The status of South Africa's ecosystems and biodiversity. Synthesis Report. South African National Biodiversity Institute, an entity of the Department of Environment, Forestry and Fisheries. South African National Biodiversity Institute* (2019).

14. Myers, N., Mittermeier, R. A., Mittermeier, C. G., da Fonseca, G. A. B. & Kent, J. Biodiversity hotspots for conservation priorities. *Nature* **403**, 853–858 (2000).

15. Filho, V. C. *Natural Products as Source of Molecules with Therapeutic Potential. Natural Products as Source of Molecules with Therapeutic Potential: Research and Development, Challenges and Perspectives* (Springer International Publishing, 2018). doi:10.1007/978-3-030-00545-0.

16. Khorombi, T. *et al.* Investigation of South African plants for anti cancer properties. (2006).

17. Seto, M., Honma, K. & Nakagawa, M. Diversity of genome profiles in malignant

12

lymphoma. *Cancer science* **101**, 573–8 (2010).

18. Matlashewski, G. *et al.* Isolation and characterization of a human p53 cDNA clone: expression of the human p53 gene. *The EMBO Journal* **3**, 3257–3262 (1984).

19. Poon, S., McPherson, J. R., Tan, P., Teh, B. & Rozen, S. G. Mutation signatures of carcinogen exposure: genome-wide detection and new opportunities for cancer prevention. *Genome Medicine* **6**, 24 (2014).

20. Parkin, D. M. The global health burden of infection-associated cancers in the year 2002. *International Journal of Cancer* **118**, 3030–3044 (2006).

21. Hassanpour, S. H. & Dehghani, M. Review of cancer from perspective of molecular. *Journal of Cancer Research and Practice* **4**, 127–129 (2017).

22. Meacham, C. E. & Morrison, S. J. Tumour heterogeneity and cancer cell plasticity. *Nature* **501**, 328–37 (2013).

23. Fisher, R., Pusztai, L. & Swanton, C. Cancer heterogeneity: implications for targeted therapeutics. *British journal of cancer* **108**, 479–85 (2013).

24. Siegel, R. L., Miller, K. D. & Jemal, A. Cancer statistics, 2016. *CA: a cancer journal for clinicians* **66**, 7–30 (2016).

25. The Global Cancer Observatory. Estimated number of new cases in 2020. *Word Health Organization* vol. 291 1 http://gco.iarc.fr/today (2020).

26. Zugazagoitia, J. *et al.* Current Challenges in Cancer Treatment. *Clinical therapeutics* **38**, 1551–66 (2016).

27. Tohme, S., Simmons, R. L. & Tsung, A. Surgery for cancer: A trigger for metastases. *Cancer Research* **77**, 1548–1552 (2017).

28. Yamaguchi, K., Takagi, Y., Aoki, S., Futamura, M. & Saji, S. Significant Detection of Circulating Cancer Cells in the Blood by Reverse Transcriptase–Polymerase Chain Reaction During Colorectal Cancer Resection. *Annals of Surgery* **232**, 58–65 (2000).

29. Saidel, G. M. Quantitative Relationships of Intravascular Tumor Cells, Tumor Vessels, and Pulmonary Metastases following Tumor Implantation. *Cancer Research* **34**, 997–1004 (1974).

30. Coffey, J. C. *et al.* Excisional surgery for cancer cure: Therapy at a cost. *Lancet Oncology* **4**, 760–768 (2003).

31. Anand, U. *et al.* Cancer chemotherapy and beyond: Current status, drug candidates, associated risks and progress in targeted therapeutics. *Genes & Diseases* (2022) doi:10.1016/j.gendis.2022.02.007.

32. Tonissi, F. *et al.* The effect of paclitaxel and nab-paclitaxel in combination with anti-angiogenic therapy in breast cancer cell lines. *Investigational new drugs* **33**, 801–9 (2015).

33. Baloglu, E. & Kingston, D. G. I. A new semisynthesis of paclitaxel from baccatin III.

Journal of natural products **62**, 1068–71 (1999).

34.   Jackson, S. P. & Bartek, J. The DNA-damage response in human biology and disease. *Nature* **461**, 1071–1078 (2009).

35.   Begg, A. C., Stewart, F. A. & Vens, C. Strategies to improve radiotherapy with targeted drugs. *Nature Reviews Cancer* **11**, 239–253 (2011).

36.   Baskar, R., Lee, K. A., Yeo, R. & Yeoh, K. W. Cancer and radiation therapy: Current advances and future directions. *International Journal of Medical Sciences* **9**, 193–199 (2012).

37.   Kennedy, L. B. & Salama, A. K. S. A review of cancer immunotherapy toxicity. *CA: a cancer journal for clinicians* **70**, 86–104 (2020).

38.   Pardoll, D. M. The blockade of immune checkpoints in cancer immunotherapy. *Nature reviews. Cancer* **12**, 252–64 (2012).

39.   D'Aloia, M. M., Zizzari, I. G., Sacchetti, B., Pierelli, L. & Alimandi, M. CAR-T cells: the long and winding road to solid tumors. *Cell death & disease* **9**, 282 (2018).

40.   GLOBOCAN, T. G. C. O. *Population Fact Sheets - South Africa.* vol. 491 https://gco.iarc.fr/ (2020).

41.   The Griffith Institute for Drug Discovery. NatureBank. https://www.griffith.edu.au/institute-drug-discovery/unique-resources/naturebank.

Chapter 2: Creation and validation of the South African natural product library

2.1   Introduction

The conventional techniques used in the preparation and screening of natural products are often tedious, costly, and time consuming. Additionally, the isolation of bioactive compounds from hits are even more challenging. A bioactive compound is a compound that exhibits biological or pharmacological activity and has potential therapeutic applications. Often in natural product chemistry, the crude extract of a plant, marine or bacterial organism is biologically screened to determine if one or more bioactive compounds are present in the crude extract. Generally, the bioactive crude extracts i.e., "hits" are further investigated through an iterating process of rescreening and purification until the compound that is responsible for the bioactivity has been identified. This is known as a bioassay-guided approach that requires extensive amounts of biological material, consumables and time to thoroughly investigate a single bioactive compound from a hit. The bioassay-guided approach is unable to keep up with the fast turnaround demand and tight deadlines expected in HTS programs. In the past the assay guided approach has been successful but has become incompatible with modern drug research deadlines. In addition, the loss of bioactivity during purification procedures and the re-isolation of previously reported compounds are not unusual[1].

In an effort to overcome the many challenges of natural product-based drug discovery, new innovative approaches and technologies have been developed. One highly successful approach is the creation of a large, biologically diverse natural product library that contains standardised crude extracts ready for HTS[2]. The creation of natural product libraries that are compatible with HTS procedures are used throughout the pharmaceutical industry and recently an increased use in academic institutions[3]. HTS procedures accelerate the hit rate in natural product-based drug discovery in a large-scale and cost-effective manner. At the University of Basel, Division of Pharmaceutical Biology, Switzerland, an academic natural product library with a HPLC-based profiling approach has been created by Professor Matthias Hamburger. The platform is HTS compliant by standardising plant extracts in dimethylsulfoxide (DMSO) at 10 mg/mL in a 96-well format. The plant material is extracted using a pressurised accelerated solvent extractor and dried using a parallel vortex evaporator. The dried plant extracts are weighed into individual glass vials and placed onto the bed of an automated liquid handler. The automated liquid handler prepares crude plant extracts in DMSO at 10 mg/mL. The standardised extracts are automatically transferred to 96-well storage plates and stored in 1.8 mL in racked microtubes. The platform uses the natural

product crude extract library in combination with HPLC-based activity profiling for the discovery of new bioactive scaffolds in natural product extracts. This approach couples the high-performance separation and the chemical information recorded, e.g., light absorption wavelengths and mass spectral (MS), with the biological activity obtained from screening. The platform is highly versatile and facilitates the prioritisation of compounds of interest for targeted purification[1]. As HTS procedures have become more automated and high-throughput, the requirement for standardised semi-purified fractions has increased as crude natural product extracts are no longer compatible[3]. The demand for standardised semi-purified samples resulted in the development of preparative methods e.g., extraction, fractionation and standardisation that accommodate extensive ranges of biologically and chemically unique crude extracts. In most modern natural product library platforms, the sample preparative methods are completed using automated robotic instruments and automated liquid handlers. The integration of automated robotic instruments and liquid handlers in the preparative methods significantly increases the number of semi-purified samples produced in the least amount of time.

Many aspects must be considered at each stage of sample preparation for standardisation. Since the conventional extraction methods such as Soxhlet extraction, laborious sequential extractions or supercritical fluid extractions (SFE) are either destructive, timely and/or inadequate for high-throughput extraction, a different extraction method must be considered[7]. The selected extraction method must be inexpensive and time effective as well as capable of high-throughput extraction for a range of chemically diverse biological materials. Most importantly, the selected extraction method must produce quality crude extracts that are an unchanged and undegraded representation of all the compounds found within the biological material. It was reported that plant materials (after being dried and ground) soaked overnight in an organic solution produced a quality crude extract[4]. All these aspects are taken into consideration when selecting an adequate extraction method. Just like the extraction method, the method developed for reducing the complexity of crude natural product extracts must accommodate a chemically diverse range of unique crude extracts. Conventional separation methods like packed silica columns, high-performance liquid chromatograph (HPLC), or supercritical fluid chromatograph (SFC) are deemed low-throughput as well as too costly for their use. Often such chromatographic techniques require large quantities of crude extract which require additional sample clean-up before use. For the reasons previously mentioned, the use of disposable solid-phase extraction (SPE) cartridges were chosen in natural product library platforms. Additionally, SPE cartridges are more accommodating to the chemical diversity of crude extracts e.g., polarity of compounds and allow for the development of clean-up and concentration elution methods[5]. The elution methods used by the SPE cartridges are

often optimised to remove undesirable compounds such as polyphenolics while concentrating drug-like compounds in other fractions[3]. As a result, certain semi-purified fractions exhibit better bioactivity than their respective crude extracts during screening. Finally, the standardisation format and storage conditions of the crude extracts and respective fractions must be carefully considered. The standardised crude extracts and fractions should be compatible with HTS processes but in a suitable form for long-term cold storage that retains sample integrity. Only a few academic institutions around the world have successfully created natural product libraries with standardised extracts and fraction and even a few incorporating internal HTS to their workflow.

2.1.1 The significant academic natural product libraries of standardised crude extracts and fractions

Located in Australia, The Griffith Institute for Drug Discovery (GRIDD) has created the GRIDD's NatureBank drug discovery platform. The NatureBank platform contains standardised biological samples of Australian plants, fungi and marine invertebrates that are compatible with HTS applications. The platform represents Australia's unique biodiversity and has archived over 30 000 biota with the associated novel chemical diversity. The NatureBank platform is made up of a crude extract library that contains around 20 000 standardised crude extracts and a fractionated library that contains an estimated 112 000 standardised fractions[6]. GRIDD's aim is to utilise Australia's unique biodiversity to drive the discovery and development of revolutionary novel treatments to improve human health.

In January 2019, the NCI Program for Natural Product Discovery (NCI NPNPD) was launched in Washington DC, the United States of America[7]. To date, the NCI NPNPD collection remains one of the most extensive natural product collection worldwide with over 500 000 standardised fractions available to the public free of charge[8]. The NCI NPNPD aims at improving the technologies and techniques used for natural product-based drug discovery and has made their natural product prefractionation library creation methods available to the public. The NCI NPNPD platform uses highly-automated SPE techniques to fractionate crude natural product extracts into seven fractions of decreasing polarity that are then standardised at 10 mg/mL in DMSO and stored in 384-well plates. The platform creates plant extracts by allowing the material to soak for 24 hours in a (1:1) methanol (MeOH)/dichloromethane (DCM) solution[4]. The dried crude plant extracts are weighed out and dissolved in an organic solution to be adsorbed onto dental cotton rolls. The extract loaded cotton rolls are then placed inside an empty SPE cartridge and using a robotic liquid handler each plant extract is fractionated on a C8 SPE cartridge into seven fractions of decreasing polarity. The automated and high-throughput fractionation methodology developed produces semi-purified fractions of crude

17

extracts with an even distribution of metabolites across the fractions. Additionally, the fractionation method concentrated the minor bioactive compounds while simultaneously removing the unwanted nuisance compounds. The fractions are dried using high-performance centrifugal solvent evaporators and the dried masses of each fraction are recorded. The dried contents of each extract and fraction are standardised in DMSO and placed in a 384-well plate for cold storage[5].

Not only does the fractionation of natural product extracts improve the performance of HTS but also post-HTS activities which facilitate the rapid identification and isolation of bioactive compounds. Traditionally, the task of dereplication was often challenging and unsuccessful due to the complexity of active crude extracts. The fractionation of plant crude extracts decreased the complexity of the crude extract across numerous fractions which eased the identification of known active or nuisance compounds i.e., dereplication from bioactive samples. The incorporating of a semi-purification step before the dereplication decreases the likelihood of re-isolating identified or nuisance compounds thus improving post-HTS activities.

2.1.2   The creation of a South African natural product library

By the late 1990's, the CSIR undertook a systematic study of creating a natural product collection of South African plant extracts and evaluated the collection for potential anti-cancer activity[9]. The project resulted in the production of over 30 000 plant extracts that represented approximately 7 000 plant species collected across South Africa. The CSIR screened a total of 7 500 plant extracts *in vitro* against an internal anti-cancer screening panel of the following three human cell lines: breast-MCF7, renal-TK10 and melanoma-UACC62[9]. However, the replication and purification of the hits were more challenging than expected and the CSIR abandoned the internal screening efforts. The remaining repository of plant material and plant extracts was subsequently transferred to the University of Pretoria which is being used to build the first South African natural product library of plant extracts and semi-purified fractions. With South Africa being one of 17 megadiverse countries in the world, this is the first initiative to create a trusted South African natural product library for research purposes. The project will adopt and implement the validated plant preparative methods developed by the NCI NPNPD for the creation of a South African natural product library containing both standardised plant extracts and fractions in a HTS compatible format.

2.1.3   The validation of the South African natural product library's standardised plant preparative methods using the NCI-60 anti-cancer assay

It is critical to validate the plant preparative methods developed to ensure that bioactivity is retained throughout the preparation. The biological screening of a positive and negative

method control standardised using the South African natural product library plant preparative methods will ensure that sample integrity is not compromised, and bioactivity is not lost.

In the late 1980's, the NCI developed an anti-cancer drug screening panel i.e., the NCI-60 of 60 human tumour cell lines. The NCI-60 screening panel was used to replace the use of transplantable animal carcinomas to human solid tumours in past anti-cancer drug screens[10]. The NCI-60 screening panel measured the cell growth of 60 different human tumour cell lines that represent the following nine distinct tumour types: breast, colon, central nervous system, leukaemia, lung, melanoma, ovarian, prostate and renal. The NCI-60 screening panel is one of the oldest *in vitro* biological assays used to identified small molecules exhibiting cell proliferative inhibition, cytotoxicity and cytostatic activity against human cancer cell lines.

The NCI-60 selected screening methodology is comprised of two screening steps. The initial step screens all the natural products crude extracts at a high single dosage ranging from 15 to 150 µg/mL against the 60 different cancer cell lines. The second step selects the samples that meet the pre-determined threshold inhibition criteria for rescreening against the same panel of cancer cell lines but at 5 different concentrations. The initial screening selects only the samples that are worth further investigation since high-throughput biological screening is extremely costly and time consuming. Re-screening the selected samples at 5 different concentrations allows for dose-response relationships to be calculated for each extract against each cell line. A dose response relationship/cure plots the response of the cells, generally inhibition or cell viability, against a decreasing screening concentration of the sample. From this relationship, the concentrations at which the samples are toxic e.g., LD_{50}, exhibit a beneficial response e.g., ED_{50} or inactive can be calculated. At the time the NCI-60 was developed, tritiated thymidine incorporation assays were considered for use in the assay as it was widely used for growth inhibition studies but was too costly for large scale screening[10]. Alternatively, the 3-(4,5-dimethylthiazol-2yl)-2,5-diphenyl tetrazolium bromide (MTT **(13)**) assay was considered as it is a simple and inexpensive colorimetric assay. The MTT **(13)** assay is both a sensitive and quantitative technique that is primarily used in small laboratory projects to measure cell viability i.e., proliferation of cells[14]. As shown in Figure 2-1, the fundamental principal relies on the metabolism of viable cells containing cellular mitochondrial oxidoreductase enzymes to reduce the water-soluble yellow tetrazolium to an insoluble purple formazan product. The insoluble purple formazan product then accumulates inside living cell as it cannot cross the cell membrane due low permeability. During analysis, the insoluble purple formazan product is solubilised using DMSO and the optical density (OD) absorption is measured spectrophotometrically at 540 nm and quantified[14]. Therefore, the amount of insoluble purple formazan product present is directly proportional to the number of living cells.

MTT **(13)**   MTT-Formazan **(14)**
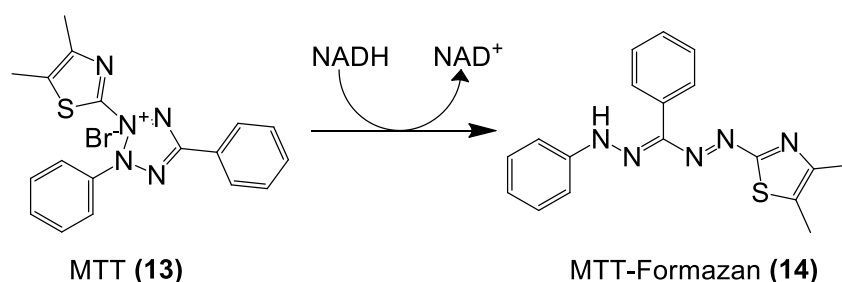
Figure 2-1 Structures of the MTT **(13)** dye and MTT-Formazan **(14)** product after reduction by the enzyme mitochondrial oxidoreductase

The NCI-60 eventually adopted the sulphorhodamine B (SRB **(15)**) assay as it was more amendable for large scale screening[10,11]. Apart from the SRB **(15)** assay being robust and practicable for HTS processes, it is also able to differentiate cells killed from growth inhibition [12,13]. SRB **(15)** assays are more commonly used in HTS endeavours to measure the rate cell of proliferation and cytotoxic effects of compounds. SRB **(15)** has a high affinity to bind to cellular protein and is used as a protein dye. The principal of the SRB **(15)** colorimetric assay relies on the dye's ability to electrostatically bind to the basic amino acid residues of proteins only in cells that have been fixed with trichloroacetic acid (TCA)[15]. The SRB **(15)** protein dye attaches to the proteins under acidic conditions and detaches from proteins under basic conditions which allows for its easy extraction and OD measurement[16]. The SRB **(15)** assay is a simple measurement of the cellular protein content present. The SRB **(15)** assay has many benefits such as a) having equivalent sensitivity to other type of commonly used fluorescence assays b) good stability of the protein dye c) a high signal-to-noise ratio when recording fluorescence and d) the non-destructive behaviour of the assay[16]. The chemical structure of unbound SRB **(15)** protein dye is shown below in Figure 2-2:
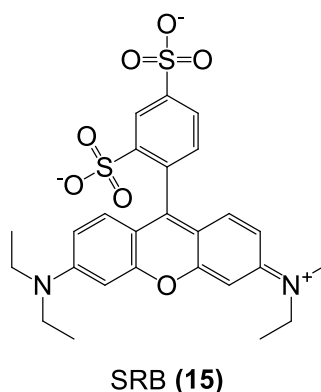
SRB **(15)**

Figure 2-2 The chemical structure of the unbound SRB **(15)** protein dye.

20

2.2 Materials and methods

2.2.1 Development of the South African natural product library's standardised plant preparative methods

The plant preparative methods developed in this project were adapted from the developed procedures selected for the production of standardised extracts and fractions in the NCI NPNPD library[5]. The only distinguishable difference is the downscaled extraction and the final standardisation concentration. Additionally, this project used the leaves of *Brassica oleracea* (*B. oleracea*) for the development and validation of the standardised plant preparative methods created for the South African natural product library.

2.2.1.1 Internal barcoding format and database structure

An internal barcoding format is used for all the plant materials used and subsequent samples created during all preparative methods. All the internal barcodes were printed (thermal transfer) onto chemically resistant barcode rolls using a Zebra ZT230 barcode printer (Zebra technologies, Separations, South Africa) shown in Figure 2-3. All the printed internal barcodes were derived from the herbarium specimen voucher number of the respective plant species. For every plant sample collected and deposited by the CSIR, the South African National Biodiversity Institute (SANBI) provided a voucher number that began with the letter "P" followed by a five-digit number. For every subsequent sample generated from the material, a suffix was added to the existing voucher number. As plant materials were extracted, the letter "x" was added as a suffix to their respective voucher numbers. As the plant extracts were fractionated into 7 unique fractions, the suffix "f" followed by a number 1 to 7 was added to denote the fraction number. For clarification, the barcode "P12345xf7" would be the seventh fraction of the plant extract "P12345x" for the plant material with the voucher number "P12345". All the plant extracts were relabelled in a separate container with the suffix "e8" added to the voucher numbers denoting the sample is a plant extract e.g., "P12345xe8". After standardisation, the plant extracts and corresponding fractions were transferred to pre-barcoded 1 ml screw cap storage vials and linked to the respective internal barcode format. The long-term cold storage position of the pre-barcoded 1 ml vials were recorded.

The barcodes of each sample were catalogued and correlated using a single Microsoft Excel worksheet i.e., database. The contents of the Excel worksheet were adjustable by both the researcher and the respective liquid handler. The database consisted of the following columns that were populated by either the researcher or the liquid handler: Plant Name; Extract P number; Fraction#; P linked barcode; UnloadedWeight (mg); Initial FractionVolume (µL); TransferredVolume (µL); LoadedWeight (mg); TransferredWeight (mg); BoxBarcode; Box

Division; Sample Status; FluidXPlateBarcode; FluidXPlatePosID; FluidXPlatePosIDBarcodes; Concentration (mg/mL); Remaining Volume (µL); Status; Duplicate; DWP Pos ID; Dilute.

Figure 2-3 An image of the Zebra ZT230 barcode printer used in this project.

2.2.1.2   Ultrasonic bath extraction

Approximately 7.0 g of the dried leaf material of *B. oleracea* was sequentially extracted in an ultrasonic bath for 2 hours. A 50 mL MeOH/DCM solution (1:1) was used for the first 60 minutes followed by a 50 mL MeOH solution for the remaining time. The plant material and solvent was contained within a custom glass percolator shown in Figure 2-4 (Listco Glassblowers Ltd., South Africa). The glass percolators were held upright inside the ultrasonic bath using a custom fabricated stainless-steel frame that is shown in Figure 2-5 and is capable of simultaneously holding 12 percolators. The glass percolator was made of borosilicate glass and was fitted with a fixed glass-ceramic frit (16-40 µm porosity) with a polytetrafluoroethylene (PTFE) stopcock. After each 60-minute ultrasonication period, the solvent was filtered through the ceramic frit at the bottom of the glass percolator and collected in round bottom flasks. The two solvent systems were combined and concentrated using a Buchi R300 rotary vacuum evaporator (Labotec, South Africa) then dried to completion in a SP Scientific Genevac® HT-6 solvent evaporator (United Scientific Ltd., South Africa) shown in Figure 2-6. The dry crude plant extracts were labelled according to the format outlined in Section 2.2.1.1 and the mass recorded.

Figure 2-4 An image of the custom glass percolator used during plant material ultrasonic bath extraction.
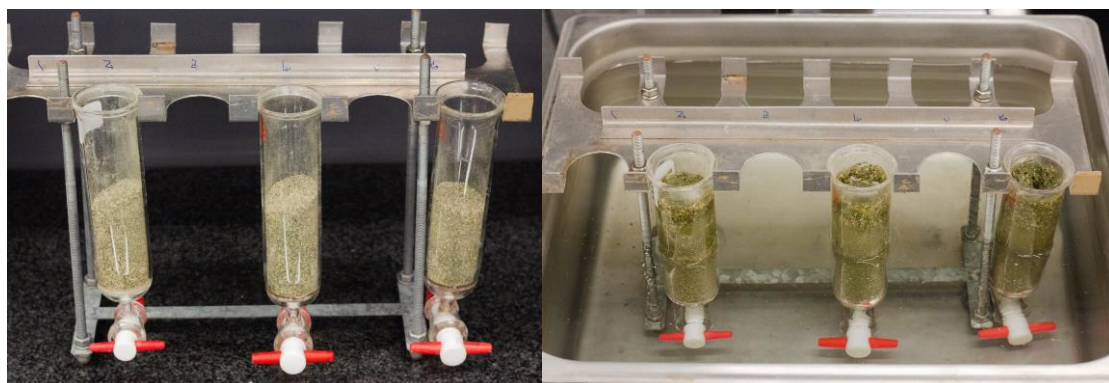
Figure 2-5 An image of the custom stainless-steel frame (left) used to suspend up to 12 glass percolators inside the ultrasonic bath (right).

Figure 2-6 An image of two Genevac® HT-6 solvent evaporators used in this project.

23

2.2.1.3 Automated plant extract fractionation

Each plant extract (200-300 mg) was weighed into a pre-weighed barcoded vial and loaded onto the Hamilton Microlab® STARlet™ liquid handler's deck. Using the Hamilton Microlab® STARlet™ automated liquid handler, each extract was dissolved in a 4.5 mL solution of MeOH/ethyl acetate (EtOAc)/methyl tert-butyl ether (MTBE) (6:3:1). After each plant extract was fully dissolved, a calculated aliquot was transferred to a BioPointe Scientific 2.2 mL, v-bottom 96 well plate (Separations, South Africa) for standardisation purposes. The dissolved plant extracts were then allowed to dry onto large, non-sterile, 1.27 cm x 3.81 cm dental cotton rolls (TIDI Products, Wisconsin, United States) inside a Genevac® HT-6 solvent evaporator. Once dried, the extract loaded cotton rolls were placed inside an empty Phenomenex SPE, 6 mL cartridge (Separations, South Africa) and closed with a Gilson® SPE cartridge sealing cap (Lasec SA, South Africa). The plant extracts were automatically fractionated using a Gilson GX-241 ASPEC® liquid handler with a VERITY® 4060 Single Syringe Pump and a single 220.5 x 1.5 x 1.1 mm probe shown in Figure 2-7 (Lasec SA, South Africa). The Gilson GX-241 ASPEC® liquid handler's deck was configured with two racks (code 376 and 346) and a solvent reservoir rack with six 100 mL reservoirs as shown in Figure 2-8. The code 376 rack consists of a mobile Disposable Extraction Cartridge (DEC) rack that holds fifteen 6 mL SPE cartridges and collection block rack that holds fifteen 15 mm x 85 mm (10 mL) tubes. The code 346 rack holds forty-four 16 mm x 100 mm tubes.

Method development and instrument operation was performed on the TRILUTION® LH v4.0. DB-Build 3 software. The automated extract fractionation method developed was adapted from the fractionation method of natural product extracts outlined in the NCI NPNPD project[5]. Using the Gilson GX-241 ASPEC® liquid handler, the plant extracts were fractionated into 7 fractions of decreasing polarity on a ThermoFisher™ HyperSep™ C8, 6 mL, 2 g reverse phase SPE cartridge (Anatech instruments, South Africa). Prior to extract fractionation, the HyperSep™ C8 SPE cartridges were washed and conditioned at a flow rate of 6 mL/min with 20 mL of MeOH and 20 mL of H_2O/MeOH (95:5) using the Gilson GX-241 ASPEC® liquid handler. Once washing and conditioning was completed, the SPE cartridges containing the extract loaded dental cotton rolls were connected first in series to the HyperSep™ C8 SPE cartridges using PTFE SPE tube adaptors (Sigma-Aldrich- Merck, Germany) as shown in Figure 2-9. Each fraction (1 to 7) was collected on a volume-basis at a flow rate of 6 mL/min. The Gilson GX-241 ASPEC® liquid handler produced seven 8 mL fractions using the following solvent systems of decreasing polarity: H_2O/MeOH (95:5), H_2O/MeOH (80:20), H_2O/MeOH (60:40), H_2O/MeOH (40:60), H_2O/MeOH (20:80), MeOH (100), MeOH/acetonitrile (ACN) (1:1). Each fraction was individually collected in an internally barcoded and pre-weighed 10 mL polypropylene (PP) screwcap vial (Lasec SA, South Africa).

24
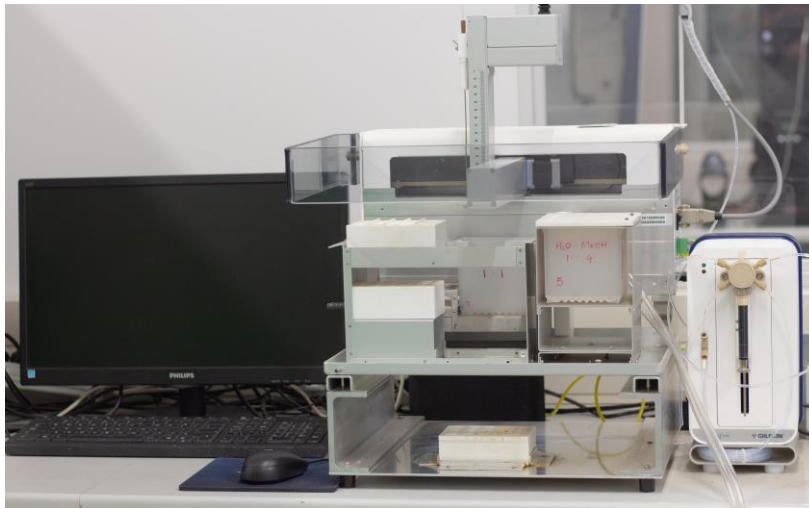
Figure 2-7 An image of the Gilson GX-241 ASPEC® liquid handler.
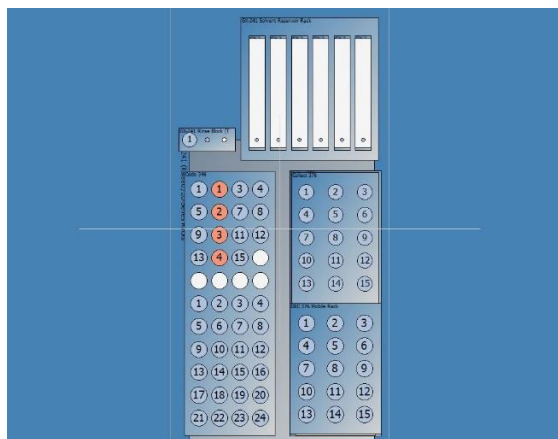
Figure 2-8 The deck layout of the Gilson GX-241 ASPEC® liquid handler.
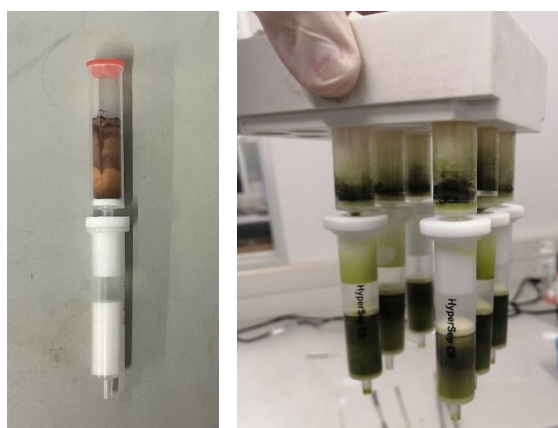
Figure 2-9 An image (left) of a extract loaded cotton roll containing SPE cartridge connected first in series to a HyperSep™ C8 SPE cartridges by an SPE tube adaptor and a placed inside the Gilson GX-241 ASPEC® liquid handler mobile rack (right).

25

2.2.1.4   Automated plant extract and fraction standardisation

All the plant extracts and fractions were standardised at 5 mg/mL in DMSO using the Hamilton Microlab® STARlet™ automated liquid handler, shown in Figure 2-10, that was scripted on VENUS five software. The software allowed the integration of a Hamilton Storage LabElite® DeCapper™ SL operated with LabElite® software V2.3.1. (Separation, South Africa) and a FluidX Impression™ Whole Rack Scanner 2D barcode reader with mirror that was operated with the software IntelliCode V11.8.0.1120 (Separation, South Africa) shown in Figure 2-11 and Figure 2-12, respectively. The Hamilton Microlab® STARlet™ automated liquid handler is fitted with an Autoload unit and barcode scanner, 8 independent compression-induced O-ring expansion (CO-RE) 1000 µL pipetting channels and an internal swivel arm plate handler (iSwap) as seen in Figure 2-13.

Figure 2-10 An image of the Hamilton Microlab® STARlet™ automated liquid handler (right) coupled to the Hamilton Storage LabElite® DeCapper™ SL (left).
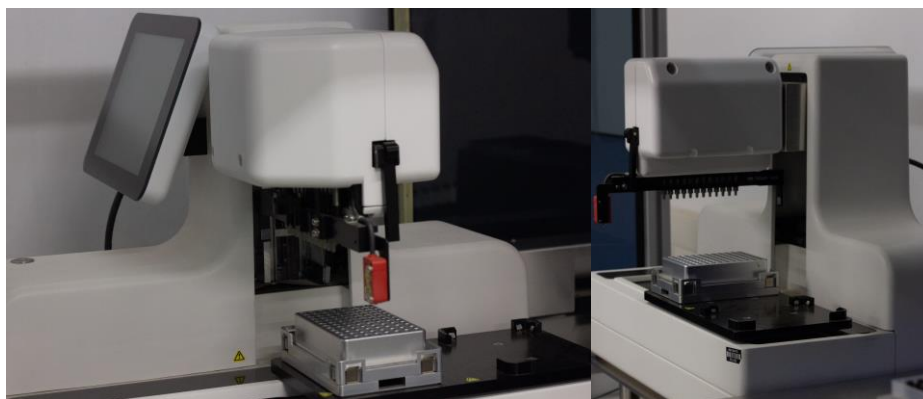
Figure 2-11 A front (left) and back (right) image illustrating the Hamilton Storage LabElite® DeCapper™ SL Hamilton Microlab® STARlet™.

Figure 2-12 An image of the FluidX Impression™ Whole Rack Scanner 2D barcode reader with mirror.

Figure 2-13 An image showing the 8 independent CO-RE pipetting channels and the iSwap arm of the Hamilton Microlab® STARlet™.

As shown in Figure 2-14, the STARlet™ automated liquid handler's deck is equipped with a Tip Carrier, Reagent Trough Carrier, three 32-Tube carrier, four 24-Tube carrier and a Multiflex (MFX) carrier base with 2x MFX DWP Modules and a Hamilton Heater Shaker (HHS) mounted on the top. The pipette Tip Carrier was configured to carry three racks of 300 µL Slim Tips and two racks of 1000 µL Conductive CO-RE Tips, the Reagent Trough Carrier was configured to hold three 120 mL solvent troughs, the three 32-Tube carriers were configured to carry a total of 96 tubes between the sizes 11 mm OD x 60 mm length - 14 mm OD x 120 mm length while the four 24-Tube carriers were configured to carry a total of 96 tubes between the sizes 14.5 mm OD x 60 mm length - 18 mm OD x 120 mm length and finally the MFX DWP Modules along with the HSS was configured to hold a deep 96 well plates with an SBS footprint.

27
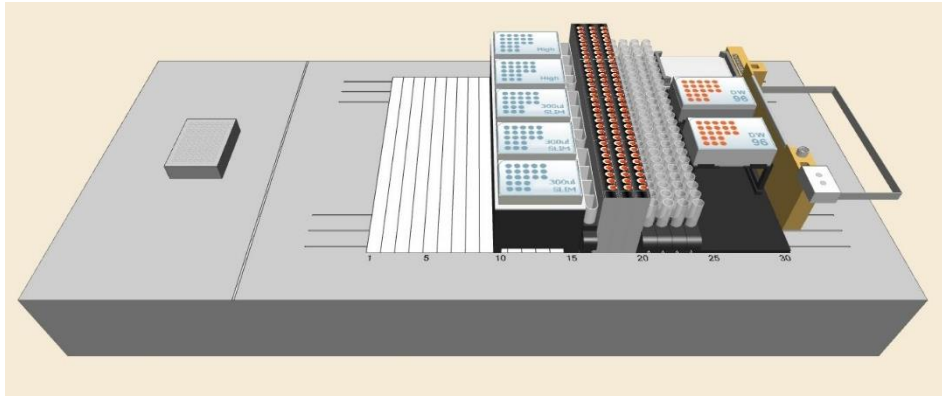
Figure 2-14 The deck layout of the Hamilton Microlab® STARlet™ automated liquid handler.

The standardisation procedure was completed as a multi-step process. Initially the STARlet™ automated liquid handler volumetrically transferred 5.55 mg of 12 dissolved plant extract to the last well (Row H) of every column (Column 1-12) in a BioPointe 96 well plate using Equation 2-1. After the plant extracts were fractionated, the STARlet™ automated liquid handler measured and recorded the volume of each fraction before transferring 1.6 mL of each fraction to the corresponding column in the BioPointe 96 well plate that contained the respective plant extract as seen in Figure 2-15. The BioPointe 96 well plate and fraction tubes were dried until completion in a Genevac® HT-6. The dry weights of each fraction were recorded in the database Excel worksheet. By using the information in the database and Equation 2-2, the STARlet™ automated liquid handler calculated the dry weight of every sample in each well of the BioPointe 96 well plate. The STARlet™ automated liquid handler then calculated and added the volume of DMSO needed to standardise each well at 5 mg/mL using Equation 2-3. Finally, the STARlet™ automated liquid handler transferred the dissolved contents of the BioPointe 96 well plate to the pre-barcoded storage FluidX 96-format 1.0 mL screw cap vials (Separations, South Africa) as shown in Figure 2-16. For the wells with insufficient masses (< 0.5 mg) and excessive masses (> 10 mg) to be standardised at 5 mg/mL, the STARlet™ automated liquid handler added 100 µL or 2000 µL of DMSO, respectively. For the wells dissolved in 100 µL DMSO, the full volume was transferred to the respective pre-barcoded vials. For wells dissolved in 2000 µL DMSO, an aliquot volume was calculated using Equation 2-4 and transferred to the respective pre-barcoded vials then further diluted using Equation 2-5 till the samples were standardised at 5 mg/mL at a final volume of 800 uL DMSO. The final concentrations (mg/mL) and volumes (µL) were recorded and populated in the database by the STARlet™ automated liquid handler.

Equation 2-1 The equation used to determine the volume (µL) needed to volumetrically transfer 5.55 mg of each dissolved plant extract.

$$\text{Calculated volume to be transferred (µL)} = \frac{5.55 \text{ (mg)}}{\left(\dfrac{\text{Extract weight (mg)}}{\text{Solvent volume used (µL)}}\right)}$$

Equation 2-2 The equation used to determine the mass of dried fraction in each well.

$$\text{Transferred weight (mg)} = \frac{\text{Dried fraction weight (mg)}}{\text{Measured fraction volume (µL) - 1600 (µL)}} \times 1600 \text{ (µL)}$$

Equation 2-3 The equation used to calculate the volume of DMSO required by each well to standardise at 5 mg/mL.

$$\text{Volume (µL) of DMSO to be added} = \frac{\text{Equation 2-2}}{5 \text{ (mg/mL)}}$$

Equation 2-4 The equation used to calculate the volume to be transferred for samples with excessive weights.

$$\text{Volume (µL) to be transferred} = \frac{0.005 \text{ (mg/µL)} \times 800 \text{ (µL)}}{\left(\dfrac{\text{Equation 2-2}}{2000 \text{ (µL)}}\right)}$$

Equation 2-5 The equation used to calculate the dilution volume of DMSO needed to standardise the samples with excessive weights at 5 mg/mL.

$$\text{Dilution volume (µL) of DMSO to be added} = 800 \text{ (µL)} - \text{Equation 2-4}$$
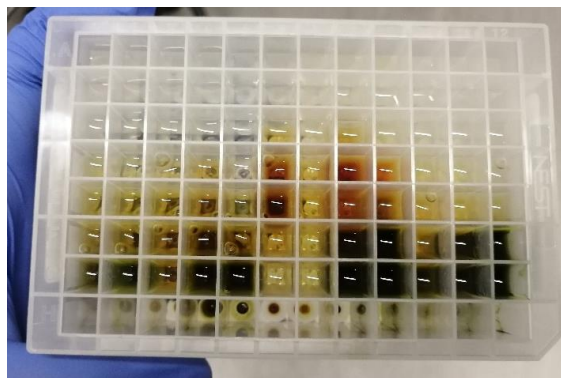
Figure 2-15 An image of the plant extracts and fractions within a BioPointe Scientific 2.2 mL, v-bottom 96 well plate before being dried.

29

Figure 2-16 An image of the pre-barcoded FluidX 96-format 1.0 mL screw cap vials.

2.2.1.5 Automated vial storage and retrieval

The standardised plant extracts and fractions were stored at -20 °C in a Hamilton Verso® Q20 robotic freezer using Instinct® S software (Separations, South Africa) shown below in Figure 2-17. The Hamilton Verso® Q20 continuously flows dry air throughout the system to obtain an almost waterless environment. The storage vials were held in a FluidX 96 well plate as the Verso® Q20 automatically loaded and scanned the barcodes of each vial. To increase storage capacity, the Verso® Q20 transferred the vials to a high-density 138-format storage rack thus allowing the storage of up to 17 600 vials. The Verso® Q20 recorded the location and position of each vial which made the retrieval of selected vials from the storage easier.

Figure 2-17 An image of two automated robotic freezer Hamilton Verso® Q20.

2.2.1.6 Automated duplication of standardised vials

The STARlet™ automated liquid handler was used to transfer a 30 µL aliquot of each selected standardised sample to a NEST® 2.0 mL, square v-bottom 96-Well Deep Well Plate (Lasec SA, South Africa) for biological screening. The STARlet™ automated liquid handler then updated the remaining volume of each standardised sample in the appropriate database Excel worksheet. For shipping, the NEST® 96 well plate was foil sealed with AlumaSeal® 96 film (Sigma-Aldrich- Merck, South Africa) as shown in Figure 2-18, using a SealBio-2 semi-automated plate sealer (Apex Scientific, South Africa) shown in Figure 2-19. The standardised samples were returned to the Verso® Q20 and the sealed NEST® 96 well plate was kept frozen at -40 °C till shipment.
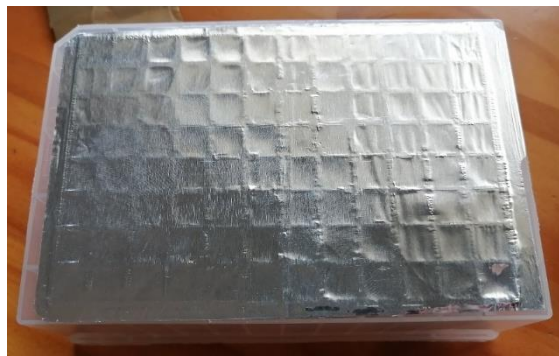
Figure 2-18 An image of a foil sealed NEST® 2.0 mL 96-Well Deep Well plate.

Figure 2-19 An image of the SealBio-2 semi-automated plate sealer with the AlumaSeal® 96 film used.

31

2.2.2   Validation of the South African natural product library's standardised plant preparative methods

2.2.2.1   Preparation of the method controls

A positive (cytotoxic) and negative (non-cytotoxic) method control was used to ensure that sample integrity was not compromised during the plant preparative methods. A standard of paclitaxel **(1)** ≥ 95 % HPLC (Sigma-Aldrich- Merck, South Africa) and a head of cabbage, *B. oleracea* purchased from Woolworths was used. Shown in Table 2 is the family name, the plant species name, the plant part used, the reported traditional usage and phytochemical constituents of *B. oleracea*. The cabbage was extracted twice and standardised using the South African natural product library's plant preparative methods outline in Section 2.2.1 . The positive method control entailed spiking one of the preparations with 1.13 mg of paclitaxel **(1)** during extraction making the unspiked preparation the negative method control.

Table 2 Information pertaining to *Brassica oleracea.*

Family name	Plant species, part and voucher number	Traditional usage	Reported phytochemical constituents
Brassicaceae	*Brassica oleracea* Leaves (130973)	The plant leaves are eaten as a vegetable.	Alkaloids, cardiac glycosides, coumarins, flavonoids, phenols, phlobatannins, quinines, saponins, terpenoids[17].

2.2.2.2   Chemical analysis of the positive method control and quantification of paclitaxel

Chemical separation and detection of the positive method control was done using ultra-high pressure liquid chromatography (UPLC) with a photodiode array detector (PDA) coupled to a quadrupole time-of-flight mass spectrometer (QTOF) as seen in Figure 2-20. The instrument used was a Waters® ACQUITY UPLC® system coupled to a Waters® XEVO-G2-XS-QTOF detector (UPLC-PDA-HRMS). The ACQUITY UPLC® system consisted of a Binary Solvent Manager, AutoSampler and PDA detector. The instrument concurrently collected light absorption and mass spectral data. The system operation, data acquisition and analysis used the software MassLynx® v4.1 (Waters Inc., Milford, Massachusetts, USA). The ACQUITY® AutoSampler kept the samples at a constant 8 °C and is fitted with a 10 µL injection loop. The ACQUITY PDA detector was set to collect light absorption wavelengths between 220 and 600 nm at a sampling rate of 20 points/sec. The Waters® XEVO-G2-XS-QTOF collected mass spectral scans every 0.3 seconds between a mass range of 50 and 1200 *m/z*. Raw data was collected in MS^E data-independent acquisition (DIA) mode which allowed the collection of both

low and high collision energy data. The detector used a leucine enkephalin (555.2693 Da) solution as an internal lock mass standard which was directly infused into the source every 10 seconds through a secondary orthogonal electron spray ionisation (ESI) capillary. The detector was calibrated using a sodium caesium iodide calibrant in both positive and negative ESI modes between the mass range of 173.047 and 1071.868 Da. The source capillary voltage was set at 2.8 kV and 2.0 kV for positive and negative ESI mode, respectively. The source temperature was set at 120 °C, the sampling cone voltage was set at 30.0 V, the extraction cone voltage was set at 4.0 V, the cone gas (nitrogen) flow was set at 20.0 L/Hr and the source desolvation temperature was set at 350 °C with a desolvation gas (nitrogen) flow at 600.0 L/Hr. Separation was achieved using a reverse phase step gradient on a UPLC reverse phase analytical column. The gradient consisted of an aqueous mobile phase A and an organic mobile phase B. Mobile phase A consisted of ultra-pure water spiked with 0.1 % formic acid while the mobile phase B consisted of ultra-pure methanol spiked with 0.1 % formic acid. The flow rate was set at 0.300 mL/min throughout the entire run. The gradient started with an isocratic hold of 3 % B for 1.0 min followed by a linear increase to 100 % B at 14.0 min. The gradient was held at 100 % B for 3.0 min then returned to initial conditions over 0.5 min. The gradient was held at 3 % B till the final run time of 20 minutes. The data collection of positive and negative ESI mode was done independently requiring two 5 µL injections of a single sample. The analytical column used was an ACQUITY UPLC® C18 Ethylene Bridged Hybrid (BEH) (2.1 mm ID x 100 mm, 1.7 µm). During runs the column was kept at a temperature of 50 °C.

For the quantification of paclitaxel **(1)**, a standard curve was prepared from a 1000 ppm paclitaxel **(1)** stock solution in MeOH/H_2O (1.9:1). The stock solution was used to prepare the following calibration points by serial dilution: 50, 25, 12.5, 6.25, 3.125 and 1.563 ppm. 5 µL of each calibration point and sample (1000 ppm) was injected three times. The peak areas of paclitaxel **(1)** were integrated from the extracted ion (m/z = 854.3, Retention Time (RT) = 11.22 (min)) in positive ESI mode. A standard curve was plotted using GraphPad Prism v5.03. The Limit of Detection (LOD) and Limit of Quantification (LOQ) of paclitaxel **(1)** were calculated using the 2022 Validation of Analytical Procedures ICH Q2(R2) guidelines that were outlined by the International Council For Harmonisation (ICH) Of Technical Requirements For Pharmaceuticals For Human Use. The LOD and LOQ were calculated as a response using Equation 2-6 and Equation 2-7 and the concentrations (ppm) were then calculated using the line of regression from the standard curve. The variables used in Equation 2-6 and Equation 2-7 are defined as the following: Sy.x = standard deviation of the response curve, S = the slope of the calibration curve.

Equation 2-6 The equation used to calculate the response of the LOD.

$$\text{LOD response} = 3.3 \times \left(\frac{\text{Sy.x}}{\text{S}}\right)$$

Equation 2-7 The equation used to calculate the response of the LOQ.

$$\text{LOQ response} = 10 \times \left(\frac{\text{Sy.x}}{\text{S}}\right)$$
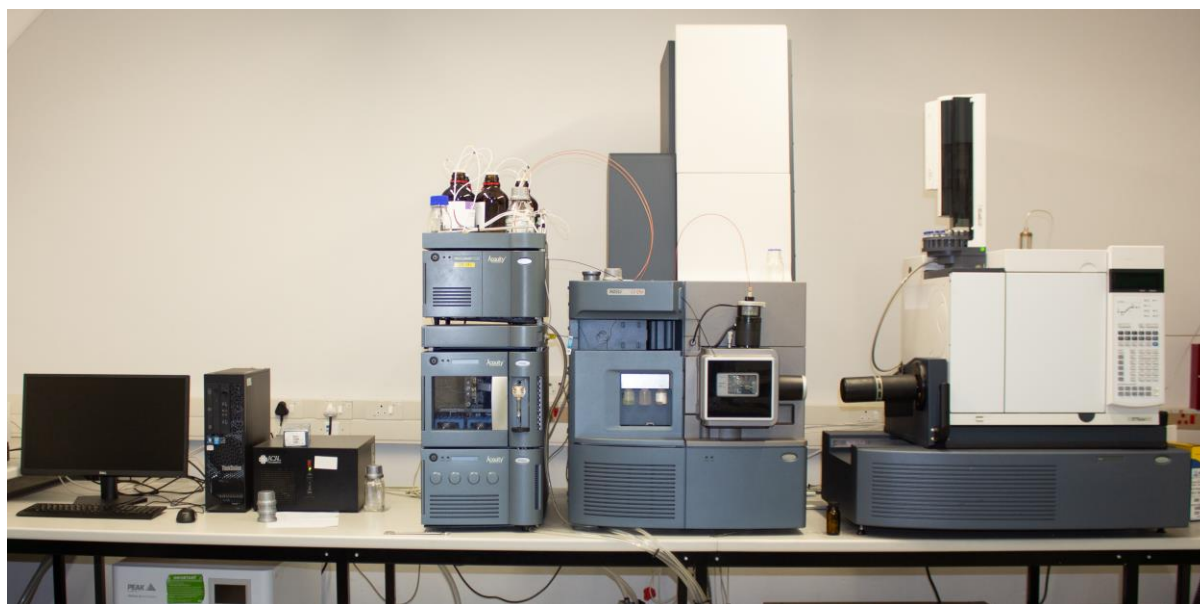
Figure 2-20 An image of the Waters® ACQUITY UPLC® system coupled to a Waters® XEVO-G2-XS-QTOF (UPLC-PDA-HRMS).

2.2.2.3 Biological screening of the method controls and paclitaxel against the cell line A549

The method controls and a paclitaxel **(1)** standard were screened in an *in vitro* SRB **(15)** assay against the human cancer cell line A549. The screening was completed by Professor SubbaRao V. Madhunapantula in his cancer research laboratory located at the Cellular and Molecular Biology Centre in the Department of Biochemistry at the JSS Medical College in Mysuru, Karnataka India. 30 µL of each standardised plant extract and fraction was provided as outlined in Section 2.2.1.6. and diluted 100-fold to a final concentration of 50 µg/mL. A standard of paclitaxel **(1)** was prepared in serial dilution and screened by Professor SubbaRao V. Madhunapantula at 0.02, 0.45, 0.91, 1.83, 29.31 and 58.63 µM.

The reagents used were Dulbecco's modified eagle medium- High glucose (DMEM-HG) and Foetal bovine serum (FBS), Glutamax, PenStrep, Trypsin, SRB **(15)**, cisplatin **(6)**, TCA and DMSO. The cells were maintained in a DMEM-HG with 10 % FBS and containing 4.5 g/L glucose, sodium bicarbonate, phenol red, Glutamax (2 mM) and PenStrep (0.5 mg/mL) while incubated at 37 °C with 5 % CO_2. The cancer cell line selected for the *in vitro* screening were human lung carcinoma epithelial cells A549. The cells were seeded in 96 well plates at 10 000 cells per well (100 µL aliquots) and incubated till 60-70 % confluence. Cisplatin **(6)** (100 µM) was used as a positive control. The wells were then treated with the prepared library samples at 50 µg/mL and incubated for 48 hours. After incubation, 50 µL of 50 % TCA was used to fix the cells in each well after which the plate was kept for 1 hour at 4 °C. After fixation was completed, each well was washed with water and left to dry. Once dry, 100 µL of SRB **(15)** was added to each well of the plate and left to incubate for half an hour. Unbound SRB **(15)** dye was removed, and each well was washed with 1 % acetic acid then left to dry. 100 µL of a 10 mM tris base solution was used to dissolve the protein bound SRB **(15)** in each well before OD absorbance was recorded at 510 nm on a multimode plate reader (PerkinElmer, Massachusetts, USA). The cell proliferation inhibition (%) was calculated using Equation 2-8 and reported.

Equation 2-8 The equation used to calculate cell proliferation inhibition (%) from the OD absorbance of each sample.

$$\text{Cell proliferation inhibition (\%)} = \frac{(\text{mean OD}_{control} - \text{mean OD}_{sample})}{(\text{mean OD}_{control})} \times 100$$

2.3 Results and discussion

2.3.1 Development of the South African natural product library's standardised plant preparative methods

2.3.1.1 Internal barcoding format and database structure

The internal barcoding format was successful as it resulted in easy labelling, tracking and data correlation of samples. The use of a single amendable Microsoft Excel worksheet allowed the consolidation of information of plant extracts and fractions all throughout the plant preparative processes, making the database an excellent record of all samples.

2.3.1.2   Ultrasonic bath extraction

It is well known that plants produce a variety of secondary metabolites with varying polarities. To date, there isn't a single solvent or solvent system that can completely extract all secondary metabolites. The ultrasonic bath extraction method used in this project was developed to created quality plant secondary metabolite extracts in the shortest time possible with the least amount of plant material required. The goal was to obtain sufficient amounts of quality plant extract for downstream processing. The solvent system consisted of an a 1:1 DCM/MeOH solvent mixture followed by a 100 % MeOH wash which has shown to yield quality bioactive organic extracts[4]. Extraction is a diffusion process governed by time, which is important to recognise when trying to obtain a quality extract. The solvent system must first penetrate the plant material, dissolve the soluble secondary metabolites and then diffuse out of the plant material. The extraction time of 2 hours selected was based on a study that showed just less than 50 % yield of a 20-hour extraction was obtained after just 1 hour extraction time[4]. It was determined that approximately 7.0 g of dried and ground plant material was enough to yield a quality extract for the required 250 mg. To make the ultrasonic bath extraction protocol high-throughput, a custom stainless-steel frame was fabricated that allowed 12 different plant materials to be extracted simultaneously. Using the ultrasonic bath extraction method outlined in Section 2.2.1.2, it was observed that the positive (PM0106) and negative (PM0105) controls unexpectedly produced different crude extract weights using the same plant material as shown in Table 3.

Table 3 The ultrasonic bath extraction yields of the positive and negative control

Plant species (Specimen number)	Plant extract number	Plant material (g)	Plant extract (g)	Yield* (%)
Brassica oleracea (130973)	PM0105x (Negative control)	6.89	0.876	12.72
	PM0106x (Positive control)	7.26	2.279	31.38

w/w, extract mass (g) per plant material mass (g).

The positive control had a yield of 31.38 % while the negative control only had a yield of 12.72 %. The discrepancy was due to the mechanical stirring of the positive control plant material as it was spiked with paclitaxel **(1)**. It was noted that for future ultrasonic bath extractions, the plant material must be stirred during the initial stages of extraction to allow the dry plant material to absorb the solvent and remain below the solvent volume level.

2.3.1.3   Automated plant extract fractionation

The extract fractionation method used was adapted from the automated fractionation method of natural product extracts in the NCI NPNPD project. The extract fractionation worked well in eluting and concentrating compounds with similar polarities together. Identical weights of each method control extract were weighed out, loaded onto individual cotton rolls and fractionated using the method outlined in Section 2.2.1.3. Shown below in Table 4 are the yields for every fraction of the positive and negative control.

Table 4 The fraction yields of the positive and negative method control.

Plant extract number	Weight of plant extract fractionated (mg)	Fraction barcode	Mass (mg)	Yield (%)
PM0205x (Negative control)	218.5	PM0205xf1	82.81	37.90
		PM0205xf2	13.87	6.35
		PM0205xf3	2.42	1.11
		PM0205xf4	1.84	0.84
		PM0205xf5	1.39	0.64
		PM0205xf6	1.90	0.87
		PM0205xf7	2.85	1.30
PM0206x (Positive control)	219.0	PM0206xf1	100.88	46.06
		PM0206xf2	25.81	11.79
		PM0206xf3	3.42	1.56
		PM0206xf4	1.98	0.90
		PM0206xf5	1.44	0.66
		PM0206xf6	1.97	0.90
		PM0206xf7	3.68	1.68

The positive method control had a greater mass recovery of 63.55 % than the negative control of 49.00 %. The mass recovery of both methods controls were relatively low when compared to the average 87.7 % mass recovery for the NCI NPNPD fraction library's fractionation method[3]. This was due to the intensity of the drying technique used when the dissolved plant extracts are adsorbed onto the dental cotton rolls. The drying technique resulted in the formation of a hard extract plug at the bottom of each dental cotton thus preventing it to fully dissolve during fractionation. However, a higher yield was observed for every fraction of the positive control. It was also noted that if the fractions of each method control were ordered by yield, the order would be the same for both controls. The difference was merely due to the extract quality difference between the positive and negative control. It was considered that the mechanical stirring of plant material during ultrasonic bath extraction produced a better quality of plant extract. The extract fractionation method developed by the NCI NPNPD project was

37

less demanding and easily up scalable than conventional fractionation techniques such as packed silica columns.

2.3.1.4   Automated plant extract and fraction standardisation

The decision to standardise all the samples at 5 mg/mL in DMSO was proven to be reasonable. There was sufficient mass in most of the fractions to be standardised at 5 mg/mL. Further, the use of DMSO proved to be advantageous for its ability to solubilise a wide polarity range of compounds for standardisation and its use as compound vehicle during biological screening. The Hamilton STARlet™ liquid handler successfully standardised the positive and negative control fractions in a manner that is ready for HTS processes. The final concentration, volume and pre-barcoded storage vials of the method controls are shown below in Table 5. The liquid-handling errors for fractions with insufficient yield worked as seen by fractions that have been standardised at a concentration lower than 5 mg/mL in 100 µL DMSO. It was determined that the scripts and protocols developed for standardisation will work for all types of plant extracts and fractions. The pre-barcoded storage vials are linked with the fraction number by the STARlet™ liquid handler.

Table 5   The final concentration, volume and associated pre-barcoded vials for each method control.

Standardised plant extract and fraction barcodes	Concentration (mg/mL)	Volume (µL)	Pre-barcoded vial label
PM0205xf1	5	154.57	FR18782294
PM0205xf2	5	693.5	FR18782295
PM0205xf3	5	121	FR18782296
PM0205xf4	4.6	100	FR18782297
PM0205xf5	3.475	100	FR18782298
PM0205xf6	4.75	100	FR18782299
PM0205xf7	5	142.5	FR18782300
PM0205xe8	5	329.5	FR18782301
PM0206xf1	5	126.88	FR18782302
PM0206xf2	5	495.9	FR18782303
PM0206xf3	5	171	FR18782304
PM0206xf4	4.95	100	FR18782305
PM0206xf5	3.6	100	FR18782306
PM0206xf6	4.925	100	FR18782307
PM0206xf7	5	184	FR18782308
PM0206xe8	5	296	FR18782309

2.3.1.5 Automated vial storage and retrieval

The use of an automated robotic freezer has shown to be necessary when working with large quantities of samples. The robotic freezer generated an inventory of all the vial stored and their exact locations. The inventory allowed for easy retrieval of vials by selecting either the pre-barcoded vial label, location or position to be returned. The locations and positions for each unique pre-barcoded vial stored within the Hamilton Verso® Q20 robotic freezer are shown below in Table 6.

Table 6 The location and position of a pre-barcoded vial that corresponds to a single standardised plant extract and fraction barcode.

Pre-barcoded vial label	Location	Position
FR18782294	Storage B1.1, Column 2, Shelf 7	Rack F6
FR18782295	Storage B1.1, Column 2, Shelf 7	Rack G6
FR18782296	Storage B1.1, Column 2, Shelf 7	Rack H5
FR18782297	Storage B1.1, Column 2, Shelf 7	Rack I5
FR18782298	Storage B1.1, Column 2, Shelf 7	Rack J3
FR18782299	Storage B1.1, Column 2, Shelf 7	Rack K3
FR18782300	Storage B1.1, Column 2, Shelf 8	Rack A2
FR18782301	Storage B1.1, Column 2, Shelf 8	Rack B1
FR18782302	Storage B1.1, Column 2, Shelf 7	Rack F7
FR18782303	Storage B1.1, Column 2, Shelf 7	Rack G7
FR18782304	Storage B1.1, Column 2, Shelf 7	Rack H6
FR18782305	Storage B1.1, Column 2, Shelf 7	Rack I6
FR18782306	Storage B1.1, Column 2, Shelf 7	Rack J4
FR18782307	Storage B1.1, Column 2, Shelf 7	Rack K4
FR18782308	Storage B1.1, Column 2, Shelf 8	Rack A3
FR18782309	Storage B1.1, Column 2, Shelf 8	Rack B2

Concerns of sample viability and stability have been addressed by storing the standardised extracts and fractions under strict inert conditions. The standardised extracts and fractions are stored in an airtight screw capped polypropylene vial that is kept frozen at -20 °C in a dry atmosphere until needed. Humidity control is the most critical factor for maintaining the integrity of screening compounds. It has been well documented that samples stored in DMSO with 5 % water are at a higher risk of instability than samples stored in only DMSO[18]. DMSO is extremely hygroscopic and readily absorbs water from the atmosphere which could promote the precipitation of compounds with poor aqueous solubility while also promoting side reactions that result in degraded compounds. Other concerns such as storage material e.g., borosilicate glass or polypropylene and freezing/thawing cycles have not shown significant

39

decomposition nor precipitation of compounds during 5 months of sample storage[18]. Additionally, in a stability study on a diverse collection of screening compounds prepared in DMSO, limited decomposition was observed for samples stored at -20 °C[19]. After considering the storage conditions used in this platform, the standardised extracts and fractions are expected to have a lifespan of 5-10 years.

2.3.1.6   Automated duplication of standardised vials

The Hamilton STARlet™ liquid handler successfully transferred 30 μL of each standardised pre-barcoded storage vial to specified wells of a disposable deep 96 well plate. The script successfully updated the remaining volume of each standardised vial in the database Excel worksheet.

2.3.2   Validation of the South African natural product library's standardised plant preparative methods

2.3.2.1   Preparation of the method controls

The positive method control was spiked with the natural abundance (0.01-0.02 % dry weight[20]) of paclitaxel **(1)** in the bark of *Taxus brevifolia*. Paclitaxel **(1)** is a well-known diterpenoid and a potent microtubule disrupter that is widely used in the treatment of non-small cell lung cancer[15]. *B. oleracea* was selected as the control material as the leaf extracts are known to exhibit relatively poor cell proliferation inhibition against human non-small cell lung cancer cell line H1299[21].

2.3.2.2   Chemical analysis of the positive method control and quantification of paclitaxel

UPLC-PDA-HRMS analysis of the standardised fractions of the positive method control indicated that paclitaxel **(1)** was largely present in the fraction PM0206xf6 (fraction 6) as seen in Figure 2-21 and Figure 2-22. The extracted ion 854.3 *m/z* in PM0206xf6 had an identical RT (min) and mass fragment pattern as the 50 ppm paclitaxel **(1)** standard, confirming the presence of paclitaxel **(1)**. The concentration of paclitaxel **(1)** was quantified in fraction PM0206xf6 using the UPLC-PDA-HRMS standard curve shown in Figure 2-23. The standard curve had a regression line expressed in Equation 2-9.
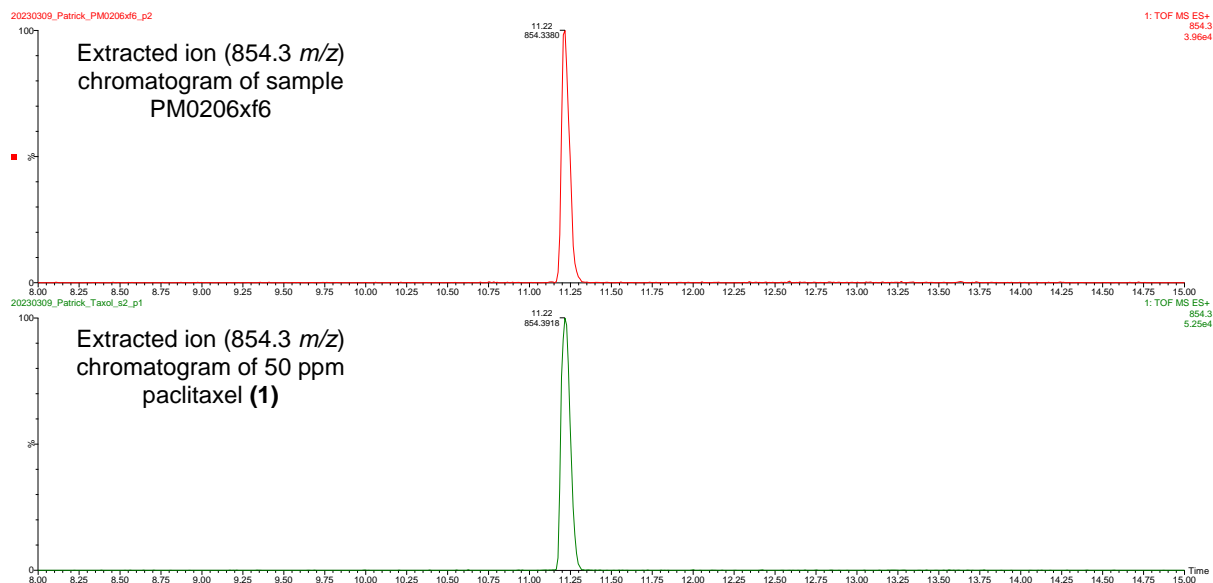
Figure 2-21 The UPLC-PDA-HRMS extracted ion 854.3 *m/z* chromatograms in positive ESI mode of the fraction PM0206xf6 (top) and a 50 ppm paclitaxel **(1)** standard (bottom).
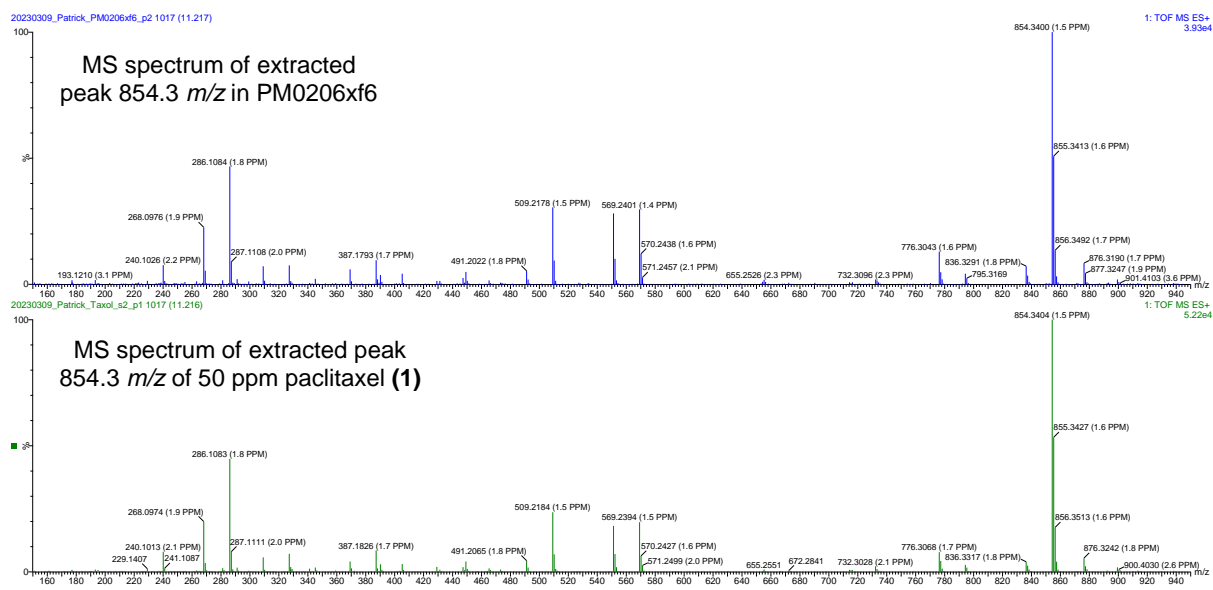
Figure 2-22 The positive ESI mode mass spectra of the extracted ion 854.3 *m/z* peaks shown in the UPLC-PDA-HRMS chromatograms in Figure 2-21.

41
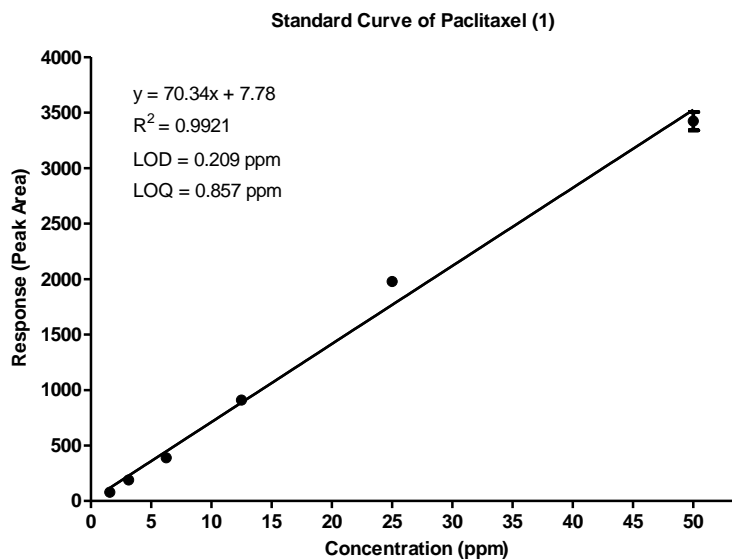
Figure 2-23 The UPLC-PDA-HRMS standard curve of paclitaxel **(1)**.

Equation 2-9 The formula describing the Line of Regression for the standard curve of paclitaxel **(1)**.

$$F(x) = 70.34x + 7.78$$

The coefficient of determination (R^2) was calculated as $R^2 = 0.9921$ which indicated a strong correlation that further justified the accuracy of calculated paclitaxel **(1)** concentrations. The calculated LOD and LOQ concentrations of paclitaxel **(1)** on the UPLC-PDA-HRMS were 0.209 ppm (0.245 µM) and 0.857 ppm (1.00 µM), respectively. Other than fraction PM0206xf6, paclitaxel **(1)** was detected in the sequential fraction PM0206xf7 but was below the limit of quantification thus its presence is presumed to be negligible This demonstrated that the fractionation method developed by the NCI NPNPD project was able to concentrate compounds within a few fractions. It was determined that the concentration of paclitaxel **(1)** in the fraction PM0206xf6 standardised at 4.925 mg/mL in DMSO was 0.1409 mg/mL (140.9121 ppm). It was calculated that the recovery was extremely poor as only 6.23 % of the spiked paclitaxel **(1)** was recovered. This was due to the intensive drying technique used when adsorbing the spiked extract onto the dental cotton roll during pre-extract fractionation. Not all of the loaded extract was completely dissolved during the fractionation as the mass recovery was less than 30 % as seen in Section 2.3.1.3.

42

2.3.2.3 Biological screening of method controls and paclitaxel against the cell line A549

The *in vitro* screening results of the negative and positive method controls along with paclitaxel **(1)** against the cell line A549 in an SRB **(15)** assay are shown in Figure 2-24 and Figure 2-25.
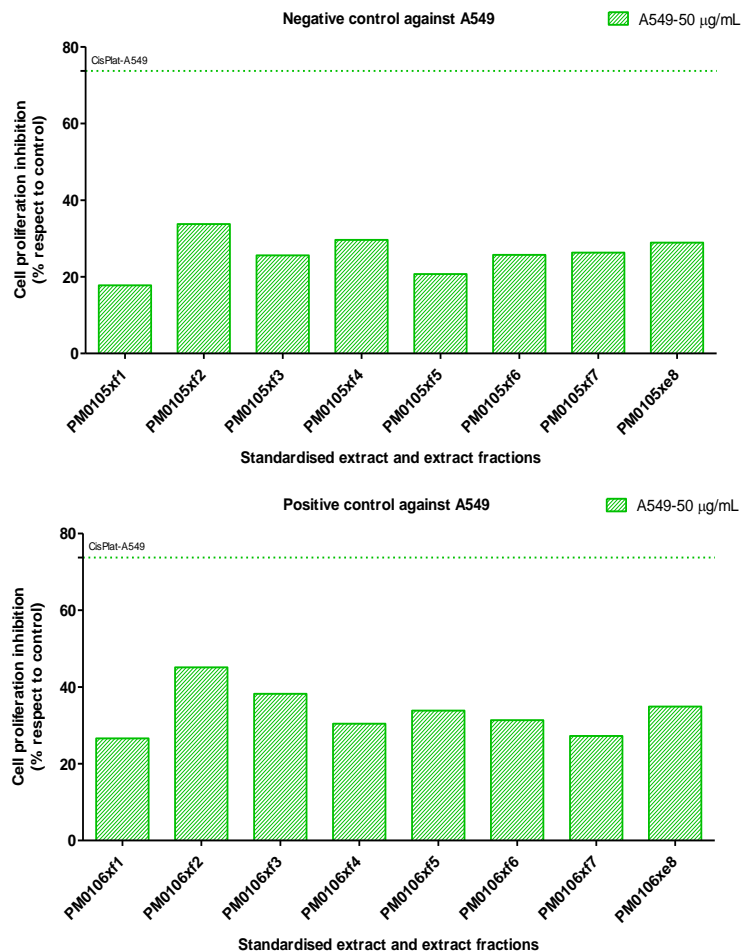
Figure 2-24 The cell proliferation inhibition (%) of the negative (top) and positive (bottom) method controls against the cell line A549.
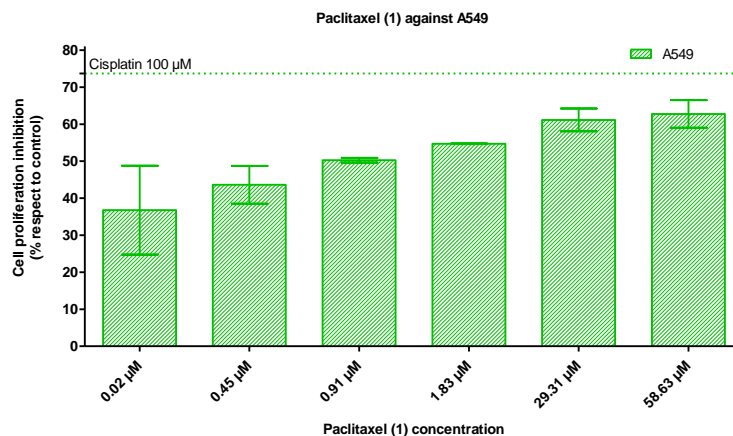
Figure 2-25 The cell proliferation inhibition (%) of paclitaxel **(1)** at different concentrations against cell line A549.

43

As shown in Figure 2-24, both method controls did not exhibit any cell proliferation inhibition greater than 50 % against the cell line A549. This verified that no contamination was introduced during the plant preparative methods that could have resulted in false activity but the loss of activity was suspected. As the standardised fraction PM0206xf6 was diluted 100-fold to a screening concentration of 49.25 µg/mL as outlined in Section 2.2.2.3, the actual concentration of paclitaxel **(1)** screened was calculated to be 1.65 µM (1.409 ppm). In Figure 2-24, the fraction PM0206xf6 unexpectedly exhibited a cell proliferation inhibition of 31.43 %. As shown in Figure 2-25, in the dose-response of paclitaxel **(1)** against the cell line A549, a cell proliferation inhibition greater than 50 % at 1.83 µM was observed. It was taken into consideration that the likely presence of other interfering compounds in the positive control extract was the reason for not observing similar activities. This phenomenon is a common occurrence in natural product chemistry. Thus, the plant preparative methods do not destroy or degrade possible bioactive compounds present in the extract or fractions.

Additionally, the decrease in the cell proliferation inhibition activity of paclitaxel **(1)** is expected as the screening concentration decreases. The experimental IC_{50} of paclitaxel **(1)** against the cell line A549 in the SRB **(15)** assay was calculated to be 0.867 µM, shown in Figure 2-26. The reported IC_{50} of paclitaxel **(1)** against the cell line A549 was 0.947 µM (0.8087 mg/mL) in a Cell Counting Kit-8 assay (CCK-8)[22]. After taking into consideration that the IC_{50} values from different assay methods should not be directly compared, the experimental IC_{50} is fairly similar to the reported IC_{50} concentration. This verified that the integrity of the cell line was not compromised and that there was a sufficient concentration of paclitaxel **(1)** present during screening to have produced a similar response as the reported IC_{50} concentration.
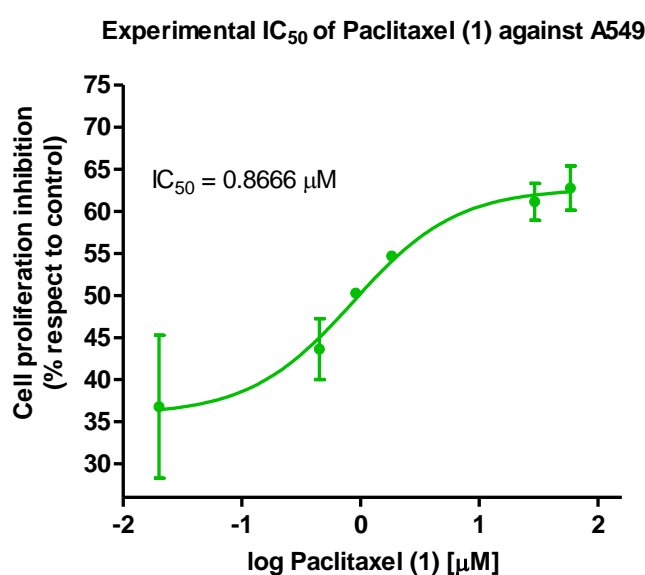
Figure 2-26 The dose-response graph of paclitaxel **(1)** against the cell line A549.

44

2.4 Conclusion

Despite South Africa being a megadiverse country and having a rich multicultural heritage with an impressive traditional knowledge about medicinal plants, limited resources and unavailable technologies have prevented the creation of an open access platform to fully utilise the opportunity of conducting world leading research. The successful creation of a natural product library will continue to allow open access to a growing trusted collection of South Africa's biodiversity for drug discovery research. The platform is the first South African natural product library that standardises plant materials in a format that is compatible with HTS and long-term storage. To expand the diversity of compounds available in the library, the sample preparative methods will be later optimised for biological materials from sources other than terrestrial plants such as microbial and marine samples. Further work includes the creation and open access of over 80 000 standardised plant extracts and fractions from the 10 000 plant samples stored in the Chemistry Department at the University of Pretoria. To date, the South African natural product library contains approximately 4 000 standardised semi-purified plant fractions and over 500 standardised crude plant extracts. The library has already been used in other projects to identify bioactive compounds against diseases like anti-plasmodial, anti-trypanosomal, anti-viral (SARS-CoV-2) and antitubercular (efflux pump and biofilm formation inhibitors). The success of developing a functioning platform provides a reenergised determination for drug discovery by investigating South Africa's medicinal plants and biodiversity for potentially novel compounds.

2.5 References

1. Potterat, O. & Hamburger, M. Combined use of extract libraries and HPLC-based activity profiling for lead discovery: potential, challenges, and practical considerations. *Planta Med.* **80**, 1171–81 (2014).

2. Atanasov, A. G., Zotchev, S. B., Dirsch, V. M., International Natural Product Sciences Taskforce & Supuran, C. T. Natural products in drug discovery: advances and opportunities. *Nat. Rev. Drug Discov.* **20**, 200–216 (2021).

3. Wilson, B. A. P., Thornburg, C. C., Henrich, C. J., Grkovic, T. & O'Keefe, B. R. Creating and screening natural product libraries. *Nat. Prod. Rep.* **37**, 893–918 (2020).

4. McCloud, T. G. High throughput extraction of plant, marine and fungal specimens for preservation of biologically active molecules. *Molecules* **15**, 4526–63 (2010).

5. Thornburg, C. C. *et al.* NCI Program for Natural Product Discovery: A Publicly-Accessible Library of Natural Product Fractions for High-Throughput Screening. *ACS Chem. Biol.* **13**, 2484–2497 (2018).

6. The Griffith Institute for Drug Discovery. NatureBank.

https://www.griffith.edu.au/institute-drug-discovery/unique-resources/naturebank.

7. NIH: National Cancer Institute. The NCI Program for Natural Product Discovery (NPNPD) Prefractionated Library. https://dtp.cancer.gov/organization/npb/npnpd_prefractionated_library.htm.

8. Evans, J. R. *et al.* National Cancer Institute (NCI) Program for Natural Product Discovery: Exploring NCI-60 Screening Data of Natural Product Samples with Artificial Neural Networks. *ACS Omega* **8**, 9250–9256 (2023).

9. Fouche, G. *et al.* In vitro anticancer screening of South African plants. *J. Ethnopharmacol.* **119**, 455–461 (2008).

10. Shoemaker, R. H. The NCI60 human tumour cell line anticancer drug screen. *Nat. Rev. Cancer* **6**, 813–823 (2006).

11. Alley, M. C. *et al.* Feasibility of Drug Screening with Panels of Human Tumor Cell Lines Using a Microculture Tetrazolium Assay1. *Am. Assoc. Cancer Res.* **48**, 589–601 (1988).

12. Rubinstein, L. V. *et al.* Comparison of in vitro anticancer-drug-screening data generated with a tetrazolium assay versus a protein assay against a diverse panel of human tumor cell lines. *J. Natl. Cancer Inst.* **82**, 1113–8 (1990).

13. Monks, A. *et al.* Feasibility of a high-flux anticancer drug screen using a diverse panel of cultured human tumor cell lines. *J. Natl. Cancer Inst.* **83**, 757–66 (1991).

14. Sylvester, P. W. Optimization of the tetrazolium dye (MTT) colorimetric assay for cellular growth and viability. *Methods Mol. Biol.* **716**, 157–68 (2011).

15. Amin, A., Gali-Muhtasib, H., Ocker, M. & Schneider-Stock, R. Overview of major classes of plant-derived anticancer drugs. *Int. J. Biomed. Sci.* **5**, 1–11 (2009).

16. Voigt, W. Sulforhodamine B assay and chemosensitivity. *Methods Mol. Med.* **110**, 39–48 (2005).

17. Salehi, B. *et al.* Phytotherapy and food applications from Brassica genus. *Phytother. Res.* **35**, 3590–3609 (2021).

18. Cheng, X. *et al.* Studies on repository compound stability in DMSO under various conditions. *J. Biomol. Screen.* **8**, 292–304 (2003).

19. Zitha-Bovens, E. *et al.* COMDECOM: predicting the lifetime of screening compounds in DMSO solution. *J. Biomol. Screen.* **14**, 557–65 (2009).

20. Evans, W. C. & Evans, D. The search for naturally derived anticancer agents. in *Trease and Evans' Pharmacognosy* 416–427 (Elsevier, 2009). doi:10.1016/B978-0-7020-2933-2.00027-7.

21. ALANI, H., OZASLAN, M., KARAGOZ, I. D. & SIMITCIOGLU, B. Investigation of Antimicrobial, DNA Protective and Cytotoxic Activity of Red Cabbage (Brassica Oleracea L. Var. Capitata F. Rubra) Plant. *Eurasia Proc. Sci. Technol. Eng. Math.* **12**,

123–129 (2021).

22.   Pu, J., Shen, J., Zhong, Z., Yanling, M. & Gao, J. KANK1 regulates paclitaxel resistance in lung adenocarcinoma A549 cells. *Artif. Cells, Nanomedicine, Biotechnol.* **48**, 639–647 (2020).

Chapter 3: High-throughput screening a small subset of the South African natural product library against cancer

3.1   Introduction

3.1.1   Plants selection strategies

The selection of medicinal plant species is arguably the first crucial step when planning to start a successful natural product drug discovery project. The selection of medicinal plant species can either be completely random or a tailored selection of medicinal plant species with some significance towards reaching the desired outcome. This project makes use of the latter approach by selecting plant species that have been used in South Africa traditional medicinal practices i.e., an ethnopharmacological approach. An ethnopharmacological approach helps expedite the selection of medicinal plants based on their reported traditional usage.

Selecting plant species using an ethnopharmacological approach is more complicated and time consuming than it seems. Aspects such as the accessibility and availability of the plant material or even the preference for certain medicinal plants over others must be evaluated. The selection criteria in the ethnopharmacological preferential scoring systems must favourably score the medicinal plant species with plant material available and reported usage for treating cancer related symptoms. Previously, ethnopharmacological preferential scoring systems have been successful in preferentially selecting medicinal plant species that have shown excellent *in vitro* activity against diseases like malaria and Alzheimer's disease[1,2]. One disadvantage of an ethnopharmacological preferential scoring system is that the majority of plant species used in traditional medicinal practises are often only reported for the treatment of symptoms. Rarely are plant species described for the treatment of specific diseases and even less so for variants of the same disease[3]. Plant selection becomes even more challenging as the treatment of cancer is not clearly described in traditional medicinal practises. To overcome this, a correlation between the common symptoms of different cancer types as described by the NCI and summarised in Table 7, was used to associate and correlate the medicinal plant species described for treating similar symptoms.

Table 7 A correlation between 10 common symptoms and possible cancer types.

Symptom	Cancer Type
Abdominal pain	Colon, renal, Leukaemia, hepatic and pancreatic cancer
Rheumatic	Leukaemia
Diarrhoea	Colon cancer
Back pain	Bladder, hepatic, pancreatic and prostate cancer

48

Appetite loss	Renal, Leukaemia, hepatic, lung and pancreatic cancer
Urinary	Bladder, renal and prostate cancer
Internal pain	Leukaemia
Nausea	Hepatic cancer
Blood urine	Bladder, renal and prostate cancer
Vomiting	Colon and hepatic cancer

3.1.2 Standardisation of the selected medicinal plant species using the South African natural product library's preparative methods

As the bioassay protocols have progressed and developed over the years, they've become more orientated towards target-specific and higher throughput applications[4]. This resulted in the decreased usage of crude natural product extracts in screening programs in both academia and industry. The decline in usage of crude plant extractions in screening programs resulted in the creation of semi-purified or fractionated natural product extract libraries. The use of standardised fractionated natural product extracts in screening programs quickly showed improvement in screening performances[5]. Additionally, another benefit of screening fractionated natural product extract libraries include the lower production costs of standardised samples when compared to pure compound libraries[4]. The application of fractionated natural product extract libraries in automated, HTS programs is a big advantage for bioactive compound discovery in both academia and industry[6]. The medicinal plant species selected were prepared and standardised using the methods described in Chapter 2 Section 2.2.1.

3.1.3 High-throughput screening against human cancer cell lines

3.1.3.1 Lung cancer

Currently, lung cancer is the second most prevalent cancer type in the world with over 2.2 million new cases reported in 2020. In 2020, it was estimated worldwide that over 1.1 million men and over 600 000 women lost their lives to lung cancer[7]. In South Africa, an estimated 108 168 new cases of cancer were reported in 2020 of which 8.3 % were lung cancer as shown in Figure 3-1.

Estimated number of new cases in 2020, South Africa, both sexes, all ages

Total : 108 168
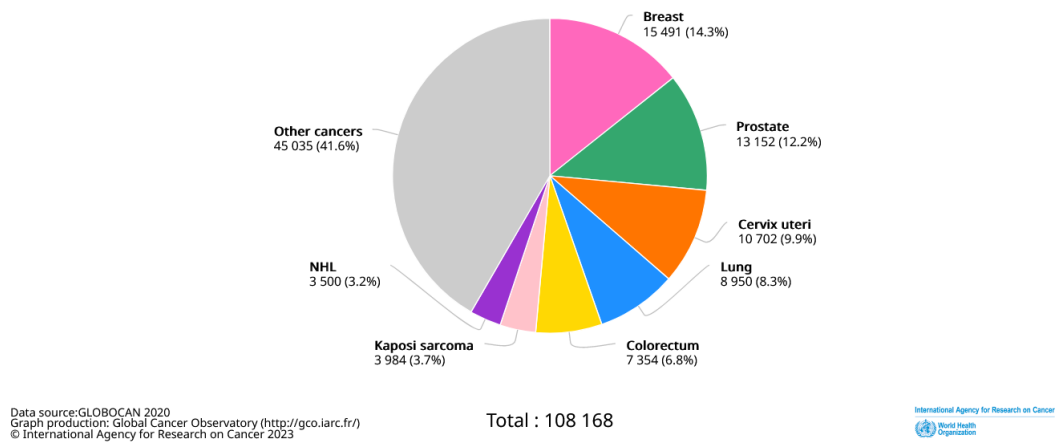
Figure 3-1 The estimated number of new cancer cases in South Africa 2020.

Lung cancer types are classified by their histology into non-small cell lung cancer (NSCLC) and small cell lung cancer (SCLC). Close to 85 % of all reported lung cancer cases are NSCLC, which mainly consist of the following subtypes: adenocarcinoma, large cell carcinoma and squamous cell carcinoma[8]. Since the treatment and prognoses of NSCLC subtypes are similar, they are collectively referred to as NSCLC. The current treatments for NSCLC are chemotherapy, radiotherapy and surgical removal. It is well recognised that the occurrence and proliferation of lung cancer is controlled by both epigenetic and genetic events[9]. Many variants of human NSCLC cell lines are available for use in research and drug discovery fields. A commonly used NSCLC cell line is A549, an epithelial adenocarcinoma that was derived from a 58-year-old male patient in 1972[10]. The A549 cell line is a hypotriploid human cell line with a modal chromosome number of 66 found in approximately 24 % of all cells. Additionally, the cell line was selected to be 1 of 9 NSCLC cell lines on the NCI-60 human tumour cell lines panel as it was considered a relatively sensitive cell line[11].

3.1.3.2   Breast cancer

Breast cancer is the most prominent cancer type with more than 2.26 million new cases and close to 700 000 deaths worldwide in 2020[12]. As seen in Figure 3-1, 14.3 % of new cancer cases estimated in South Africa 2020 were breast cancer related highlighting the prevalence of breast cancer. A few recognised factors that contribute to an increased risk of breast cancer are: age, geographical location, ethnic background, frequency of pregnancies, genetic predisposition, diet and intake of oral contraceptives[13]. Unfortunately, the incidence and

50

mortality rates of breast cancer are still increasing irrespective of the massive advancement in treatment and awareness programs[14].

Breast cancer is classified into 3 major categories: non-hormonal related human epidermal growth factor receptor 2 (HER2) positive breast cancer (HER2+), triple-negative breast cancer (TNBC) and luminal breast cancer (LBC)[15]. The categories are differentiated by the expression of HER2, oestrogen receptor (ER) and progesterone receptor (PR) of each cancer type[16,17]. About 70 % of all breast cancers are reported to over express ER resulting in cancer cells to be dependent on high levels of oestrogen to support cell proliferation[18]. One treatment approach is hormonal therapy which prevents or limits oestrogen from binding to ER in oestrogen dependent breast cancers. Breast cancer cells are known to vary a lot in expression profiles which makes identifying, targeting and treatment of the cancer even more problematic. HER2+ is formed due to over-expression of the HER2 gene that encodes for the transmembrane glycoprotein receptor p185, which is detected in nearly 30 % of all invasive breast cancer cases. The over-expression of the HER2 gene was also reported in oesophageal, gastric and other non-breast cancer types[15]. TNBC occurs when there is no expression in the HER2, ER or PR membrane receptors, making it resistant to the available chemotherapy treatments[17,19]. TNBC is the most aggressive form of breast cancer with the worst survival rate, amongst the breast cancer types, for patients with cancer recurrence. The TNBC has an incidence rate of 10-20 %, mainly in younger women[19]. LBC is characterised by the definite expression of the ER on cell membranes with either HER2 or PR. Based on immunohistochemical profiles, LBC is sub-categorised in luminal A or luminal B subtypes. In the luminal A subtype, the PR is present and the HER2 is absent where in the luminal B subtype, the PR is absent and the HER2 is present[15]. Luminal A represents a breast cancer subtype that is associated with a low relapse occurrences, better prognosis and higher survival rates when compared to the luminal B subtype. The use of human cancer-derived cell lines in cancer research is extremely beneficial as they carry the specific genetic alterations of the cancer cells they were isolated from[15]. A commonly research human breast cancer cell line is MCF7 (luminal A subtype) that was isolated from the pleural effusion of a 69-year-old patient with breast cancer. Treatment with anti-oestrogen chemotherapy drugs have shown to slow or stop the growth of MCF7 by blocking the binding of oestrogen to ER. Additionally, MCF7 was selected to be 1 of 7 breast cell lines on the NCI-60 human tumour panel[11].

3.1.3.3 Colorectum cancer

Colorectum cancer is the third most prevalent cancer in the world with an estimated 1.9 million new cases in 2020. In 2020, it was estimated that over 515 000 men and 419 000 women lost their lives to colorectum cancer[20]. In South Africa 2020, there was an estimated 7 354 new

cases of colorectum as seen in Figure 3-1. There has been a gradual increase in the incidence of colorectum cancer with an estimated increase in the death toll of more than 60 % by the year 2035[21]. There are several non-invasive and invasive detection methods to identify colorectal cancer before symptoms appear. Non-invasive techniques such as a stool tests require a small stool sample to be tested for the presence of blood in specific tests like the guaiac (FOBT) and faecal immunochemical test[22]. Invasive techniques such as sigmoidoscopy and colonoscopy are still commonly used today and are often paired with precancerous lesion removal[23]. Colorectum cancer is regularly diagnosed in younger individuals as the following factors are associated with an increase in incidence: bad nutritional habits and diets, obesity, sedentarism, drinking and smoking[23]. In most cases, colorectal cancers start off as abnormal tissue growth i.e., polyps, that form on the inner epithelial layer of the colon or rectum. Some of the polyps, not all, become malignant over long periods of time. If a polyp becomes malignant, it will grow into the lining of the colon or rectum until it expands into blood or lymph vessels and travels throughout the body[24]. Most colorectal cancers are epithelial adenocarcinomas as they start in mucus cells that line the inside of the colon and rectum. In both academia and industry, the human epithelial cancer cell line Caco2 has been extensively used as a model of the intestinal epithelial layer. The cell line was derived from a human colorectal adenocarcinoma isolated in the 1970's by Jorgen Fogh at the Sloan-Kettering Cancer Research Institute[25]. The Caco2 cell line is heterogeneous and contains cells with slightly different properties that are similar to the absorptive enterocytes found in the intestines[25]. A common cell membrane receptor of Caco2 is the epidermal growth factor receptor (EGFR), found on almost all cell types including MCF7, along with the following sugar transporters: GLUT1, GLUT2, GLUT3, GLUT5 and SGLT1[23]. The cell line Caco2 is routinely used in studies of transepithelial drug transport to investigate whether a drug is actively or passively transported across the intestinal epithelium[25].

3.1.3.4 FDA approved chemotherapeutic drugs in cancer treatment

Over the last 38 years, the FDA has approved 156 natural products for the treatment of cancers[26]. Shown in Figure 3-2 are a few FDA approved unaltered or dervied natural product drugs used in the treatment of NSCLC, breast cancer and colorectal cancer.

52
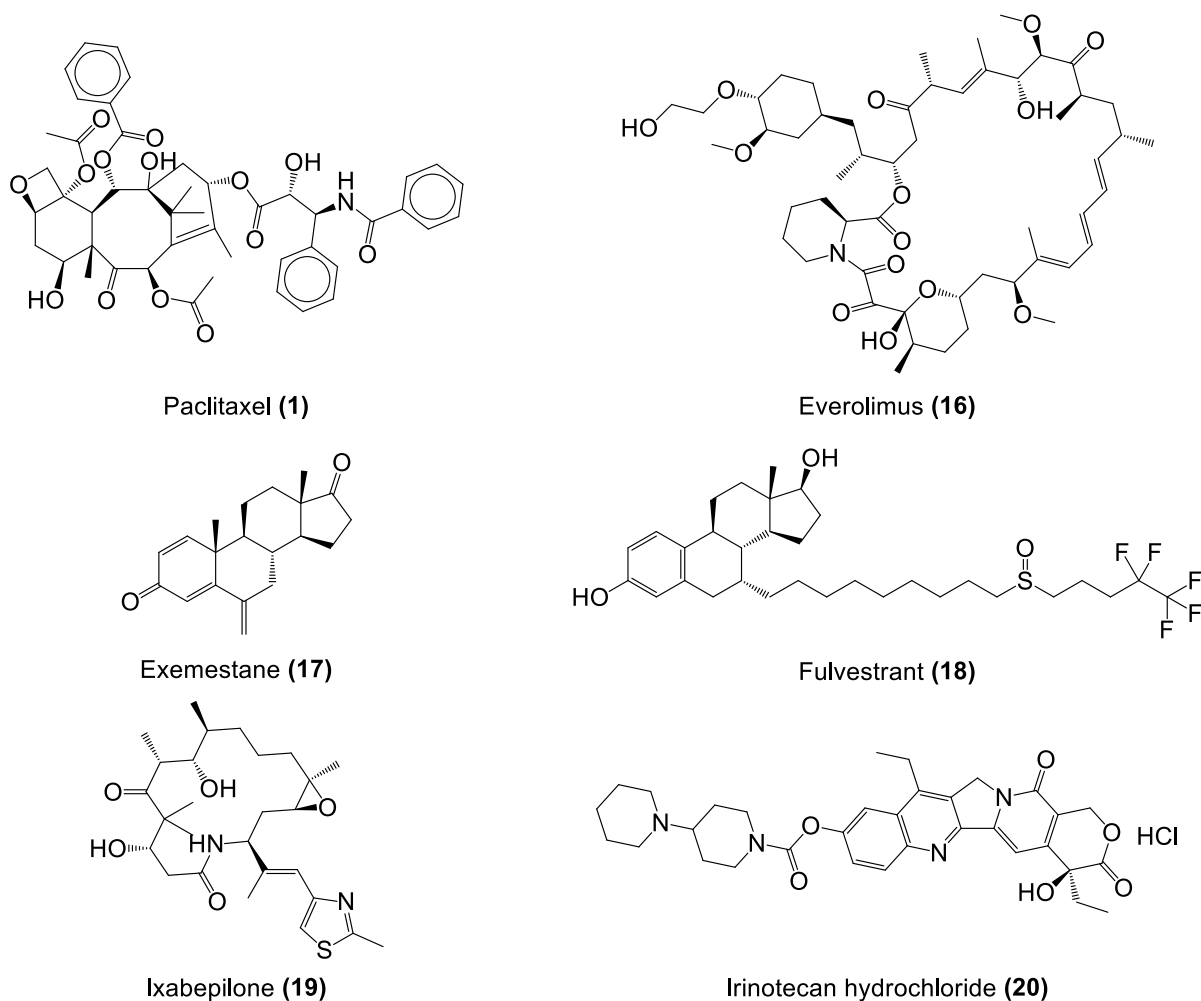
Figure 3-2 The chemical structures of a few FDA approved unaltered or dervied natural products used in the treatment of lung, breast and colorectal cancer.

Paclitaxel **(1)** is extensively used in the treatment of NSCLC as well as various types of breast cancer[9,15]. Everolimus **(16)**, exemestane **(17)**, fulvestrant **(18)** and ixabepilone **(19)** are all currently used in the treatment of various breast cancers[27–30]. Irinotecan hydrochloride **(20)** is one of the key chemotherapeutic drugs used in the treatment of metastatic colorectal cancer[31].

3.2 Materials and methods

3.2.1 Preferential plant scoring and selection

A relevant literature study (1 book and 6 review publications) was carried out that identified indigenous or naturalised medicinal plant species used within South Africa[3,32–37]. The majority of the literature study referenced the works of Anne Hutchings and two articles published by the CSIR. The book Zulu Medicinal Plants: An Inventory by Anne Hutchings contained detailed information of over 1 000 plants species that are traditionally used by the Nguni (Zulu) ethic

group native to South Africa[32]. The two articles published by the CSIR reported on the moderate and potent activity of different South African plant species from a larger screening of 7 500 plant extracts against the human cancer cell lines: MCF7, TK10 and UACC62[3,37]. The medicinal plant species identified during the literature study were listed if the traditional medicinal usage explicitly stated for the treatment of cancer and/or the treatment of one or more cancer related symptoms. The list of identified plant species was further refined to plant species with material available in the plant depository at the University of Pretoria. The resultant list contained the plant species, with material available, that have the highest likelihood of success to be used as a treatment against different cancer types. Finally, the list of medicinal plant species was ranked based on the scores from the ethnopharmacological preferential scoring system similar to other projects that used this approach[1,2].

The following scoring criteria and score assignments were used to rank the list of potential medicinal plant species:

a) Has the plant's traditional usage been reported for treatment of a cancer (1= the plant species has been specifically reported to not be used in the treatment of cancer, 2= no usage has been reported for treatment of a cancer, 3= the plant species has been reported for the treatment of cancer),

b) Has the plant's traditional usage been reported for the treatment of a cancer related symptom (1= the plant species has been specifically reported to treat no cancer related symptoms, 2= the plant species has been reported to treat one cancer related symptom, 3= the plant species has been reported to treat two or more cancer related symptoms),

c) Has the plant's traditional usage been reported for treatment of cancer related symptoms of two different cancer types (1= the plant species has been specifically reported to treat a symptom against one cancer type, 2= the plant species has been reported to treat a symptom of two different cancer types, 3= the plant species has been specifically reported to treat two symptoms against two different cancer types),

d) Has the plant's toxicity been reported (1= it has been reported that all plant parts are toxic, 2= it has been reported that one of the plant parts is toxic, 3= it has been reported that none of the plant parts are toxic),

e) Has the plant's anti-cancer activity been reported in published articles (1= the plant has been reported inactive or not tested, 2= the plant's anti-cancer activity has been reported with the active compound identified, 3= the plant's anti-cancer activity has been reported without the active compound identified),

f) Has a related species in the same genus of the plant been reported for anti-cancer activity (1= the entire genus is inactive or not tested for activity, 2= the plant's genus is reported to have moderate activity, 3= the plant's genus is reported to have excellent activity).

54

The selection of plant species appropriate for continuation of the project were finalised by applying a minimum cut-off score of 13. A few plant species from the published work of the CSIR were of interest and given a perfect score of 18.

3.2.2 Standardisation using the South African natural product library's plant preparative methods

3.2.2.1 Plant material collection and handling

A few plant species were collected from the Manie van der Schijff Botanical Gardens on Hatfield campus, University of Pretoria. The remaining plant species were retrieved from the plant depository. The collected plant material was oven dried at 40 °C for 3 days and ground to a particle size of < 40 μm. Herbarium specimens of the collected plant species were deposited and identified at the H.G.W.J. SCHWEICKERDT HERBARIUM (PRU). The herbarium specimens from the plant depository were deposited and identified at SANBI by the CSIR.

3.2.2.2 Ultrasonic bath extraction

As outlined in Chapter 2 Section 2.2.1.2., approximately 7.0 g of each dried plant material was sequentially extracted in an ultrasonic bath for 2 hours using a 50 mL MeOH/DCM (1:1) solution for the first 60 minutes followed by a 50 mL MeOH solution for the remaining time. The plant materials were mechanically stirred before the first 60 minutes of extraction. The plant materials and solvents were kept within individual custom glass percolators that were held upright inside the ultrasonic bath using a custom stainless-steel framework. The extracts were concentrated using a Buchi R300 rotary vacuum evaporator and dried to completion in a SP Scientific Genevac® HT-6 solvent evaporator. The extract yields were reported as a percentage of extract weight (g) per plant material weight (g).

3.2.2.3 Automated plant extract fractionation

As outlined in Chapter 2 Section 2.2.1.3, approximately 200-300 mg of each plant extract was dried onto individual dental cotton rolls using a Genevac® HT-6 solvent evaporator. The extract loaded dental cotton rolls were then fractionated on a HyperSep™ C8 SPE cartridge using a Gilson GX-241 ASPEC® liquid handler into 7 fractions with 7 unique eluent systems of decreasing polarity. The individual fractions were collected on a volume-basis in pre-weighed internally barcoded tubes and dried to completion in a Genevac® HT-6 solvent evaporator. The yields of each fraction were recorded in the appropriate Excel worksheet and reported as a percentage of fraction mass (mg) per weight of plant extract fractionated (mg).

3.2.2.4　Automated plant extract and fraction standardisation

As outlined in Chapter 2 Section 2.2.1.4, all plant extracts and fractions were standardised at a concentration of 5 mg/mL in DMSO and transferred to pre-barcoded storage vials using the Hamilton Microlab® STARlet™ automated liquid handler. The final concentrations and volumes of each standardised plant extract and fraction were automatically recorded in the appropriate Excel worksheet.

3.2.2.5　Automated vial storage and retrieval

As outlined in Chapter 2 Section 2.2.1.5, the pre-barcoded storage vials of the standardised plant extracts and fractions were transferred to high-density 138-format storage racks inside a Hamilton Verso® Q20 at -20 °C. The locations and positions of each pre-barcoded storage vial was recorded by the Verso® Q20.

3.2.2.6　Automated duplication of standardised vials

As outlined in Chapter 2 Section 2.2.1.6, the STARlet™ automated liquid handler transferred 30 µL aliquots of each standardised plant extract and fraction from the pre-barcoded storage vials to three NEST® 2.0 mL Deep Well Plates that were then foil sealed and kept at -40 °C until required for biological screening.

3.2.3　High-throughput screening of the standardised plant extracts and fractions against human cancer cell lines

3.2.3.1　Biological screening against the human cancer cell line A549

The *in vitro* screening was conducted at the Cellular and Molecular Biology centre in the Department of Biochemistry at the JSS Medical College in Mysuru, Karnataka, India and supervised by Professor SubbaRao V. Madhunapantula as part of a collaborative project. The first 10 plant species were screened against the NSCLC cell line A549 in an SRB **(15)** assay. The standardised extracts and fractions were provided as per the method outlined in Chapter 2 Section 2.2.1.6 and screened at a concentration of 50 µg/mL with the positive control cisplatin **(6)** at 100 µM. The cell proliferation inhibition (%) was calculated and reported. The full details of the screening method is outlined in Chapter 2 Section 2.2.2.3.

3.2.3.2　Biological screening against the human cancer cell lines MCF7 and Caco2

The remaining plant species were screened against the cell lines MCF7 and Caco2 at Bioassaix, in an MTT **(13)** assay. Bioassaix is a screening research laboratory supervised by Professor Maryna van de Venter located in the Department of Biochemistry and Microbiology at the Nelson Mandela University in Port Elizabeth, South Africa. I received training and preformed the *in vitro* screening of the remaining plant extracts and fractions at Bioassaix.

56

The reagents Dulbecco's modified eagle media-Low glucose (DMEM-LG) and FBS were purchased from GE Healthcare Life Sciences (Logan, UT, USA). Trypsin and a phosphate buffered saline (PBS) with and without Ca^{2+} and Mg^{2+} was purchased from Lonza (Wakersville, MD, USA). MTT **(13)**, melphalan **(7)** and DMSO were purchased from Sigma (St. Louis, MO, USA). Both the human breast cancer cell line MCF7 and the human colorectal adenocarcinoma cell line Caco2 were purchased from Cellonex, South Africa. 30 µL of each standardised plant extract and fraction was provided as per the method outlined in Chapter 2 Section 2.2.1.6. Melphalan **(7)** (30 µM) was used as a positive control and 2.5 % DMSO was used as a vehicle control. The cells were maintained in 10 cm culture dishes in 10 mL complete medium (DMEM-LG + 10 % FBS + 1x penicillin/streptomycin) and incubated at 37 °C, 5 % CO_2, and 100 % relative humidity. The cells were seeded into 96 well plates at 4 000 cells per well (100 µL aliquots) and left overnight to attach. The seeded cells were treated in duplicates with 100 µL of the standardised extracts and fractions at both 25 µg/mL and 50 µg/mL and incubated for 48 hours at 37 °C and 5 % CO_2. After 48 hours, the medium was removed and followed by the addition of 100 µL MTT **(13)** (0.5 mg/mL) to each well which was left to incubate. After 3 hours, DMSO was added to each well and the OD absorbance was recorded at 540 nm. Cell viability was calculated and the cell proliferation inhibition (%) was reported for each well.

3.3 Results and discussion

3.3.1 Preferential plant scoring and selection

The use of a preferential plant scoring system modelled on the traditional usage of plant species improved the selection process by refining the pool of possible candidates to only the plant species with material available and with a greater potential of identifying anti-cancer compounds. A listing of 1 126 medicinal plant species was refined after the removal of plants species that were not recorded for treating one or more symptoms of cancer and without any material in the plant repository. Only 368 medicinal plant species were scored using the criteria mentioned in Section 3.2.1. Maximum scores were awarded to the plant species of interest from published work by the CSIR[3,37]. After the cut-off score was applied, exactly 100 plant species remained and were deemed suitable for investigation. It was noted that after the cut-off criterium was applied, all the remaining 100 plant species were seen equally preferential and that it was unnecessary to prioritise the plant species with the higher scores. During material collection from the plant repository, it was decided that only the first 34 plant species would be used for the completion of the project. Shown in Table 8 are the final 34 plant species selected for the completion of the study. The table consists of the family name, the plant species name, the plant part used, the voucher number, reported traditional usage, phytochemical constituents and the final score of the collected plant species.

57

Table 8 Information pertaining to the selected plant species.

Family name	Plant species, part and voucher number	Traditional usage	Reported phytochemical constituents	Final score
Plumbaginaceae	*Plumbago zeylanica* Leaves & Stem (130972-23/10/2020)	The roots powdered are applied to warts and used as snuff. Plant infusions are used to treat inflamation[32].	Alkaloids, flavonoids, glycosides, naphthoquinones, plumbagin, steroids, triterpenoids, tannins[38].	18
Asteraceae	*Xanthium strumarium* Stems (P12696)	The fruit is the consumed to treat headaches, rhinitis, nasal diseases, itching and to alleviate pain[39].	Anthraquinones, coumarins, flavonoids, glycosides, lignanoids, naphthoquinones, phenylpropenoids, sesquiterpenoids, steroids, thiazides, xanthinine[39,40].	18
Apiaceae	*Heteromorpha trifoliata* Leaves (P20913)	Leaves are used to treat scrofula and prepared as enemas for abdominal disorders. Root infusions are used for shortness of breath, chest pains, asthma coughs, dysentery, scrofula, colic and as a blood purifier[32].	Falcarindiol and sarisan (antifungal compounds) have been isolated from the leaves[32].	17
Pittosporaceae	*Pittosporum viridiflorum* Bark (P21236)	Bark tinctures or enemas are administered for the treatment of fevers and lower back pain[32].	Alkaloids, flavonoids, saponins, phenols, proanthocyanidin[41].	16
Anacardiaceae	*Sclerocarya birrea* Bark (P25361)	Bark extracts are administered via enemas for the treatment of	Coumarins, flavonoids, phytosterols, polyphenols, tannins, triterpenoids[42].	16

58

		diarrhoea and malaria. The fruits are also used to destroy ticks[32].		
Rutaceae	*Zanthoxylum capense* Leaves (P18523)	The leaves are applied to open sores to accelerate healing while the leaves and stems are inserted into the mouth for toothache[32].	Alkaloids, triterpene steroids, saponins, tannins, quinones, isocomene, siliphinen, modhephene, delta-cadinene, isobienol[32,43].	16
Asteraceae	*Helichrysum nudifolium* Roots (P13625)	Root extracts are consumed as emetics for chest complaints and the treatment of colds[32].	Flavonoids, phloroglucinols, terpenes[44].	14
Euphorbiaceae	*Croton sylvaticus* Roots (P17237)	The bark is administered for abdominal and urinary disorders, dropsical swellings and internal inflammations[32].	Alkaloids, anthraquinones, flavonoids, lignan, phenolics, sterols, tannins, terpenoids, crotin[32,45].	14
Plumbaginaceae	*Plumbago auriculata* Leaves (130591-23/10/2020)	The powdered roots are applied to warts and used as snuff. Plant infusions are used to treat swelling[32].	Alkaloids, carbohydrates with phenol, flavonoids, phenols, plumbagin, proteins, saponins, tannins[46].	14
Lamiaceae	*Plectranthus barbatus* Leaves (130592-21/10/2020)	The plant has been used for digestive, respiratory, circulatory, nervous disorders, infections, aborticide, contraception and pain managment[47].	Diterpenoids[48].	14
Myrsinaceae	*Rapanea melanophloeos* Leaves	The bark is administered as enemas and emetics	Tannins, embelin, triterponoids, sakurasaponin[32].	18

	(P21589)	for treating muscular and stomach pains as well as fevers[32].		
Amaranthacea	*Achyranthes aspera* Whole Plant (P12437)	The powdered roots are used in infusions to treat chest pain and stomach emetics[32].	Alkaloids, carbohydrates, flavonoids, glycosides, phenols, saponins, steroids, tannins, terpenoids[49].	17
Rutaceae	*Zanthoxylum capense* Twigs (P18524)	The leaves are applied to open sores and infusions are ingested as purgative parasiticides[32].	Alkaloids, triterpene steroids, saponins, tannins, quinones[43].	16
Solanaceae	*Physalis peruviana* Roots (P24891)	The leaf infusions are used as enemas to relieve stomach pains and the root sap is used to treat gastric ulcers[32].	Flavonoids, phenols, saponins[50].	16
Asteraceae	*Brachylaena elliptica* Leaves (P21731)	The leaves are used in infusions for enemas to treat biliousness and backache[32].	Alkaloids, flavonoids, flavonols, phenols, proanthocyanidins, saponins, sesquiterpene lactones, tannins[51].	15
Combretaceae	*Combretum molle* Leaves (P25462)	The leaves are used to treat open wounds while the roots are used as for constipation and as an aborticide. A blend of the leaves and roots are used as snakebite antidotes[32].	Alkaloids, cardiac glycosides, coumarins, flavonoids, phenols, steroids, tannins, terpenoids[52].	15
Polygalaceae	*Polygala fruticose* Whole Plant (P22227)	The roots are used to treat diseases affecting veins and arteries, intestinal	Not reported.	15

60

		sores as well as venereal diseases[32].		
Solanaceae	*Solanum aculeastrum* Seeds (P24535)	Fruit decoctions are used as enemas for pain in the lower back, the burn fruit ash is rubbed over the body to relieve pain from rheumatism and the fruits are applied to wounds and injected for haemorrhoids and dysentery[32].	Alkaloids, coumarins, flavonoids, lignans, terpenes, phenolic compounds, sterols, steroidal saponins, solanine[32,53].	15
Strychnaceae	*Strychnos usambarensis* Stems (P23578)	The plant is used to alleviate stomach aches. The stembark and leaves are ingested for local pain and general weakness[32].	Alkaloids (oxindole and bis-indole alkaloids), harmin, strychnofoline, strychnophylline, usambarine[32].	15
Euphorbiaceae	*Euphorbia ingens* Stems (P23438)	The plant latex is applied to skin diseases and warts or taken as a purgative. The plant is also burnt and inhaled for asthma and bronchitis[32].	Tetracyclic diterpenes, macrocyclic terpen alcohols, ingol, steroids[32].	14
Asteraceae	*Helichrysum odoratissimum* Leaves (P24835)	Root decoctions are used as emetics for chest complaints while root infusions aretaken for colds. Water infusions are used in the treatment of prolapsed rectums[32].	α-Pyrone phloroglucinols have been identified[32].	14
Plumbaginaceae	*Plumbago auriculata*	The powdered roots are applied to warts	Alkaloids, carbohydrates with	14

61

	Roots (P24988)	and used as snuff. Plant infusions are used to treat swelling[32].	phenol, flavonoids, phenols, plumbagin, proteins, saponins, tannins[46].	
Solanaceae	*Solanum tomentosum* Whole Plant (P21314)	The plant is used to treat sore throats while root decoctions are used to treat syphilis. The fruit of the plant is applied to skin areas affected by disease[32].	Not reported.	14
Lamiaceae	*Plectranthus cylindraceus* Leaves (P13964)	The plant is ingested to alleviate digestive, respiratory, circulatory and nervous disorders. The plant is used for the relief of colds, cough and bronchitis[47].	Diterpenes, oxygenated monoterpenes, sesquiterpenes, sesquiterpene hydrocarbons[54].	14
Asteraceae	*Brachylaena discolor* Roots (P20791)	Leaf infusions are used for the treatment of diabetes and renal conditions. Root infusions are ingested for stomach haemorrhages and the treatment of chest pain[32].	Onopordopicrin[32].	13
Euphorbiaceae	*Clutia pulchella* Leaves (P24653)	Leaf infusions are ingested to treat stomach-ache as well as diarrhoea and dysentery. Infusions of the leaves, stems and roots are administered as enemas to children	Not reported.	13

		with gastrointestinal pains[32].		
Asteraceae	*Conyza scabrida* Leaves (P23558)	Leaf infusions are taken for coughs and colds. The whole plant is administered for fevers during influenza, for chest and heart complaints. Leaf dressings are applied to inflammation of abdomen[32].	Clerodane derivatives, diterpenoids, hautriwaic acid[32].	13
Lauraceae	*Cryptocarya latifolia* Stems (P17029)	Ground bark is used in the treatments of chest ailments, internal pains, muscle cramps and urinary tract diseases[32].	Copaene, nerolidol, α-pyrone, quercetin-3-O-rhamnoside, β-sitosterol **(29)**[55].	13
Araliaceae	*Cussonia spicata* Stems (P20773)	Root infusions are administered for the treatment of fever. Fruit, stems and roots are used to alleviate nausea. The bark is used for the treatment of stomach ulcers[32].	Not reported.	13
Meliaceae	*Ekebergia capensis* Leaves (P17761)	Bark decoctions are taken for heartburn or chest complaints and coughs. The leaves are used for abscesses[32].	Coumarins, limonoids, phenolic compounds, steroids, triterpenoids[56].	13
Fabaceae	*Erythrina caffra* Leaves (P19980)	The leaves are used as a poultice that is applied to the bladder for urinary complications[32].	Alkaloids (erysitrine, erythraline), 11-methoxyerythraline, erysodine, erysovine, erythrinine and erysopine[32].	13

Rubiaceae	*Gardenia thunbergia* Leaves (P24165)	The rootbark is used for the treatment of febrile and biliousness[32].	Scopoletin, syringaldehyde **(32)**, tigmasterol, vanillic acid[57].	13
Asteraceae	*Mikania capensis* Leaves (P21619)	Leaves are used for urinary complaints and venereal infections[32].	Not reported.	13
Asteraceae	*Mikania natalensis* Leaves (P24150)	Leaves are used for urinary complaints and venereal infections[32].	Not reported.	13

Since medicinal plant species are often only described for the treatment of symptoms and the treatment of cancer is not clearly described in traditional medicinal practises, a correlation between the common symptoms of different cancer types was successfully related to medicinal plant species that are described to treat similar symptoms. The use of an ethnopharmacological preferential plant scoring system demonstrated how a massive pool of over 2 000 South Africa medicinal plant species were drastically refined down to the plant species most likely to succeed. The refinement step helped mitigate the waste of limited time and resources nonrelevant plant species.

It was observed that the number of plant species decreased as the final scores increased as shown in Figure 3-3. The decrease indicated that the criteria preformed as expected by preferentially scoring the medicinal plant species. However, the trend was slightly skewed as the following species were selected from the published work by the CSIR and awarded a perfect score of 18 points: *Plumbago zeylanica*, *Xanthium strumarium* and *Rapanea melanophloeos*. These plant species showed moderate activity (log $GI_{50} > 0$ to 1.10) when screened by the NCI against sixty human cancer cell lines[37].
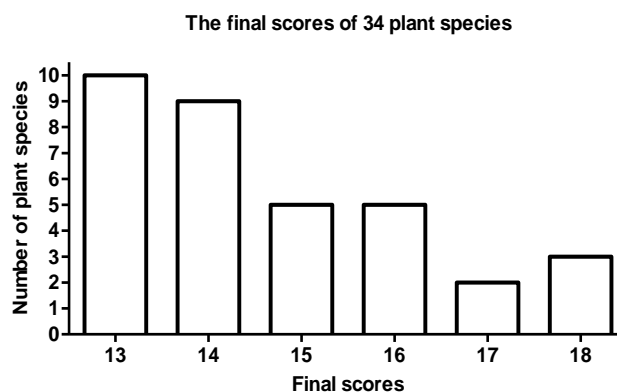
Figure 3-3   The final scored of the selected 34 plant species.

64

Of the final 34 plant species selected for the completion of the study, it was noted that 8 of the plant species are members of the *Asteraceae* family belonging to either the *Brachylaena*, *Conyza*, *Helichrysum, Mikania* or *Xanthium* genera. The *Asteraceae* family is one of the largest flowering plant families that includes over 1 600 genera and 25 000 species worldwide[58]. The members of the *Asteraceae* family include a range of phytochemical compounds such as acetylenes, flavonoids, phenolic acids, polyphenols and triterpenes which have been used in traditional medicines for over 3 000 years. The *Asteraceae* family also includes significant medicinal plants like chamomile, dandelion and wormwood. The members of the *Asteraceae* family have shown anti-inflammatory, antimicrobial and antioxidant activity[59].

3.3.2 Standardisation using the South African natural product library's plant preparative methods

3.3.2.1 Ultrasonic bath extraction

The ultrasonic bath extraction method showed to be both high-throughput and robust for the large and diverse number of plant species. The ultrasonic bath extraction yields of all the selected plant species are shown in Table 9.

Table 9 The ultrasonic bath extraction yields of all the selected plant species.

Plant species (Specimen number)	Plant extract barcode	Plant material (g)	Plant extract (g)	Yield (%)
Plumbago zeylanica (130972)	PM0204x	7.00	0.377	5.38
Xanthium strumarium (P12696)	P12696x	7.00	0.865	12.35
Heteromorpha trifoliata (P20913)	P20913x	6.92	1.022	14.77
Pittosporum viridiflorum (P21236)	P21236x	6.97	0.397	5.70
Sclerocarya birrea (P25361)	P25361x	7.37	0.870	11.80
Zanthoxylum capense (P18523)	P18523x	6.98	0.435	6.24
Helichrysum nudifolium (P13625)	P13625x	7.01	0.413	5.89
Croton sylvaticus (P17237)	P17237x	7.12	0.923	12.96

Plumbago auriculata (130591)	PM0203x	7.37	0.429	5.82
Plectranthus barbatus (130592)	PM0102x	7.09	0.816	11.50
Rapanea melanophloeos (P21589)	P21589x	7.13	0.559	7.84
Achyranthes aspera (P12437)	P12437x	6.91	0.329	4.76
Zanthoxylum capense (P18524)	P18524x	6.96	0.343	4.93
Physalis peruviana (P24891)	P24891x	7.14	0.519	7.27
Brachylaena elliptica (P21731)	P21731x	6.93	0.480	6.93
Combretum molle (P25462)	P25462x	7.06	0.627	8.88
Polygala fruticose (P22227)	P22227x	7.18	1.179	16.41
Solanum aculeastrum (P24535)	P24535x	6.92	1.498	21.64
Strychnos usambarensis (P23578)	P23578x	7.12	0.834	11.71
Euphorbia ingens (P23438)	P23438x	14.17	0.359	2.53
Helichrysum odoratissimum (P24835)	P24835x	7.14	0.741	10.37
Plumbago auriculata (P24988)	P24988x	7.11	0.459	6.46
Solanum tomentosum (P21314)	P21314x	7.07	0.423	5.98
Plectranthus cylindraceus (P13964)	P13964x	6.90	0.484	7.01
Brachylaena discolor (P20791)	P20791x	7.07	0.447	6.32
Clutia pulchella (P24653)	P24653x	6.57	0.415	6.32
Conyza scabrida (P23558)	P23558x	7.01	1.242	17.71

Cryptocarya latifolia (P17029)	P17029x	6.92	0.348	5.03
Cussonia spicata (P20773)	P20773x	7.06	0.371	5.26
Ekebergia capensis (P17761)	P17761x	7.20	0.563	7.82
Erythrina caffra (P19980)	P19980x	6.74	0.553	8.20
Gardenia thunbergia (P24165)	P24165x	7.07	0.294	4.15
Mikania capensis (P21619)	P21619x	7.09	0.924	13.03
Mikania natalensis (P24150)	P24150x	6.98	0.865	12.39

The extraction method was successful as nearly all of the selected plant species required a single extraction to obtain enough quality plant extract (> 250 mg) for fractionation. The mechanical stirring of the plant materials allowed the dry plant material to easily absorb the solvent and remain below the solvent volume level thus improving the quality. However, the extraction method had to be repeated a second time for the stems of *Euphorbia ingens* (P23438). Shown in Table 10 are the average extract yields of each plant part reported in Table 9.

Table 10 The average extract yield (%) of individual plant parts.

Plant Part	Average Yield (%)
Seeds	21.64
Leaves	9.54
Whole plant	9.05
Roots	7.78
Bark	8.75
Stems	7.38
Leaves and Stems	5.60
Twigs	4.93

It was concluded that approximately 7.0 g of any dried plant part e.g., leaves, stems, roots etc., is sufficient to obtain a minimum of 250 mg required of plant extract using the ultrasonic bath extraction method.

3.3.2.2 Automated plant extract fractionation

All the plant extracts were fractionated on a HyperSep™ C8 SPE cartridge using a Gilson GX-241 ASPEC® liquid handler into 7 fractions with 7 unique eluent systems of decreasing polarity. The automated fractionation method worked as expected producing 238 unique fractions from 34 plant extracts that was adequate for standardisation. The average fraction yield of each fraction number is shown below in Figure 3-4 and the full fractionation details are shown in Supplementary data 3-1.

The average yield for each of the 7 fractions
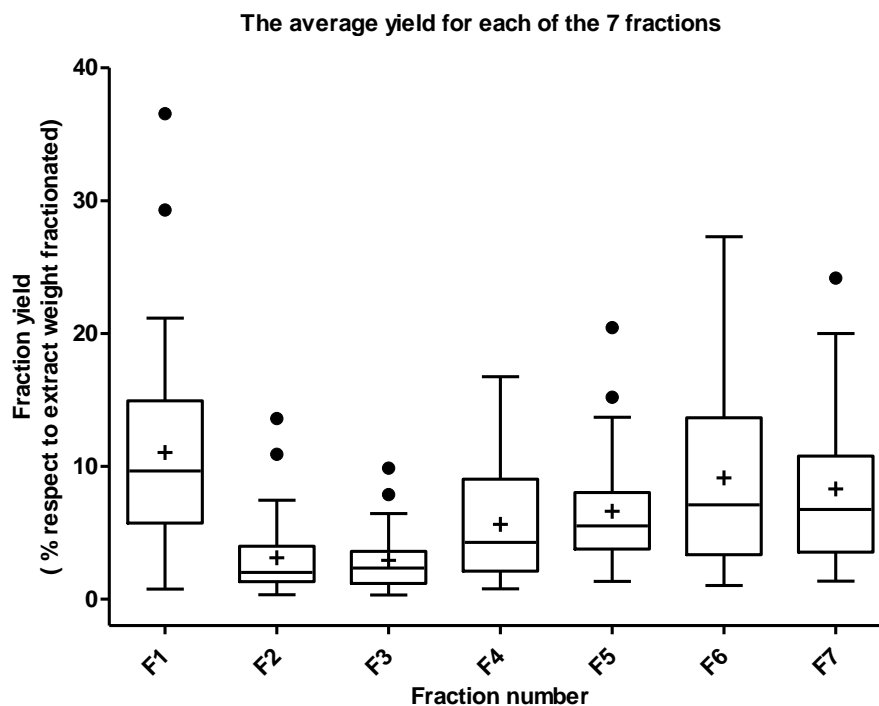
Figure 3-4   The average yield for each of the 7 fractions. The crosses in each box represent the average yield (%) for that particular fraction number while the solid black dots are outliers that are more than 1.5 times the interquartile range[60].

On average, it was observed that the first fraction had the highest yield (%) followed closely by fraction 6 and fraction 7 as shown in Figure 3-4. The higher yields were expected as the NCI NPNPD project's fractionation method was developed around removing artifacts in these fractions[5]. The average mass recovery for each of the plant extracts fractionated using the adapted fractionation method was calculated as 46.75 %. This is relatively low when compared to the average 87.7 % recovery for the fractionation method selected for generating the NCI NPNPD fraction library[4]. It was determined that the mass recovery was poor due to the intensity of the drying technique used when the plant extracts were adsorbed onto the dental cotton rolls. The dental cotton rolls, after soaking up the dissolved plant extract, was dried in a Genevac® HT-6 solvent evaporator that resulted in non-uniform drying and the formation of

a hard extract plug at the bottom of each dental cotton roll. During fractionation, the hard extract plug took a while to fully dissolve resulting in poor mass recovery. Nevertheless, adequate quantities were obtained to standardised the fractions.

3.3.2.3   Automated plant extract and fraction standardisation

The Hamilton STARlet™ liquid handler successfully standardised the 34 plant extracts and 238 fractions at 5 mg/mL in DMSO. Shown in Figure 3-5 are the final storage volumes of each extract and fraction standardised at 5 mg/mL in DMSO. The full details of every standardised extract and fraction are shown in Supplementary data 3-2.

The volume (µL) of each standardised plant extract and fraction in DMSO
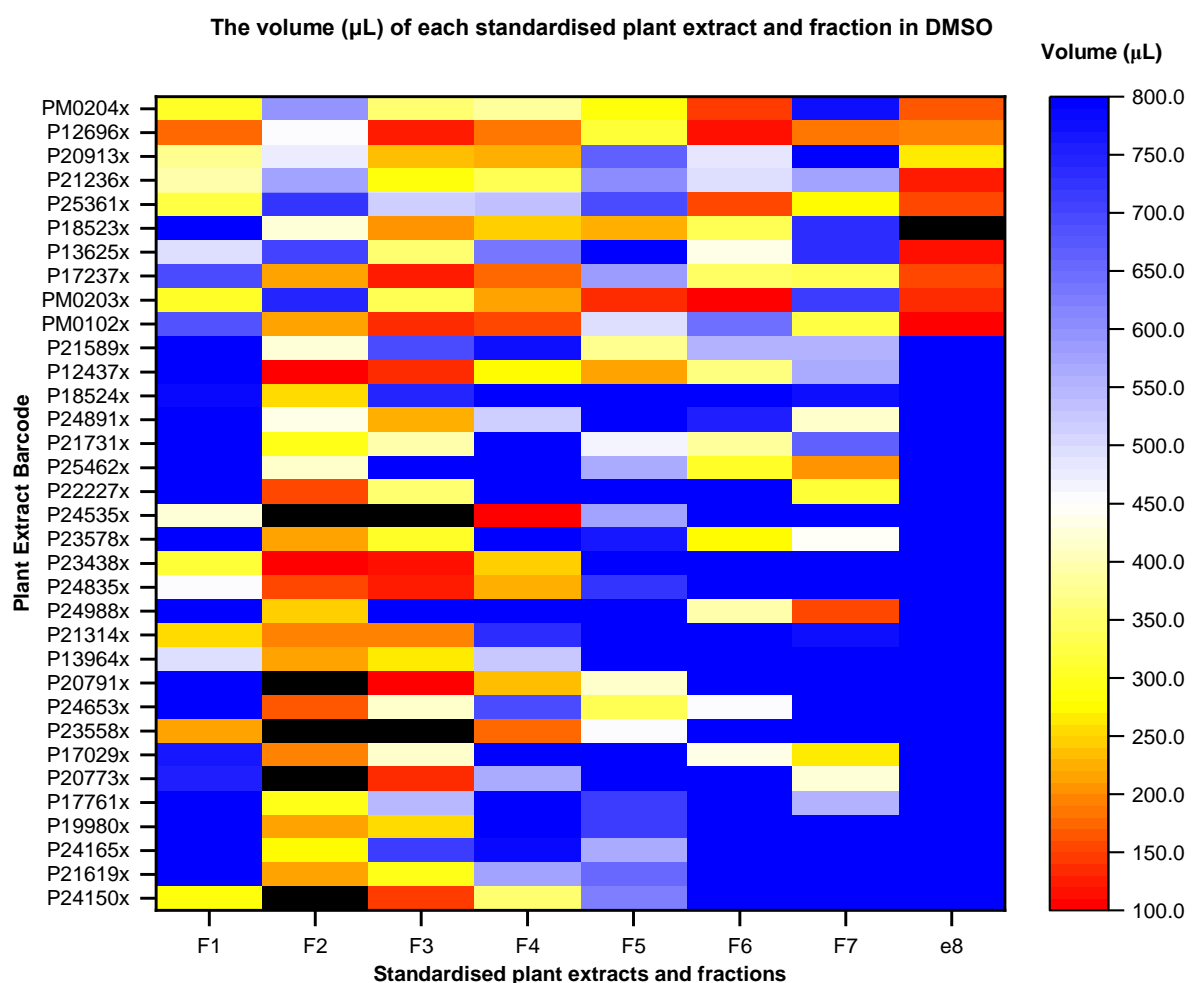
Figure 3-5   The volume of every plant extract and fraction standardised at 5 mg/mL in DMSO.

The volumes of each plant extract and fraction standardised at 5 mg/mL is shown by the respective colour gradient in Figure 3-5. The colour blue represents the max storage volume of 800 µL while the colour black represents the samples that were not standardised at 5 mg/mL

and stored at the minimum DMSO volume of 100 µL. It was observed that only 8 samples (primarily fraction 2) had insufficient mass (< 0.5 mg) transferred to the respective wells in the BioPointe 96 well plate which resulted in a lower standardisation concentration. The liquid-handling errors also corrected 58 fractions with excess mass (> 10.0 mg) transferred to the respective wells in the BioPointe 96 well plate that were successfully diluted and stored at a max DMSO volume of 800 µL. Considering that only 2.94 % of the plant extracts and fractions were not standardised at 5 mg/mL due to insufficient mass transferred indicated that 5 mg/mL was the ideal storage concentration for a large number of samples. The number of extracts and fractions standardised at a lower concentration will decrease as the mass recovery is improved during automated plant extract fractionation.

3.3.2.4   Automated vial storage and retrieval

The pre-barcoded vials of the standardised plant extracts and fractions were transferred to high-density 138-format storage racks inside a Hamilton Verso® Q20 at -20 °C as shown in Figure 3-6. The location and position of each pre-barcoded vial was recorded by the Verso® Q20 and was done according to the automated software programme.

Figure 3-6 The standardised plant extracts and fractions stored in high-density 138-format storage rack inside the Verso® Q20.

It was more than evident that the use of a robotic freezer like the Hamilton Verso® Q20 is a requirement when working with large quantities of samples. In minutes the robotic freezer

automatically scanned and transferred 272 pre-barcoded vials to high-density 138-format storage racks while recording their exact locations.

3.3.2.5 Automated duplication of standardised vials

As shown in Figure 3-7, the Hamilton STARlet™ liquid handler successfully transferred 30 μL from each standardised plant extract and fraction from the pre-barcoded storage vials to three NEST® 2.0 mL Deep Well Plates that were then foil sealed and kept at -40 °C until required for biological screening.
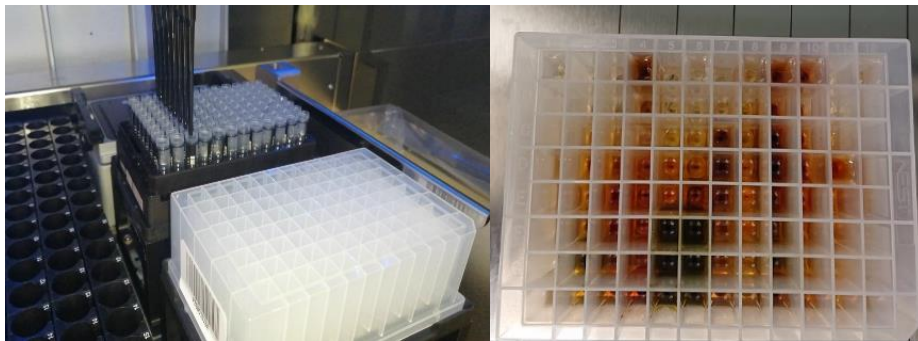
Figure 3-7 The automated duplication of the standardised plant extracts and fractions to a DWP for biological screening.

3.3.3 High-throughput screening of the standardised plant extracts and fractions against human cancer cell lines

3.3.3.1 Biological screening against the human cancer cell line A549

The first 10 standardised plant extracts and respective fractions were screened *in vitro* at 50 μg/mL for 48 hours against the human cancer cell line A549 in an SRB **(15)** assay. The cell proliferation inhibition (%) of the standardised extracts and fractions are summarised in Figure 3-8 with the full details shown in Supplementary data 3-3 to Supplementary data 3-6.
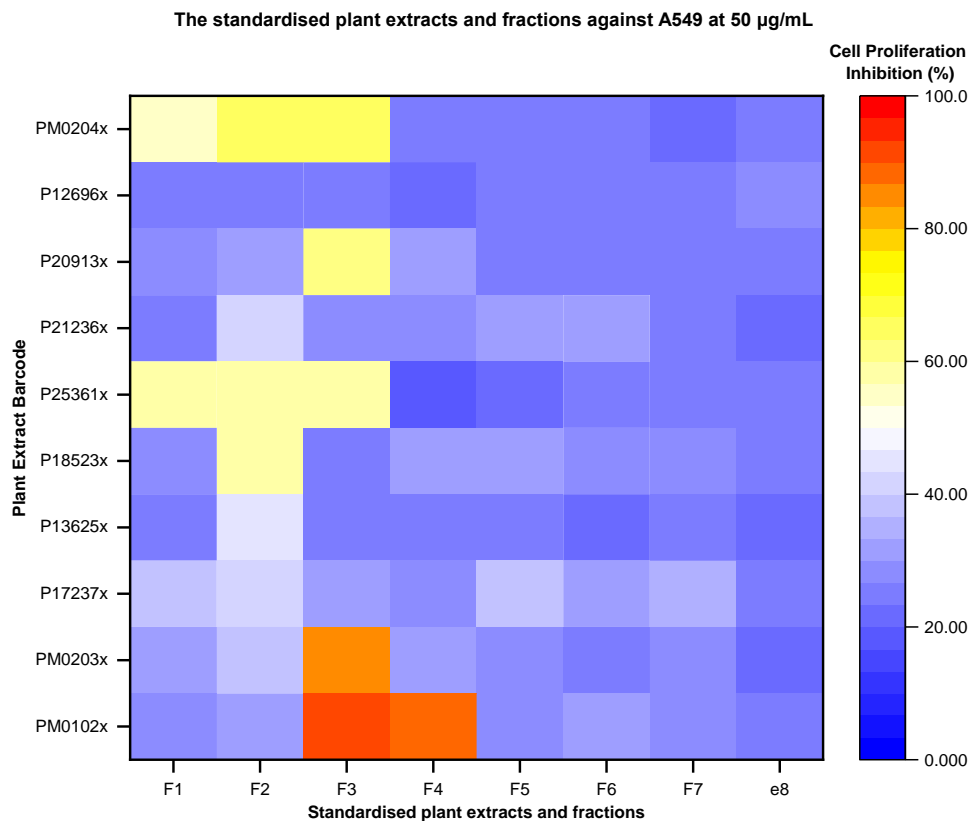
Figure 3-8 The cell proliferation inhibition (%) of the first 10 plant extracts and respective fractions against the cell line A549 at 50 µg/mL.

The standardised extracts and fractions were screened at 50 µg/mL against the cell line A549 with an adapted procedure of the single dose NCI-60 screening methodology. The SRB **(15)** assay did not include any repeats which was taken into consideration when the data was examined. The screening results showed more than 50 % cell proliferation inhibition after 48 hours for the following 11 samples: PM0204xf1, PM0204xf2, PM0204xf3, P20913xf3, P25361xf1, P25361xf2, P25361xf3, P18523xf2, PM0203xf3, PM0102xf3 and PM0102xf4. After further investigation, it was noted that the 11 fractions were from 6 different plant species that belonged to 5 different families. This illustrated that potential anti-cancer compounds can be found across different plant species and how natural products should be seen as a rich source of chemically diverse compounds. The fractions that displayed potent activity were from either fraction 3 or fraction 4. Of the above mentioned 11 fractions, only the following 3 fractions, from two plant species, showed excellent cell proliferation inhibition activity above 80 %: PM0203xf3, PM0102xf3 and PM0102xf4 shown in Figure 3-9.

72
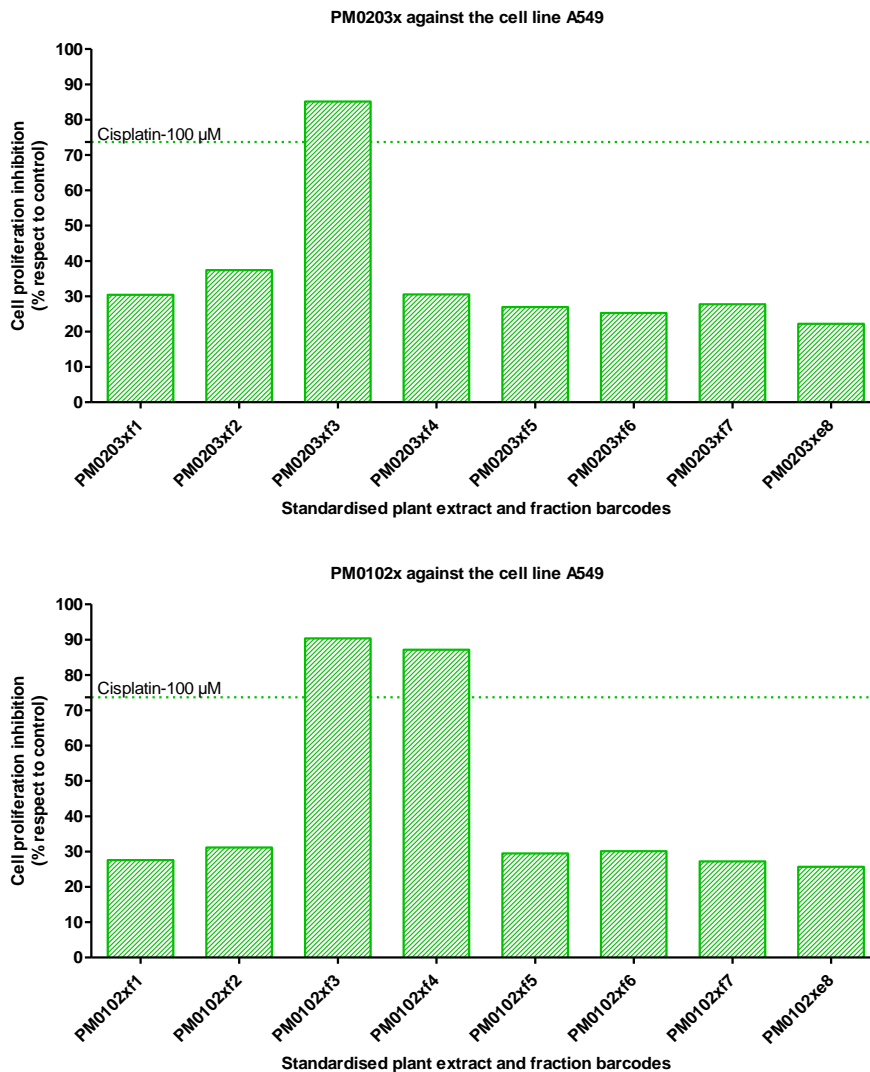
Figure 3-9 The cell proliferation inhibition (%) of PM0203x (top) and PM0102x (bottom) against the cell line A549.

The third standardised fraction (PM0203xf3) of *Plumbago auriculata* (Leaves) exhibited a cell proliferation inhibition of 85 % while the third (PM0102xf3) and fourth (PM0102xf4) standardised fraction of *Plectranthus barbatus* (Leaves) had a cell proliferation inhibition of 90 % and 87 %, respectively. It was observed that the activity for either plant species was concentrated in either fraction 3 or fraction 4. Both plant species received a score of 14 which was amongst the lowest scores of the 10 plant species screened against the cell line A549.

Plumbagin is reported as one of the potent and broad-spectrum bioactive compounds in the plant extracts of *Plumbago auriculata*. Plumbagin has shown antibacterial, anti-cancer, antifungal, anti-inflammatory, and antiplasmodial activity[46]. It is postulated that plumbagin is

73

present in PM0203xf3 but confirmation by chemical analysis is required. *Plectranthus barbatus* (*P. barbatus*) is the most used medicinal plant species in the genus *Plectranthus*. The main phytochemical constituents of *P. barbatus* are essential oils, abietanoids (abietane diterpenoids) and 8,13-epoxy-labd-14-en-11-one diterpenoids. The majority of abietanoids were isolated from the leaves and stems of *P. barbatus*. The methanolic leaf extract of *P. barbatus* has shown cytotoxic activity against leukaemia cells in dose-response biological screening. It was reported that the methanolic extract had an IC_{50} value against sensitive and multidrug-resistant leukaemia cells of 5.7 ± 1.29 µg/mL and 7.93 ± 0.64 µg/mL, respectively[35]. Chemical analysis of PM0102xf3 and PM0102xf4 is needed to confirm the presence of cytotoxic abietanoids found in the leaves of *P. barbatus*. It is important to note that none of the standardised extracts showed cell proliferation inhibition above 50 %. In natural product chemistry, it is commonly seen that plant species are not further investigated due to the inactivity of their crude extracts. This demonstrated the importance to fractionate crude plant extracts into semi-purified fractions for screening purposes as to not omit compounds with desirable activity that were suppressed due to the presence of interfering compounds.

The positive control cisplatin **(6)** was screened at 100 µM and exhibited 73.71 % cell proliferation inhibition after 48 hours. Cisplatin **(6)** worked well as a positive standard however the properties of cisplatin **(6)** must be taken into consideration when compared to the standardised extracts and fractions. One cannot directly compare the activities between pure compounds and chemical mixtures as there is no pre-existing knowledge of the contents in the fraction mixtures. The compounds present in fractions i.e., chemical mixtures might have a completely different absorption, metabolism, mechanism of action and target than that of the positive standard used. However, the 3 fractions did show a higher activity than the positive control and are considered for further investigation.

3.3.3.2   Biological screening against the human cancer cell lines MCF7 and Caco2

The remaining 24 standardised extracts and their respective fractions were screened *in vitro* at 25 µg/mL and 50 µg/mL for 48 hours against the human cancer cell lines MCF7 and Caco2 in an MTT **(13)** assay. The cell proliferation inhibition (%) against the cell lines are summarised in Figure 3-11 with the full detailed biological results shown in Supplementary data 3-7 to Supplementary data 3-14.

74
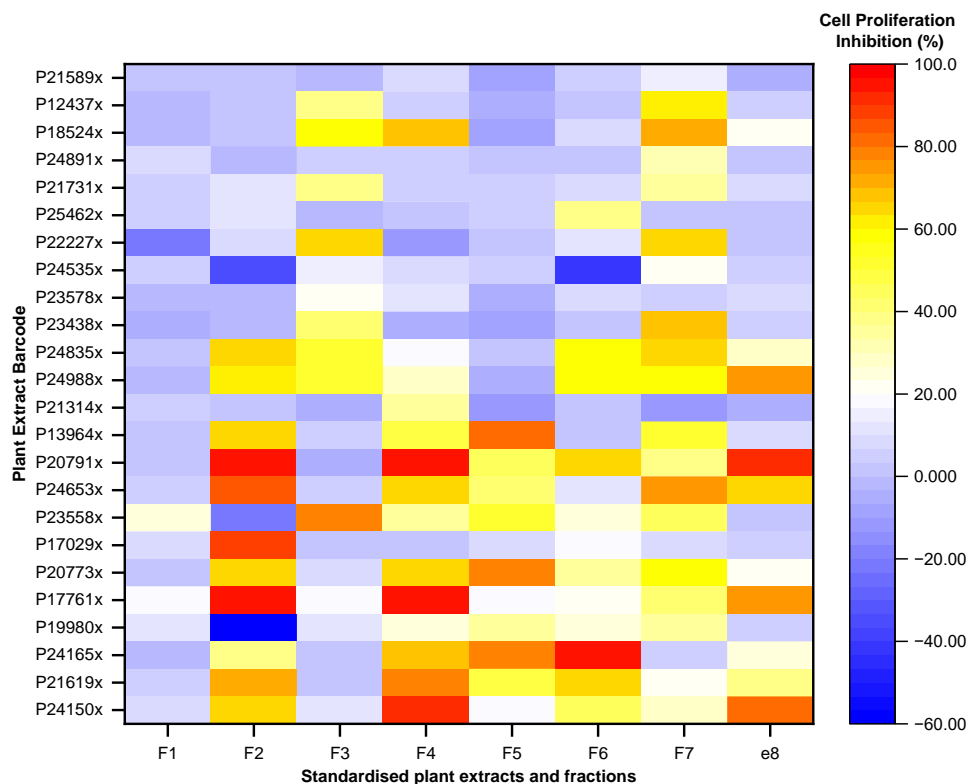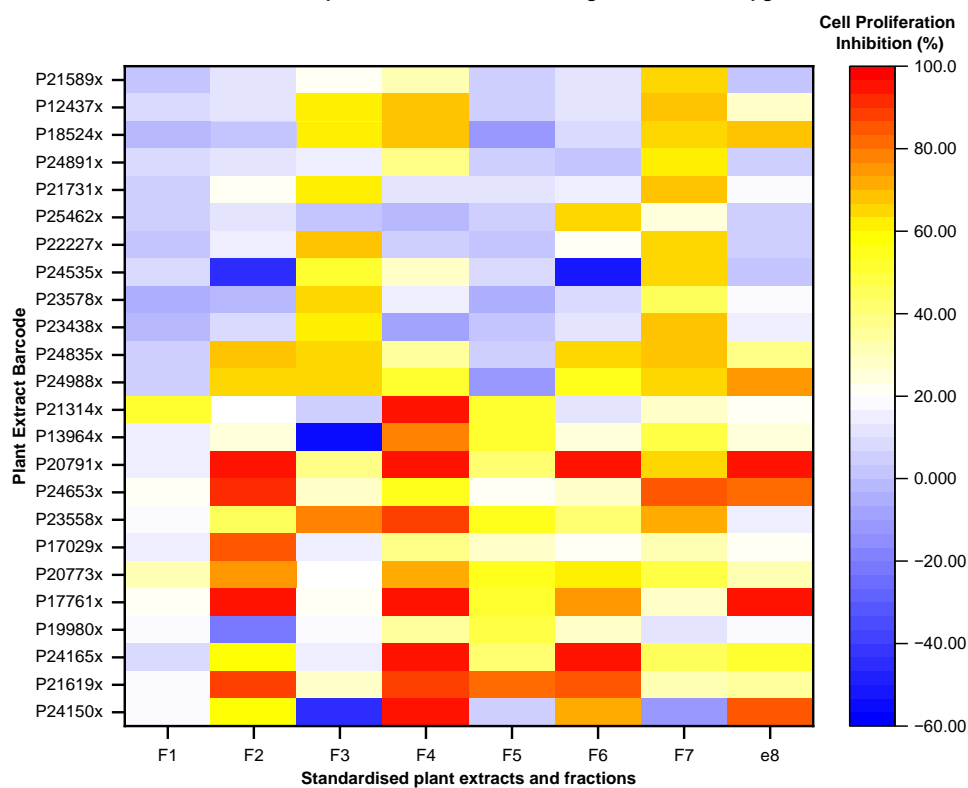
Figure 3-10   The cell proliferation inhibition (%) of the remaining standardised plant extracts and fractions against the cell line MCF7 at 25 µg/mL (top) and 50 µg/mL (bottom).
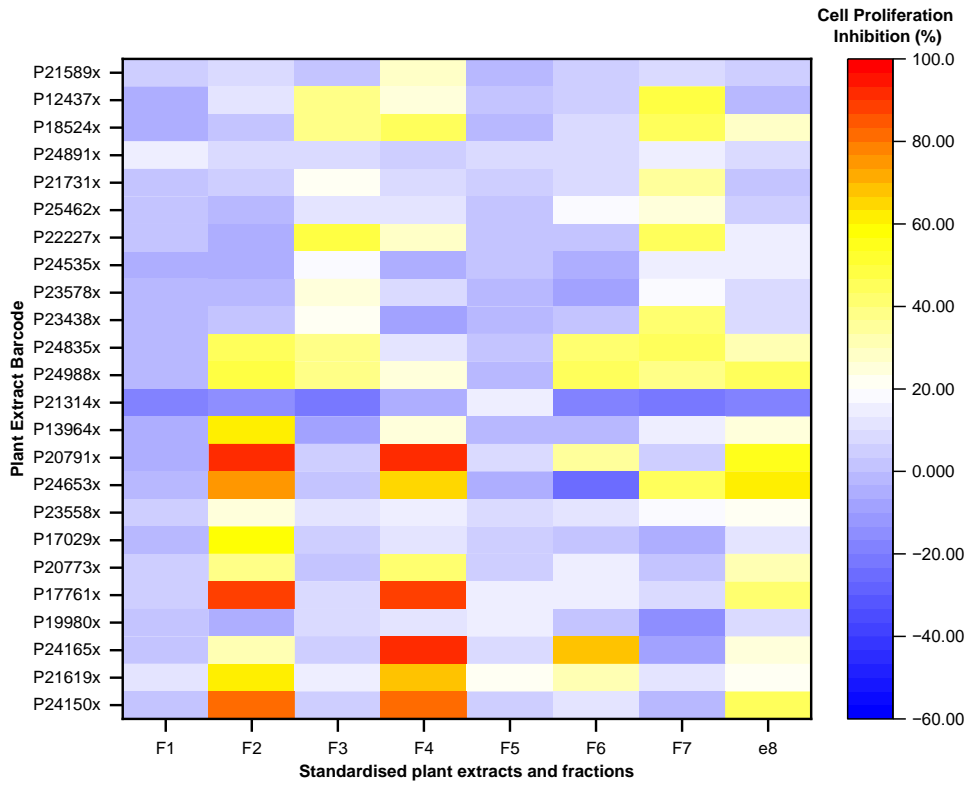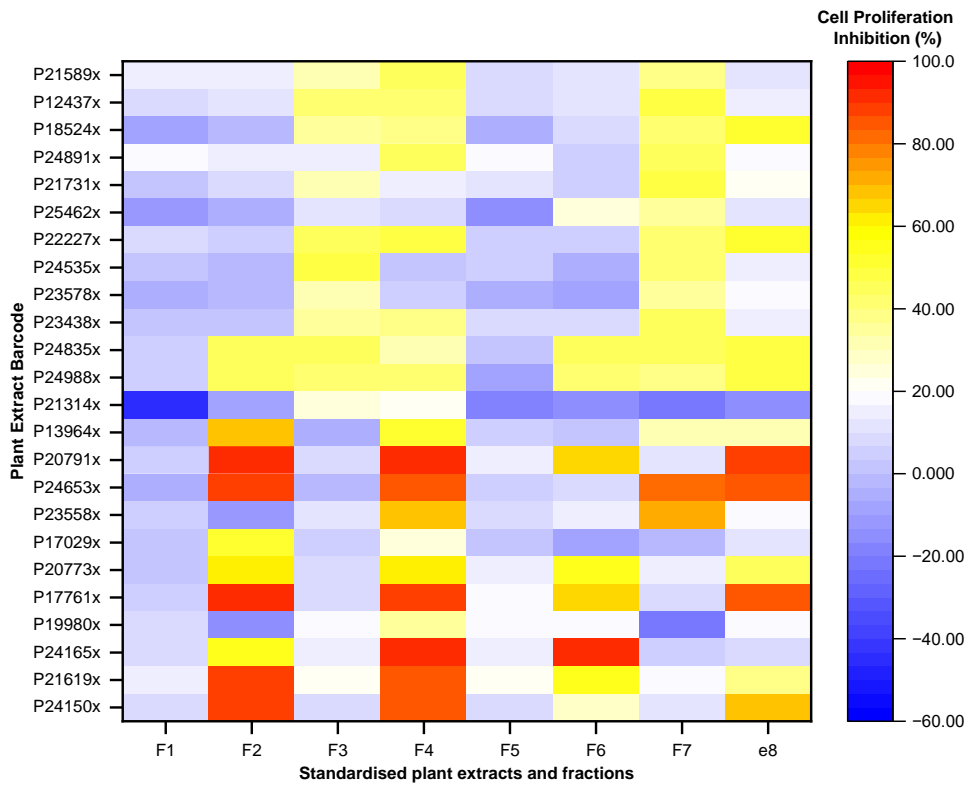
Figure 3-11 The cell proliferation inhibition (%) of the remaining standardised plant extracts and fractions against the cell line Caco2 at 25 µg/mL (top) and 50 µg/mL (bottom).

After 48 hours, melphalan **(7)** (30 µM) showed 49.42 % and 51.22 % cell proliferation inhibition against the cell lines MCF7 and Caco2, respectively. At both screening concentrations against both cell lines, the hits of fractions 3 and 7 showed moderate activity while the hits of fractions 2 and 4 showed the mostly potent activity. This demonstrated how the automated plant extract fractionation method concentrated the bioactive compounds within the plant extracts to certain only a certain number of fractions. As expected, there were more standardised extracts and fractions that exhibited above 50 % cell proliferation inhibition at 50 µg/mL than at 25 µg/mL against both cell lines. This is observed since the standardised extracts and fractions are more concentrated i.e., potent at higher concentrations. Additionally, it was observed that a considerable amount of the standardised fractions showed greater activity than their respective standardised extracts.

Shown in Figure 3-10 are the 24 standardised plant extracts and respective fractions screened at 25 µg/mL and 50 µg/mL against the cell line MCF7 for 48 hours. At 50 µg/mL, only 72 and 12 standardised extracts and fractions exhibited above 50 % and 90 % cell proliferation inhibition, respectively. At 25 µg/mL, 46 and 7 standardised extracts and fractions exhibited above 50 % and 90 % cell proliferation inhibition, respectively. It was noted that when the screening concentration was halved from 50 µg/mL to 25 µg/mL, the number of standardised extracts and fractions that exhibited cell proliferation > 90 % reduced by more than 40 %. Shown in Figure 3-11 are the same 24 standardised plant extracts and respective fractions screened at 25 µg/mL and 50 µg/mL against the cell line Caco2 for 48 hours. At 50 µg/mL, 30 and 5 standardised extracts and fractions exhibited above 50 % and 90 % cell proliferation inhibition, respectively. At 25 µg/mL, 16 and 3 standardised extracts and fractions exhibited above 50 % and 90 % cell proliferation inhibition, respectively. It was noted that when the screening concentration was halved from 50 µg/mL to 25 µg/mL, the number of standardised extracts and fractions that exhibited cell proliferation > 90 % reduced by 40 %.

At both screening concentrations, the cell line MCF7 had more than double the number of "hits" than Caco2. This could be due to the nature and/or mechanism of action of the compounds present in the standardised extracts and fractions. This demonstrates at a basic level a higher selectivity of the standardised extracts and fractions towards the cell line MCF7. It was noted that no growth hormones were present in the cell culture medium implying that any proliferation or inhibition of MCF7 was not dependent on hormones or antagonistic compounds binding to receptors such as HER2, ER or PE. The standardised extracts and fractions that exhibited above 80 % cell proliferation inhibition at 25 µg/mL against both cell lines, such as those shown in Figure 3-12, were worth further investigation.

77
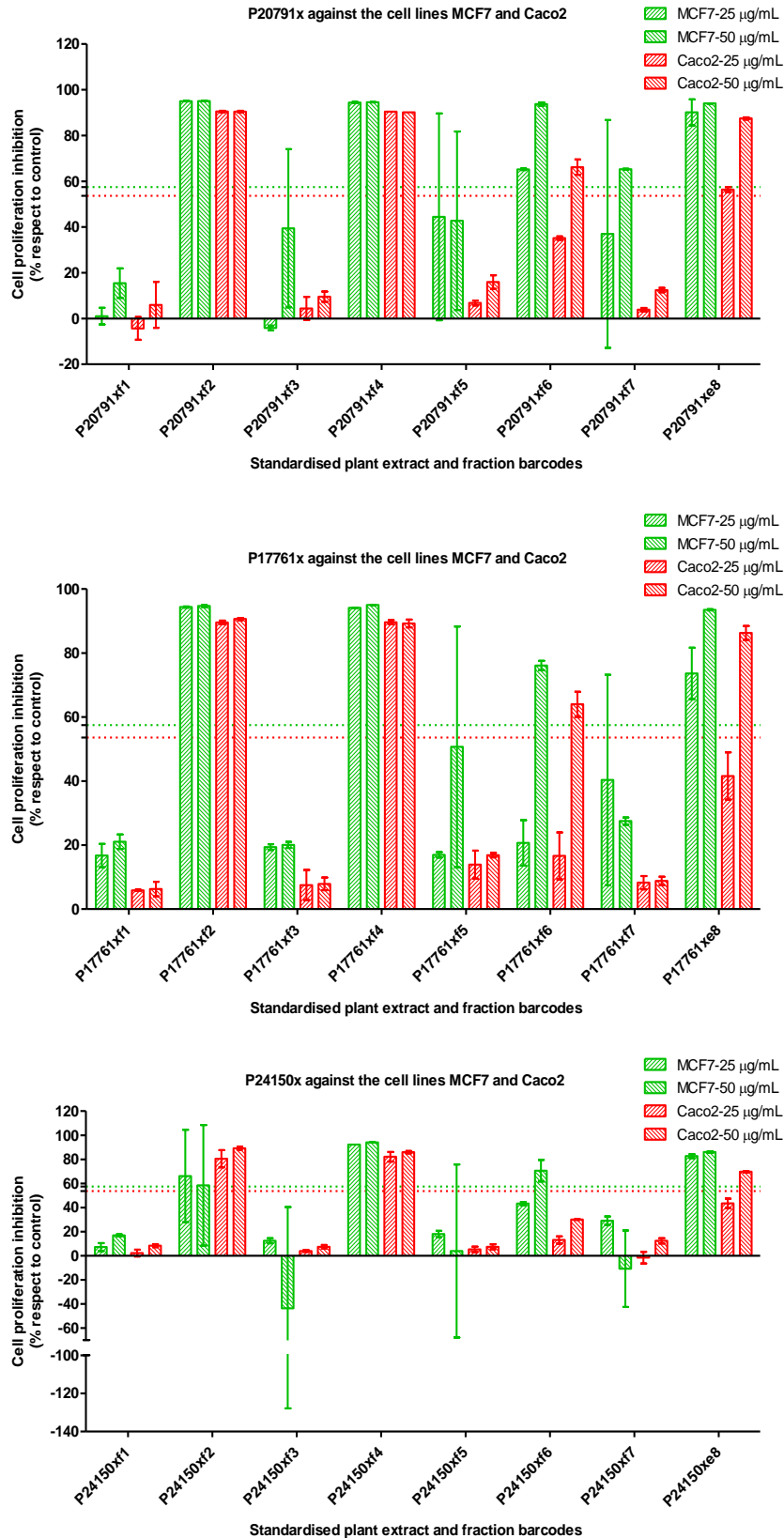
Figure 3-12 The cell proliferation inhibition (%) of P20791x (top), P17761x (middle) and P24150x (bottom) against the cell lines MCF7 and Caco2.

Both *Brachylaena discolor*-P20791x (*B. discolor*) and *Mikania natalensis*-P24150 (*M. natalensis*) are members of the *Asteraceae* family while *Ekebergia capensis*-P17761x (*E. capensis*) is a member of the *Meliaceae* family. These three plants were scored amongst the lowest plant species with a score of 13. Traditionally, the roots of *B. discolor* are ingested for the treatment of stomach haemorrhages and chest pains[32]. The sesquiterpene lactone onopordopicrin has been reported to be abundantly present in the aerial parts and roots of the *Brachylaena* genus[32]. Onopordopicrin has shown antibacterial, antifungal, anti-inflammatory, phytotoxic, antiplasmodial, anti-ulcerogenic and anti-cancer activity[61–67]. It was reported that onopordopicrin had an IC_{50} value of 20 mM against the human cancer cell line HeLa (cervical cancer) and a cell proliferation inhibition above 70 % against the human cancer cell lines HepG 2 (liver cancer) and A549 (lung cancer)[67]. As seen in Figure 3-12, the excellent activity of *B. discolor* fractions 2, 4, 6 and the extract 8 are most likely due to onopordopicrin and other similar sesquiterpene lactones in the species.

E. capensis is one of the most commonly used plant species in African traditional medicine for the treatment of a broad range of diseases. In the *Ekebergia* genus, limonoids were reported as the major class of secondary metabolites making up around 30 % of the total reported metabolites while triterpenoids and coumarins accounted for 26 % and 17 %, respectively[56]. The MeOH/DCM root extracts of *E. capensis* have shown anti-inflammatory, antiplasmodial, hypotensive, antituberculotic and anti-cancer activities. The reported IC_{50} concentration of a *E. capensis* root extract against Vero (African monkey kidney), 4T1 (mouse breast cancer) and HEp2 (human larynx carcinoma) cell lines were 2.8 ± 0.1 µg/mL, 9.3 ± 0.1 µg/mL and 61 ± 1.4 µg/mL, respectively[68]. It was postulated that the anti-cancer compounds present in fractions 2 and 4 are most likely limonoids and/or triterpenes.

Fractions 2, 4 and the extract 8 of *M. natalensis* showed relatively good cell proliferation inhibition against both cell lines at both screening concentrations. Traditionally, only the aerial parts of the *Mikania* genus are used in medicinal practises. It was reported that mainly sesquiterpene lactones are found in the aerial parts i.e., the leaves and flowers[69]. Other chemical classes such as coumarins, flavonoids, terpenoids and phytosterols are also described to a lesser extent within the genus[70]. Many species in the *Mikania* genus have shown different pharmacological activities mainly analgesic, anti-allergic, anti-inflammatory, antioxidant, and antimicrobial[71]. As the phytochemistry of *M. natalensis* unpublished, it was selected for further investigation.

79

The large standard deviation bars and negative cell proliferation inhibition values seen throughout all the biological data in Supplementary data 3-7 to Supplementary data 3-14 were attributed to bacterial contamination during screening. The bacteria present during screening metabolised and reduce the tetrazolium MTT **(13)** dye to the MTT-Formazan **(14)** product resulting in higher optical densities recorded. This appeared as a negative cell proliferation percentage i.e. the amount of MTT **(13)** dye metabolised was greater than the control groups depicting that cell proliferation had occurred. It is also worth noting that bacterial contamination is not the only source of obtaining high absorption values. A few chemical related issues may influence the reduction of tetrazolium such as a) chemical interference within the cell affecting the reduction of the tetrazolium, b) chemical reduction of the tetrazolium by the testing samples and c) the metabolic conditions of the cells which might alter the reduction rate of the tetrazolium[72]. For this project, chemical related interferences were ruled out as the presence of bacteria was visually confirmed under a microscope.

3.4   Conclusion

Currently the University of Pretoria has over 12 000 plant material samples available in its plant depository that represents just over 7 000 plant species collected throughout South Africa. The ethnopharmacological preferential scoring system worked well by refining the available medicinal plant material down to a final selection of 100 plant species that had the highest probability of containing potential chemotherapeutic agents. As cancer is not clearly described in traditional medicinal practises, a table of associated cancer symptoms helped identify potential medicinal plants by their reported usage for treating cancer-like symptoms. The cut-off score of 13 allowed a non-bias final selection of medicinal plant species based on obtaining a higher, more preferential score than others. According to the plant scoring system, the basic exclusion principle allowed the plant species that have the highest likelihood of succeeding to be investigated. Only 34 plant species were selected for the continuation of the project.

The plant standardisation methods worked well in standardising all 34 selected plant species. The methods were robust, high-throughput and accommodating to all types of plant material while lowering the production cost. The extraction method was able to produce high-quality extracts with sufficient yields to be used throughout the standardisation process. The extract fractionation method developed by the NCI NPNPD project worked well as it was observed to concentrate drug-like compounds in certain fractions while removing interfering compounds evident by the high mass of the first fraction. However, the mass recovery was only half of what was expected which was attributed to the intensive drying conditions. During the

80

intensive drying step, the dissolved extracts were loaded onto individual dental cotton rolls and dried which formed a hard plug that did not completely dissolve during fractionation which affected the mass recovery. It was concluded that 5 mg/mL was a suitable storage concentration as only 2.94 % of the plant extract and fractions were not standardised at 5 mg/mL due to insufficient mass. This will be less frequent when the mass recovery is improved during the fractionation step. The Hamilton STARlet™ liquid handler successfully standardised all the plant extracts and fractions while generating faultless database Excel worksheets. It was determined that the utilisation of the Hamilton Verso® Q20 for storage decreased the risk of possible human errors that would occur when working with large numbers of samples. Both the SRB **(15)** and MTT **(13)** assay proved to be adequate and sensitive enough for high-throughput screening against the human cell lines A549, MCF7 and Caco2. The influence and benefit of fractionating the plants extract on a HyperSep™ C8 SPE cartridge before screening was shown as most bioactive fractions were exhibiting better activity than their respective crude extracts. The cell lines A549, MCF7 and Caco2 were adequately chosen as they closely resemble the most common subtypes of the three most common cancer types in the world. Out of 80 samples, only 3 fractions showed above 80 % cell proliferation inhibition at 50 µg/mL against the cell line A549. Out of 192 samples, only 10 fractions showed above 90 % cell proliferation inhibition at 25 µg/mL between the cell lines MCF7 and Caco2. The fractionation of plant extracts before screening has shown to improve the biological results as well as post screening investigations such as selecting hits for the isolation and chemical characterisation of active ingredients.

In a cost-friendly and time efficient manner, the HTS of a small subset of the South African natural product library against different cancer cell lines has identified numerous "hits" for investigation in an effort to discovery potential chemotherapeutic compounds. Future work will be on improving the adapted automated plant extract fractionation method and to complete the standardisation of the remaining plant material from the selected 100 plant species. Additionally, consideration has been made towards screening the current and future subset of standardised plant extracts and fractions against different cancer cell lines to identify "hits" against more than 3 cell lines.

3.5   References

1.   Clarkson, C. *et al.* In vitro antiplasmodial activity of medicinal plants native to or naturalised in South Africa. *J. Ethnopharmacol.* **92**, 177–191 (2004).

2.   Thakur, A., Chun, Y. S., October, N., Yang, H. O. & Maharaj, V. Potential of South African medicinal plants targeting the reduction of Aβ42 protein as a treatment of Alzheimer's disease. *J. Ethnopharmacol.* **231**, 363–373 (2019).

3.   Fouche, G. *et al.* In vitro anticancer screening of South African plants. *J. Ethnopharmacol.* **119**, 455–461 (2008).

4.   Wilson, B. A. P., Thornburg, C. C., Henrich, C. J., Grkovic, T. & O'Keefe, B. R. Creating and screening natural product libraries. *Nat. Prod. Rep.* **37**, 893–918 (2020).

5.   Thornburg, C. C. *et al.* NCI Program for Natural Product Discovery: A Publicly-Accessible Library of Natural Product Fractions for High-Throughput Screening. *ACS Chem. Biol.* **13**, 2484–2497 (2018).

6.   Atanasov, A. G., Zotchev, S. B., Dirsch, V. M., International Natural Product Sciences Taskforce & Supuran, C. T. Natural products in drug discovery: advances and opportunities. *Nat. Rev. Drug Discov.* **20**, 200–216 (2021).

7.   WCRFI. World Cancer Research Fund International: Lung cancer statistics. https://www.wcrf.org/cancer-trends/lung-cancer-statistics/%0A (2019).

8.   Lukeman, J. M. What Is Lung Cancer? in *Perspectives in Lung Cancer* 30–40 (S. Karger AG, 2015). doi:10.1159/000400400.

9.   Pu, J., Shen, J., Zhong, Z., Yanling, M. & Gao, J. KANK1 regulates paclitaxel resistance in lung adenocarcinoma A549 cells. *Artif. Cells, Nanomedicine, Biotechnol.* **48**, 639–647 (2020).

10.   Roggen, E. L., Soni, N. K. & Verheyen, G. R. Respiratory immunotoxicity: An in vitro assessment. *Toxicol. Vitr.* **20**, 1249–1264 (2006).

11.   Shoemaker, R. H. The NCI60 human tumour cell line anticancer drug screen. *Nat. Rev. Cancer* **6**, 813–823 (2006).

12.   World Health Organization, Global Cancer Observatory & International Agency for Research on Cancer. Breast cancer statistics. *World Cancer Research Fund International* https://www.wcrf.org/dietandcancer/cancer-trends/breast-cancer-statistics%0Ahttp://globocan.iarc.fr (2022).

13.   McPherson, K., Steel, C. M. & Dixon, J. M. ABC of breast diseases: Breast cancer - Epidemiology, risk factors, and genetics. *Br. Med. J.* **321**, 624–628 (2000).

14.   JI, K. & PI, H.-R. Breast cancer: magnitude of the problem and descriptive epidemiology. *Epidemiol. Rev.* **15**, 7–16 (1992).

15.   Samaan, T. M. A., Samec, M., Liskova, A., Kubatka, P. & Büsselberg, D. Paclitaxel's mechanistic and clinical effects on breast cancer. *Biomolecules* **9**, 1–22 (2019).

16.   Riaz, M. *et al.* MiRNA expression profiling of 51 human breast cancer cell lines reveals subtype and driver mutation-specific miRNAs. *Breast Cancer Res.* **15**, (2013).

17.   Zubor, P. *et al.* MiRNA in a multiomic context for diagnosis, treatment monitoring and personalized management of metastatic breast cancer. *Futur. Oncol.* **14**, 1847–1867 (2018).

18.   Wu, Q. *et al.* Analysis of the miRNA-mRNA-lncRNA networks in ER+ and ER- breast

cancer cell lines. *J. Cell. Mol. Med.* **19**, 2874–87 (2015).

19. Yao, Y., Chu, Y., Xu, B., Hu, Q. & Song, Q. Risk factors for distant metastasis of patients with primary triple-negative breast cancer. *Biosci. Rep.* **39**, 1–10 (2019).

20. Ferlay J, Soerjomataram I, Ervik M, Dikshit R, Eser S, Mathers C, Rebelo M, Parkin DM, Forman D, Bray, F. Colorectal cancer statistics | World Cancer Research Fund International. *GLOBOCAN 2012 v1.1, Cancer Incidence and Mortality Worldwide: IARC CancerBase No. 11* http://www.wcrf.org/int/cancer-facts-figures/data-specific-cancers/colorectal-cancer-statistics (2012).

21. Sawicki, T. *et al.* A Review of Colorectal Cancer in Terms of Epidemiology, Risk Factors, Development, Symptoms and Diagnosis. *Cancers (Basel).* **13**, 1–23 (2021).

22. Points, K. Tests to Detect Colorectal Cancer and Polyps. *Nature cancer Institute* vol. 2011 1–8 http://www.cancer.gov/types/colorectal/screening-fact-sheet (2013).

23. Granados-Romero, J. J. *et al.* Colorectal cancer: a review. *Int. J. Res. Med. Sci.* **5**, 4667 (2017).

24. Centre for Disease Control and Prevention. What Is Colorectal Cancer? | CDC. *Cdc* vol. 13 104–116 https://www.cdc.gov/cancer/colorectal/basic_info/what-is-colorectal-cancer.htm (2021).

25. Verhoeckx, K. *et al. The Impact of Food Bioactives on Health. The Impact of Food Bioactives on Health: In Vitro and Ex Vivo Models* (Springer International Publishing, 2015). doi:10.1007/978-3-319-16104-4.

26. Newman, D. J. & Cragg, G. M. Natural Products as Sources of New Drugs over the Nearly Four Decades from 01/1981 to 09/2019. *J. Nat. Prod.* **83**, 770–803 (2020).

27. Heigener, D. F. & Reck, M. Crizotinib. *Recent Results Cancer Res.* **201**, 197–205 (2014).

28. Van Asten, K., Neven, P., Lintermans, A., Wildiers, H. & Paridaens, R. Aromatase inhibitors in the breast cancer clinic: focus on exemestane. *Endocr. Relat. Cancer* **21**, R31-49 (2014).

29. Nathan, M. R. & Schmid, P. A Review of Fulvestrant in Breast Cancer. *Oncol. Ther.* **5**, 17–29 (2017).

30. Li, J., Ren, J. & Sun, W. Systematic review of ixabepilone for treating metastatic breast cancer. *Breast Cancer* **24**, 171–179 (2017).

31. Fujita, K., Kubota, Y., Ishida, H. & Sasaki, Y. Irinotecan, a key chemotherapeutic drug for metastatic colorectal cancer. *World J. Gastroenterol.* **21**, 12234–48 (2015).

32. Hutchings, A., Scoff, A. H., Lewis, G. & Cunningham, A. Zulu medicinal plants: an inventory. *Choice Rev. Online* **34**, 34-6265-34–6265 (1997).

33. Kooti, W. *et al.* Effective Medicinal Plant in Cancer Treatment, Part 2: Review Study. *J. Evid. Based. Complementary Altern. Med.* **22**, 982–995 (2017).

34. Mbele, M., Hull, R. & Dlamini, Z. African medicinal plants and their derivatives: Current efforts towards potential anti-cancer drugs. *Exp. Mol. Pathol.* **103**, 121–134 (2017).

35. Saeed, M. E. M., Meyer, M., Hussein, A. & Efferth, T. Cytotoxicity of South-African medicinal plants towards sensitive and multidrug-resistant cancer cells. *J. Ethnopharmacol.* **186**, 209–223 (2016).

36. Koduru, S., Grierson, D. S. & Afolayan, A. J. Ethnobotanical information of medicinal plants used for treatment of cancer in the Eastern Cape Province, South Africa. *Curr. Sci.* **92**, 906–908 (2007).

37. Khorombi, T. *et al.* Investigation of South African plants for anti cancer properties. (2006).

38. Kapare, H., Metkar, S. & Shirolkar, S. Anticancer potential of Plumbago zeylanica Linn. and its isolated constituent plumbagin: a review. *Int. J. Pharm. Sci. Res.* **11**, 4859–4865 (2020).

39. Fan, W. *et al.* Traditional Uses, Botany, Phytochemistry, Pharmacology, Pharmacokinetics and Toxicology of Xanthium strumarium L.: A Review. *Molecules* **24**, (2019).

40. Wink, M. & van Wyk, B.-E. Mind-altering and poisonous plants of the world. *Choice Rev. Online* **46**, 46-6198-46–6198 (2009).

41. Otang, W. M., Grierson, D. S. & Ndip, R. N. Phytochemical studies and antioxidant activity of two South African medicinal plants traditionally used for the management of opportunistic fungal infections in HIV/AIDS patients. *BMC Complement. Altern. Med.* **12**, 43 (2012).

42. Ojewole, J. A. O., Mawoza, T., Chiwororo, W. D. H. & Owira, P. M. O. Sclerocarya birrea (A. Rich) Hochst. ['Marula'] (Anacardiaceae): a review of its phytochemistry, pharmacology and toxicology and its ethnomedicinal uses. *Phytother. Res.* **24**, 633–9 (2010).

43. Amabeoku, G. J. & Kinyua, C. G. Evaluation of the Anticonvulsant Activity of Zanthoxylum capense (Thunb.) Harv. (Rutaceae) in Mice. *Int. J. Pharmacol.* **6**, 844–853 (2010).

44. Lourens, A. C. U., Viljoen, A. M. & van Heerden, F. R. South African Helichrysum species: a review of the traditional uses, biological activity and phytochemistry. *J. Ethnopharmacol.* **119**, 630–52 (2008).

45. Maroyi, A. Traditional usage, phytochemistry and pharmacology of Croton sylvaticus Hochst. ex C. Krauss. *Asian Pac. J. Trop. Med.* **10**, 423–429 (2017).

46. Singh, Ka., Naidoo, Y. & Baijnath, H. A COMPREHENSIVE REVIEW ON THE GENUS PLUMBAGO WITH FOCUS ON PLUMBAGO AURICULATA (PLUMBAGINACEAE). *African J. Tradit. Complement. Altern. Med.* **15**, 199–215 (2017).

47. Soto-Blanco, B., Borges Fernandes, L. C. & Campos Cmara, C. Anticonvulsant activity of extracts of Plectranthus barbatus leaves in mice. *Evidence-based Complement. Altern. Med.* **2012**, 1–4 (2012).

48. Alasbahi, R. H. & Melzig, M. F. Plectranthus barbatus: a review of phytochemistry, ethnobotanical uses and pharmacology - part 2. *Planta Med.* **76**, 753–65 (2010).

49. Rajeshwari T, S. R. and S. M. Phytochemical Investigation and Antioxidant Potential of Two Amaranthaceae Plants: Achyranthes Aspera Linn and Chenopodium Album Linn. *Int. J. Pharm. Sci. Res.* **13**, 902–911 (2020).

50. Arun, M. & Asha, V. V. Preliminary studies on antihepatotoxic effect of Physalis peruviana Linn. (Solanaceae) against carbon tetrachloride induced acute liver injury in rats. *J. Ethnopharmacol.* **111**, 110–4 (2007).

51. Alfred Maroyi. Brachylaena elliptica and B. ilicifolia (Asteraceae): A Comparative Analysis of their Ethnomedicinal Uses, Phytochemistry and Biological Activities. *J. Pharm. Nutr. Sci.* **10**, 223–229 (2020).

52. Oloya, B., Namukobe, J., Ssengooba, W., Afayoa, M. & Byamukama, R. Phytochemical screening, antimycobacterial activity and acute toxicity of crude extracts of selected medicinal plant species used locally in the treatment of tuberculosis in Uganda. *Trop. Med. Health* **50**, 16 (2022).

53. Kaunda, J. S. & Zhang, Y.-J. The Genus Solanum: An Ethnopharmacological, Phytochemical and Biological Properties Review. *Nat. Products Bioprospect.* **9**, 77–137 (2019).

54. Khan, M., Al-Saleem, M. S. M. & Alkhathlan, H. Z. A detailed study on chemical characterization of essential oil components of two Plectranthus species grown in Saudi Arabia. *J. Saudi Chem. Soc.* **20**, 711–721 (2016).

55. Hamza, M. F., Shaik, S. & Moodley, R. PHYTOCHEMICAL, ELEMENTAL AND BIOTECHNOLOGICAL STUDY OF CRYPTOCARYA LATIFOLIA. *African J. Tradit. Complement. Altern. Med. AJTCAM* **13**, 74–80 (2016).

56. Kemayou, G. P. M. *et al.* Phytochemistry, traditional uses, and pharmacology of the genus ekebergia (Meliaceae): A review. *Trends Phytochem. Res.* **5**, 110–125 (2021).

57. Mohamed, S., Ross, S. & Mohamed, N. EXPLORATION OF COMPONENTS CONTRIBUTING TO POTENT CYTOTOXICITY OF GARDENIA THUNBERGIA L. F. AGAINST HUMAN LEUKEMIA AND HEPATOMA. *Bull. Pharm. Sci. Assiut* **45**, 153–162 (2022).

58. Nikolić, M. & Stevović, S. Family Asteraceae as a sustainable planning tool in phytoremediation and its relevance in urban areas. *Urban For. Urban Green.* **14**, 782–789 (2015).

59. Rolnik, A. & Olas, B. The Plants of the Asteraceae Family as Agents in the Protection

of Human Health. *Int. J. Mol. Sci.* **22**, 1–10 (2021).

60. Kannan, K. S., Manoj, K. & Arumugam, S. Labeling Methods for Identifying Outliers. *Int. J. Stat. Syst.* **10**, 231–238 (2015).

61. Lonergan, G. *et al.* Isolation, NMR studies, and biological activities of onopordopicrin from Centaurea sonchifolia. *J. Nat. Prod.* **55**, 225–8 (1992).

62. Móricz, Á. M. *et al.* Layer chromatography-bioassays directed screening and identification of antibacterial compounds from Scotch thistle. *J. Chromatogr. A* **1524**, 266–272 (2017).

63. Bordignon, A. *et al.* In vitro antiplasmodial and cytotoxic activities of sesquiterpene lactones from Vernonia fimbrillifera Less. (Asteraceae). *Nat. Prod. Res.* **32**, 1463–1466 (2018).

64. Suzuki, M., Iwasaki, A., Suenaga, K. & Kato-Noguchi, H. Phytotoxic activity of crop residues from Burdock and an active substance. *J. Environ. Sci. Health. B.* **54**, 877–882 (2019).

65. de Almeida, A. B. A. *et al.* Anti-ulcerogenic mechanisms of the sesquiterpene lactone onopordopicrin-enriched fraction from Arctium lappa L. (Asteraceae): role of somatostatin, gastrin, and endogenous sulfhydryls and nitric oxide. *J. Med. Food* **15**, 378–83 (2012).

66. de Almeida, A. B. A. *et al.* Anti-inflammatory intestinal activity of Arctium lappa L. (Asteraceae) in TNBS colitis model. *J. Ethnopharmacol.* **146**, 300–10 (2013).

67. Zhang, J. *et al.* Onopordopicrin from the new genus Shangwua as a novel thioredoxin reductase inhibitor to induce oxidative stress-mediated tumor cell apoptosis. *J. Enzyme Inhib. Med. Chem.* **36**, 790–801 (2021).

68. Irungu, B. N. *et al.* Constituents of the roots and leaves of Ekebergia capensis and their potential antiplasmodial and cytotoxic activities. *Molecules* **19**, 14235–46 (2014).

69. Yu, H., Le Roux, J. J., Zhao, M. & Li, W. Mikania sesquiterpene lactones enhance soil bacterial diversity and fungal and bacterial activities. *Biol. Invasions* **25**, 237–250 (2023).

70. Abdellah, Y. A. Y. *et al.* Phytochemical and underlying mechanism of Mikania micrantha Kunth on antibiotic resistance genes, and pathogenic microbes during chicken manure composting. *Bioresour. Technol.* **367**, 128241 (2023).

71. Brigida da Silva, A., Owiti, A. & Barbosa, W. R. Pharmacology of Mikania genus: A systematic review. *Pharmacogn. Rev.* **12**, 230 (2018).

72. Rubinstein, L. V. *et al.* Comparison of in vitro anticancer-drug-screening data generated with a tetrazolium assay versus a protein assay against a diverse panel of human tumor cell lines. *J. Natl. Cancer Inst.* **82**, 1113–8 (1990).

Chapter 4: Investigation into the anti-cancer activity of *Mikania natalensis*

4.1 Introduction

4.1.1 Classification and geographic distribution

The plant species *M. natalensis* is classified under the geneus *Mikania* and belongs to the *Asteraceae* family. It is estimated that approximately 22 800 plant species belong to the *Asteraceae* family[1]. The species name "*natalensis*" refers to the region of origin, KwaZulu-Natal, South Africa. Today *M. natalensis* can be found throughout South Africa mainly spanning from Zoutpansberg to the Transvaal Drakensberg, throughout eastern Natal and even as far south as the Tsitsikamma forest in the Cape[2]. The genus was first documented in Brazil, South America by Johann Christian Mikan who was an Austrian-Czech botanist, entomologist and zoologist. Johann C. Mikan was one of three leading naturalists who participated in an Austrian expedition to Brazil, where he described many new animal and plant species. Among his discoveries, Johann named the genus *Mikania* Willd. to commemorate his father Joseph Gottfried Mikan, a professor of chemistry and botany. The *Mikania* genus is believed to have originated from the tropical south and central regions of South America and is colloquially referred to as 'guaco' in Brazil[1]. The genus is now widely distributed across the world and commonly observed in India, Southeast Asia, Pacific islands and South China. The *Mikania* genus is reported to contain around 450 different species however, only the following species have been extensively studied: *Mikania glomerata (M. glomerata)*, *Mikania laevigata* (*M. laevigata*) and *Mikania micrantha* (*M. micrantha*).

4.1.2 Botany

M. natalensis is described as a herbaceous, wide-climbing perennial. The plants hairless stems can reach a thickness of 3 mm in diameter while the leaf stalks can reach up to a length of 3 cm. The leaves are opposite, petioled and in some instances have been reported to cover an area of 10 cm x 7 cm. The leaf blade is long-pointed and triangular with backward facing extensions. The edges of the leaf can be found as either sub-entire, sinuate-dentate or denticulate. The leaves are 5-nerved from the base with a hairless to thinly haired face and a velvety underside[2]. The flowers generally grow up to 8-10 mm long containing purple-coloured anthers with membranous appendage and cream-white coloured corollas. The flowers are arranged in loosely branched inflorescences. The flowers are fragrantful and are found throughout the year especially from July to September.

4.1.3 Traditional usage of *Mikania natalensis*

Generally, only the aerial parts of the plant species from the *Mikania* genus that are used in traditional medicinal practises around the globe. In South Africa, the Zulu people use the leaves of *M. natalensis* as leaf-paste dressings for the treatment of venereal diseases and urinary complications. The leaves are also prepared as a snuff and snorted for the relief of headaches. Leaf infusions are also taken as a nauseant for headaches and influenza[3]. In Brazil, the "guaco" leaves are traditionally prepared as extracts or infusions for the treatment of respiratory tract diseases such as asthma and pleurisy bronchitis. Additionally, the leaves have used for the treatment of the common flu, gastrointestinal disorders and rheumatism[4].

4.1.4 Phytochemistry and biological activity of the genus *Mikania*

The genus *Mikania* has been extensively reported for its rich abundance in sesquiterpene lactones[4]. Sesquiterpene lactones are mainly found in the aerial parts i.e., the leaves and flowers[5] in the plant species of the *Mikania* genus. Other chemical classes such as coumarins, flavonoids, terpenoids and phytosterols are also described within the genus[6]. Shown in Figure 4-1 are a few of the secondary metabolites described in the *Mikania* genus. The major chemical constituents reported in *M. glomerata* are campesterol **(21)**, caryophyllene oxide **(22)**, coumarin **(23)**, germacrene D **(24)**, kaurenoic acid **(25)**, lupeol, lupeol acetate **(26)**, spathulenol **(27)**, sabinene **(28)** and β-sitosterol **(29)**[7–9]. It was reported that in *M. laevigata,* the major chemical constituents are coumarin **(23)**, germacrene D **(24)**, grandifloric acid **(30)**, kaurenoic acid **(25)**, myrcene **(31)**, spathulenol **(27)** and syringaldehyde **(32)**[7,10]. Lastly, *M. micrantha* was reported to mainly contain epifriedelinol **(33)**, friedelin **(34)**, fructose, fumaric acid **(35)**, germacrene D **(24)**, mikanin **(36)**, mikanin 3-O-sulfate **(37)**, mikanolide **(38)**, dihydromikanolide **(39)**, deoxymikanolide, α- pienene, β-pienene **(40)**, scandenolide **(41)**, stigmasterol **(42)** and α-thujene **(43)**[7,11,12].

The published biological data revealed that the chemical constituents of the *Mikania* genus were investigated primarily investigated for antibacterial activity. Preparations from *M. glomerata* have shown excellent *in vitro* antibacterial activity against the oral bacterium *Streptococcus mutans (S. mutans)* that cause tooth loss. It was reported that hexane fractions of a methanolic extract from *M. glomerata* had a minimum inhibitory and bactericidal concentration between 12.5-25 µg/mL and between 25-400 µg/mL against *S. mutans*, respectively[13]. In a different study, the hexane fraction of a DCM and MeOH/H_2O extract, with a high kaurenoic acid **(25)** content, had a minimum inhibitory and bactericidal concentration between 6.25-400 µg/mL[14]. It is postulated that kaurenoic acid **(25)** is a potential biofilm inhibitory agent against cariogenic bateria[15]. *M. glomerata* has been identified for potential pharmacological applications in the following areas: arthritis, appetite stimulant, anticoagulant,

antifungal, antispasmodic, antioxidant, antipyretic, antisyphilitics, antitumoral, itchy eczema treatment, neuralgia, rheumatism and as a sudorific[7]. The hexane fractions of a methanolic extract from *M. laevigata* were found to have a minimum inhibitory and bactericidal concentration between 12.5-100 µg/mL and between 25-400 µg/mL against *S.* mutans, respectively[13]. The hexane and ethanolic extracts of *M. laevigata* also had a greater selective inhibitory activity against the tumour cells Hep-2, HeLA than the nontumor cell line MRC-5[16]. *M. laevigata* has been reported to have the pharmacological application as a potential analgesic, anti-allergic, anti-inflammatory, antimicrobial, antispasmodic and antiulcer remedy[7]. The aqueous and methanolic extracts of *M. micrantha* have shown antibacterial activity against *Bacillus subtilis*, *Escherichia coli*, *Proteus vulgaris* and *Staphylococcus aureus* (*S. aureus*)[17]. Mikanolide **(38)** and two derivatives were isolated from a *M. micrantha* organic extract that exhibited antibacterial activity against pathogenic *S. aureus* and β-hemolytic *Streptococcus* at 100 µg of each compound per disc[18]. In a different study, numerous sesquiterpene lactones were isolated from an organic extract of the aerial parts of *M. micranth*a and screened for anti-cancer activity. The isolated sesquiterpene lactones showed moderate activity against six human tumour cell lines[19]. Additionally, the sesquiterpene lactones from *M. micranth*a were reported to show antiviral activity against the respiratory syncytial virus and influenza virus[20]. The identified pharmacological applications of *M. micrantha* were as a potential antibacterial and antifungal[7].
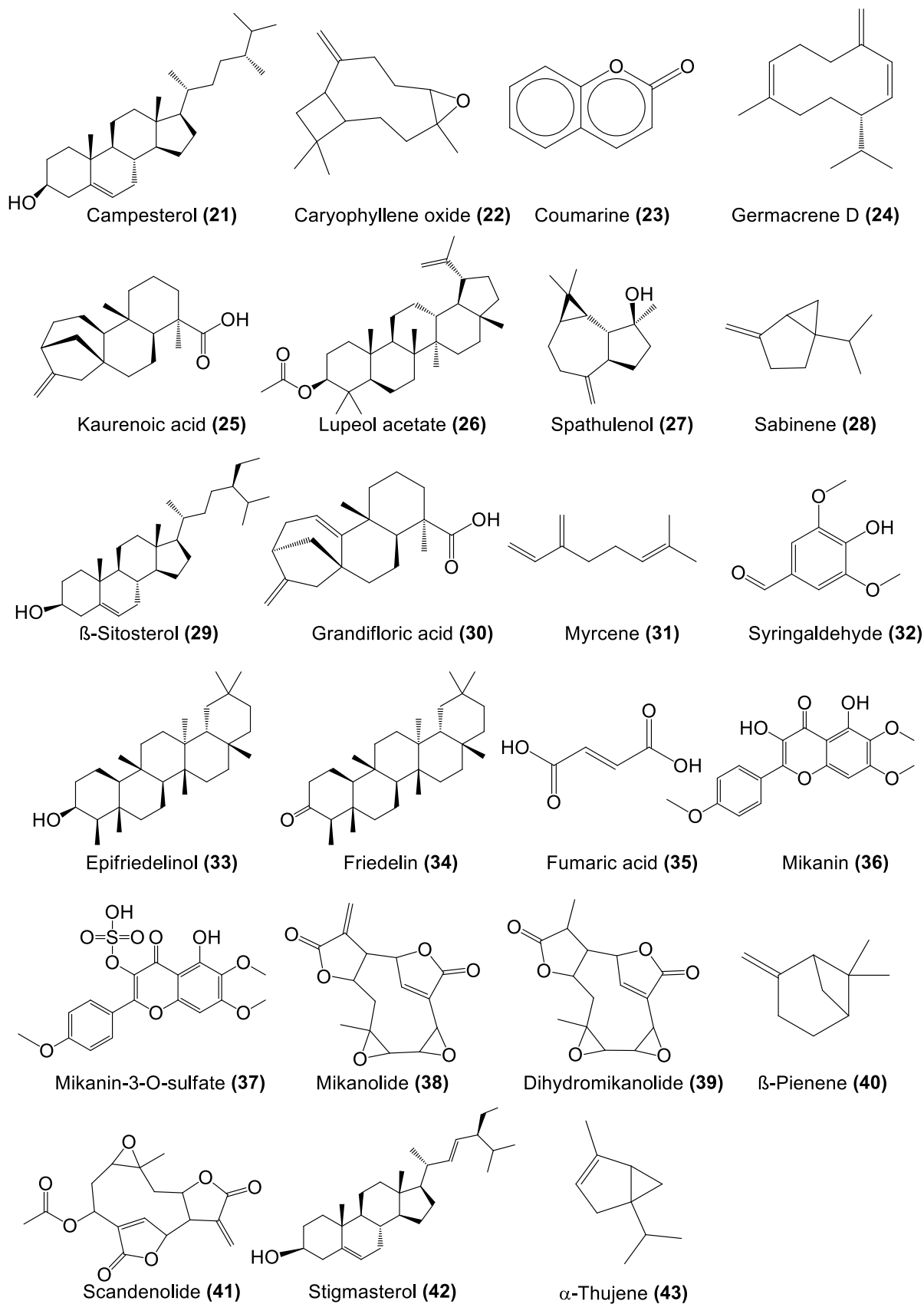
Figure 4-1 The chemical structures of a few secondary metabolites described in the *Mikania* species.

4.2   Materials and methods

M. natalensis was standardised using the South African natural product library's plant preparative methods as described in Chapter 2 Section 2.2.1. After the selection and dereplication of the hit fraction, the plant preparative methods were upscaled for the isolation, structural confirmation and IC_{50} determination.

4.2.1   Standardisation using the South African natural product library's plant preparative methods

4.2.1.1   Ultrasonic bath extraction of *M. natalensis*

Approximately 6.98 g the dried leaf material was sequentially extracted in an ultrasonic bath for 2 hours. A 50 mL DCM/MeOH (1:1) solution was used for the first 60 minutes followed by a 50 mL MeOH solution for the remaining time. The plant material and solvents were kept within a custom glass percolator that was held upright inside the ultrasonic bath using a custom stainless-steel framework. After extraction, the extract was filtered through the fixed frit at the bottom of the glass percolator and concentrated using a Buchi R300 rotary vacuum evaporator (Labotec). The extract was dried to completion in a Genevac HT-6 solvent evaporator (United Scientific) and the dry crude mass was recorded. The detailed method is outlined in Chapter 2 Section 2.2.1.2.

4.2.1.2   Automated plant extract fractionation *of M. natalensis*

The extract fractionation of *M. natalensis* was done according to the detailed method outlined in Chapter 2 Section 2.2.1.3 on a HyperSep™ C8 SPE cartridge using a Gilson GX-241 ASPEC® liquid handler. Approximately 0.242 g of the leaf extract was loaded onto a single dental cotton roll and fractionated into 7 fractions of decreasing polarity with 7 unique eluent systems. The fractions were collected on a volume-basis in pre-weighed internally barcoded PP tubes and dried to completion in a Genevac® HT-6 solvent evaporator. The dried weights were recorded in the appropriate database Excel document.

4.2.1.3   Automated plant extract and fraction standardisation of *M. natalensis*

The extract and fractions of *M. natalensis* were standardised at a concentration of 5 mg/mL in DMSO before being transferred to pre-barcoded storage vials in a 96 well plate as outlined in Chapter 2 Section 2.2.1.4. This was completed using a Hamilton Microlab® STARlet™ automated liquid handler.

4.2.1.4 Biological screening of the standardised extract and fractions of *M. natalensis* against the cell lines MCF7 and Caco2

The standardised extract and fractions of *M. natalensis* were screened in an *in vitro* MTT **(13)** assay against the human cancer cell lines MCF7 (breast cancer) and Caco2 (colorectal adenocarcinoma). Two stock solutions of the standardised samples were prepared at 25 and 50 µg/mL in DMSO. The seeded cells were treated in duplicates with 100 µL of each stock solution and incubated at 37 °C and 5 % CO_2 for 48 hours. Melphalan **(7)** (30 µM) was used in duplicate as a positive control. The reagents, standardised sample preparation, cell maintenance and treatment protocol are described in detail in Chapter 3 Section 3.3.3.2. The data obtained was analysed using Microsoft Excel and the graphs were plotted using GraphPad Prism v5.03.

4.2.2 Dereplication and upscaled production of the hit fraction with isolation, structural confirmation and IC_{50} determination of the bioactive compound

4.2.2.1 Hit dereplication and tentative identification of the bioactive compound using UPLC-PDA-HRMS

Chemical separation and detection of the standardised extract and fractions used a Waters® ACQUITY UPLC® system coupled to a Waters® XEVO-G2-XS-QTOF (UPLC-PDA-HRMS) detector as described in full detail in Chapter 2 Section 2.2.2.2. The Waters® XEVO-G2-XS-QTOF collected mass spectral scans every 0.3 seconds with a mass range of 50-1200 *m/z*. The raw data was collected in MS^E DIA mode and used a leucine enkephalin (555.2693 Da) solution as an internal standard. Separation was achieved using a reverse phase step gradient on an ACQUITY UPLC® C18 BEH column (2.1 mm ID x 100 mm, 1.7 µm) that was kept at 50 °C during runs. The gradient consisted of an aqueous mobile phase A and an organic mobile phase B. Mobile phase A consisted of ultra-pure water spiked with 0.1 % formic acid while the mobile phase B consisted of ultra-pure methanol spiked with 0.1 % formic acid. The flow rate was set at 0.300 mL/min throughout the entire run. The gradient started with an isocratic hold of 3 % B for 1.0 min followed by a linear increase to 100 % B at 14.0 min. The gradient was held at 100 % B for 3.0 min then returned to initial conditions over 0.5 min. The gradient was held at 3 % B till the final run time of 20 minutes. Data collection of the positive and negative ESI mode was done independently which required two 5 µL injections per sample.

The tentative identification of the bioactive compound used the mass spectral data obtained from the UPLC-PDA-HRMS to search online chemical databases. The calculated monoisotopic mass (corrected with lock mass), light absorption (λ_{max}) and the calculated molecular formula were used to search the following online databases: ChemSpider, PubChem, Reaxys and the Dictionary of Natural Products.

4.2.2.2 Upscaled production of the hit fraction

The upscaled extraction of *M. natalensis* was completed as a sequential extraction over 3 days that used 18.26 g of plant material. The plant material was suspended in a 500 mL Erlenmeyer flask with 300 mL DCM/MeOH (1:1) and shaken on an orbital shaker bed for 24 hours. After 24 hours, the plant material was filtered off using a Büchner funnel and Whatman No. 1 filter paper. The extract was concentrated using a Buchi R300 rotary vacuum solvent evaporator. The plant material was resuspended for a second time in 300 mL DCM/MeOH (1:1) and was shaken for an additional 24 hours. After the second extraction, the solvent was filtered off and concentrated as described above. The plant material was resuspended for a final time in 300 mL MeOH and shaken for 24 hours. After the final extraction, all the concentrated extracts were combined and dried to completion using a Genevac® HT-6 solvent evaporator. The resulting dried plant extract was weighed and the yield recorded.

Approximately 0.745 g of the upscaled plant extract was loaded onto 3 individual dental cotton rolls (250 mg per cotton roll) and fractionated using the method outlined in Chapter 2 Section 2.2.1.3 on a HyperSep™ C8 SPE cartridge using a Gilson GX-241 ASPEC® liquid handler. Unlike the previous fractionation method, identical fractions were collected as a single collection in a pre-weighed glass polytops and dried until completion in a Genevac® HT-6. The weights of each upscaled fraction was recorded and stored at -20 °C until needed.

4.2.2.3 Mass targeted isolation of mikanin 3-O-sulfate using HPLC-PDA-MS

The isolation of the bioactive compound was done on a Waters® Preparative HPLC system equipped with a Waters PDA and coupled to an ACQUITY QDa mass detector (HPLC-PDA-MS)(Waters, Milford, MA, USA), shown in Figure 4-2. System operation, data acquisition and data analysis were performed using the software MassLynx® v4.1 (Waters Inc., Milford, Massachusetts, USA). The Waters PDA detector was set to collect light absorption wavelengths between 210-400 nm at a sampling rate of 10 points/sec with a resolution of 2.4 nm. The Waters QDa mass detector was set to acquire only in positive ESI mode during runs, with the data collection set at a mass range of 150-1000 Da. The source temperature was set at 120 °C with a probe temperature of 600 °C. The capillary voltage was set to 0.80 kV and the cone voltage at 30.00 V.

Separation and isolation were accomplished using a reverse phase step gradient on an XBridge® BEH C18 OBD™ semi-preparative column (10 mm × 150 mm, 5 μm). The gradient was made up of a mobile phase A and a mobile phase B. Mobile phase A consisted of ultra-pure water spiked with 0.1 % formic acid while mobile phase B consisted of HPLC grade ACN spiked with 0.1 % formic acid. The flow rate was set to 5.0 mL/min throughout the entire run.

The gradient started with an isocratic hold of 5 % B for 0.10 minutes followed by a linear increase to 100 % B at 18.0 minutes. The gradient was held at 100 % B for 2.0 minutes then returned to initial conditions over 0.5 min. The gradient was then held at 5 % B till the final run time of 24.0 minutes. A mass-trigger based collection method was used to isolate the bioactive compound during the semi-preparative run. The mass-trigger based collection method was set to collect any peak in the positive ESI mode with a nominal mass of 345.0 m/z that was detected above a Minimum Intensity Threshold (MIT) of 100 000. The upscaled fraction sample PP24150xf4 was prepared in 1.0 mL ACN/H_2O (1:2), filtered and 900 µL was injected as a single volume onto the semi-preparative column for isolation.

Figure 4-2   An image of the Waters® Preparative HPLC system equipped with a Waters PDA and coupled to an ACQUITY QDa mass detector (HPLC-PDA-MS).

4.2.2.4   Structural confirmation of mikanin 3-O-sulfate using nuclear magnetic resonance

The 1D and 2D Nuclear Magnetic Resonance (NMR) spectral data was collected on a Bruker Avance III-HD Ascend™ 500 NMR Spectrometer fitted with a CryoProbe Prodigy BBO500 (5 mm coils) and equipped with a SampleCase for automated loading of samples, shown in Figure 4-3. System operation and data acquisition was managed by TopSpin 3.5pl7 software from Bruker. The ^{1}H and ^{13}C spectra were collected at the operating frequency 500.0100 MHz and 125.728 MHz, respectively. The isolated compound PP24150xf4t1 (0.96 mg) was prepared in 60 µL deuterated methanol (CD$_3$OD) and placed inside an NMR tube (1.7 mm ID). The software ACDLabs™ Spectrus Processor v 2021.1.1 was used for the analysis of the experimental 1D and 2D NMR spectral data. Additionally, the software was used to generate calculated NMR spectra and atom number assignment of mikanin 3-O-sulfate **(37)**. All chemical shifts were reported in ppm (δ-scale), with coupling constants "*J*" reported in Hertz (Hz) and spectra calibrations used the trace protons from CD$_3$OD = δ$_H$ 3.31 and δ$_C$ 49.1.

94

Figure 4-3 The Bruker Avance III-HD Ascend™ 500 NMR Spectrometer fitted with a CryoProbe Prodigy BBO500 and SampleCase.

4.2.2.5 IC_{50} determination of mikanin 3-O-sulfate against the cell lines MCF7 and Caco2

The isolated M3S **(37)** was screened *in vitro* in an MTT **(13)** assay against the human cancer cell lines MCF7 and Caco2. The cell lines were cultivated in DMEM-LG with 10 % FBS and 1x penicillin/streptomycin antibiotics. The cells were incubated at 37 °C, 5 % CO_2, and 100 % relative humidity until needed. The cultivated cells were seeded into 96 well plates at 4 x10^4 cells per well (100 μL) and incubated overnight to attach. A stock solution of M3S **(37)** was prepared at 50 μg/mL in DMSO. From the stock solution, serial dilutions were prepared at the following concentrations: 50.0 μg/mL (177.82 μM), 25.0 μg/mL (58.91 μM), 12.5 μg/mL (29.45 μM), 6.3 μg/mL (14.73 μM), 3.1 μg/mL (7.4 μM) and 1.7 μg/mL (3.7 μM). The seeded cells were treated in quadruplicates with 100 μL of each serial dilution concentration and incubated for 48 hours at 37 °C with 5 % CO_2. Melphalan **(7)** was used in quadruplicates as a positive control at 25 and 50 μM. After incubation, 100 μL cell medium was removed from each well. 100 μL of a 0.5 mg/mL MTT **(13)** solution was added to each well and left to incubate for 30 minutes. After incubation, the MTT **(13)** solution was removed and 100 μL of DMSO was added. OD absorbance was recorded at 540 nm and the cell proliferation inhibition (%) was calculated using Equation 2-8. The biological data was analysed using Microsoft Excel and the respective graphs along with the IC_{50} values were calculated using GraphPad Prism v5.03.

95

4.2.3 Single crystal X-ray diffraction analysis

4.2.3.1 Crystallisation technique

The crystals of dihydromikanolide **(39)** were obtained from a dried upscaled fraction produced from the method outlined in Section 4.2.2.2. Upon inspection, fine yellow needle-like crystals were found in fraction 5 (PP24150xf5- a non-bioactive fraction) with the solvent system 20:80 H_2O/MeOH. The crystals were stored at 8 °C in a refrigerator until analysed.

4.2.3.2 Single crystal X-ray diffraction analysis

The X-ray diffraction data for the single crystal (SCXRD) was measured using monochromatic Cu-Kα radiation (λ = 1.54184 Å) at 149.99(10) K with use of an Oxford Cryogenics Cryostat on a Rigaku XtaLAB Synergy R diffractometer with a rotating-anode X-ray source and a Hybrid Pixel Array CCD detector, shown in Figure 4-4. The data reduction and absorption corrections were performed using the CrysAlis[Pro] v. 1.171.41.123a. (Rigaku OD, 2022) software package. The crystal structure was solved by intrinsic phasing using SHELXT 2018/2 and refined using SHELXL 2018/3. During calculations, all hydrogen atoms were positioned in geometrically idealised sites and were constrained to ride on their parent atoms. Structure elucidation and graphics were done on the software Olex2-1.5. The X-ray crystallographic coordinates of dihydromikanolide **(39)** have been previously published and deposited in the Cambridge Crystallographic Data Centre (CCDC) with the deposit numbers 161086 and 1139991[20].

Figure 4-4 An image of the Rigaku XtaLAB Synergy R diffractometer.

4.3 Results and discussion

4.3.1 Standardisation using the South African natural product library's plant preparative methods

4.3.1.1 Ultrasonic bath extraction of *M. natalensis*

The ultrasonic bath extraction method worked well for the dried leaf material of *M. natalensis* as sufficient plant extract was produced for the extract fractionation. It was determined that a 12.39 % yield was obtained from 6.98 g of the dry leaf material as shown in Table 11.

Table 11   The ultrasonic bath extraction yield of *M. natalensis*.

Plant species (Specimen number)	Plant extract number	Plant material weight (g)	Plant extract weight (g)	Yield (%)
M. natalensis (P24150)	P24150x	6.98	0.865	12.39

4.3.1.2 Automated plant extract fractionation of *M. natalensis*

Approximately 0.242 g of plant extract P24150x was weighed and dried onto a single dental cotton roll. The extract loaded cotton roll was fractionated into 7 unique fractions of decreasing polarity and the results are shown in Table 12.

Table 12   The fraction yields of the extract P24150x.

Plant extract number	Weight of plant extract fractionated (mg)	Fraction barcode	Eluent systems	Mass (mg)	Yield (%)
P24150x	242.0	P24150xf1	95:5 H_2O/MeOH	1.42	0.59
		P24150xf2	80:20 H_2O/MeOH	0.43	0.18
		P24150xf3	60:40 H_2O/MeOH	0.75	0.31
		P24150xf4	40:60 H_2O/MeOH	1.77	0.73
		P24150xf5	20:80 H_2O/MeOH	3.13	1.29
		P24150xf6	100 MeOH	10.57	4.37
		P24150xf7	50:50 MeOH/ACN	10.40	4.30

© University of Pretoria

Overall, the fraction yields were relatively low and the total mass recovered from the loaded extract mass was 11.76 % (w/w). The mass recovery can be improved by loading more extract mass onto the cotton roll or by preventing the plant extract from over drying onto the dental cotton thus preventing the plant extract from forming a solid plug. A large majority of the compounds present in the leaf extract were mid-polar in nature as seen by the progressive increase in yields of each fraction as the eluent systems became gradually less polar. However, the trend was not seen for the first fraction as it had the 3rd highest yield. This was observed as most of the extremely polar compounds were unretained by the stationary phase of the SPE C8 RP cartridge and eluted out with the very polar eluent system 95:5 H_2O/MeOH.

4.3.1.3 Automated plant extract and fraction standardisation of *M. natalensis*

The extract and fractions of *M. natalensis* were standardised and transferred to pre-barcoded storage vials using the Hamilton Microlab® STARlet™ automated liquid handler. The final concentration, volume and pre-barcoded storage vials of the standardised extract and fractions are shown below in Table 13.

Table 13 The final concentration, volume and associated pre-barcoded storage vials of the standardised extract and fractions of P24150x.

Standardised plant extract and fraction barcode	Concentration (mg/mL)	Volume (µL)	Pre-barcoded vial label
P24150xf1	5.00	283.33	FR18784126
P24150xf2	4.31	100.00	FR18784127
P24150xf3	5.00	149.11	FR18784128
P24150xf4	5.00	353.08	FR18784129
P24150xf5	5.00	626.57	FR18784130
P24150xf6	5.00	800.00	FR18784131
P24150xf7	5.00	800.00	FR18784132
P24150xe8	5.00	800.00	FR18784133

The standardisation method completed by the STARlet™ automated liquid handler was successfully executed and handled all samples with insufficient (< 0.5 mg) and excessive masses (>10.0 mg) accordingly. It was evident after examining Table 13, that the fraction P24150xf2 had an insufficient mass to be standardised at 5 mg/mL while the fractions P24150xf6 and P24150xf7 had excess masses, evident by the maximum storage volume of 800 µL.

4.3.1.4 Biological screening of the standardised extract and fractions of *M. natalensis* against the cell lines MCF7 and Caco2

The standardised extract and fractions of *M. natalensis* were screened *in vitro* in an MTT **(13)** assay against the human cancer cell lines MCF7 and Caco2. The cell proliferation inhibition (%) of the standardised extract and fractions against the human cancer cell line MCF7 are shown in Figure 4-5.
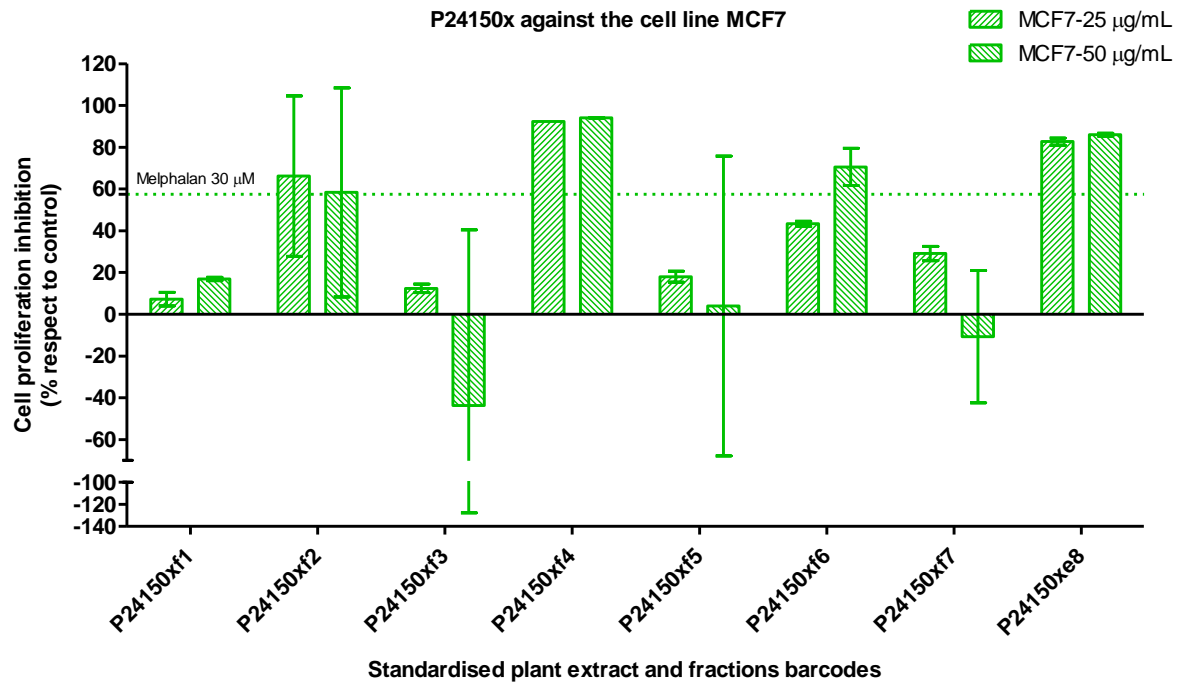
Figure 4-5   The cell proliferation inhibition (%) of the standardised extract and fractions of *M. natalensis* against the human cancer cell line MCF7.

The large standard deviation bars and negative cell proliferation inhibition values seen in fractions P24150xf2, P24150xf3, P24150xf5 and P24150xf7 were attributed to bacterial contamination during screening. At the screening concentrations 25 µg/mL and 50 µg/mL, only the following samples showed a cell proliferation inhibition above 40 %: P24150xf2, P24150xf4, P24150xf6 and P24150xfe8 (the plant extract). It was concluded that the bioactive compound(s) were concentrated in the fraction P24150xf4 than any other fraction. At the screening concentrations of 25 µg/mL and 50 µg/mL against the cell line MCF7, the fraction P24150xf4 showed a cell proliferation inhibition of 92 % and 94 %, respectively. The cell proliferation inhibition (%) of the *M. natalensis* extract and fractions against the human cancer cell line Caco2 is shown in Figure 4-6.

99
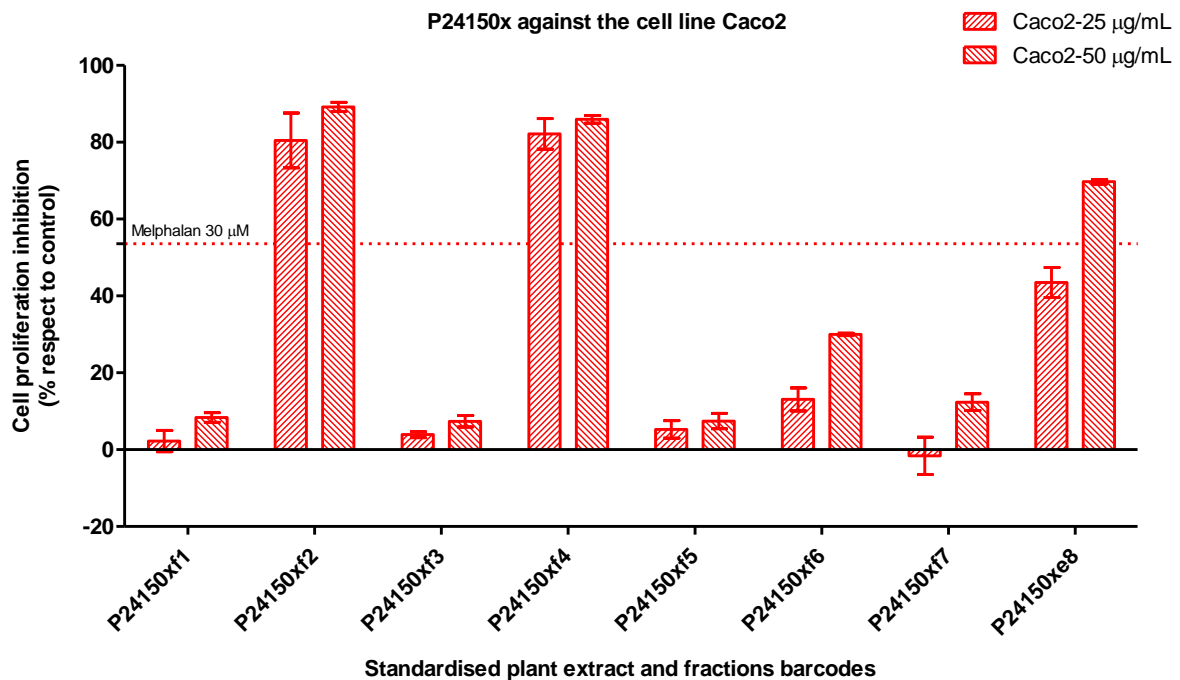
Figure 4-6 The cell proliferation inhibition (%) of the standardised extract and fractions of *M. natalensis* against the human cancer cell line Caco2.

The large standard deviation bars and the negative cell proliferation inhibition values seen in fractions P24150xf1 and P24150xf7 were attributed to bacterial contamination during screening. At the screening concentrations 25 µg/mL and 50 µg/mL, only the following samples showed more than 40 % cell proliferation inhibition against the cell line Caco2: P24150xf2, P24150xf4 and P24150xfe8. At the screening concentrations of 25 µg/mL and 50 µg/mL against the Caco2 cell line, the fractions P24150xf2 and P24150xf4 showed cell proliferation inhibitions above 80 %. At 25 µg/mL, the fraction P24150xf4 showed the highest cell proliferation inhibition of 82 % while P24150xf2 showed 80 %. At 50 µg/mL it was the fraction P24150xf2 that showed a higher cell proliferation inhibition of 89 % while P24150xf4 only showed 85 % inhibition. It was concluded that the bioactive compounds were concentrated in the fractions P24150xf2 and P24150xf4. Overall, only the fraction P24150xf4 had 80 % cell proliferation inhibition against both cancer cell lines at both test concentrations. This resulted in only the fraction P24150xf4 selected for post-HTS investigated to identify a possible anti-cancer compound.

4.3.2   Dereplication and upscaled production of the hit fraction with isolation, structural confirmation and IC$_{50}$ determination of the bioactive compound

4.3.2.1   Hit dereplication and tentative identification of the bioactive compound using UPLC-PDA-HRMS

The UPLC-PDA-HRMS analysis of the bioactive fraction P24150xf4 was done in both positive and negative ESI mode. The BPI (base peak ion) PDA and MS chromatograms of the bioactive fraction P24150xf4 in positive ESI mode are shown in Figure 4-7.
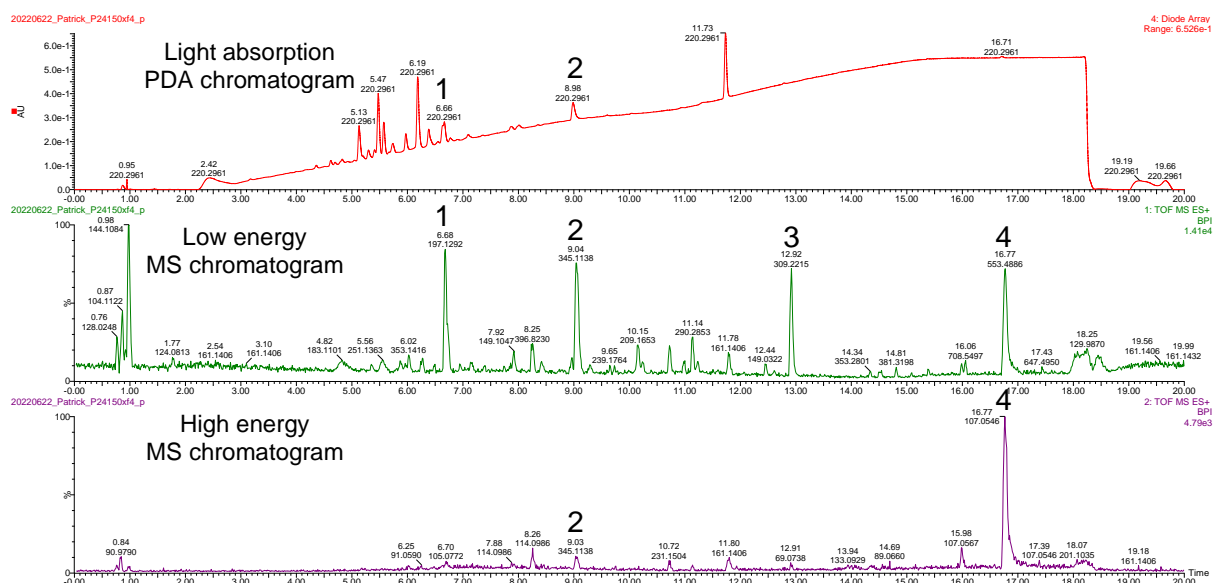
Figure 4-7 The UPLC-PDA-HRMS BPI chromatograms of the bioactive fraction P24150xf4 in positive ESI mode. Shown above is the PDA chromatogram (top), the low (middle) and high (bottom) energy MS chromatograms of the bioactive fraction P24150xf4.

The chemical analysis indicated the presence of 4 well ionising compounds in the positive ESI mode. It was determined that the peaks numbered 1,3 and 4 were mobile phase contaminates and thus ignored. In positive ESI mode, peak 2 (RT = 9.03 min) was unique to the bioactive fraction and the corresponding PDA spectrum along with the low and high energy mass spectra in positive ESI mode were extracted and shown in Figure 4-8 and Figure 4-9, respectively.
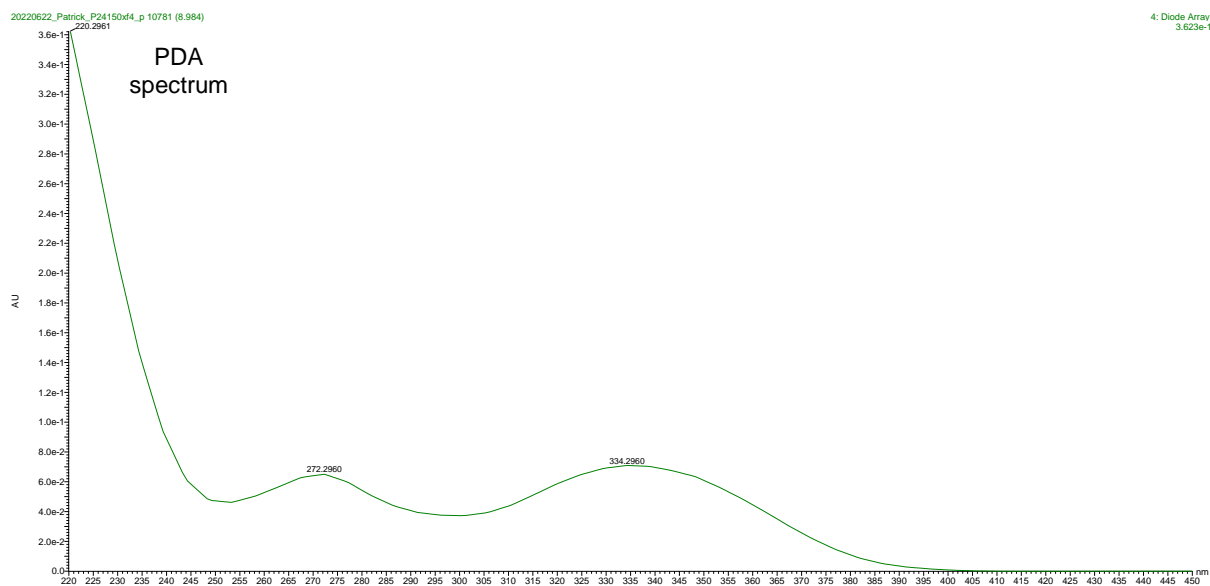
Figure 4-8 The extracted PDA spectrum of peak 2 from the PDA chromatogram shown in Figure 4-7.
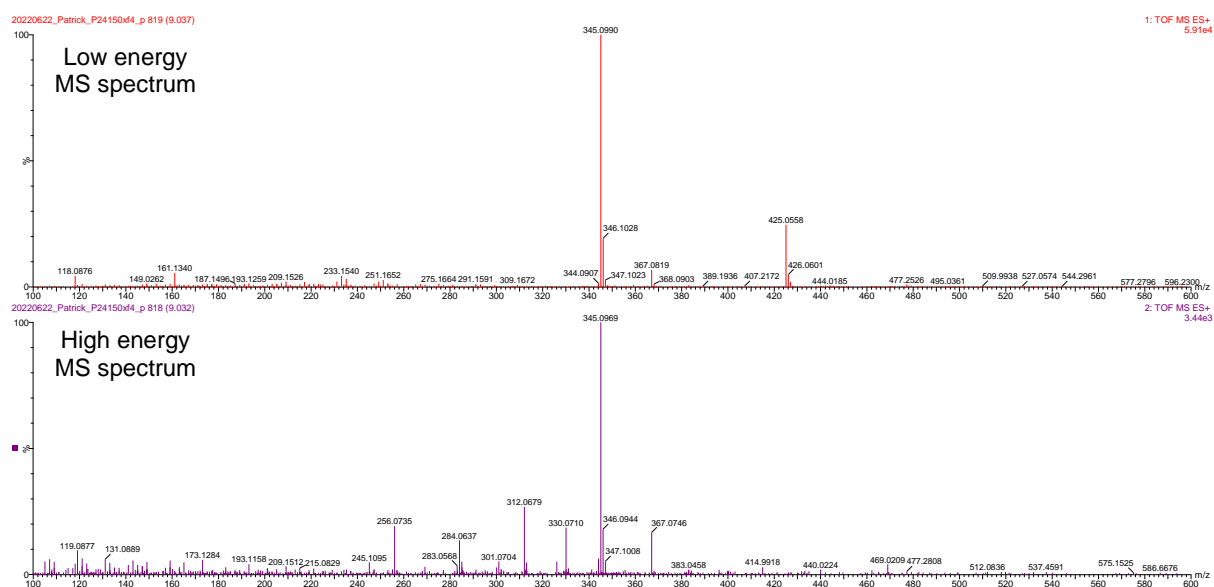
Figure 4-9 The lock mass corrected low (top) and high (bottom) energy mass spectra of peak 2 from the BPI MS chromatograms in positive ESI mode shown in Figure 4-7.

The extracted PDA spectrum of peak 2 indicated that the compound had a light absorption wavelength of λ_{max} = 272 and 334 nm. The extracted low and high energy mass spectra of peak 2 in positive ESI mode showed the quasi-molecular ion [M+H]$^+$ at 425.0556 m/z along with 5 high energy fragments shown in Table 14. It was also noted that peak 2 had a base peak ion with the nominal mass 345 m/z in positive ESI mode.

102

The BPI PDA and MS chromatograms of the bioactive fraction P24150xf4 in negative ESI mode are shown in Figure 4-10. The analysis indicated the presence of only one well ionising compound at a similar RT as peak 2. The corresponding PDA spectrum along with the low and high energy mass spectra in negative ESI mode were extracted and shown in Figure 4-11 and Figure 4-12, respectively.
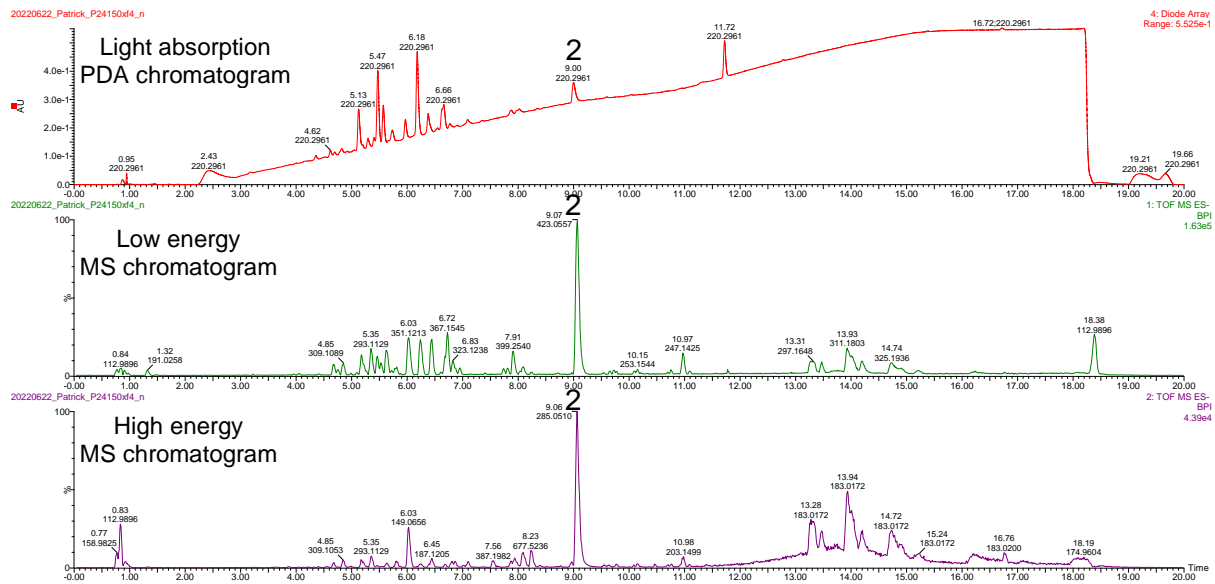
Figure 4-10 The UPLC-PDA-HRMS BPI chromatograms of the bioactive fraction P24150xf4 in negative ESI mode. Shown above is the PDA chromatogram (top), the low (middle) and high (bottom) energy MS chromatograms of the bioactive fraction P24150xf4.
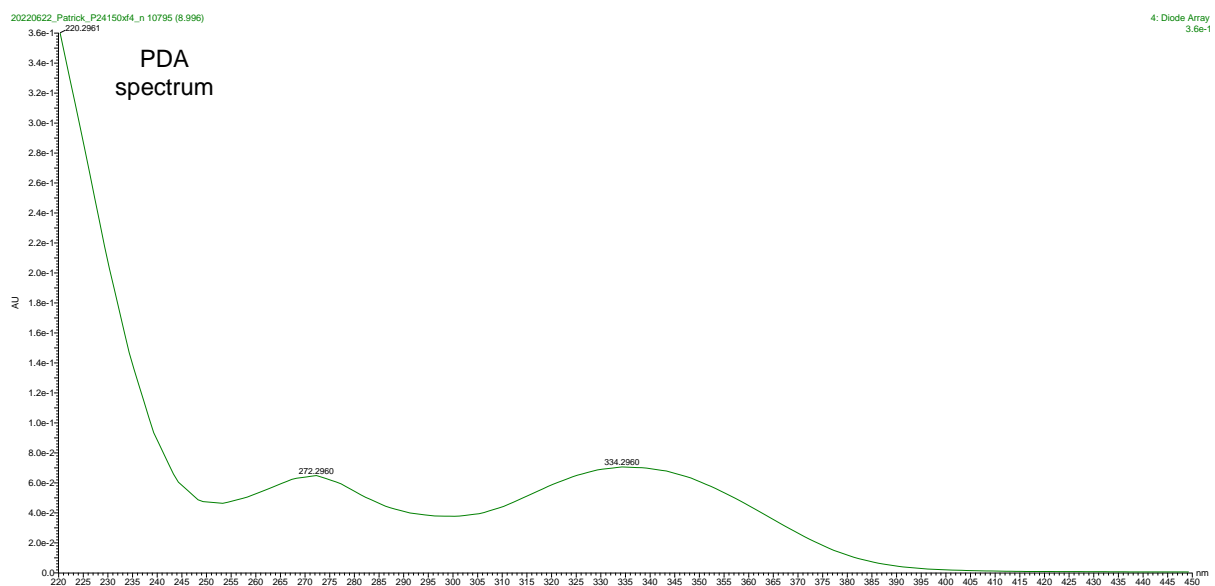
Figure 4-11 The extracted PDA spectrum of peak 2 from the PDA chromatogram shown in Figure 4-10.

103
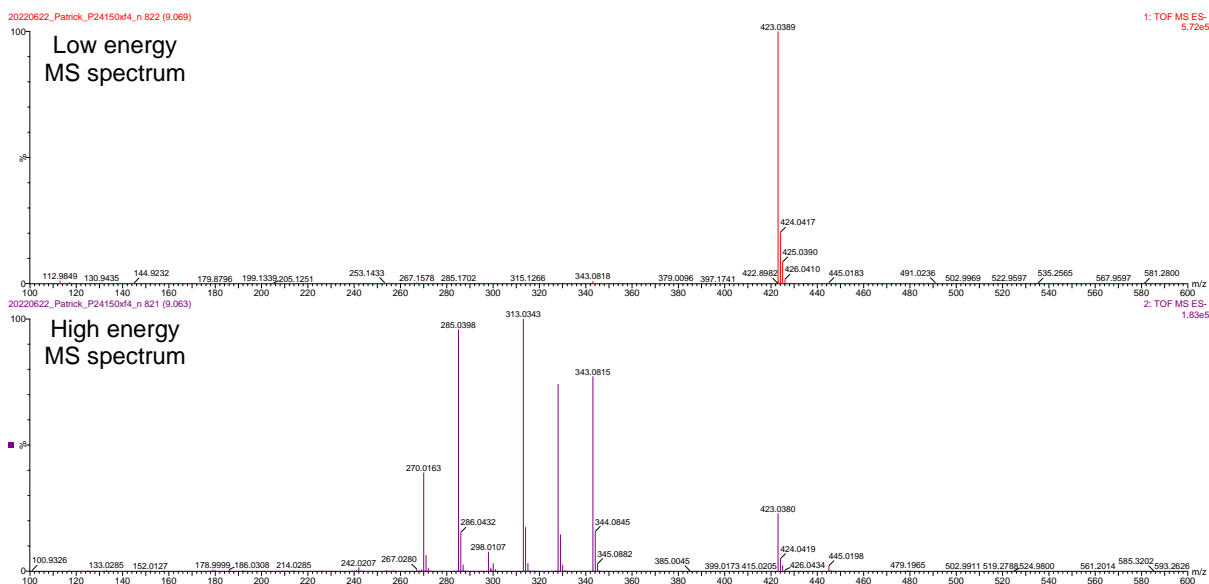
Figure 4-12 The lock mass corrected low (top) and high (bottom) energy mass spectra of peak 2 from the BPI MS chromatograms in negative ESI mode shown in Figure 4-10.

The extracted PDA spectrum showed that the compound had a light absorption wavelength at λ_{max} = 272 and 334 nm, confirming that peak 2 is the same compound that ionises well in both ESI modes. The extracted low and high energy negative ESI mass spectra's of peak 2 showed a quasi-molecular ion [M-H]⁻ at 423.038 *m/z* along with 5 high energy fragments shown in Table 14.

Table 14 The high energy positive and negative ESI mode mass spectral data of peak 2.

ESI Mode	RT* (min)	Observed *m/z*** (mass error (mDa))	Observed quasi-molecular ion and formula	Observed fragment (*m/z***) (mass error (mDa)) and fragment formula
Positive	9.03	425.0558 (-1.6)	[M+H]⁺ [$C_{18}H_{17}O_{10}S$]⁺	345.0969 (-0.5) [$C_{18}H_{17}O_7$]⁺
				330.0710 (-3.0) [$C_{17}H_{14}O_7$]⁺
				312.0679 (5.5) [$C_{17}H_{12}O_6$]⁺
				284.0637 (-4.8) [$C_{16}H_{12}O_5$]⁺
				256.0735 (-0.1) [$C_{15}H_{12}O_4$]⁺

Negative	9.06	423.0380 (-0.6)	[M-H]⁻ [C₁₈H₁₅O₁₀S]⁻	343.0815 (-0.3) $[C_{18}H_{15}O_7]^-$
				328.0580 (-0.3) $[C_{17}H_{12}O_7]^-$
				313.0343 (-0.5) $[C_{16}H_9O_7]^-$
				285.0398 (-0.1) $[C_{15}H_9O_6]^-$
				270.0163 (-0.1) $[C_{14}H_6O_6]^-$

*RT, retention time; **m/z, mass to charge ratio*

In both positive and negative ESI mode, the molecular formula of the quasi-molecular ion and high energy fragments were reported with the mass error in mDa. The calculated molecular formulas of each fragment with a mass error greater than ± 2.5 mDa were deemed inaccurate. It was noted that the high energy fragments in positive ESI mode 330.0710 *m/z*, 312.0679 *m/z* and 284.0637 *m/z* had mass errors of -3.0, 5.5 and -4.8 mDa, respectively. This may be due to the calibration of the mass detector in positive ESI mode. It was recognised that the high energy fragments in negative ESI mode had the lowest mass error.

Using the database Dictionary of Natural Products and Table 14, peak 2 was tentatively identified as mikanin 3-O-sulfate **(37)** and labelled as M3S **(37)**. As seen in Figure 4-1, M3S **(37)** is the sulphated analogue of mikanin **(36)** with a calculated monoisotopic weight 424.0464 Da and the molecular formula $C_{18}H_{16}O_{10}S$. M3S **(37)** was observed at RT = 9.06 min in the BPI MS chromatogram in negative ESI mode at 285.0398 *m/z* with the base peak ion 313.0343 *m/z* as shown in Figure 4-10 and Figure 4-12, respectively. The quasi-molecular ion [M-H]⁻ of M3S **(37)** was observed at 423.0380 *m/z* with a mass error of -0.6 mDa and the molecular formula $[C_{18}H_{15}O_{10}S]^-$ with the corresponding light absorption wavelengths of λ_{max} = 272 and 334 nm. At the time of writing, there was no published data on the light absorption wavelengths or high-resolution low and high energy mass fragments of M3S **(37)**. Further analysis of the extracted high energy mass spectrums in both the positive and negative ESI mode corresponded to the predicted fragmentation patterns shown in Figure 4-13 and Figure 4-14. The structural fragments were only matched to the observed mass fragments (*m/z*) if the chemical formula was an exact match. The tentative identification was accepted as the experimental accurate mass had a low mass error of -0.6 ppm when compared to the calculated monoisotopic weight of 424.0464 Da. The successful assignment of all the experimental high energy mass fragments in positive and negative ESI mode further confirmed

the tentative identification. Although no published HRMS or light absorption data existed, the above reported spectra may be helpful for future research on M3S **(37)**.

345 *m/z*

330 *m/z*

312 *m/z*

284 *m/z*

256 *m/z*
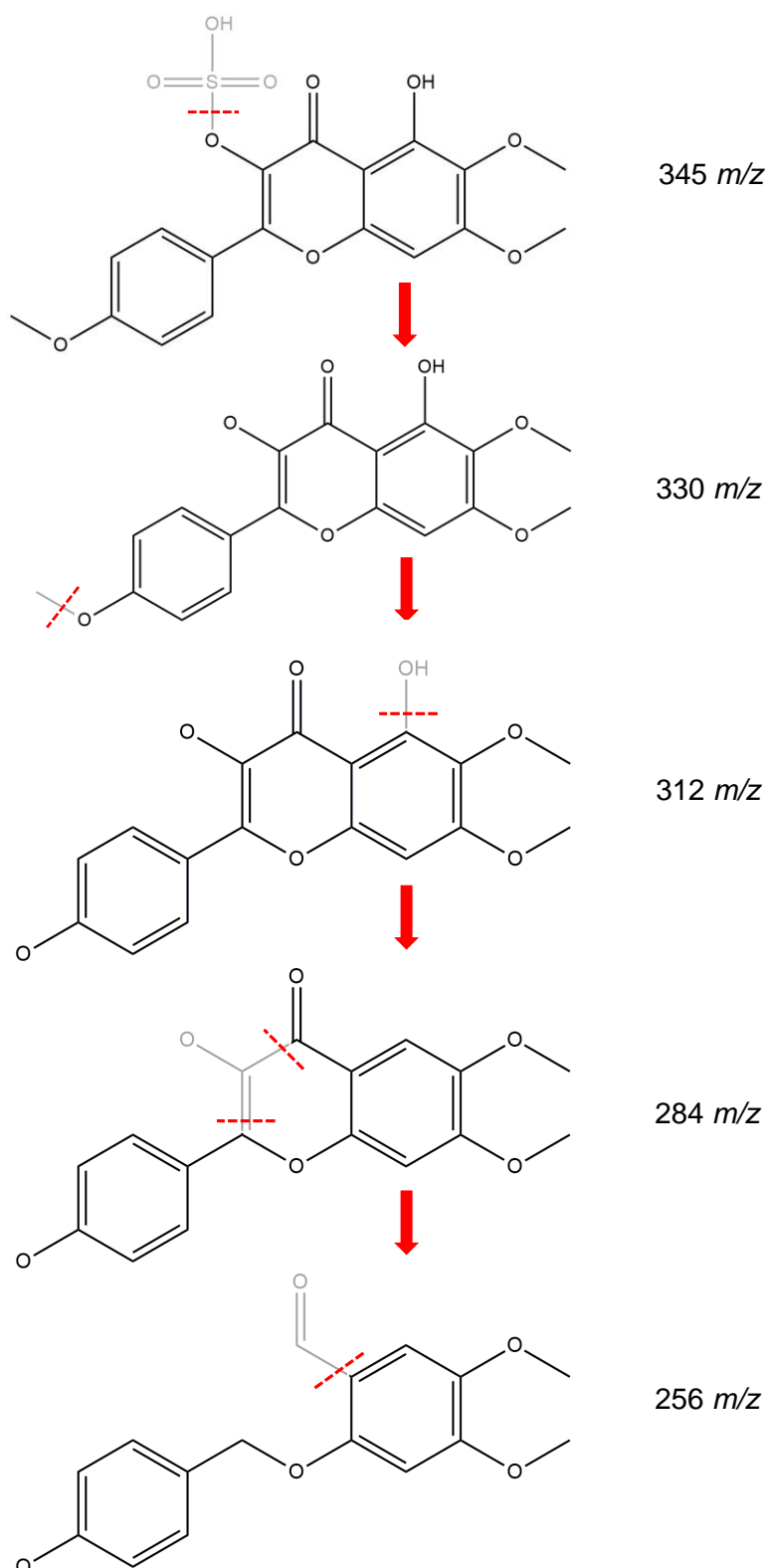
Figure 4-13 A proposed fragmentation pathway of M3S **(37)** from the high energy MS positive ESI mode fragments.

343 *m/z*

328 *m/z*

313 *m/z*

285 *m/z*

270 *m/z*
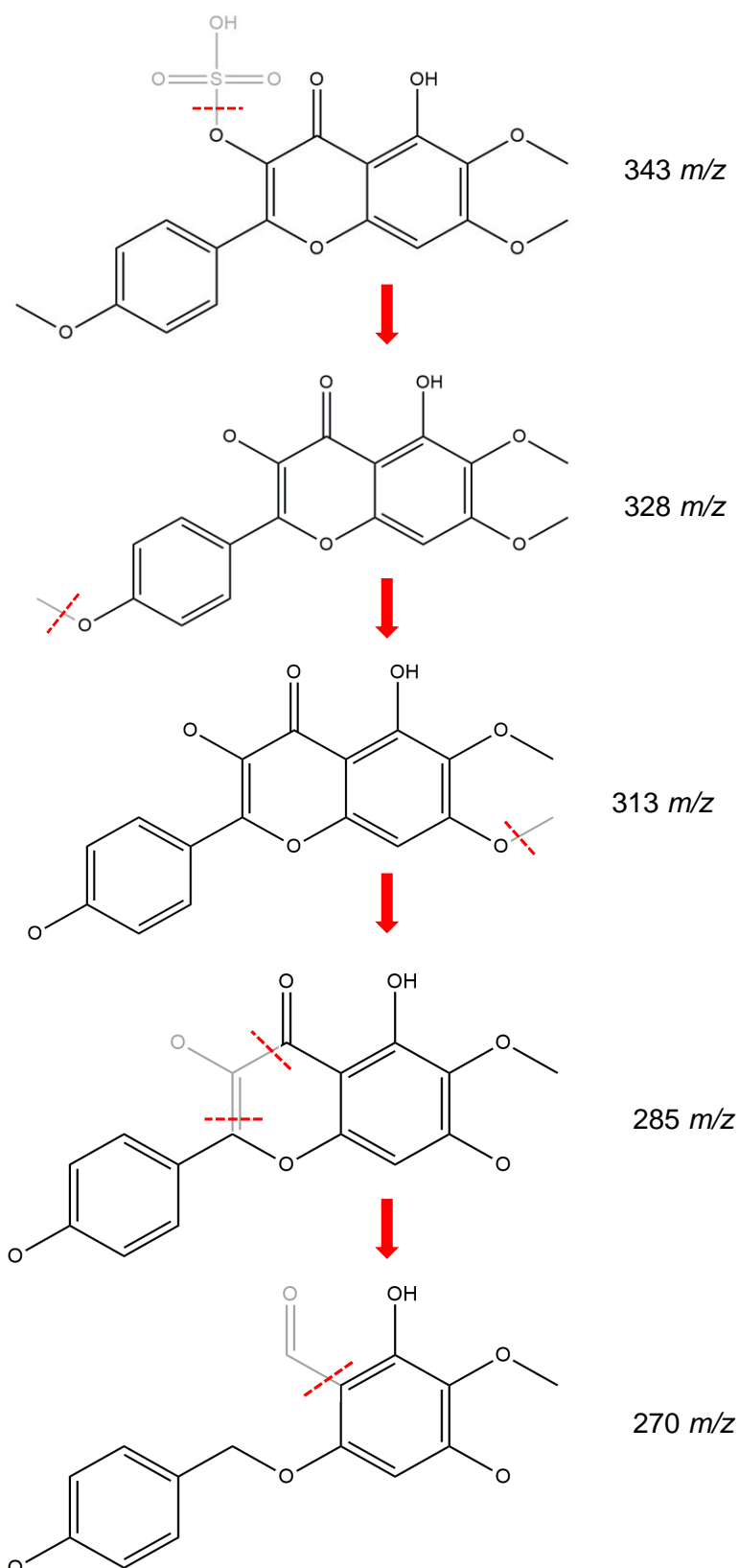
Figure 4-14 A proposed fragmentation pathway of M3S **(37)** from the high energy MS negative ESI mode fragments.

4.3.2.2　　Upscaled production of the hit fraction

After 3 days of extraction, 18.26 g of *M. natalensis* dry leaf material produced an extract (PP24150x) dry mass of 2.30 g. The upscaled plant extraction method using the orbital shaker bed had a yield of 12.60 % (w/w) which was only 0.21 % more than the extract yield obtained from the ultrasonic bath extraction.

Approximately 0.745 g of the upscaled leaf extract (PP24150x) was adsorbed onto 3 individual dental cotton rolls and fractionated on a HyperSep™ C8 SPE cartridge using a Gilson GX-241 ASPEC® liquid handler. Shown in Table 15 are the yields of each upscaled fraction collected using the respective eluent systems.

Table 15　The upscaled plant fraction yields of the extract PP24150x.

Plant extract number	Total weight of plant extract fractionated (mg)	Fraction barcode	Eluent systems	Mass (mg)	Yield (%)
PP24150x	0.745	PP24150xf1	95:5 H_2O/MeOH	10.28	1.38
		PP24150xf2	80:20 H_2O/MeOH	7.52	1.01
		PP24150xf3	60:40 H_2O/MeOH	12.04	1.62
		PP24150xf4	40:60 H_2O/MeOH	24.66	3.31
		PP24150xf5	20:80 H_2O/MeOH	34.53	4.63
		PP24150xf6	100 MeOH	83.2	11.16
		PP24150xf7	50:50 MeOH/ACN	143.85	19.31

It was determined that only 0.316 g (42.43 %) of the total loaded upscaled extract mass was recovered. It was noted that the upscaled fractionation had a larger extract mass recovery than the natural product library automated fractionation method. The trends described in Section 4.3.1.2 were also observed. The upscaled fractionation of the extract resulted in 24.66 mg of the fraction PP24150xf4.

4.3.2.3 Mass targeted isolation of mikanin 3-O-sulfate using HPLC-PDA-MS

The fraction PP24150xf4 (24.66 mg) was prepared in 1.0 mL ACN/H_2O (1:2), filtered and injected (900 µL) as a single volume onto the semi-preparative column where M3S **(37)** was isolated using a mass-trigger based collection on the HPLC-PDA-MS. The BPI MS chromatogram in positive ESI mode of PP24150xf4 is shown in Figure 4-15.
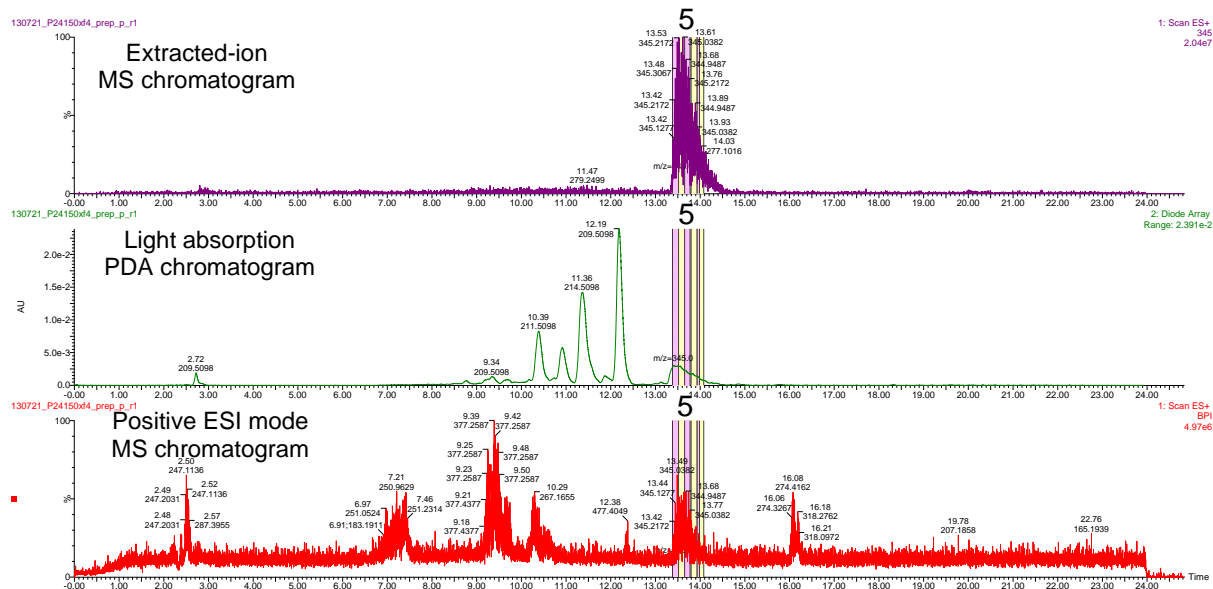
Figure 4-15 The HPLC-PDA-MS BPI chromatograms of the the upscaled fraction PP24150xf4 in positive ESI mode. Shown above is the extracted-ion MS chromatogram (top) of 345 *m/z*, the PDA chromatogram (middle) and the MS chromatogram (bottom) in ESI positive mode

After extracting the nominal mass for the base peak ion (345 *m/z)* of M3S **(37)** previously mentioned in Section 4.3.2.1, it was determined that peak 5 at RT= 13.40-14.08 (min) was M3S **(37)**. During the run, peak 5 was collected across 6 individual vials. Only the first three vials were combined due to the presence of a minor second compound in the remaining vials. The contents of the first three vials were combined and dried resulting in 0.96 mg of M3S **(37)** isolated. The mass-trigger based collection was successful as seen by the coloured collection bands in Figure 4-15. The extracted-ion chromatogram of nominal mass 345 *m/z* showed only a single occurrence of that mass, ensuring no other compounds with a similar fragment could have been collected. The MIT of 100 000 was set perfectly as the entire peak was collected and prevented the collection of any target masses found in the base noise.
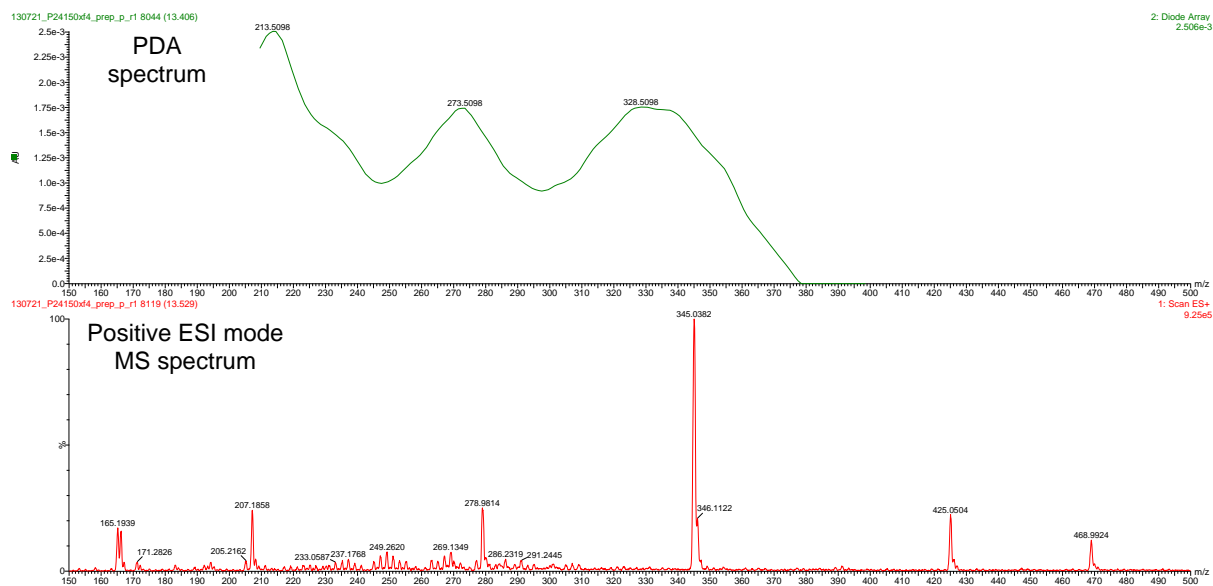
Figure 4-16 The extracted PDA and mass spectra in positive ESI mode of peak 5 from the HPLC-PDA-MS BPI chromatograms shown in Figure 4-15.

Nearly identical light absorption wavelengths were observed for peak 2 and peak 5 in Figure 4-11 and in Figure 4-16. It was also noted that only the high energy quasi-molecular ion and base peak ion seen in the HRMS of peak 2 in positive ESI mode seen in Figure 4-9, were also present in the extracted HPLC-PDA-MS MS spectrum of peak 5. However, this was taken into consideration that one cannot make a direct comparison between data collected from different detectors.

4.3.2.4 Structural confirmation of mikanin 3-O-sulfate using NMR

ACDLabs™ Spectrus Processor was used to confirm the structure of the isolated M3S **(37)**. ACDLabs™ was used to generate the atom number assignment of M3S **(37)** shown in Figure 4-17. The experimental and calculated ^{1}H and ^{13}C spectra of M3S **(37)** are shown in Figure 4-18 and Figure 4-19, respectively. The experimental HSQC and HMBC spectra of M3S **(37)** are shown in Figure 4-20 and Figure 4-21, respectively.
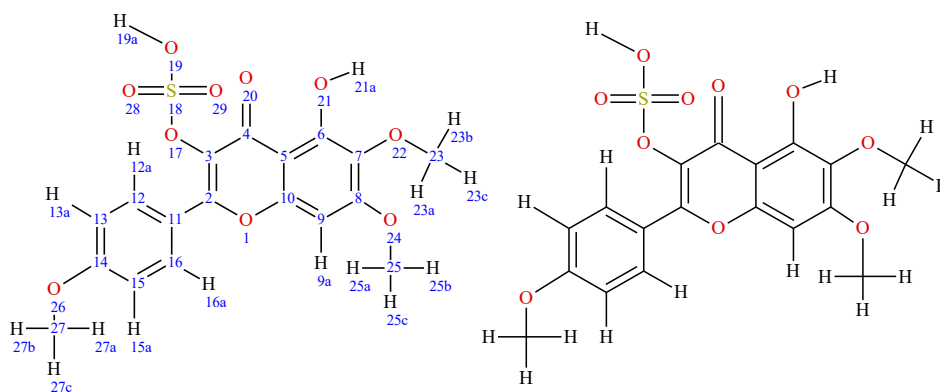
Figure 4-17 The atom number assignment (left) of M3S **(37)** (right).

110
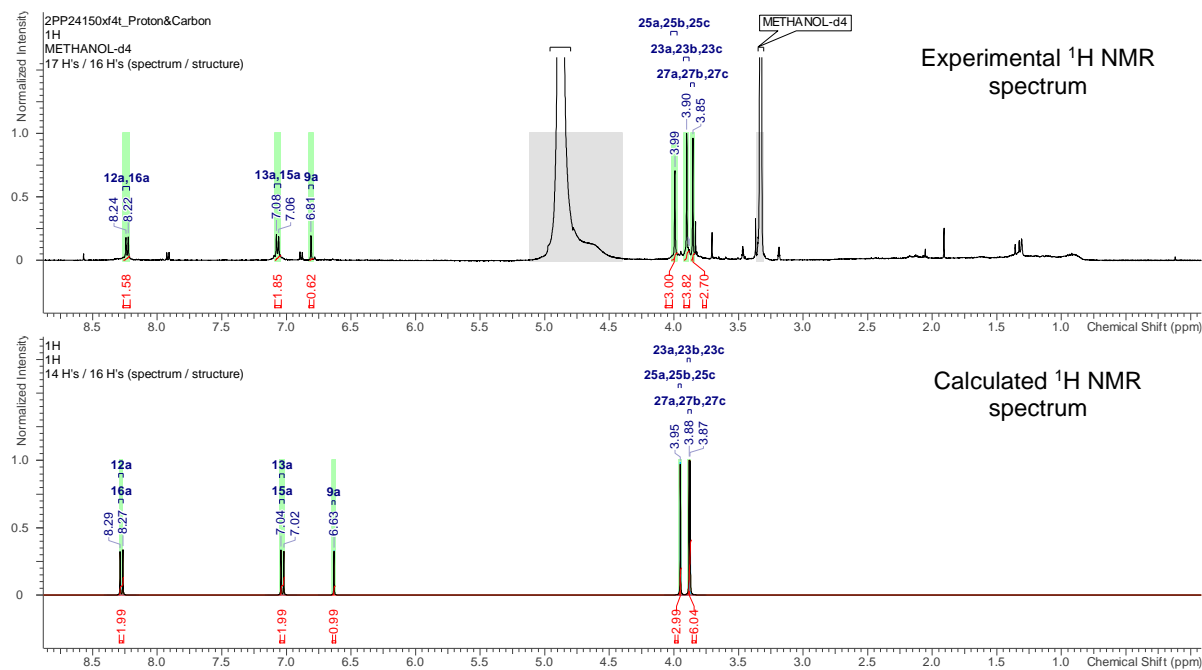
Figure 4-18 The experimental (top) and ACDLabs™ calculated (bottom) ¹H NMR spectra of M3S **(37)**, with atom number assignments.
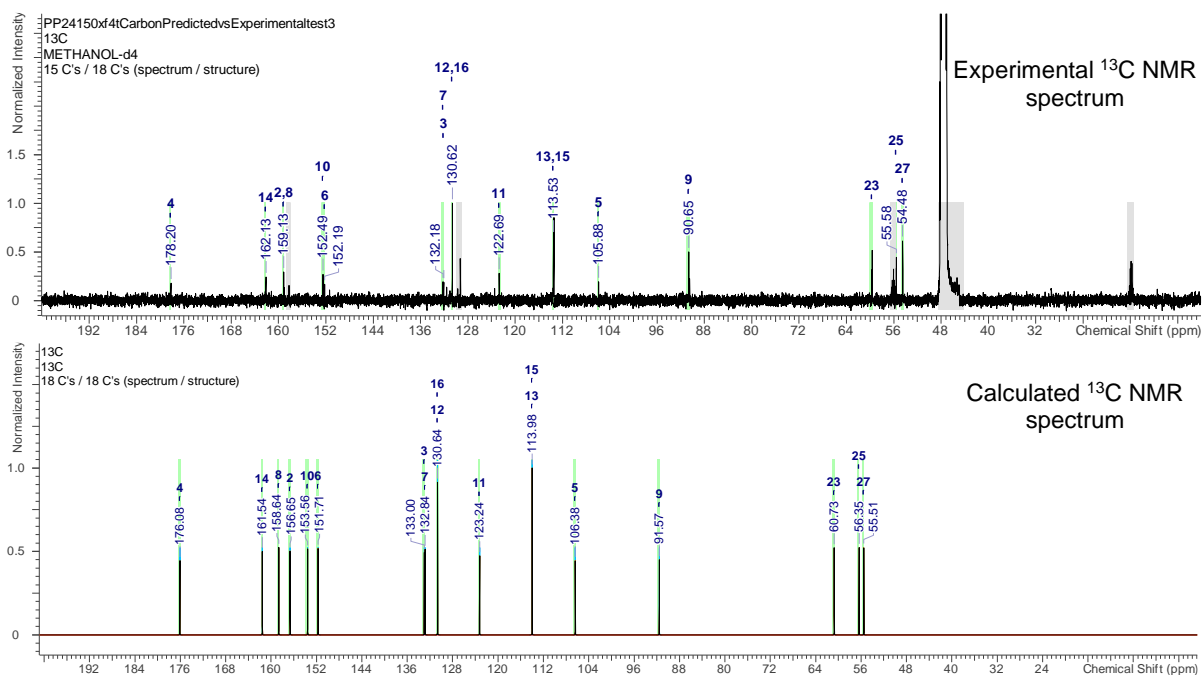
Figure 4-19 The experimental (top) and ACDLabs™ calculated (bottom) ¹³C NMR spectra's of M3S **(37)**, with atom number assignments.
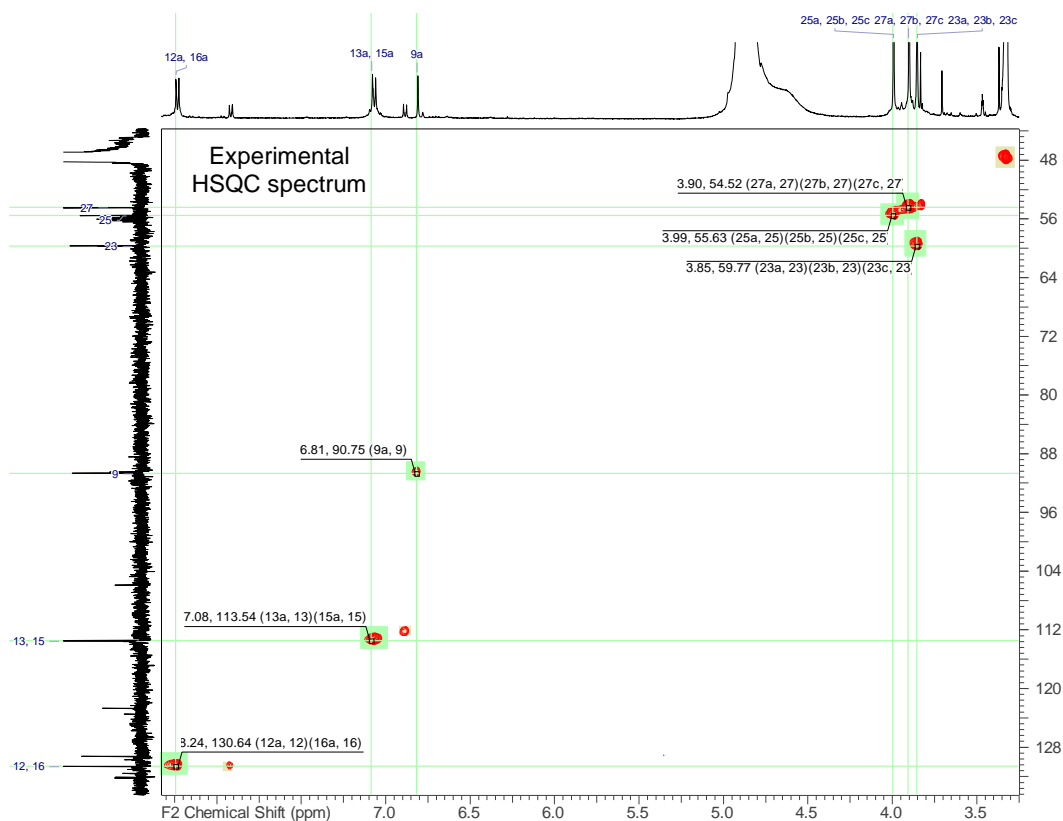
Figure 4-20 The HSQC NMR spectrum of M3S **(37)**, with atom number assignments, shifts and atom number correlations.
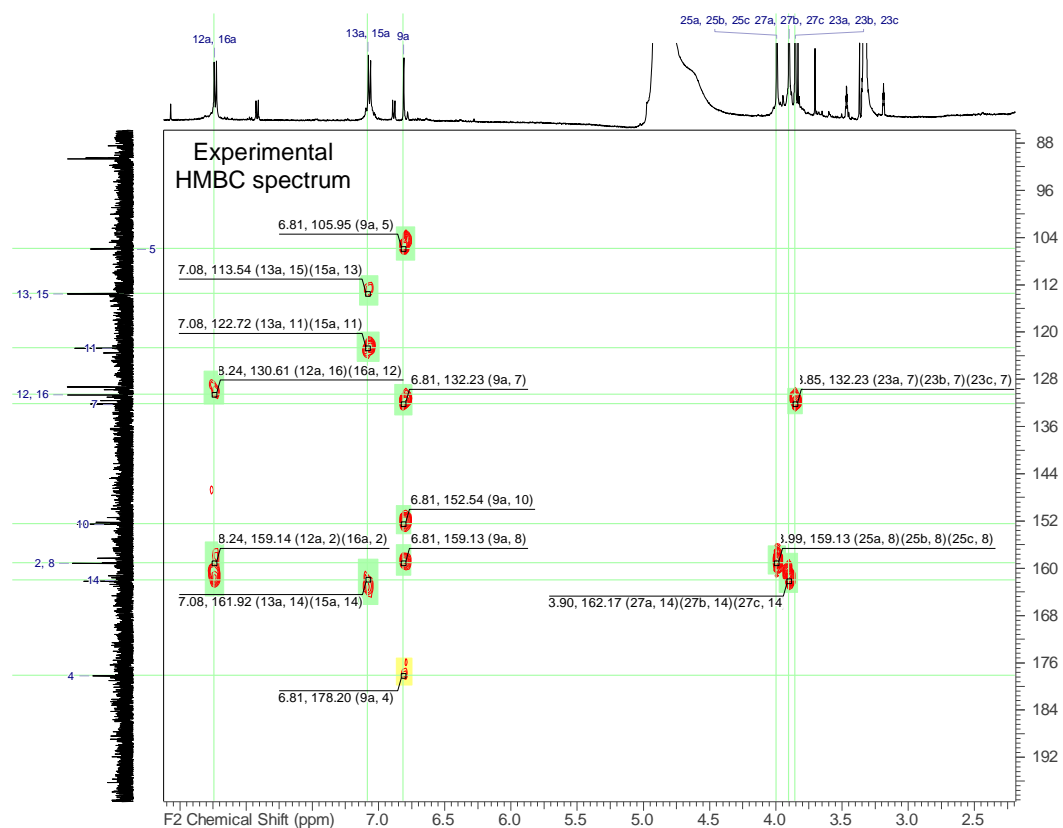
Figure 4-21 The HMBC NMR spectrum of M3S **(37)**, with atom number assignments, shifts and atom number correlations.

112

As no published NMR spectral data was available, the experimental ^{1}H and ^{13}C NMR shifts of M3S **(37)** were compared to the ACDLabs™ calculated NMR shifts as shown in Table 16 and Table 17. The calculated ^{1}H spectrum of M3S **(37)** did not include multiplicity and coupling of protons but still provided the predicated atom shifts. The experimental ^{1}H shifts of M3S **(37)** were observed as: ^{1}H NMR (CD$_3$OD, 500 MHz): δ 3.85 (s, 3H), 3.90 (s, 3H), 3.99 (s, 3H), 6.81 (s, 1H), 7.06 (d, 1H, J = 9.0 Hz), 7.08 (d, 1H, J = 9.0 Hz), 8.22 (d, 1H, J = 9.0 Hz), 8.24 (d, 1H, J = 9.0 Hz). Ortho-coupling was observed between H-12a and H-13a as well as ortho-coupling between H-15a and H-16a. No meta-coupling was observed since the meta-positioned aromatic protons 13a and 15a/12a and 16a have the same properties. The experimental ^{1}H shifts of M3S **(37)** are almost an identical match to the calculated shifts as shown in Table 16.

Table 16 The experimental and ACDLabs™ calculated ^{1}H shifts of M3S **(37)**.

Atom number assignments	XHn	H Count	Experimental [1]H δ (ppm) and J (Hz) (CD$_3$OD)	Calculated [1]H δ (ppm)
9a	C<u>H</u>	1H	6.81 (s)	6.63
12a	C<u>H</u>	1H	8.24 (d, J = 9.0)	8.29
13a	C<u>H</u>	1H	7.08 (d, J = 9.0)	7.04
15a	C<u>H</u>	1H	7.06 (d, J = 9.0)	7.02
16a	C<u>H</u>	1H	8.22 (d, J = 9.0)	8.27
23a, 23b, 23c	C<u>H</u>$_3$	3H	3.85 (s)	3.88
25a, 25b, 25c	C<u>H</u>$_3$	3H	3.99 (s)	3.95
27a, 27b, 27c	C<u>H</u>$_3$	3H	3.90 (s)	3.87

The experimental ^{13}C shifts of M3S **(37)** were as follows: ^{13}C NMR (CD$_3$OD, 126 MHz): δ 54.5, 55.6, 59.7, 90.7, 105.9, 113.5, 122.7, 130.6, 132.1, 132.2, 152.2, 152.5, 159.1, 162.1, 178.2. After investigation of the ^{13}C NMR spectra, it was determined that a carbonyl group was present at δ$_C$ 178.2 (C-4), quaternary carbons at δ$_C$ 122.7 (C-11), δ$_C$ 132.1 (C-3), δ$_C$ 132.2 (C-7), δ$_C$ 152.2 (C-6), δ$_C$ 152.5 (C-10), δ$_C$ 159.1 (C-2/C-8), δ$_C$ 162.1 (C-14), δ$_C$ 178.2 (C-4), a deshielded quaternary unsaturated carbon δ$_C$ 105.9 (C-5) and an aromatic carbon at δ$_C$ 90.7 (C-9). Symmetry was observed in the aromatic carbon region at δ$_C$ 113.5 (C-13/C-15) and δ$_C$ 130.6 (C-12/C-16). Three methoxy carbons were also seen at δ$_C$ 54.5 (C-27), δ$_C$ 55.6 (C-25) and δ$_C$ 59.7 (C-23). The experimental ^{13}C spectra shifts are a close match to the calculated shifts of M3S **(37)** as shown in Table 17.

Table 17 The experimental and ACDLabs™ calculated ^{13}C shifts of M3S **(37)**.

Atom number assignments	XHn	Experimental ^{13}C δ (ppm) (CD₃OD)	Calculated ^{13}C δ (ppm)
2	C	159.1	156.7
3	C	132.1	133.0
4	C	178.2	176.1
5	C	105.9	106.4
6	C	152.2	151.7
7	C	132.2	132.8
8	C	159.1	158.6
9	CH	90.7	91.6
10	C	152.5	153.6
11	C	122.7	123.2
12	CH	130.6	130.6
13	CH	113.5	114.0
14	C	162.1	161.5
15	CH	113.5	114.0
16	CH	130.6	130.6
23	CH₃	59.7	60.7
25	CH₃	55.6	56.4
27	CH₃	54.5	55.5

Upon inspection, the HSQC NMR spectra displayed all the expected proton-carbon single bond correlations of M3S **(37)**. All the protons, apart from H-19a and H-21a which are not bonded to carbon, were successfully correlated to a carbon of M3S **(37)**. As shown in Figure 4-20, the signals from impurities were ignored and the relevant correlations are shown in Table 18.

Table 18 The experimental HSQC correlations of M3S **(37)**.

Carbon Atom number	Proton Atom number	XHn	H Multiplicity	Experimental ^{1}H δ (ppm) (CD₃OD)	Experimental ^{13}C δ (ppm) (CD₃OD)
9	9a	CH	s	6.81	90.7
12	12a	CH	d	8.24	130.6
13	13a	CH	d	7.08	113.5
15	15a	CH	d	7.06	113.5
16	16a	CH	d	8.22	130.6
23	23a, 23b, 23c	CH₃	s	3.85	59.7
25	25a, 25b, 25c	CH₃	s	3.99	55.6
27	27a, 27b, 27c	CH₃	s	3.90	54.5

As seen in Figure 4-21, the HMBC NMR spectra of M3S **(37)** showed 18 unique $^2J_{CH}$, $^3J_{CH}$ and $^4J_{CH}$ correlations summarised in Table 19. The only $^4J_{CH}$ correlation was seen between H-9a (δ_H 6.81) → C-4 (δ_C 90.7). As expected, there were no correlations from either H-21a and H-19a. Additionally the positions of the three methoxy groups were confirmed. The methoxy protons H-27a, H-27b, H-27c correlated to C-14 while the methoxy protons H-23a, H-23b, H-23c and H-25a, H-25b, H-25c correlated to C-7 and C-8, respectively. All the HMBC correlations are shown in Figure 4-22.

Table 19 The experimental HMBC correlations of M3S **(37)**.

Atom Number Assignment	Experimental ^1H δ (ppm) (CD$_3$OD)	Experimental ^{13}C δ (ppm) (CD3OD)	HMBC (H→C)
2		159.1	
3		132.1	
4		178.2	
5		105.9	
6		152.2	
7		132.2	
8		159.1	
9		90.7	
9a	6.81 (1H, s)		C-4, C-5, C-7, C-8, C-10
10		152.5	
11		122.7	
12		130.6	
12a	8.24 (1H, d, *J* = 9.0)		C-2, C-16
13		113.5	
13a	7.08 (1H, d, *J* = 9.0)		C-11, C-14, C-15
14		162.1	
15		113.5	
15a	7.06 (1H, d, *J* = 9.0)		C-11, C-13, C-14
16		130.6	
16a	8.22 (1H, d, *J* = 9.0)		C-2, C-12
23		59.7	
23a, 23b, 23c	3.85 (3H, s)		C-7
25		55.6	
25a, 25b, 25c	3.99 (3H, s)		C-8
27		54.5	
27a, 27b, 27c	3.90 (3H, s)		C-14
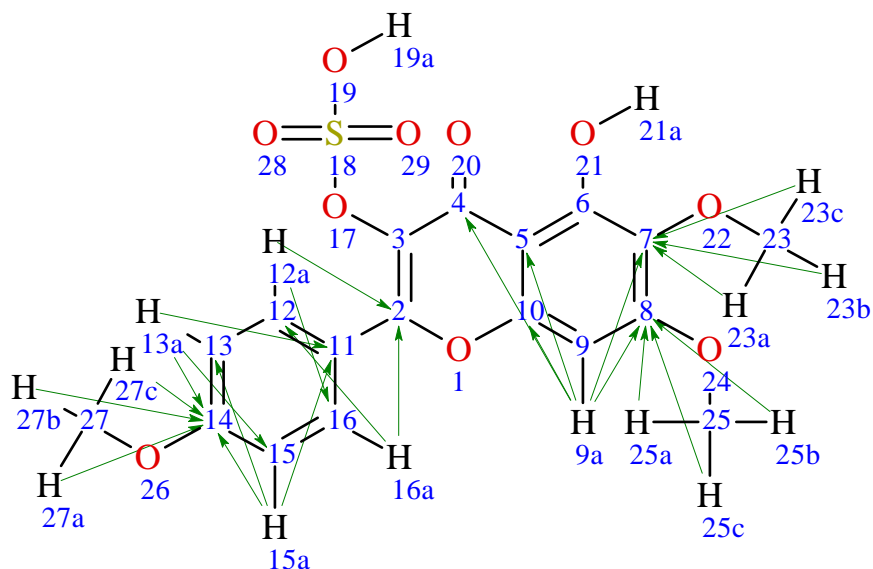
Figure 4-22 All the experimental HMBC NMR (H→C) correlations of M3S **(37)**.

Minor contamination was seen throughout the 1D and 2D spectra's which resulted in a few unassigned spectral peaks. The experimental ^{1}H and ^{13}C spectra was a close match to the ACDLabs™ calculated spectra's while the HSQC NMR spectra displayed all the expected proton-carbon single bond correlations of M3S **(37)** and the HMBC NMR spectra confirmed the positions of the three methoxy groups. Thus, it was confirmed that the isolated bioactive compound is M3S **(37)** through 1D and 2D NMR experiments. This is the first reported occurrence of M3S **(37)** isolated from the leaves of *M. natalensis*. The compound is a sulphated analogue of the flavonoid, mikanin **(36)**. In the genus *Mikania*, both mikanin **(36)** and M3S **(37)** have been reported to be found in the organic extracts of *M. micrantha* and *M. cordata*[7]. The compounds were reported to be present in the MeOH extract of the aerial parts of *M. micrantha* and in the DCM extract of *M. cordata* leaves[7,20]. At the time of writing, there were no published NMR data on mikanin **(36)** or M3S **(37)**.

4.3.2.5 IC$_{50}$ determination of mikanin 3-O-sulfate against the cell lines MCF7 and Caco2

The isolated M3S **(37)** was screened *in vitro* in an MTT **(13)** assay against the human cancer cell lines MCF7 and Caco2. The cell proliferation inhibition (%) of M3S **(37)** was determined and the dose-response curves were calculated. The cell proliferation inhibition (%) of M3S **(37)** against MCF7 is shown below in Figure 4-23.

116
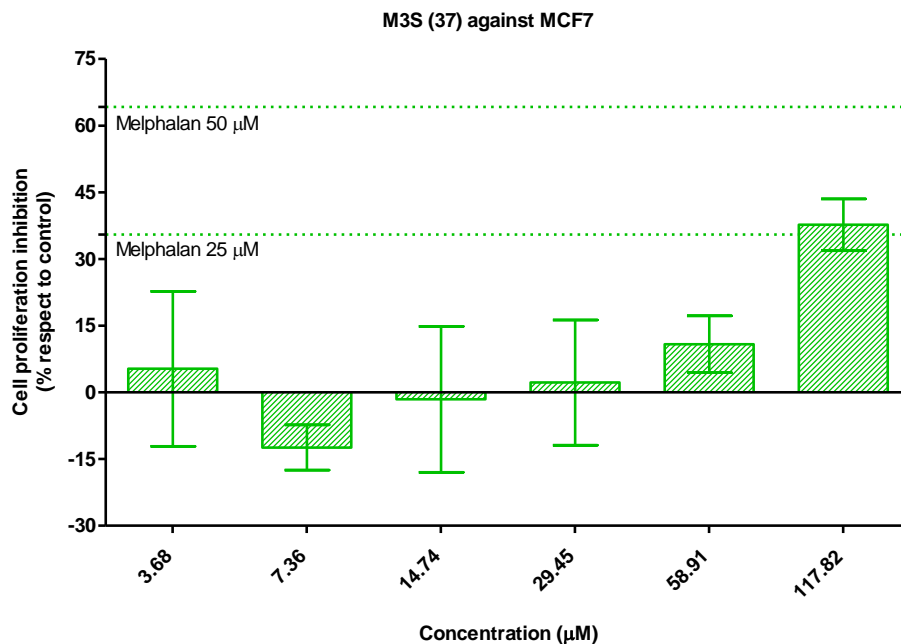
Figure 4-23 The cell proliferation inhibition (%) of M3S **(37)** against MCF7.

The large standard deviation bars and negative cell proliferation inhibition values were attributed to the bacterial contamination during screening. At the high dosage 117.82 μM, M3S **(37)** demonstrated a cell proliferation inhibition above 35 % against the cell line MCF7, which was higher than the positive standard melphalan **(7)** (25 μM). The experimental IC_{50} of M3S **(37)** against the cell line MCF7 was calculated from the dose-response curve shown in Figure 4-24.
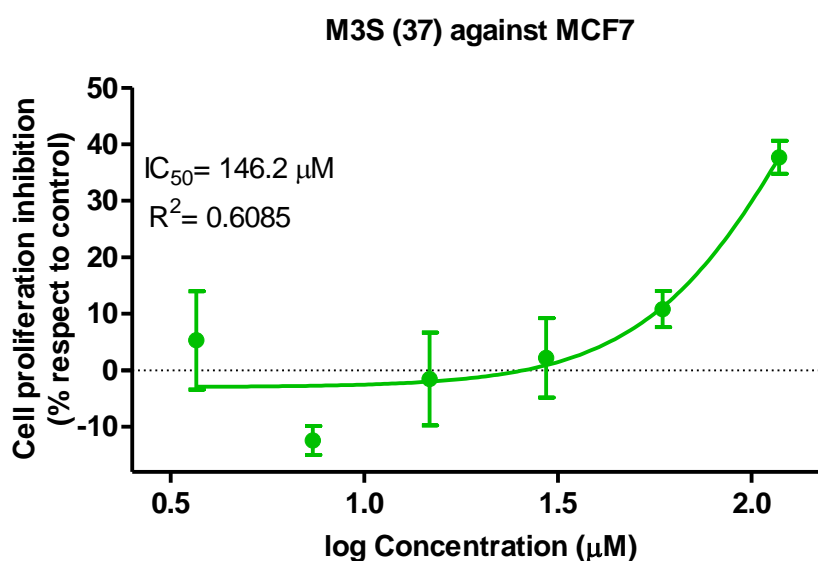
Figure 4-24 The dose-response curve of M3S **(37)** against MCF7.

The IC_{50} concentration of M3S **(37)** against MCF7 was calculated as 146.2 µM. The calculated IC_{50} concentration had a high degree of uncertainty as the coefficient of determination ($R^2 = 0.6085$) for the nonlinear regression curve was below acceptable. The cell proliferation inhibition (%) of M3S **(37)** against Caco2 is shown below in Figure 4-25.
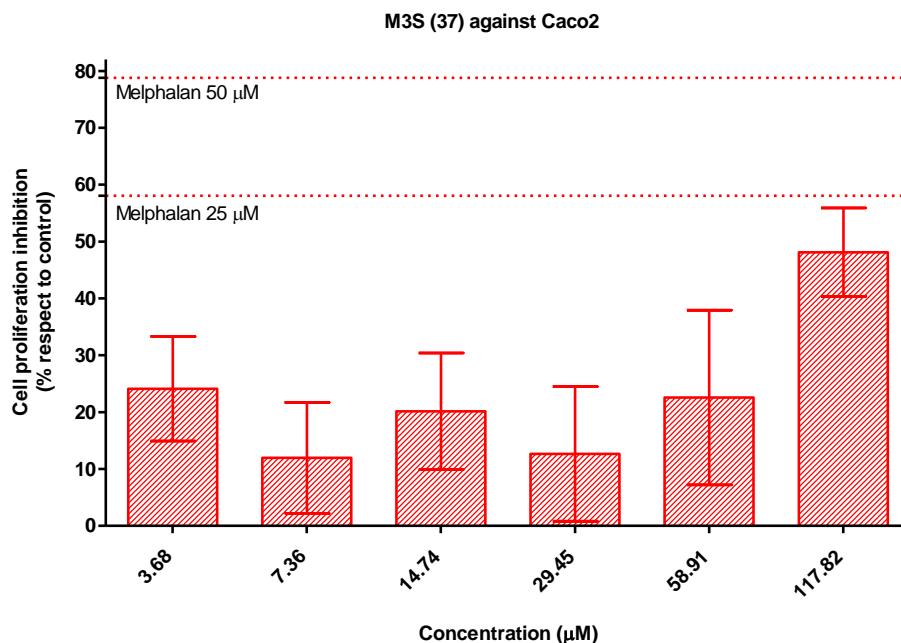
Figure 4-25 The cell proliferation inhibition (%) of M3S **(37)** against Caco2.

The large standard deviation bars were attributed to bacterial contamination during screening. M3S **(37)** did not perform better than the positive controls at either concentrations against Caco2. At the high dosage 117.82 µM, M3S **(37)** demonstrated a cell proliferation inhibition above 45 %, which was higher when compared to the cell line MCF7. The experimental IC_{50} of M3S **(37)** against the cell line Caco2 was calculated from the dose-response curve shown in Figure 4-26.
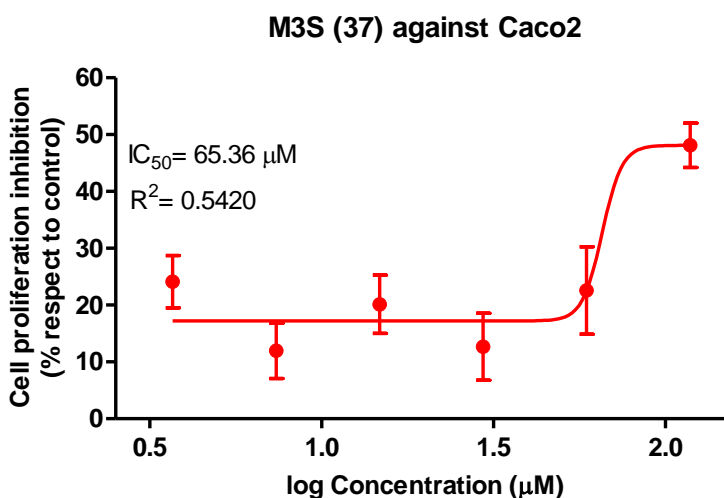
Figure 4-26 The dose-response curve of M3S **(37)** against Caco2.

118

The IC_{50} concentration of M3S **(37)** against Caco2 was calculated as 65.36 µM. The calculated IC_{50} concentration had a high degree of uncertainty as the coefficient of determination (R^2 = 0.5420) for the nonlinear regression curve was below acceptable. The dose-response MTT **(13)** assays did not provide any conclusive results other than M3S **(37)** is biologically active against MCF7 and Caco2. Bacterial contamination resulted in the inconsistent responses across all concentrations against both cell lines. Regardless, M3S **(37)** still demonstrated a higher efficacy i.e., a lower IC_{50} value towards the Caco2 cell line. This was the first reported occurrence of M3S **(37)** exhibiting any cell proliferation inhibition against the cell lines MCF7 and Caco2. When the experimental IC_{50} values of M3S **(37)** were compared to the reported IC_{50} values for paclitaxel **(1)**, M3S **(37)** was less active. Paclitaxel **(1)** was reported to have IC_{50} values of 8.0 x10^{-4} µM and 0.10 ± 0.03 µM agaisnt the cell lines MCF7 and Caco2, respectively[21,22].

4.3.3   Single crystal X-ray diffraction analysis

A suitable single crystal of dihydromikanolide **(39)** was mounted on a nylon loop and analysed on a Rigaku XtaLAB Synergy R diffractometer. The following experimental crystal data for dihydromikanolide **(39)** $C_{15}H_{16}O_6$ (M = 292.28 g/mol): monoclinic, space group $P2_1$ (no. 4), a = 9.0802(4) Å, b = 7.1086(4) Å, c = 10.4341(5) Å, β = 99.577(4)°, V = 664.11(6) Å^3, Z = 2, T = 149.99(10) K, µ(Cu-Kα) = 0.959 mm^{-1}, D_{calc} = 1.462 g/cm^3, 10 037 reflections measured (8.594° ≤ 2Θ ≤ 158.614°), 2 633 unique (R_{int} = 0.0456, R_{sigma} = 0.0333) which were used in all calculations. The final R_1 was 0.0456 (I > 2σ(I)) and wR_2 was 0.1258 (all data). The crystal data and structure refinement parameters of dihydromikanolide **(39)** are shown in Table 20.

Table 20 SCXRD crystallographic parameters of dihydromikanolide **(39)**.

Compound	Dihydromikanolide **(39)**
CCDC deposit number	161086; 1139991
Emp. Formula	$C_{15}H_{16}O_6$
Formula weight (g/mol)	292.28
Crystal description	Yellowish, fine needle-like
Temperature (K)	149.99(10)
Wavelength (Å)	1.54184 (Cu-Kα)
Crystal system	Monoclinic
Space group	$P2_1$ (No. 4)
a (Å)	9.0802(4)
b (Å)	7.1086(4)
c (Å)	10.4341(5)
α (°)	90

119

β (º)	99.577(4)
γ (º)	90
Volume (Å^3)	664.11(6)
Z	2
Density calculated (g.cm^{-3})	1.462
Absorption coefficient (mm^{-1})	0.959
F(0 0 0)	308.0
Crystal size (mm^3)	0.9 × 0.2 × 0.1
Reflections collected	10037
Unique reflections	2633
Completeness	1.0
Independent refl.	2633 [R_{int} = 0.0456, R_{sigma} = 0.0333]
Data/restraints/parameters	2633/1/195
Goodness of fit on F^2	1.035
Final R$_1$ indexes [(I > 2σ(I)]	0.0456
wR$_2$ indices (all data)	0.1258
Largest diffraction peak and hole (e.Å^{-3})	0.18/-0.19
Flack parameter	-0.07(14)

Dihydromikanolide **(39)**

A

B

C
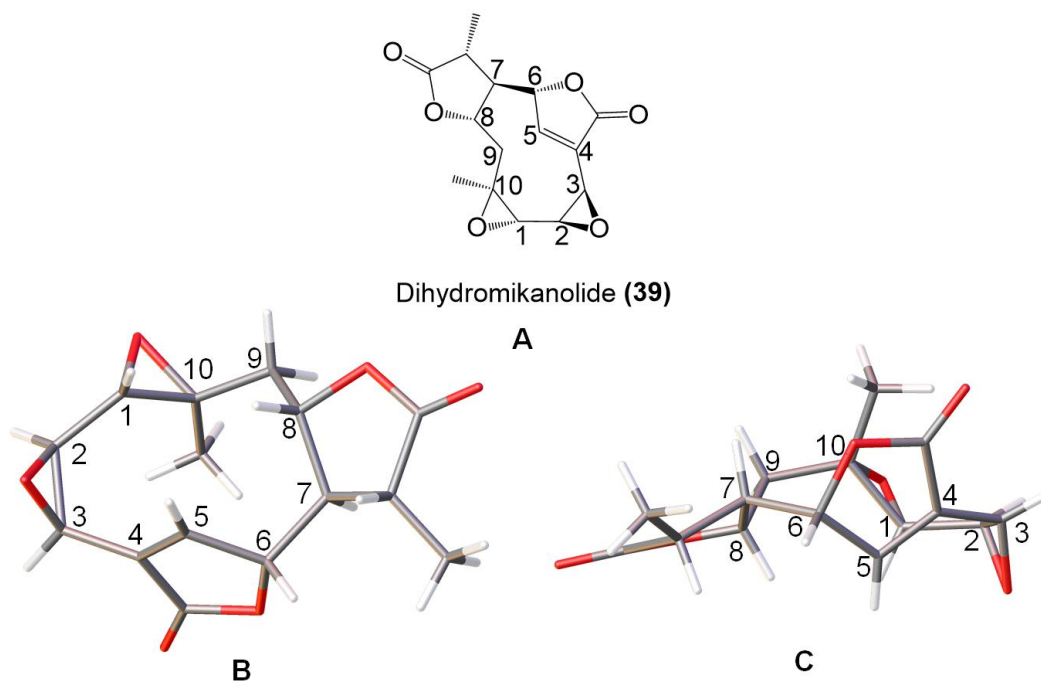
Figure 4-27 **A**-The chemical structure showing the absolute configuration of dihydromikanolide **(39)**, **B**-The SCXRD structure of dihydromikanolide **(39)** with atom-labeling of the 10 membered ring, **C**-The conformation of the 10-membered ring of dihydromikanolide **(39)**.

120

As seen in Figure 4-27A and B, the sesquiterpene lactone dihydromikanolide **(39)** has a 10 membered ring fused with an unsaturated and saturated lactone ring and additionally two epoxides. As demonstrated in Figure 4-27C, the fragment C-5-C-6-C-7-C-8-C-9-C-10-C-1 is in a boat conformation whilst the fragment C-1-C-2-C-3-C-4 is on a single plane. When measured, the two epoxide rings create a dihedral angle of 158.3°, which is higher than the 145.7° reported in literature[20]. This indicated that the crystal structure of dihydromikanolide **(39)** reported in this project is at a more favourable lower energy state since the epoxides are not introducing steric straining around that bond. Thus, the absolute configuration of this molecule has less uncertainty than the reported literature. This is consistent with the low experimental Flack parameter of -0.07, where a score near 0 indicates a low uncertainty in the absolute structure.

4.4 Conclusion

Using a subset of the University of Pretoria's natural product library for HTS against the cell lines MCF7 and Caco2, the hit fraction from *M. natalensis* was identified and easily dereplicated which resulted in the isolation and identification of the bioactive compound M3S **(37)**. The plant preparation methods in the South African natural product library allowed for easy upscaling that resulted in more of the active fraction being produced. The dereplication of the hit fraction from *M. natalenis* led to the identification of a unique peak that was tentatively identified and isolated using mass targeted isolation on the HPLC-PDA-MS. The structure of the isolated M3S **(37)** (0.96 mg) was confirmed using both 1D and 2D NMR experiments. The isolated M3S **(37)** was rescreened against the cancer cell lines MCF7 and Caco2 and the IC_{50} concentrations were determined to be 146.2 µM and 65.36 µM, respectively. The isolated M3S **(37)** exhibited a poorer cell proliferation inhibition when compared to the activity of respective hit fraction against both cell lines MCF7 and Caco2. The poor activity of the isolated M3S **(37)** could be due to the absence of compounds which synergistically contributed to the overall activity of the hit fraction or the poor solubility and stability of M3S **(37)** during biological screening. However, the IC_{50} concentrations confirmed that M3S **(37)** was an anti-cancer compound present in the hit fraction of *M. natalensis*. This is the first report of M3S **(37)** in the leaves of *M. natalensis* that has shown anti-cancer activity against the cell lines MCF7 and Caco2. Additionally, the presence of dihydromikanolide **(39)** in the leaves of *M. natalensis* was confirmed through SCXRD analysis and furthermore the absolute configuration reported was less uncertain than that reported in literature. This is the first reported incident of the bioactive M3S **(37)** and dihydromikanolide **(39)** present in the leaves extract of *M. natalensis*.

4.5 References

1. Brigida da Silva, A., Owiti, A. & Barbosa, W. R. Pharmacology of Mikania genus: A systematic review. *Pharmacogn. Rev.* **12**, 230 (2018).

2. World Flora Online. WFO (2023): Mikania natalensis DC. http://www.worldfloraonline.org/taxon/wfo-0000067088.

3. Hutchings, A., Scoff, A. H., Lewis, G. & Cunningham, A. Zulu medicinal plants: an inventory. *Choice Rev. Online* **34**, 34-6265-34–6265 (1997).

4. Singh, M. K. A Comprehensive Review on some Species of Mikania. *YMER Digit.* **21**, 299–309 (2022).

5. Yu, H., Le Roux, J. J., Zhao, M. & Li, W. Mikania sesquiterpene lactones enhance soil bacterial diversity and fungal and bacterial activities. *Biol. Invasions* **25**, 237–250 (2023).

6. Abdellah, Y. A. Y. *et al.* Phytochemical and underlying mechanism of Mikania micrantha Kunth on antibiotic resistance genes, and pathogenic microbes during chicken manure composting. *Bioresour. Technol.* **367**, 128241 (2023).

7. Rufatto, L. C., Gower, A., Schwambach, J. & Moura, S. Genus Mikania: chemical composition and phytotherapeutical activity. *Rev. Bras. Farmacogn.* **22**, 1384–1403 (2012).

8. Medeiros Mazzorana, D., Nicolau, V., Moreira, J., de Aguiar Amaral, P. & de Andrade, V. M. Influence of Mikania laevigata Extract over the Genotoxicity Induced by Alkylating Agents. *ISRN Toxicol.* **2013**, 1–7 (2013).

9. Rehder, V. L. G., Sartoratto, A. & Rodrigues, M. V. N. Essential oils composition from leaves , inflorescences and seeds of Mikania laevigata Schultz Bip . ex Baker and Mikania glomerata Sprengel. *Rev. Bras. Plantas Med.* **8**, 116–118 (2006).

10. Pedroso, A. P. D. *et al.* Isolation of syringaldehyde from Mikania laevigata medicinal extract and its influence on the fatty acid profile of mice. *Rev. Bras. Farmacogn.* **18**, 63–69 (2008).

11. Ahmed, M., Rahman, M. T., Alimuzzaman, M. & Shilpi, J. A. Analgesic sesquiterpene dilactone from Mikania cordata. *Fitoterapia* **72**, 919–21 (2001).

12. Bedi, G., Tonzibo, Z. F., N'Guessan, T. Y. & Chalchat, J.-C. Chemical Constituents of the Essential Oil of Mikania cordata (Burm.f.) B.L. Robinson from Abidjan (Ivory Coast). *J. Essent. Oil Res.* **15**, 198–199 (2003).

13. Yatsuda, R. *et al.* Effects of Mikania genus plants on growth and cell adherence of mutans streptococci. *J. Ethnopharmacol.* **97**, 183–189 (2005).

14. Moreira, M. R. *et al.* ent-Kaurenoic acid-rich extract from Mikania glomerata: In vitro activity against bacteria responsible for dental caries. *Fitoterapia* **112**, 211–216 (2016).

15. Moreti, D. L. C. *et al.* Mikania glomerata Sprengel extract and its major compound ent-

122

kaurenoic acid display activity against bacteria present in endodontic infections. *Anaerobe* **47**, 201–208 (2017).

16. Rufatto, L. C., Finimundy, T. C., Roesch-Ely, M. & Moura, S. Mikania laevigata: Chemical characterization and selective cytotoxic activity of extracts on tumor cell lines. *Phytomedicine* **20**, 883–889 (2013).

17. Ghosh, A., Das, B. K., Roy, A., Mandal, B. & Chandra, G. Antibacterial activity of some medicinal plant extracts. *J. Nat. Med.* **62**, 259–62 (2008).

18. Facey, P. C., Peart, P. C. & Porter, R. B. R. The antibacterial activities of mikanolide and its derivatives. *West Indian Med. J.* **59**, 249–52 (2010).

19. Ríos V., E. *et al.* Sesquiterpene lactones from Mikania micrantha and Mikania cordifolia and their cytotoxic and anti-inflammatory evaluation. *Fitoterapia* **94**, 155–163 (2014).

20. But, P. P.-H. *et al.* Antiviral constituents against respiratory viruses from Mikania micrantha. *J. Nat. Prod.* **72**, 925–8 (2009).

21. Tonissi, F. *et al.* The effect of paclitaxel and nab-paclitaxel in combination with anti-angiogenic therapy in breast cancer cell lines. *Invest. New Drugs* **33**, 801–9 (2015).

22. Fohlen, A. *et al.* Anticancer Drugs for Intra-Arterial Treatment of Colorectal Cancer Liver Metastases: In-Vitro Screening after Short Exposure Time. *Pharmaceuticals* **14**, 639 (2021).

Chapter 5: Conclusion

Cancer is one of the major public health problems worldwide and although treatments are improving and personalised medicine promises advancements, incident rates are predicted to increase exponentially over the next 10 years mainly due to the aging population and adjustable behavioural and lifestyle conciderations[1,2]. Cancer is a disease that arises from gene mutations that allow the unregulated proliferation of abnormal cells. The gene mutations are mainly often caused by genetic disorders or exposure to carcinogens. Gene mutations or damage to the proto-oncogenes often results in abnormalities during the cell-division cycle causing uncharacteristic proliferation at any point in the cycle[3]. The randomness of abnormality in the cell-division cycle makes all cancers, at the cellular level, a variety disease that consequently makes diagnosis and treatment challenging as each case is treated on an individual basis[4,5]. Cancer treatment is still a reductionist approach which has a continuous demand for new treatments[6].

Natural products have been used in medicinal practices since the beginning of mankind as the earliest recorded usage dates back to over five thousand years[7]. To date, over 809 natural products have been approved by the FDA since 1981 for the treatment against communicable and noncommunicable diseases such as HIV, bacterial infections and cancers[8]. This demonstrates that natural products are still a potential source for novel chemically diverse and complex therapeutic compounds for all diseases including a variety disease like cancer[9].

South Africa has one of the richest multicultural heritages in the world that has accumulated an impressive knowledge on the indigenous medicinal plants. South Africa's flora is one of the world's richest untapped sources for potential therapeutic compounds as over 2000 indigenous plant species are used in traditional medicinal practises[10]. However, South Africa has fallen behind in natural product drug discovery as biological screening efforts have become more target-specific and higher throughput that required the need for semi-purified or fractionated natural product extract libraries[11]. The previous attempts at novel drug discovery in South Africa have only utilised crude natural product extracts thus providing an opportunity to investigate South Africa's flora for the discovery of novel therapeutic agents. Since natural products are a readily available source of chemically novel, diverse and complex compounds that exhibit greater drug-likeness than synthetic compounds, their potential in drug discovery is still undisputed especially against variety diseases like cancer[12].

The work reported in this study was aimed towards creating a viable and trusted South African natural product library platform that is ready for HTS against numerous diseases. The library

124

platform was then evaluated for its anti-cancer potential against numerous cancer cell lines to rapidly isolate and characterise a biologically active compound using state of the art hyphenated analytical techniques. Since the creation of the platform, it has been used in different HTS projects to identify anti-cancer, anti-plasmodial, anti-trypanosomal, anti-viral (SARS-CoV-2) and antitubercular (efflux pump and biofilm formation inhibitors) therapeutic compounds. The creation of the South African natural product library was accomplished by adapting the modern high-throughput standardisation methods for plant material extraction, fractionation and standardisation procedures developed and used by world renowned experts and research institutions. The project mostly referred to the work done by the NCI NPNPD project lead by Dr. Barry R. O'Keefe and Prof. Matthias Hamburger at the University of Basel, Switzerland[13,14].

The procedures developed for the production of standardised plant extract and fractions in this project focused on the miniaturisation of the high-throughput methods of pre-existing and ideal natural product library platform. The miniaturisation was necessary as plant material is a limiting factor in natural product drug discovery. The developed miniaturised methods in this project worked well as it was shown to be robust, high-throughput and accommodating of all types of plant material. The ultrasonic bath extraction method was able to produce sufficient high-quality extracts (> 250 mg) needed for downstream standardisation processes by using the least amount of plant material (7.0 g). Additionally, this extraction method was high-throughput when compared to traditional methods of extraction as it took no more than 5 hours to obtain 12 quality plant crude extracts. The automated plant extract fractionation method used was identical to the method developed by the NCI NPNPD project but was adapted to be used on a Gilson GX-241 ASPEC® liquid handler. Since the liquid handler was configured with a single needle, the fractionation of 12 crude extracts took no less than 6 hours to complete. However, the unfortunate lengthy time was compensated by the full automation of the method apart from replacing sequential fraction tubes and replenishing the solvent systems. The standardisation step occurred in a multiple step process using the Hamilton Microlab® STARlet™ automated liquid handler which, as a single occurance, was able to handle all 84 fractions generated from 12 crude extracts. It took an average of 24 hours to fully complete the standardisation of 12 plant extracts and their respective fractions. The first step required an aliquot (1.6 mL) of each fraction to be transferred to the intermediate 96 well plate, after which the intermediate plate and fractions were dried to completion (± 18 hours). The third step involved recording the weights of the dried fractions (± 2 hours) and lastly to solubilise the constituents in each well of the intermediate plate to the final concentration of 5 mg/mL in DMSO before being transferred to the storage plate. The insight of using an intermediate 96 well plate was made available by the researchers of the NCI NPNPD project.

The standardisation concentration of 5 mg/mL was selected specifically for this library platform and has shown to be adequate as nearly all the extracts and fractions could be standardised. The stringent storage conditions of the standardised extracts and fractions allow for an extended life expectancy of around 5-10 years[15,16]. The standardised extracts and samples are stored in airtight screw capped polypropylene vials under dry atmospheric conditions and kept frozen at -20 °C inside a Hamilton Verso® Q20 robotic freezer until needed. To date, the South African natural product extract library contains approximately 4 000 standardised semi-purified plant fractions and over 500 standardised crude plant extracts. Further work includes the creation and open access to over 80 000 standardised plant extracts and fractions from the 10 000 plant samples stored in the Chemistry Department at the University of Pretoria. The development of standardisation methods for the incorporation of biological materials from microbial and marine sources is also being considered.

Additionally, in this project the South African natural product library was evaluated for potential anti-cancer compounds from a selection of medicinal plant species. The selection of plant species was accomplished by developing an ethnopharmacological preferential scoring system that scored South African medicinal plant which allowed for the selection of the most preferential medicinal plant species. As cancer is not clearly described in traditional medicinal practises, cancer associated symptoms helped identify potential medicinal plants by their reported usage for treating cancer-like symptoms[17]. From a list of 100 medicinal plant species, 34 were selected, standardised and screened against the human cancer cell lines A549, MCF7 and Caco2. In total, 3 fractions showed excellent cell proliferation inhibition above 80 % at 50 µg/mL against the cell line A549 while 10 fractions showed potent cell proliferation inhibition above 90 % at 25 µg/mL between the cell lines MCF7 and Caco2. The benefit of fractionating plant extracts on a HyperSep™ C8 SPE cartridge pre-HTS was demonstrated as most fractions were exhibiting better activity than their corresponding crude extracts. It was observed that the potent biological active compounds were concentrated in fraction 3 and/or 4 against the cell line A549 while the potent biological active compounds were concentrated in fractions 2 and 4 against the cell lines MCF7 and Caco2. In a time and cost-efficient manner, the HTS of a small subset of standardised plant species in the South African natural product library format has identified numerous "hits" for investigation of potentially novel chemotherapeutic agents.

Using the natural product library, a single hit fraction from *Mikania natalensis* was prioritised for post-HTS investigation. The dereplication of the hit fraction used modern analytical techniques such as UPLC-PDA-HRMS analysis and online databases such as ChemSpider, PubChem, Reaxys and the Dictionary of Natural Products. The dereplication quickly lead to

the tentative identification of a single unique peak in the hit fraction. The easy upscaling of the plant preparation methods allowed for the rapid isolation of the biologically active compound. By using mass-directed isolation on an HPLC-PDA-MS, the biologically active compound mikanin 3-O-sulphate **(37)** was isolated and purified (0.96 mg). The structural confirmation using 1D and 2D NMR in combination with ACDLabs™ Spectrus Processor further confirmed the identity of M3S **(37)**. The isolated M3S **(37)** was rescreened against the cancer cell lines MCF7 and Caco2 and the IC_{50} concentrations were determined to be 146.2 µM and 65.36 µM, respectively. It was confirmed that M3S **(37)** is the anti-cancer compound present in the hit fraction from the leaf extract of *M. natalensis*. This was the first report of M3S **(37)** in the leaves of *M. natalensis* that has shown anti-cancer activity against the cell lines MCF7 and Caco2. Furthermore, the presence of dihydromikanolide **(39)** in the leaf extract of *M. natalensis* was confirmed through SCXRD analysis.

Through this work, it can be seen that the creation of the first South African natural product library, that standardised fractionated crude extracts, has shown outstanding performance and an even greater potential than initially realised. Overall, the aims and objectives in this study were met and demonstrated that using standardisation platforms, HTS methodologies and hyphenated analytical techniques that South Africa can rapidly offer novel and lifesaving therapeutic compounds. Not only will the platform serve as an open access tool in accelerated drug discovery nationwide, but it will also be a means of preserving South Africa's biodiversity.

5.1   References

1. Siegel, R. L., Miller, K. D. & Jemal, A. Cancer statistics, 2016. *CA. Cancer J. Clin.* **66**, 7–30 (2016).

2. Aschebrook-Kilfoy, B. *et al.* An Overview of Cancer in the First 315,000 All of Us Participants. *PLoS One* **17**, e0272522 (2022).

3. Seto, M., Honma, K. & Nakagawa, M. Diversity of genome profiles in malignant lymphoma. *Cancer Sci.* **101**, 573–8 (2010).

4. Meacham, C. E. & Morrison, S. J. Tumour heterogeneity and cancer cell plasticity. *Nature* **501**, 328–37 (2013).

5. Fisher, R., Pusztai, L. & Swanton, C. Cancer heterogeneity: implications for targeted therapeutics. *Br. J. Cancer* **108**, 479–85 (2013).

6. Zugazagoitia, J. *et al.* Current Challenges in Cancer Treatment. *Clin. Ther.* **38**, 1551–66 (2016).

7. Petrovska, B. B. Historical review of medicinal plants' usage. *Pharmacogn. Rev.* **6**, 1–5 (2012).

8. Newman, D. J. & Cragg, G. M. Natural Products as Sources of New Drugs over the

Nearly Four Decades from 01/1981 to 09/2019. *J. Nat. Prod.* **83**, 770–803 (2020).

9. Atanasov, A. G., Zotchev, S. B., Dirsch, V. M., International Natural Product Sciences Taskforce & Supuran, C. T. Natural products in drug discovery: advances and opportunities. *Nat. Rev. Drug Discov.* **20**, 200–216 (2021).

10. Skowno, A. L. *et al. National Biodiversity Assessment 2018: The status of South Africa's ecosystems and biodiversity. Synthesis Report. South African National Biodiversity Institute, an entity of the Department of Environment, Forestry and Fisheries. South African National Biodiversity Institute* (2019).

11. Wilson, B. A. P., Thornburg, C. C., Henrich, C. J., Grkovic, T. & O'Keefe, B. R. Creating and screening natural product libraries. *Nat. Prod. Rep.* **37**, 893–918 (2020).

12. Najmi, A., Javed, S. A., Al Bratty, M. & Alhazmi, H. A. Modern Approaches in the Discovery and Development of Plant-Based Natural Products and Their Analogues as Potential Therapeutic Agents. *Molecules* **27**, 349 (2022).

13. Evans, J. R. *et al.* National Cancer Institute (NCI) Program for Natural Product Discovery: Exploring NCI-60 Screening Data of Natural Product Samples with Artificial Neural Networks. *ACS Omega* **8**, 9250–9256 (2023).

14. Potterat, O. & Hamburger, M. Combined use of extract libraries and HPLC-based activity profiling for lead discovery: potential, challenges, and practical considerations. *Planta Med.* **80**, 1171–81 (2014).

15. Zitha-Bovens, E. *et al.* COMDECOM: predicting the lifetime of screening compounds in DMSO solution. *J. Biomol. Screen.* **14**, 557–65 (2009).

16. Cheng, X. *et al.* Studies on repository compound stability in DMSO under various conditions. *J. Biomol. Screen.* **8**, 292–304 (2003).

17. Khorombi, T. *et al.* Investigation of South African plants for anti cancer properties. (2006).

Supplementary data

Supplementary data 3-1   The fraction yields for every plant extract fractionated.

Plant extract number	Weight of plant extract fractionated (mg)	Fraction barcode	Mass (mg)	Yield (%)
PM0204x	196.7	PM0204xf1	41.30	21.00
		PM0204xf2	21.45	10.90
		PM0204xf3	7.08	3.60
		PM0204xf4	7.76	3.95
		PM0204xf5	5.72	2.91
		PM0204xf6	2.85	1.45
		PM0204xf7	16.57	8.42
P12696x	201.0	P12696xf1	73.44	36.54
		P12696xf2	9.02	4.49
		P12696xf3	2.41	1.20
		P12696xf4	3.76	1.87
		P12696xf5	6.26	3.11
		P12696xf6	2.31	1.15
		P12696xf7	3.71	1.85
P20913x	199.3	P20913xf1	7.40	3.71
		P20913xf2	27.08	13.59
		P20913xf3	4.78	2.40
		P20913xf4	4.50	2.26
		P20913xf5	13.24	6.64
		P20913xf6	26.63	13.36
		P20913xf7	15.87	7.96
P21236x	204.2	P21236xf1	32.78	16.05
		P21236xf2	11.50	5.63
		P21236xf3	5.72	2.80
		P21236xf4	6.72	3.29
		P21236xf5	12.11	5.93
		P21236xf6	25.70	12.59
		P21236xf7	11.54	5.65
P25361x	205.4	P25361xf1	39.01	18.99
		P25361xf2	14.58	7.10
		P25361xf3	10.23	4.98
		P25361xf4	23.99	11.68
		P25361xf5	13.88	6.76
		P25361xf6	3.10	1.51

		P25361xf7	5.52	2.69
P18523x	195.4	P18523xf1	16.03	8.20
		P18523xf2	8.58	4.39
		P18523xf3	4.18	2.14
		P18523xf4	4.93	2.52
		P18523xf5	4.52	2.31
		P18523xf6	6.60	3.38
		P18523xf7	17.35	8.88
P13625x	202.5	P13625xf1	25.68	12.68
		P13625xf2	14.10	6.96
		P13625xf3	7.15	3.53
		P13625xf4	12.66	6.25
		P13625xf5	16.14	7.97
		P13625xf6	8.70	4.30
		P13625xf7	17.46	8.62
P17237x	213.9	P17237xf1	13.82	6.46
		P17237xf2	4.36	2.04
		P17237xf3	2.41	1.13
		P17237xf4	3.53	1.65
		P17237xf5	11.63	5.44
		P17237xf6	37.55	17.55
		P17237xf7	38.02	17.77
PM0203x	199.3	PM0203xf1	41.41	20.78
		PM0203xf2	14.85	7.45
		PM0203xf3	6.65	3.34
		PM0203xf4	4.25	2.13
		PM0203xf5	2.67	1.34
		PM0203xf6	2.03	1.02
		PM0203xf7	14.27	7.16
PM0102x	218.8	PM0102xf1	13.63	6.23
		PM0102xf2	4.33	1.98
		PM0102xf3	2.65	1.21
		PM0102xf4	3.04	1.39
		PM0102xf5	9.89	4.52
		PM0102xf6	19.80	9.05
		PM0102xf7	39.56	18.08
P21589x	263.1	P21589xf1	35.21	13.38
		P21589xf2	9.06	3.44
		P21589xf3	14.72	5.59

		P21589xf4	16.07	6.11
		P21589xf5	7.77	2.95
		P21589xf6	11.35	4.31
		P21589xf7	11.34	4.31
P12437x	276.8	P12437xf1	45.27	16.35
		P12437xf2	2.35	0.85
		P12437xf3	2.82	1.02
		P12437xf4	5.77	2.08
		P12437xf5	4.28	1.55
		P12437xf6	7.48	2.70
		P12437xf7	10.37	3.75
P18524x	238.9	P18524xf1	16.97	7.10
		P18524xf2	5.55	2.32
		P18524xf3	15.38	6.44
		P18524xf4	24.42	10.22
		P18524xf5	20.87	8.74
		P18524xf6	34.27	14.34
		P18524xf7	16.37	6.85
P24891x	251.7	P24891xf1	73.73	29.29
		P24891xf2	9.67	3.84
		P24891xf3	4.12	1.64
		P24891xf4	9.25	3.68
		P24891xf5	32.04	12.73
		P24891xf6	16.05	6.38
		P24891xf7	8.70	3.46
P21731x	256.4	P21731xf1	27.73	10.81
		P21731xf2	5.49	2.14
		P21731xf3	7.92	3.09
		P21731xf4	23.99	9.36
		P21731xf5	10.13	3.95
		P21731xf6	8.26	3.22
		P21731xf7	11.74	4.58
P25462x	245.0	P25462xf1	35.66	14.56
		P25462xf2	9.00	3.67
		P25462xf3	19.31	7.88
		P25462xf4	27.60	11.27
		P25462xf5	11.77	4.81
		P25462xf6	6.42	2.62
		P25462xf7	4.31	1.76

		P22227xf1	26.38	10.80
P22227x	244.2	P22227xf2	3.25	1.33
		P22227xf3	7.34	3.01
		P22227xf4	29.17	11.95
		P22227xf5	33.42	13.69
		P22227xf6	22.70	9.30
		P22227xf7	6.83	2.80
P24535x	266.0	P24535xf1	8.84	3.32
		P24535xf2	0.87	0.33
		P24535xf3	0.83	0.31
		P24535xf4	2.07	0.78
		P24535xf5	11.55	4.34
		P24535xf6	62.64	23.55
		P24535xf7	64.30	24.18
P23578x	233.9	P23578xf1	32.21	13.77
		P23578xf2	4.44	1.90
		P23578xf3	6.32	2.70
		P23578xf4	30.80	13.17
		P23578xf5	15.26	6.52
		P23578xf6	5.64	2.41
		P23578xf7	5.85	2.50
P23438x	228.9	P23438xf1	6.12	2.67
		P23438xf2	2.00	0.87
		P23438xf3	2.35	1.03
		P23438xf4	5.00	2.18
		P23438xf5	18.50	8.08
		P23438xf6	37.29	16.29
		P23438xf7	43.72	19.10
P24835x	255.9	P24835xf1	9.88	3.86
		P24835xf2	3.39	1.32
		P24835xf3	2.70	1.06
		P24835xf4	4.71	1.84
		P24835xf5	15.88	6.21
		P24835xf6	69.81	27.28
		P24835xf7	29.96	11.71
P24988x	254.2	P24988xf1	26.58	10.45
		P24988xf2	5.16	2.03
		P24988xf3	25.09	9.87
		P24988xf4	42.59	16.75

132

		P24988xf5	20.40	8.02
		P24988xf6	9.25	3.64
		P24988xf7	3.42	1.35
P21314x	240.7	P21314xf1	1.82	0.76
		P21314xf2	3.91	1.62
		P21314xf3	3.85	1.60
		P21314xf4	14.15	5.88
		P21314xf5	25.61	10.64
		P21314xf6	16.88	7.01
		P21314xf7	15.44	6.42
P13964x	237.0	P13964xf1	9.98	4.21
		P13964xf2	4.35	1.84
		P13964xf3	5.40	2.28
		P13964xf4	10.43	4.40
		P13964xf5	36.02	15.20
		P13964xf6	32.67	13.78
		P13964xf7	24.76	10.45
P20791x	259.6	P20791xf1	23.37	9.00
		P20791xf2	2.08	0.80
		P20791xf3	2.31	0.89
		P20791xf4	4.80	1.85
		P20791xf5	8.46	3.26
		P20791xf6	35.34	13.61
		P20791xf7	35.20	13.56
P24653x	272.2	P24653xf1	18.91	6.95
		P24653xf2	3.47	1.27
		P24653xf3	8.41	3.09
		P24653xf4	13.89	5.10
		P24653xf5	6.80	2.50
		P24653xf6	9.99	3.67
		P24653xf7	18.06	6.64
P23558x	228.4	P23558xf1	4.28	1.87
		P23558xf2	1.16	0.51
		P23558xf3	1.32	0.58
		P23558xf4	3.62	1.58
		P23558xf5	9.40	4.12
		P23558xf6	57.36	25.11
		P23558xf7	45.66	19.99
P17029x	252.5	P17029xf1	16.10	6.38

		P17029xf2	4.27	1.69
		P17029xf3	9.08	3.60
		P17029xf4	28.11	11.13
		P17029xf5	51.64	20.45
		P17029xf6	8.99	3.56
		P17029xf7	5.30	2.10
P20773x	241.5	P20773xf1	16.41	6.79
		P20773xf2	2.11	0.87
		P20773xf3	2.80	1.16
		P20773xf4	11.28	4.67
		P20773xf5	31.12	12.88
		P20773xf6	24.26	10.04
		P20773xf7	8.62	3.57
P17761x	254.3	P17761xf1	53.83	21.16
		P17761xf2	6.38	2.51
		P17761xf3	11.74	4.62
		P17761xf4	22.67	8.91
		P17761xf5	14.20	5.58
		P17761xf6	19.01	7.47
		P17761xf7	11.42	4.49
P19980x	248.6	P19980xf1	19.61	7.89
		P19980xf2	4.24	1.71
		P19980xf3	4.99	2.01
		P19980xf4	17.94	7.22
		P19980xf5	15.37	6.18
		P19980xf6	17.45	7.02
		P19980xf7	20.37	8.19
P24165x	228.7	P24165xf1	23.57	10.31
		P24165xf2	5.42	2.37
		P24165xf3	14.32	6.26
		P24165xf4	16.27	7.11
		P24165xf5	11.32	4.95
		P24165xf6	16.41	7.17
		P24165xf7	20.91	9.14
P21619x	282.9	P21619xf1	30.13	10.65
		P21619xf2	4.57	1.62
		P21619xf3	5.63	1.99
		P21619xf4	11.72	4.14
		P21619xf5	13.99	4.95

		P21619xf6	30.04	10.62
		P21619xf7	17.76	6.28
		P24150xf1	5.92	2.45
		P24150xf2	1.78	0.74
		P24150xf3	3.21	1.33
P24150x	241.8	P24150xf4	7.24	2.99
		P24150xf5	12.97	5.37
		P24150xf6	48.91	20.23
		P24150xf7	42.84	17.72

Supplementary data 3-2 The final concentration, volume and associated pre-barcoded vial for each plant extract and fraction barcode.

Standardised plant extract and fraction barcodes	Concentration (mg/mL)	Volume (µL)	Pre-barcoded vial label
PM0204xf1	5.00	309.90	FR18782214
PM0204xf2	5.00	596.73	FR18782215
PM0204xf3	5.00	354.00	FR18782216
PM0204xf4	5.00	388.00	FR18782217
PM0204xf5	5.00	286.00	FR18782218
PM0204xf6	5.00	142.50	FR18782219
PM0204xf7	5.00	772.48	FR18782220
PM0204xe8	5.00	168.00	FR18782221
P12696xf1	5.00	174.29	FR18782222
P12696xf2	5.00	451.00	FR18782223
P12696xf3	5.00	120.50	FR18782224
P12696xf4	5.00	188.00	FR18782225
P12696xf5	5.00	313.00	FR18782226
P12696xf6	5.00	115.50	FR18782227
P12696xf7	5.00	185.50	FR18782228
P12696xe8	5.00	194.00	FR18782229
P20913xf1	5.00	370.00	FR18782230
P20913xf2	5.00	472.67	FR18782231
P20913xf3	5.00	239.00	FR18782232
P20913xf4	5.00	225.00	FR18782233
P20913xf5	5.00	662.00	FR18782234
P20913xf6	5.00	480.66	FR18782235
P20913xf7	5.00	793.50	FR18782236
P20913xe8	5.00	265.00	FR18782237
P21236xf1	5.00	390.48	FR18782238

P21236xf2	5.00	575.00	FR18782239
P21236xf3	5.00	286.00	FR18782240
P21236xf4	5.00	336.00	FR18782241
P21236xf5	5.00	605.50	FR18782242
P21236xf6	5.00	498.05	FR18782243
P21236xf7	5.00	577.00	FR18782244
P21236xe8	5.00	122.00	FR18782245
P25361xf1	5.00	328.12	FR18782246
P25361xf2	5.00	729.00	FR18782247
P25361xf3	5.00	511.50	FR18782248
P25361xf4	5.00	533.55	FR18782249
P25361xf5	5.00	694.00	FR18782250
P25361xf6	5.00	155.00	FR18782251
P25361xf7	5.00	276.00	FR18782252
P25361xe8	5.00	158.00	FR18782253
P18523xf1	5.00	798.50	FR18782254
P18523xf2	5.00	429.00	FR18782255
P18523xf3	5.00	209.00	FR18782256
P18523xf4	5.00	246.50	FR18782257
P18523xf5	5.00	226.00	FR18782258
P18523xf6	5.00	330.00	FR18782259
P18523xf7	5.00	737.75	FR18782260
P18523xe8	4.88	100.00	FR18782261
P13625xf1	5.00	498.44	FR18782262
P13625xf2	5.00	705.00	FR18782263
P13625xf3	5.00	357.50	FR18782264
P13625xf4	5.00	633.00	FR18782265
P13625xf5	5.00	793.00	FR18782266
P13625xf6	5.00	435.00	FR18782267
P13625xf7	5.00	733.10	FR18782268
P13625xe8	5.00	115.00	FR18782269
P17237xf1	5.00	691.00	FR18782270
P17237xf2	5.00	218.00	FR18782271
P17237xf3	5.00	120.50	FR18782272
P17237xf4	5.00	176.50	FR18782273
P17237xf5	5.00	581.50	FR18782274
P17237xf6	5.00	340.87	FR18782275
P17237xf7	5.00	336.66	FR18782276
P17237xe8	5.00	150.00	FR18782277

PM0203xf1	5.00	309.10	FR18782278
PM0203xf2	5.00	742.50	FR18782279
PM0203xf3	5.00	332.50	FR18782280
PM0203xf4	5.00	212.50	FR18782281
PM0203xf5	5.00	133.50	FR18782282
PM0203xf6	5.00	101.50	FR18782283
PM0203xf7	5.00	713.50	FR18782284
PM0203xe8	5.00	132.50	FR18782285
PM0102xf1	5.00	681.50	FR18782286
PM0102xf2	5.00	216.50	FR18782287
PM0102xf3	5.00	132.50	FR18782288
PM0102xf4	5.00	152.00	FR18782289
PM0102xf5	5.00	494.50	FR18782290
PM0102xf6	5.00	646.46	FR18782291
PM0102xf7	5.00	323.56	FR18782292
PM0102xe8	5.00	109.50	FR18782293
P21589xf1	5.00	800.00	FR18783942
P21589xf2	5.00	420.86	FR18783943
P21589xf3	5.00	691.60	FR18783944
P21589xf4	5.00	778.16	FR18783945
P21589xf5	5.00	374.48	FR18783946
P21589xf6	5.00	558.82	FR18783947
P21589xf7	5.00	550.42	FR18783948
P21589xe8	5.00	800.00	FR18783949
P12437xf1	5.00	800.00	FR18783950
P12437xf2	5.00	109.66	FR18783951
P12437xf3	5.00	134.96	FR18783952
P12437xf4	5.00	271.72	FR18783953
P12437xf5	5.00	218.04	FR18783954
P12437xf6	5.00	367.40	FR18783955
P12437xf7	5.00	560.25	FR18783956
P12437xe8	5.00	800.00	FR18783957
P18524xf1	5.00	782.99	FR18783958
P18524xf2	5.00	251.00	FR18783959
P18524xf3	5.00	746.51	FR18783960
P18524xf4	5.00	800.00	FR18783961
P18524xf5	5.00	800.00	FR18783962
P18524xf6	5.00	800.00	FR18783963
P18524xf7	5.00	774.43	FR18783964

P18524xe8	5.00	800.00	FR18783965
P24891xf1	5.00	800.00	FR18783966
P24891xf2	5.00	430.69	FR18783967
P24891xf3	5.00	227.98	FR18783968
P24891xf4	5.00	511.86	FR18783969
P24891xf5	5.00	800.00	FR18783970
P24891xf6	5.00	757.55	FR18783971
P24891xf7	5.00	411.58	FR18783972
P24891xe8	5.00	800.00	FR18783973
P21731xf1	5.00	800.00	FR18783974
P21731xf2	5.00	293.52	FR18783975
P21731xf3	5.00	390.88	FR18783976
P21731xf4	5.00	800.00	FR18783977
P21731xf5	5.00	461.18	FR18783978
P21731xf6	5.00	384.57	FR18783979
P21731xf7	5.00	669.48	FR18783980
P21731xe8	5.00	800.00	FR18783981
P25462xf1	5.00	800.00	FR18783982
P25462xf2	5.00	415.25	FR18783983
P25462xf3	5.00	800.00	FR18783984
P25462xf4	5.00	800.00	FR18783985
P25462xf5	5.00	564.62	FR18783986
P25462xf6	5.00	300.26	FR18783987
P25462xf7	5.00	202.04	FR18783988
P25462xe8	5.00	800.00	FR18783989
P22227xf1	5.00	800.00	FR18783990
P22227xf2	5.00	155.91	FR18783991
P22227xf3	5.00	351.29	FR18783992
P22227xf4	5.00	800.00	FR18783993
P22227xf5	5.00	800.00	FR18783994
P22227xf6	5.00	800.00	FR18783995
P22227xf7	5.00	319.44	FR18783996
P22227xe8	5.00	800.00	FR18783997
P24535xf1	5.00	428.06	FR18783998
P24535xf2	2.11	100.00	FR18783999
P24535xf3	2.07	100.00	FR18784000
P24535xf4	5.00	105.20	FR18784001
P24535xf5	5.00	575.57	FR18784002
P24535xf6	5.00	800.00	FR18784003

P24535xf7	5.00	800.00	FR18784004
P24535xe8	5.00	800.00	FR18784005
P23578xf1	5.00	800.00	FR18784006
P23578xf2	5.00	218.08	FR18784007
P23578xf3	5.00	309.68	FR18784008
P23578xf4	5.00	800.00	FR18784009
P23578xf5	5.00	762.30	FR18784010
P23578xf6	5.00	271.83	FR18784011
P23578xf7	5.00	441.43	FR18784012
P23578xe8	5.00	800.00	FR18784013
P23438xf1	5.00	314.12	FR18784014
P23438xf2	5.00	100.40	FR18784015
P23438xf3	5.00	110.41	FR18784016
P23438xf4	5.00	247.36	FR18784017
P23438xf5	5.00	800.00	FR18784018
P23438xf6	5.00	800.00	FR18784019
P23438xf7	5.00	800.00	FR18784020
P23438xe8	5.00	800.00	FR18784021
P24835xf1	5.00	456.88	FR18784022
P24835xf2	5.00	155.71	FR18784023
P24835xf3	5.00	128.32	FR18784024
P24835xf4	5.00	224.37	FR18784025
P24835xf5	5.00	727.79	FR18784026
P24835xf6	5.00	800.00	FR18784027
P24835xf7	5.00	800.00	FR18784028
P24835xe8	5.00	800.00	FR18784029
P24988xf1	5.00	800.00	FR18784030
P24988xf2	5.00	241.33	FR18784031
P24988xf3	5.00	800.00	FR18784032
P24988xf4	5.00	800.00	FR18784033
P24988xf5	5.00	800.00	FR18784034
P24988xf6	5.00	399.01	FR18784035
P24988xf7	5.00	156.74	FR18784036
P24988xe8	5.00	800.00	FR18784037
P21314xf1	5.00	250.51	FR18784038
P21314xf2	5.00	196.27	FR18784039
P21314xf3	5.00	195.65	FR18784040
P21314xf4	5.00	735.46	FR18784041
P21314xf5	5.00	800.00	FR18784042

P21314xf6	5.00	800.00	FR18784043
P21314xf7	5.00	776.96	FR18784044
P21314xe8	5.00	800.00	FR18784045
P13964xf1	5.00	497.33	FR18784046
P13964xf2	5.00	219.97	FR18784047
P13964xf3	5.00	267.80	FR18784048
P13964xf4	5.00	522.29	FR18784049
P13964xf5	5.00	800.00	FR18784050
P13964xf6	5.00	800.00	FR18784051
P13964xf7	5.00	800.00	FR18784052
P13964xe8	5.00	800.00	FR18784053
P20791xf1	5.00	800.00	FR18784054
P20791xf2	4.80	100.00	FR18784055
P20791xf3	5.00	109.03	FR18784056
P20791xf4	5.00	230.80	FR18784057
P20791xf5	5.00	410.63	FR18784058
P20791xf6	5.00	800.00	FR18784059
P20791xf7	5.00	800.00	FR18784060
P20791xe8	5.00	800.00	FR18784061
P24653xf1	5.00	800.00	FR18784062
P24653xf2	5.00	164.92	FR18784063
P24653xf3	5.00	410.14	FR18784064
P24653xf4	5.00	695.55	FR18784065
P24653xf5	5.00	331.62	FR18784066
P24653xf6	5.00	458.87	FR18784067
P24653xf7	5.00	800.00	FR18784068
P24653xe8	5.00	800.00	FR18784069
P23558xf1	5.00	211.74	FR18784070
P23558xf2	2.86	100.00	FR18784071
P23558xf3	3.33	100.00	FR18784072
P23558xf4	5.00	175.71	FR18784073
P23558xf5	5.00	450.93	FR18784074
P23558xf6	5.00	800.00	FR18784075
P23558xf7	5.00	800.00	FR18784076
P23558xe8	5.00	800.00	FR18784077
P17029xf1	5.00	763.42	FR18784078
P17029xf2	5.00	197.46	FR18784079
P17029xf3	5.00	419.89	FR18784080
P17029xf4	5.00	800.00	FR18784081

P17029xf5	5.00	800.00	FR18784082
P17029xf6	5.00	436.35	FR18784083
P17029xf7	5.00	269.34	FR18784084
P17029xe8	5.00	800.00	FR18784085
P20773xf1	5.00	755.45	FR18784086
P20773xf2	4.82	100.00	FR18784087
P20773xf3	5.00	133.38	FR18784088
P20773xf4	5.00	567.62	FR18784089
P20773xf5	5.00	800.00	FR18784090
P20773xf6	5.00	800.00	FR18784091
P20773xf7	5.00	426.45	FR18784092
P20773xe8	5.00	800.00	FR18784093
P17761xf1	5.00	800.00	FR18784094
P17761xf2	5.00	295.03	FR18784095
P17761xf3	5.00	544.12	FR18784096
P17761xf4	5.00	800.00	FR18784097
P17761xf5	5.00	712.81	FR18784098
P17761xf6	5.00	800.00	FR18784099
P17761xf7	5.00	559.59	FR18784100
P17761xe8	5.00	800.00	FR18784101
P19980xf1	5.00	800.00	FR18784102
P19980xf2	5.00	212.84	FR18784103
P19980xf3	5.00	253.59	FR18784104
P19980xf4	5.00	800.00	FR18784105
P19980xf5	5.00	710.76	FR18784106
P19980xf6	5.00	800.00	FR18784107
P19980xf7	5.00	800.00	FR18784108
P19980xe8	5.00	800.00	FR18784109
P24165xf1	5.00	800.00	FR18784110
P24165xf2	5.00	274.08	FR18784111
P24165xf3	5.00	711.88	FR18784112
P24165xf4	5.00	787.85	FR18784113
P24165xf5	5.00	565.48	FR18784114
P24165xf6	5.00	790.90	FR18784115
P24165xf7	5.00	800.00	FR18784116
P24165xe8	5.00	800.00	FR18784117
P21619xf1	5.00	800.00	FR18784118
P21619xf2	5.00	218.21	FR18784119
P21619xf3	5.00	294.11	FR18784120

P21619xf4	5.00	579.82	FR18784121
P21619xf5	5.00	658.81	FR18784122
P21619xf6	5.00	800.00	FR18784123
P21619xf7	5.00	800.00	FR18784124
P21619xe8	5.00	800.00	FR18784125
P24150xf1	5.00	283.33	FR18784126
P24150xf2	4.31	100.00	FR18784127
P24150xf3	5.00	149.11	FR18784128
P24150xf4	5.00	353.08	FR18784129
P24150xf5	5.00	626.57	FR18784130
P24150xf6	5.00	800.00	FR18784131
P24150xf7	5.00	800.00	FR18784132
P24150xe8	5.00	800.00	FR18784133
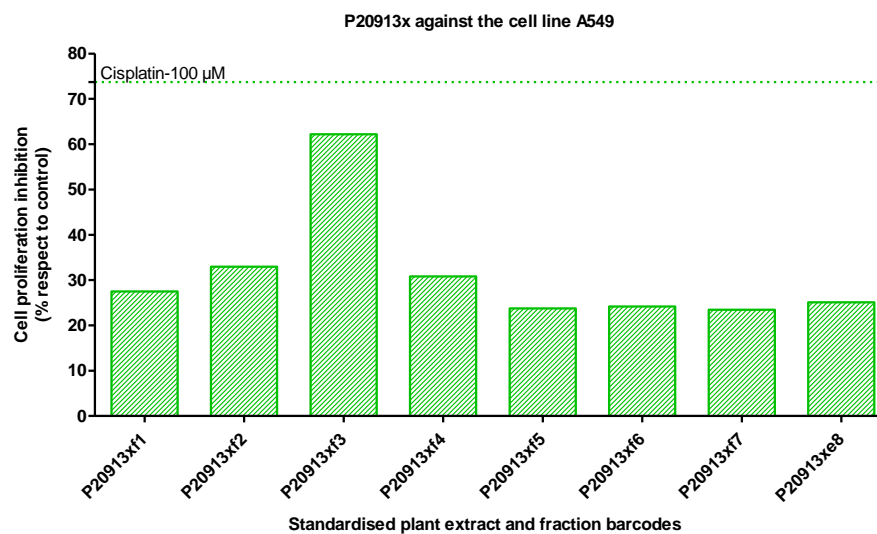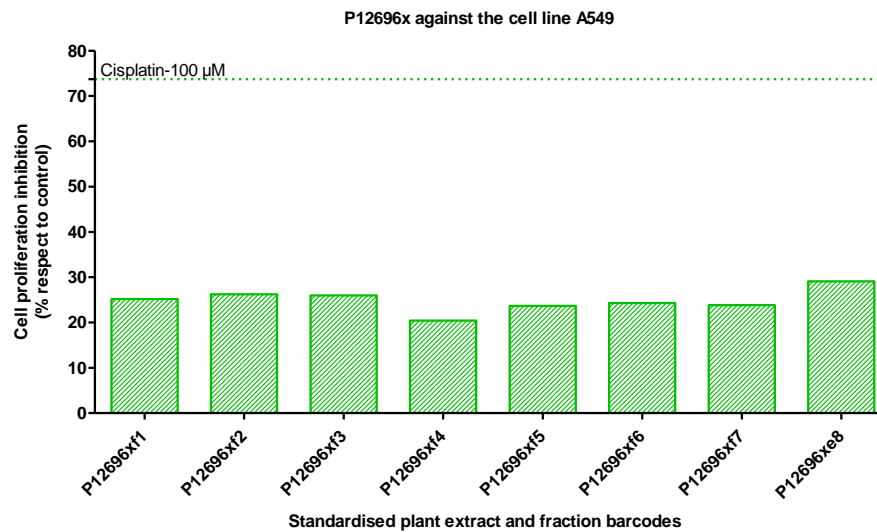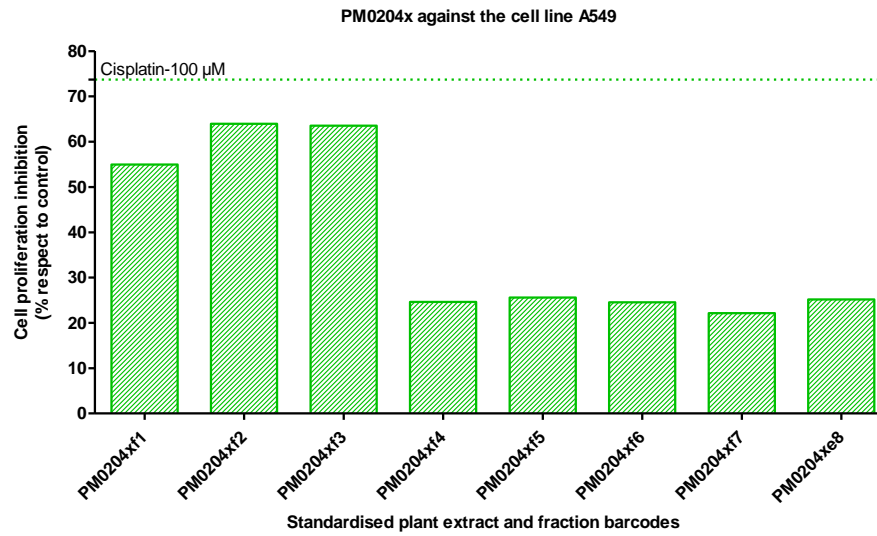
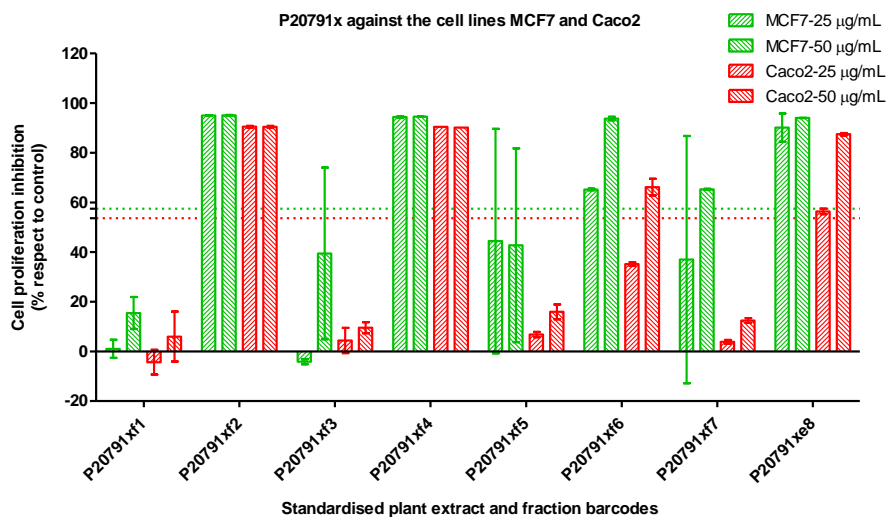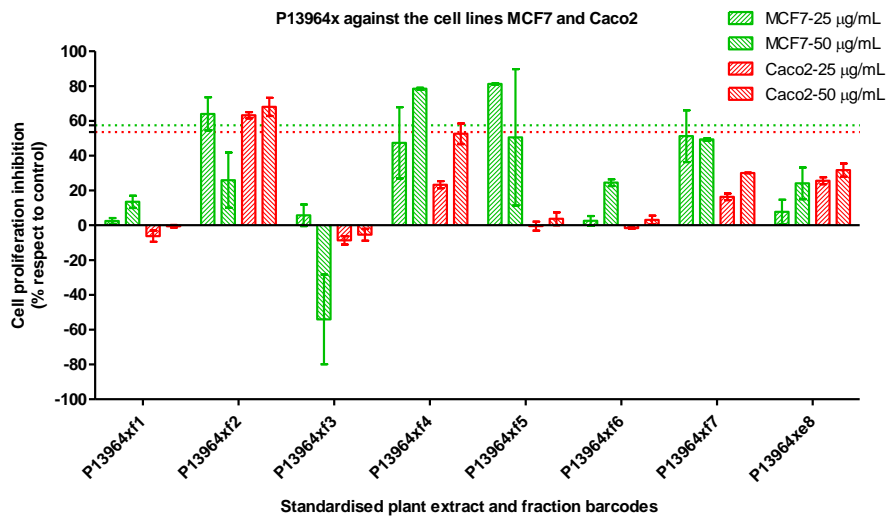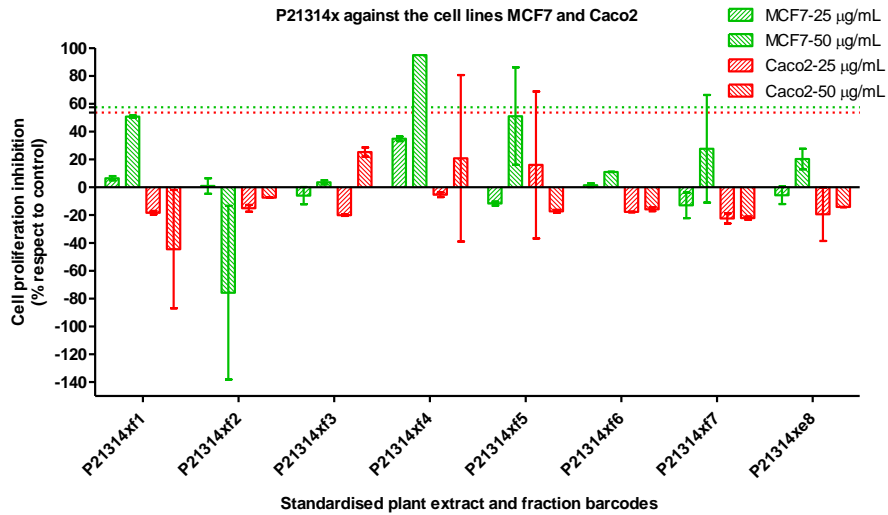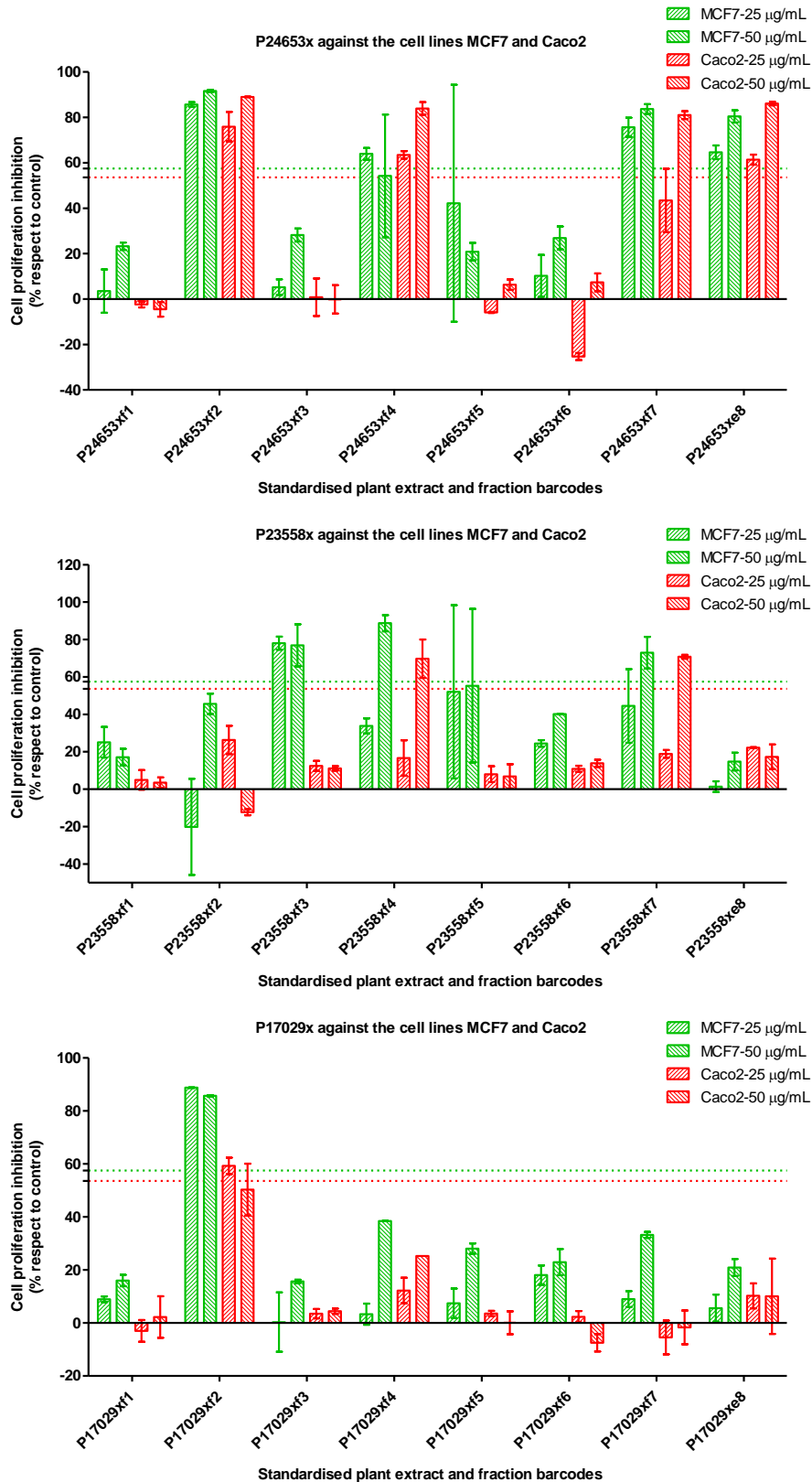**Supplementary data 3-3**   The cell proliferation inhibition (%) of PM0204x (top), P12696x (middle) and P20913x (bottom) against the cell line A549.

143

P21236x against the cell line A549

P25361x against the cell line A549

P18523x against the cell line A549
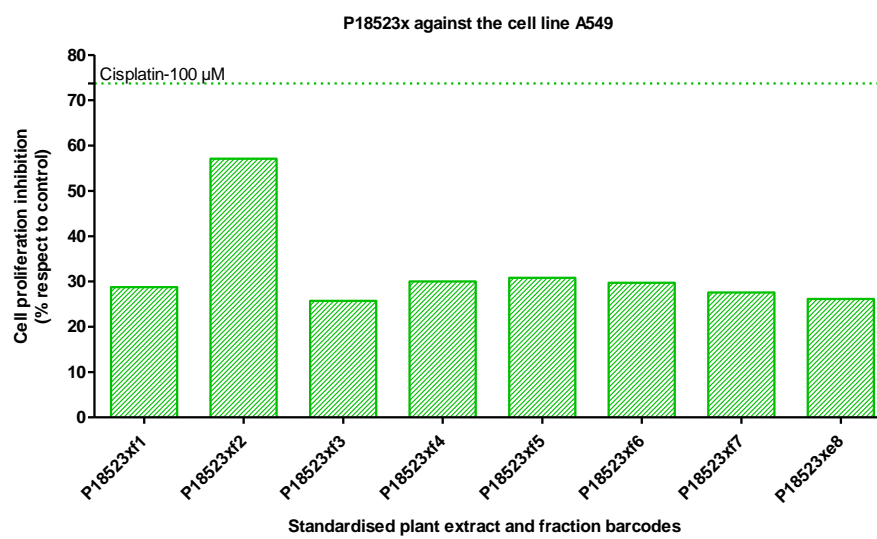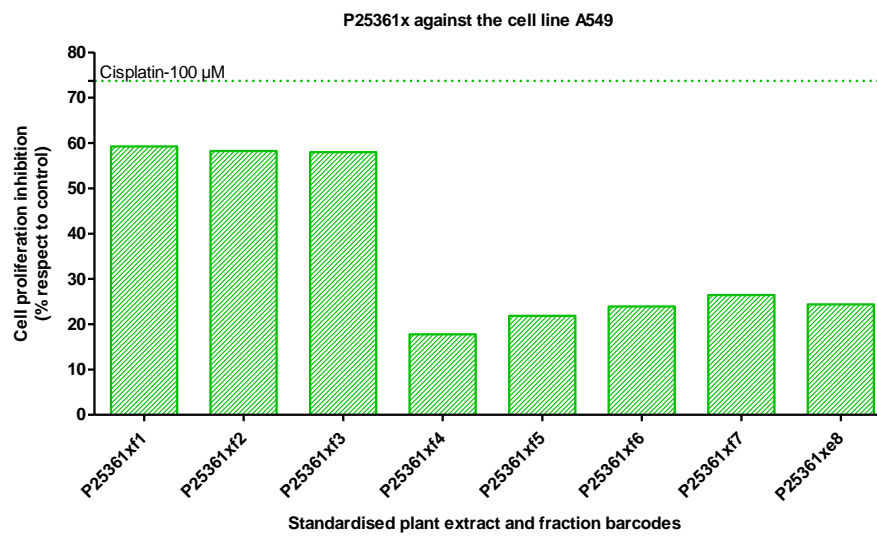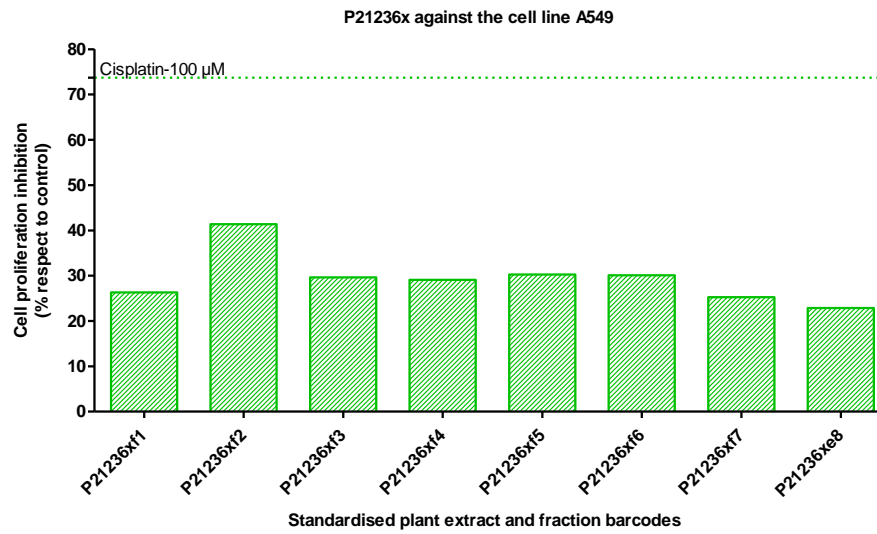
Supplementary data 3-4   The cell proliferation inhibition (%) of P21236x (bottom), P25361x (middle) and P18523x (bottom) against the cell line A549.

144
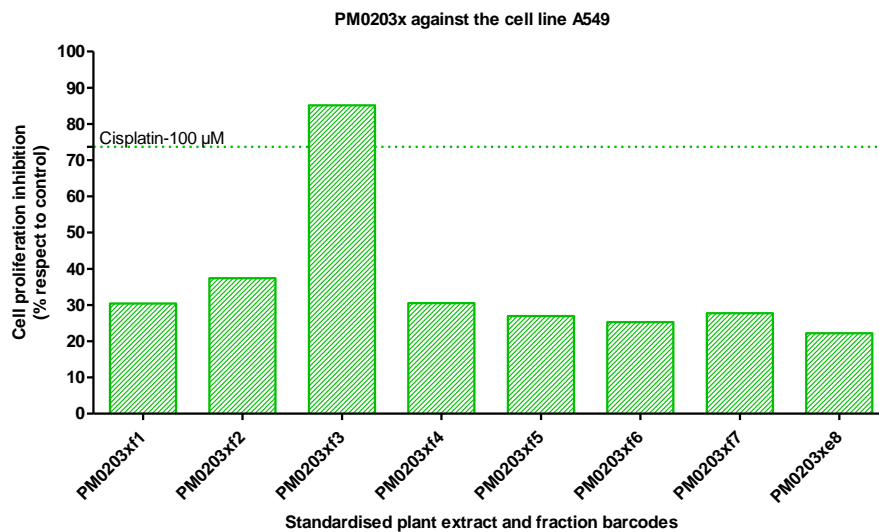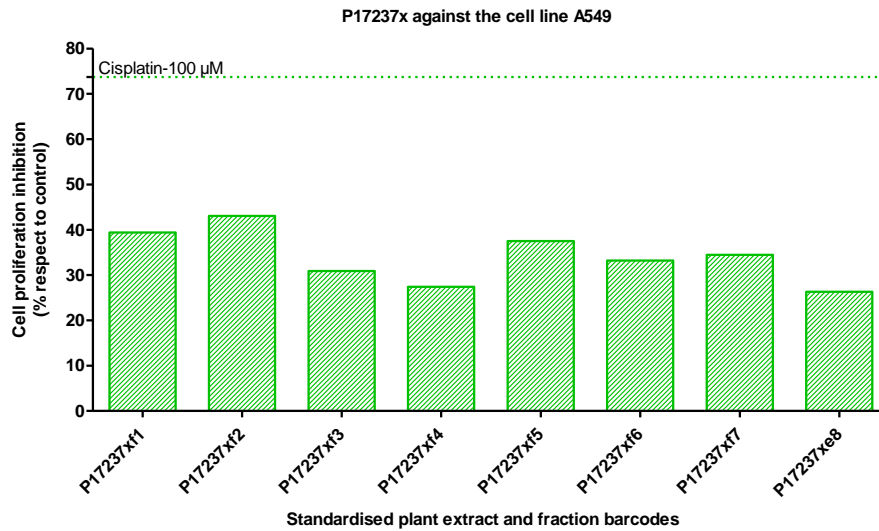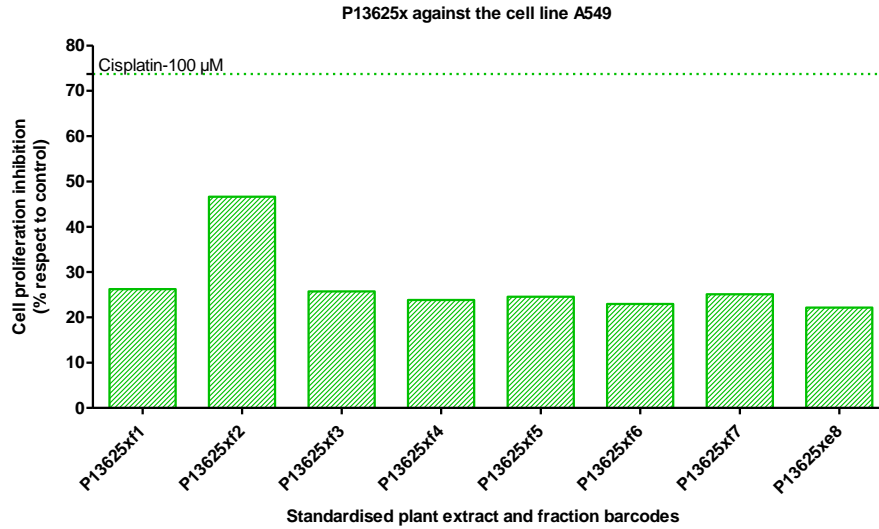
Supplementary data 3-5 The cell proliferation inhibition (%) of P13625x (top) and P17237x (middle) and PM0203x (bottom) against the cell line A549.

145

PM0102x against the cell line A549
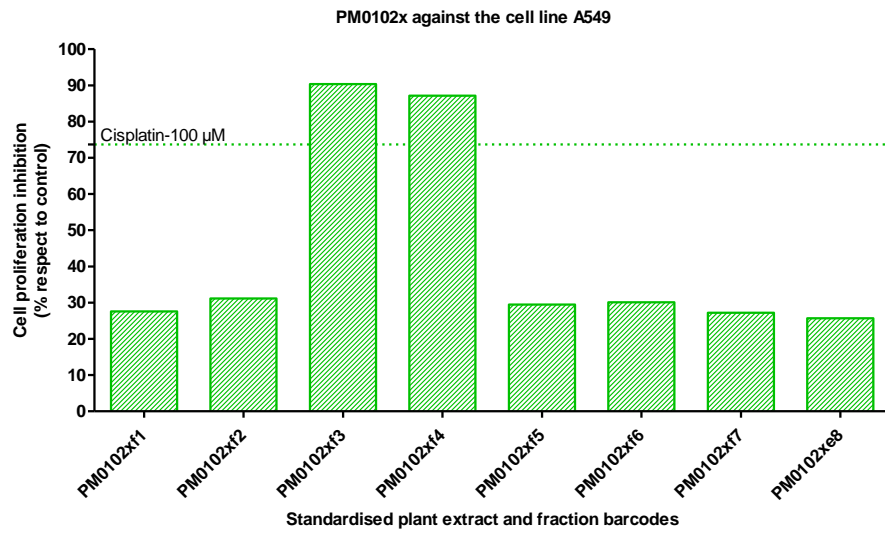
Supplementary data 3-6 The cell proliferation inhibition (%) of PM0102x against the cell line A549.
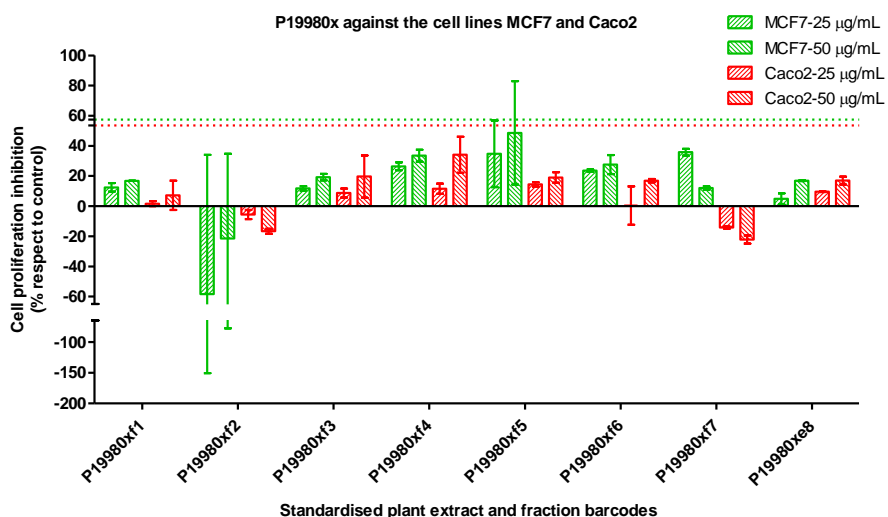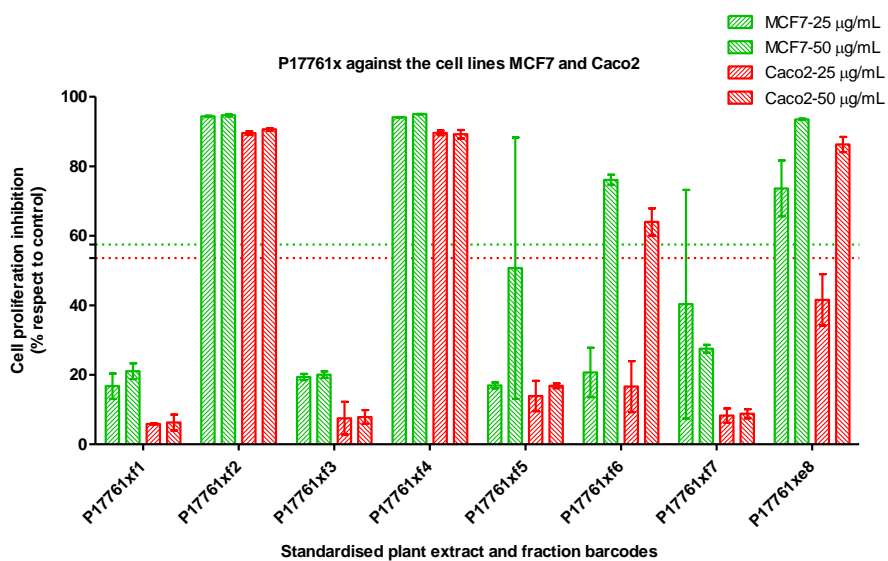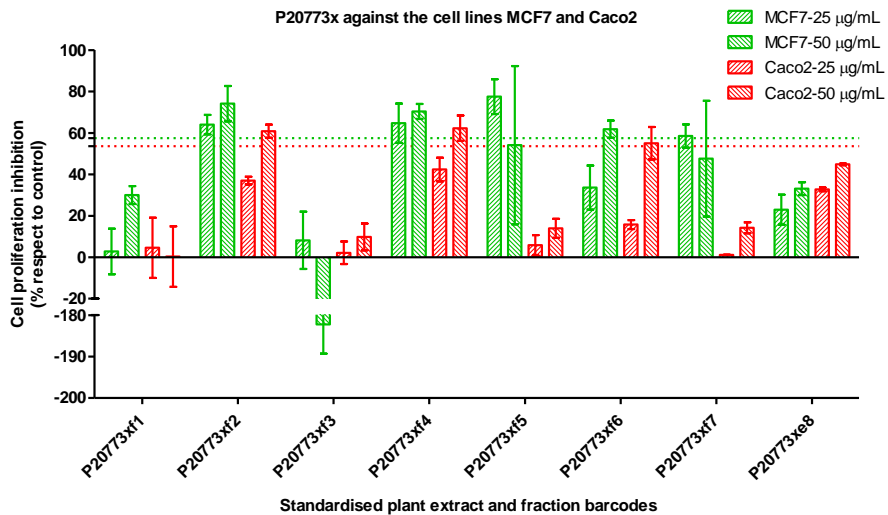
146
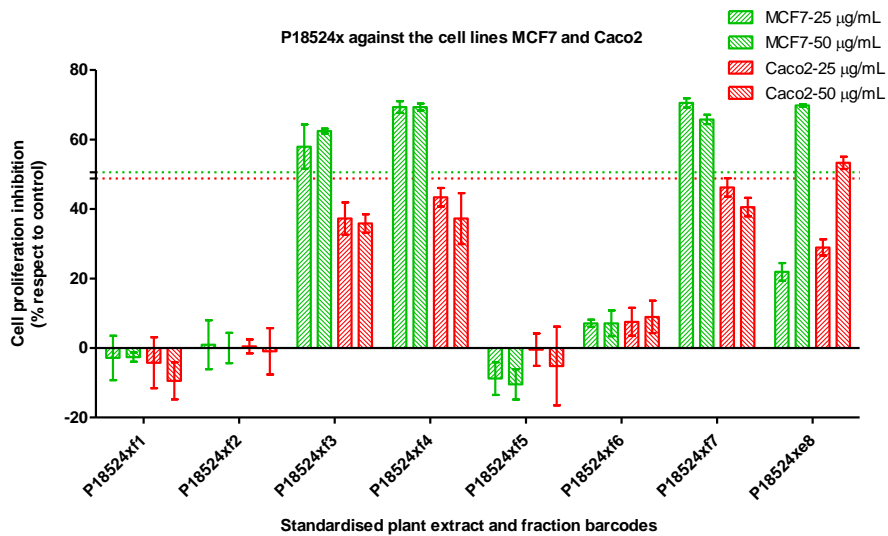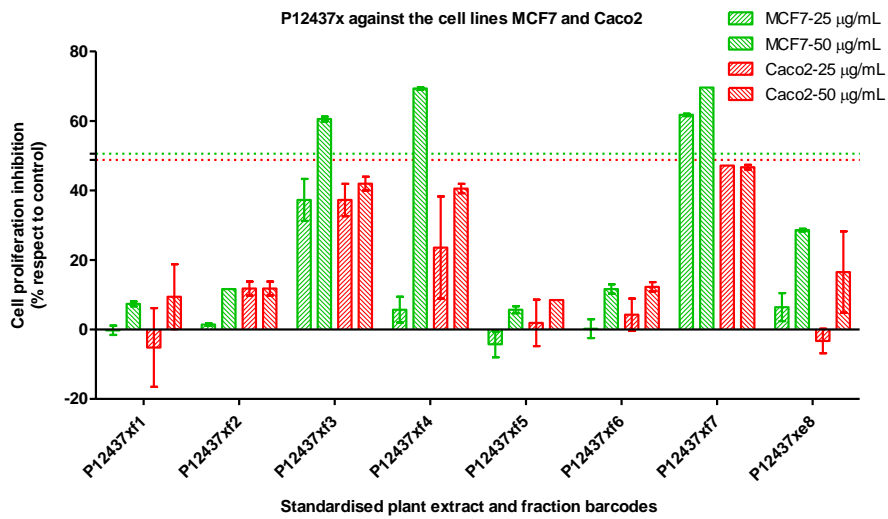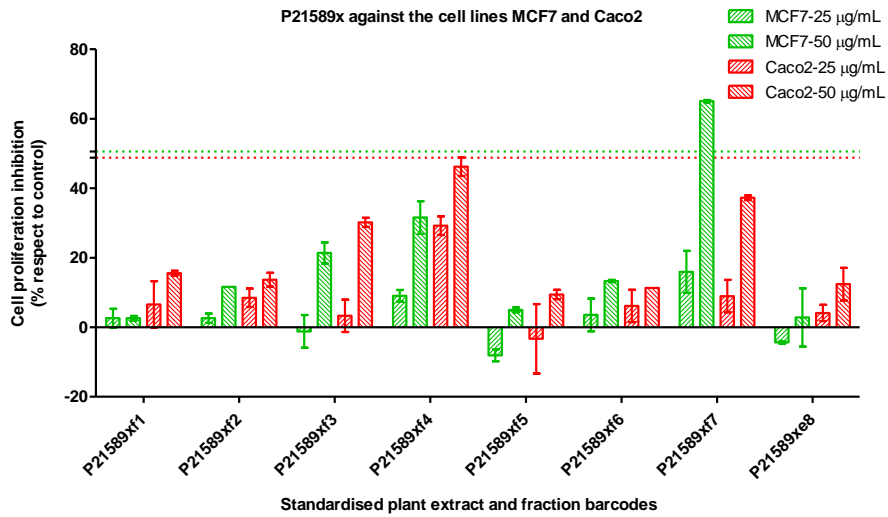
Supplementary data 3-7 The cell proliferation inhibition (%) of P21589x (top), P12437x (middle) and P18524x (bottom) against the cell lines MCF7 and Caco2.

147
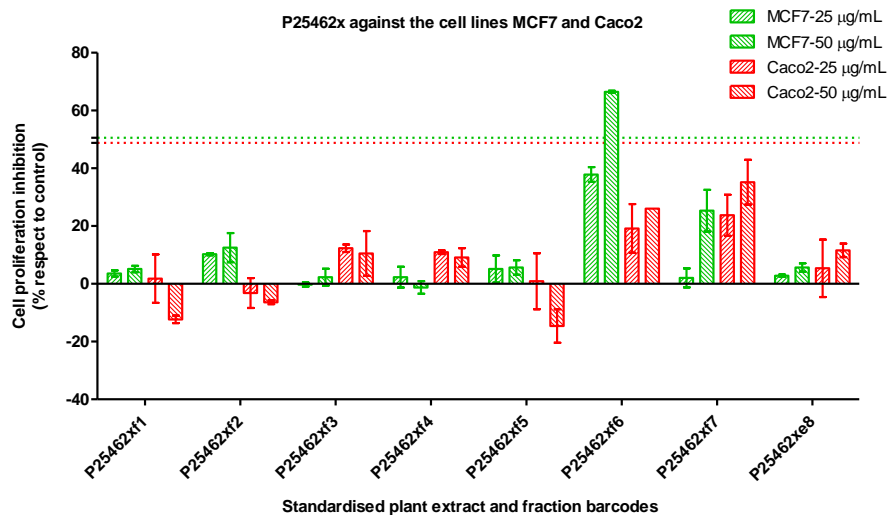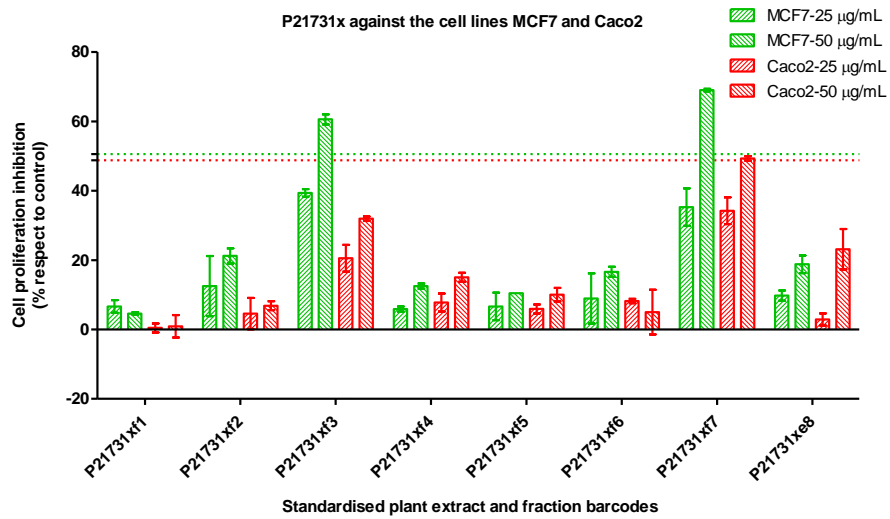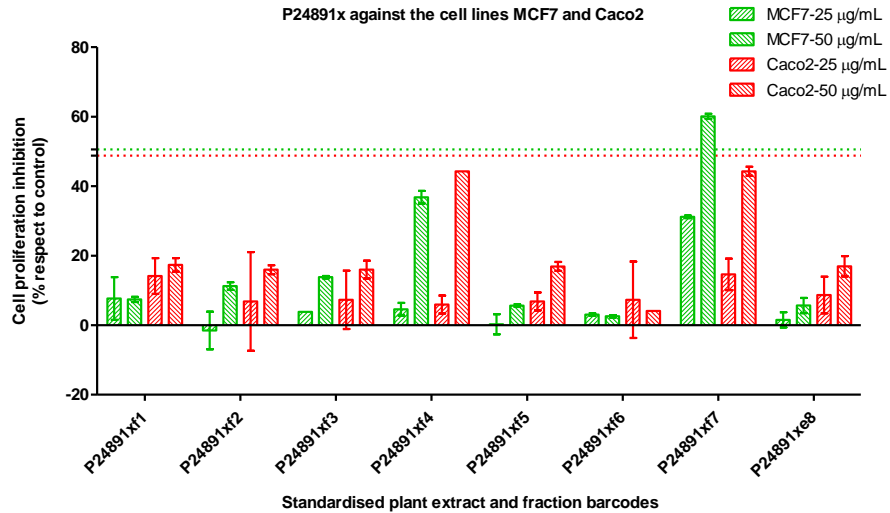
Supplementary data 3-8 The cell proliferation inhibition (%) of P24891x (top), P21731x (middle) and P25462x (bottom) against the cell lines MCF7 and Caco2.

148
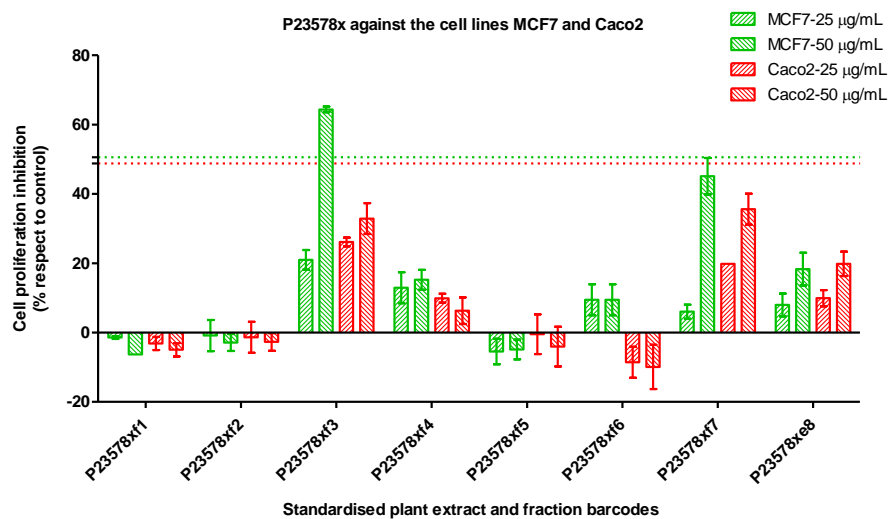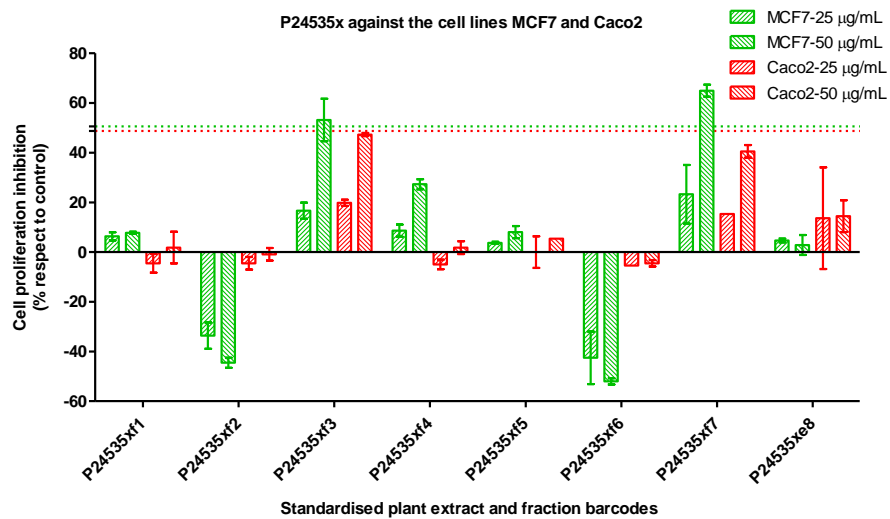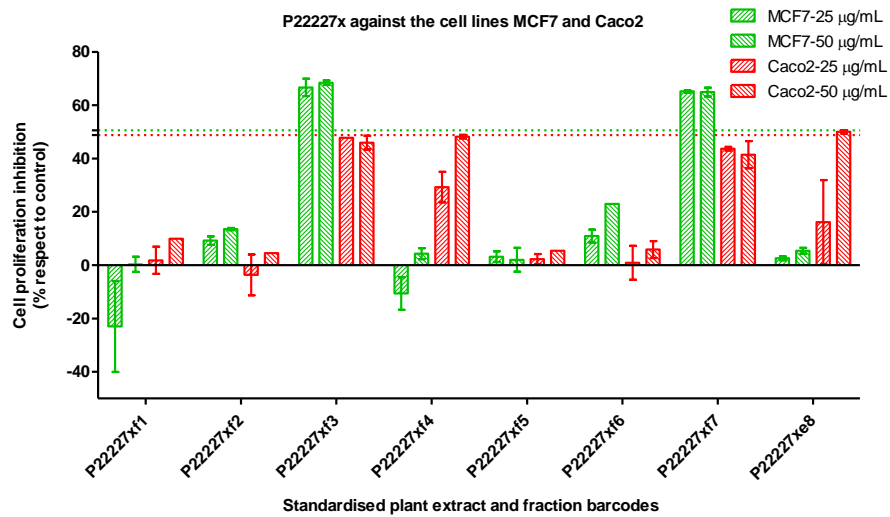
Supplementary data 3-9 The cell proliferation inhibition (%) of P22227x (top), P24535x (middle) and P23578x (bottom) against the cell lines MCF7 and Caco2.
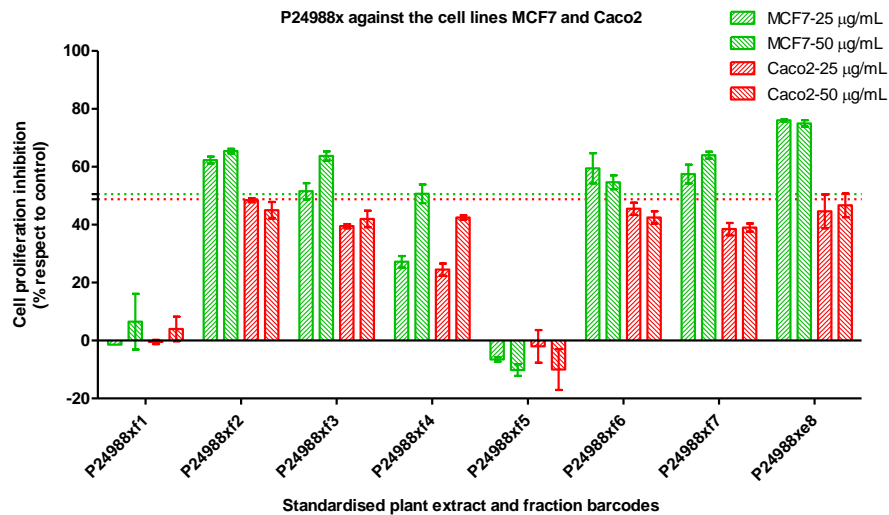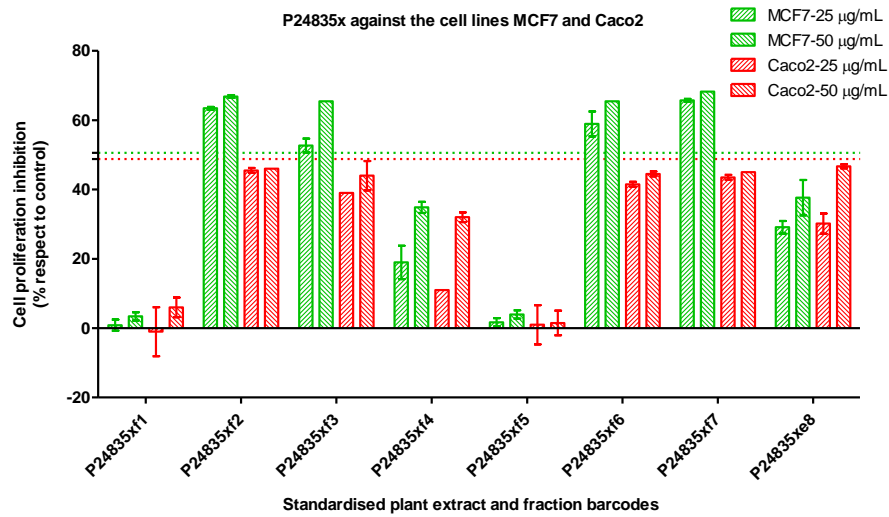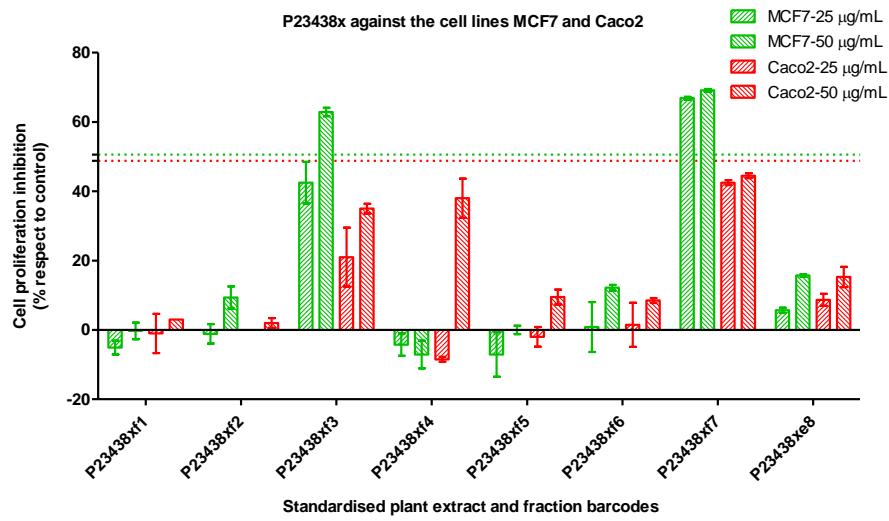
Supplementary data 3-10 The cell proliferation inhibition (%) of P23438x (top), P24835x(middle) and P24988x (bottom) against the cell lines MCF7 and Caco2.
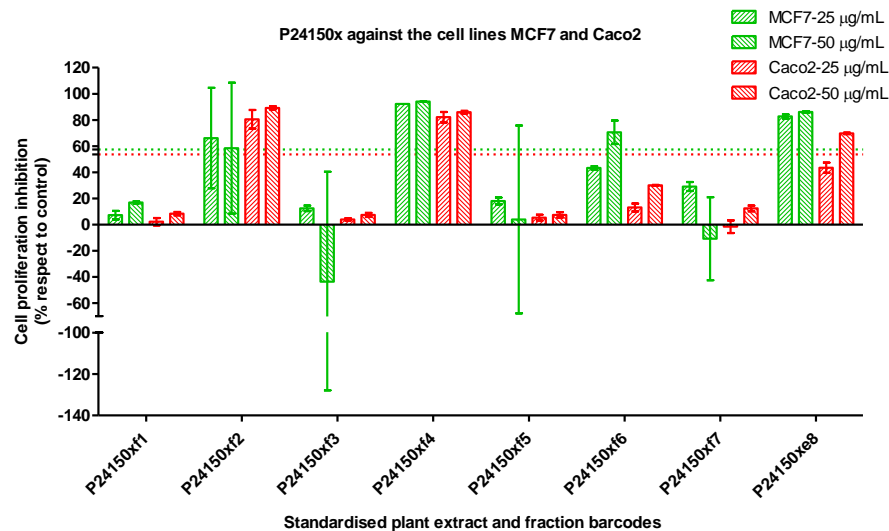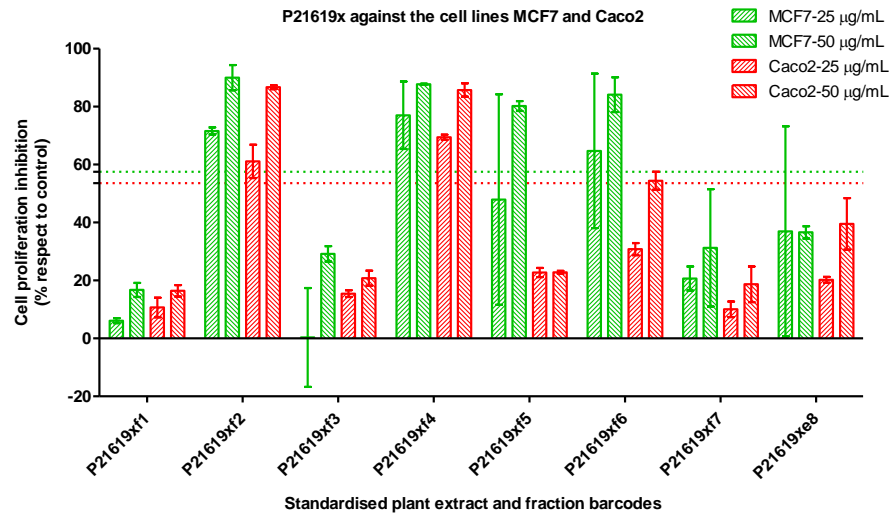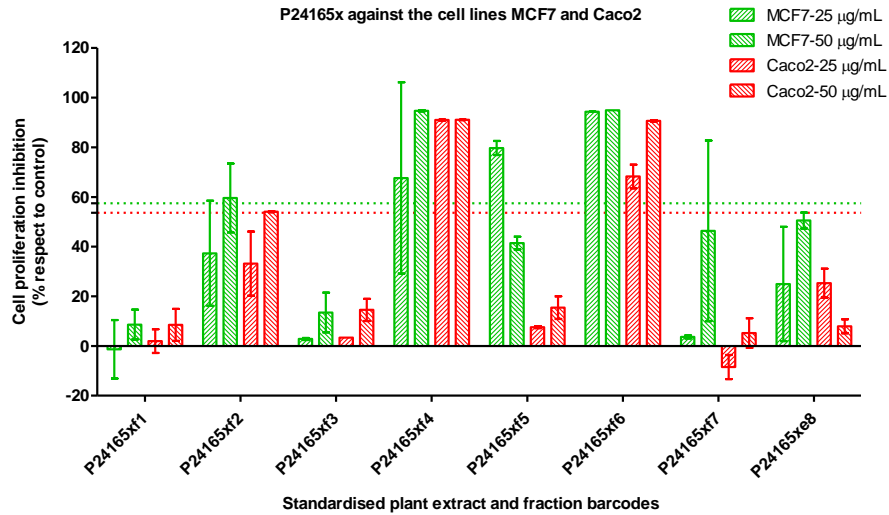
150

Supplementary data 3-11 The cell proliferation inhibition (%) of P21314x (top), P13964x (middle) and P20791x (bottom) against the cell lines MCF7 and Caco2.

Supplementary data 3-12 The cell proliferation inhibition (%) of P24653x (top), P23558x (middle) and P17029x (bottom) against the cell lines MCF7 and Caco2.

152

Supplementary data 3-13 The cell proliferation inhibition (%) of P20773x (top), P17761x (middle) and P19980x (bottom) against the cell lines MCF7 and Caco2.

Supplementary data 3-14 The cell proliferation inhibition (%) of P24165x (top), P21619x (middle) and P24150x (bottom) against the cell line MCF7 and Caco2.

154